UNIVERSIDADE FEDERAL DO RIO GRANDE DO SUL

INSTITUTO DE CIÊNCIAS BÁSICAS DA SAÚDE

DEPARTAMENTO DE BIOQUÍMICA

PROGRAMA DE PÓS-GRADUAÇÃO EM CIÊNCIAS BIOLÓGICAS:

BIOQUÍMICA

# A inibição de NFκB como estratégia para indução de morte celular em tumores

Doutorando: Alfeu Zanotto Filho

Orientador: Dr. José Cláudio Fonseca Moreira

Tese submetida ao Programa de Pós-Graduação em Ciências Biológicas: Bioquímica, como requisito parcial para obtenção do grau de Doutor em Bioquímica.

Porto Alegre, 2012

“Às vezes me questiono se, em um contexto de tantas carências básicas à boa parte da população, o mundo ainda precisa de mais tecnologia. Será que ainda sabemos onde queremos chegar com tanto conhecimento? Temos saber suficiente para viver com paz, saúde e igualdade, mas parecemos perder o foco daquilo que parece ser “viver bem”. Nossos desafios como civilização serão vencidos com crescimento tecnológico? Ou o bom senso e a humanidade seriam as melhores escolhas? Criamos novos problemas para resolvê-los com nossa ciência, talvez apenas na tentativa de sanar nossa curiosidade intrínseca ou de alimentar nosso ego insaciável. Mesmo assim, fiz o meu melhor”.

(Alfeu Zanotto Filho)

**AGRADECIMENTOS**

A minha esposa, Jussara Pisoni, pelo carinho, atenção, apoio, e principalmente por não me deixar desistir ou vacilar nos meus sonhos durante os momentos de dúvida.

Aos meus pais Alfeu e Marli Zanotto, e irmão, Mateus Zanotto, pelo respeito às minhas escolhas profissionais, pelos valores ensinados, e pelo exemplo, os quais permitiram o curso dessa trajetória.

Aos colegas do Centro Estudos em Estresse Oxidativo, Lab. 32, especialmente ao aluno de mestrado Rafael Schröder pela disposição, pelo trabalho técnico de alta qualidade e respeito com o nosso estudo. Agradeço também ao colega André Simões Pires e Guilherme Behr pela ajuda experimental e amizade. Ao colega João Paulo pelas colaborações científicas nas longas discussões aos fins de tarde e noites de trabalho.

Agradecimentos mais que especiais à minha sempre amiga Elizandra Braganhol, pela ajuda experimental, disposição, conhecimento e, principalmente, por ser uma pessoa de coração tão nobre, além de competentíssima parceira de trabalho.

Ao Mentor e Amigo, José Claudio F. Moreira, pela confiança, exemplo, respeito e liberdade proporcionados nestes 9 anos de convívio. Minha formação como profissional certamente é uma extensão de sua posição como tal;

Ao PPG: Bioquímica (UFRGS) e às agências financiadoras CAPES e CNPq, que me proveram bolsas de estudo durante todo o período, permitindo a realização de um trabalho em tempo integral.

**RESUMO**

A caracterização de vias de sinalização alteradas em células tumorais, e a validação de fármacos inibidores de transdução de sinal que interajam com as mesmas de modo a atuar como terapia principal ou adjuvante no tratamento de neoplasias sólidas e hematopoiéticas, é um campo de grande interesse em oncologia. A necessidade da caracterização de novos alvos moleculares advém da incidência considerável de recidivas, quadros de quimiorresistência e efeitos adversos associados ao tratamento com os agentes antitumorais clássicos. Nesta tese, desenvolvemos a hipótese de que o fator de transcrição NFκB poderia estar envolvido com processos de proliferação, antiapoptose e quimiorresistência em células neoplásicas, caracterizando-se como um potencial alvo para interferência farmacológica. Para isso, avaliamos: i) o papel de NFκB na resposta celular a ERO e no controle da decisão entre morte e proliferação celular; ii) o estado de ativação de NFκB em modelos tumorais in vitro e in vivo; iii) o potencial citotóxico e seletividade dos inibidores de NFκB, seus mecanismos de ação, atividade em células neoplásicas e em linhagens quimiorresistentes. Para isso, foram utilizadas abordagens in vitro (cultivos celulares), in vivo (modelo animal de implante tumoral), e análises de bancos de expressão gênica através de ferramentas de biologia de sistemas. Os resultados demonstraram que NFκB está superestimulado em linhagens de leucemia e de glioblastoma quando comparado com leucócitos e astrócitos não-transformados. O tratamento com inibidores farmacológicos de NFκB causou morte celular programada em um mecanismo seletivo para células tumorais, potenciando os efeitos de antitumorais clássicos tanto em linhagens selvagens quanto em células quimiorresistentes. Além disso, os inibidores BAY117082 e curcumina apresentaram atividade in vivo em modelo animal de glioma sem evidência de citotoxicidade aguda. Em suma, os dados aqui apresentados sugerem que o fator de NFκB constitui-se um potencial alvo para inibição farmacológica no tratamento de neoplasias. Neste contexto, a diversidade da expressão de NFκB em diferentes tipos tumorais e a segurança associada ao uso clínico de seus inibidores permanece por ser avaliada.

## ABSTRACT

Characterization of new molecular targets is one of the most important challenges in oncology. In this context, there is a growing interest in characterization of deregulated cell signaling pathways in solid and hematopoietic cancer cells in order to leverage the development of specific cell signaling inhibitors to act as principal or adjuvant therapy, and to circumvent the frequently observed chemoresistance and relapse in cancer patients. In this study, we hypothesized that the transcription factor NFκB could be involved on proliferation, antiapoptosis response and chemoresistance in cancer cells thus being a potential target for pharmacological interference. Attempting to test this, we evaluated: i) the role of NFκB in cell response against reactive oxygen species and in control of cell death and proliferation signaling; ii) NFκB activation status in cancer and noncancerous cells in vitro and in vivo; iii) cytotoxicity, selectivity and mechanisms of action of NFκB inhibitors in glioma and leukemia cells besides its biological activity against chemotherapy-resistant cell lines. Experiments were performed based on in vitro (cancer cell lines and primary cultures) and in vivo (tumor implants) models of cell growth. Moreover, in some experiments, bench-directed analysis of public gene expression databases followed by bioinformatic approach was used to ensure the significance and reliability of experimental data. Our findings showed an overstimulation of NFκB in leukemic and glioblastoma cell lines compared to healthy leucocytes and non-transformed astrocytes, respectively. Treatment with pharmacological inhibitors of NFκB induced programmed cell death in a cancer cells selective manner and potentiated the effects of classical anticancer drugs in both wild-type and chemoresistant cell lines. Indeed, the pharmacological NFκB inhibitors BAY117082 and curcumin showed significant anticancer efficacy in a model of brain-implanted gliomas without evidence of acute toxicity. Overall, the herein presented data suggest that NFκB is a potential target for cell death induction in leukemia and glioblastomas. Evaluation of its expression profile in different type of cancers beyond testing efficacy and safety of NFκB pharmacological inhibitors for clinical usefulness remains to be investigated.

## LISTA DE ABREVIATURAS

**NFκB**: Fator Nuclear kappa B

**EGFR:** Receptor para o Fator de Crescimento Epidermal

**VEGF**: Fator de Crescimento Endotelial Vascular

**IκB**: Inibidor de NFκB

**IKK:** IκB Cinase

**NIK:** Cinase Indutora de NFκB

**TNF**: Fator de Necrose Tumoral

**AP-1**: Proteína Ativadora tipo 1

**TLR**: Receptor Toll-like

**PTEN**: Proteína Homóloga da Fosfatase e Tensina

**PKC**: Proteína Cinase C

**PKA**: Proteína Cinase A

**PDGF**: Fator de Crescimento Derivado de Plaquetas

**TNFAIP3**: Proteína-3 Induzida pelo Fator de Necrose Tumoral

**LEF-1**: Fator Potencializando de Transcrição e Ligação Linfóide tipo 1

**TKI**: Inibidor de Tirosina-cinases

**SDF-1**: Fator de Crescimento Derivado de Estroma

**IGF**: Fator de Crescimento Insulina-ligado

**FDA**: Food and Drug Administration

**EMSA**: Electro Mobility Shift Assay

**siRNA**: small interference RNA (RNA de Interferência)

**MMP**: Metaloproteinases de Matriz Extracelular

**SOD2**: Superóxido dismutase tipo 2

**ERO**: Espécies Reativas de Oxigênio

**miRNA**: micro RNA

**LISTA DE FIGURAS**

## APRESENTAÇÃO

Essa tese sugere que o fator de transcrição NFκB é um potencial alvo terapêutico em tumores via inibição farmacológica. Neste estudo, avaliamos especificamente o papel deste fator de transcrição em modelos de células leucêmicas e glioblastomas in vivo e in vitro. Os “Materiais e Métodos” e os “Resultados” estão apresentados na forma de artigo científico.

No artigo 1, avaliamos o papel de NFκB no controle dos mecanismos de morte e proliferação celular em situação de estresse oxidativo induzido por retinol. Nos artigos 2 e 3, o papel do NFκB e o potencial citotóxico da sua inibição foram avaliadas em modelos de cultivo celular de linhagens de leucemia e glioblastomas, respectivamente. No quarto artigo, determinamos o efeito in vivo do inibidor de NFκB, curcumina, em modelo de implante cerebral de glioma de rato, avaliando tanto parâmetros de eficácia quanto de toxicidade.

O capítulo Discussão contém uma interpretação dos resultados obtidos nessa Tese, apoiada pela literatura científica corrente. Por fim, são apresentadas as conclusões e perspectivas.

No capítulo Referências Bibliográficas encontramos aquelas citadas nos capítulos Introdução e na Discussão. Os anexos correspondem a dados gerados durante o período de desenvolvimento desta tese e que não fazem parte do corpo principal da mesma.

# I - INTRODUÇÃO

# I. INTRODUÇÃO

## I.1 - Contextualização geral

Mesmo após muitas décadas de pesquisa científica e incontáveis avanços, a busca pela tão falada “cura do câncer” continua sendo uma meta de caminhos tortuosos, principalmente em alguns tipos de neoplasias. Isso tudo se deve à grande diversidade de tumores, tanto no que se refere à origem histológica quanto aos diferentes perfis de mutação nas diferentes populações celulares de um mesmo espécime, taxas de proliferação exacerbada, invasão/infiltração tecidual, quimio e radioresistência, além de metástases. Embora diferenças específicas nestes parâmetros sejam encontradas, os processos de transformação neoplásica compartilham, em sua gênese, uma sequência transformações em nível celular como mutações puntuais, amplificações, deleções ou translocações cromossômicas em genes codificantes de proteínas envolvidas no controle do ciclo celular, apoptose e proliferação, também conhecidas como “oncogenes”. Tais alterações em nível de genoma promovem a ativação de rotas de sinalização celular específicas, que levam ao processo de proliferação descontrolado, ativação de mecanismos de escape imunológico e resistência à apoptose. Em tumores sólidos, a excessiva angiogênese também é um fator bastante favorável ao crescimento neoplásico (Alberts et al., 2006).

Classicamente, os agentes farmacológicos utilizados na terapia antitumoral foram agrupados em: quimioterapia, terapia hormonal e imunoterapia (Kasuga et al., 2004; Zhang et al., 2007). A quimioterapia, foco deste estudo, inclui um diverso número de famílias de moléculas agrupadas em função de sua estrutura molecular (classes químicas) e mecanismos de ação, como por

exemplo: agentes alquilantes de DNA (temozolomida, ciclofosfamida, melfalan); antibióticos (mitomicina, bleomicina); antimetabólitos (metotrexato, 5-fluoracil e citarabina); inibidores de topoisomerase (doxorubicina, etoposideo, idarubicina e outras antraciclinas); inibidores de fuso mitótico (paclitaxel, vincristina e vimblastina) (Espinosa et al., 2003). Em geral, tais classes de moléculas atuam afetando processos relacionados à síntese de novas moléculas de DNA, induzindo mutações, danos de quebra de fita-simples e fita-dupla nas cadeias desoxiribonucleotídicas e desestabilização cromossômica. Consequentemente, os processos de proliferação celular são comprometidos, culminando na indução de paradas no ciclo celular, senescência e morte celular apoptótica, autofágica e, até mesmo necrótica. Tais fenômenos acabam levando à diminuição das taxas de crescimento tumoral (Hurley et al., 2002; Xiong-Zhi et al., 2006).

Na última década, novos fármacos têm sido desenvolvidos, e seus mecanismos de ação são os mais distintos, podendo variar desde a modulação de fenômenos em nível de membrana plasmática (inibição/antagonismo de receptores de membrana), inibição de alvos intracelulares proteicos, até a modulação de vias de sinalização alteradas em células tumorais como decorrência das mutações, deleções, duplicações e translocações cromossômicas que ocorrem durante a promoção e progressão tumoral (Espinosa et al., 2003; Baker e Reddy, 2010). Assim, os mecanismos de sinalização envolvidos em fenômenos como angiogênese, metástase, diferenciação, resistência celular à apoptose, e o papel das células iniciadoras tumorais (ou células-tronco tumorais) têm sido estudados e exploradas como potenciais alvos para caracterização de novas moléculas anticâncer (Mercer et

al., 2009; Sathornsumetee et al., 2009; Dancey et al., 2002). Hormônios esteróides atuando diretamente na transcrição de genes específicos (como a prednisolona e a dexametasona), anti-hormônios (como o tamoxifem e flutamida), anticorpos monoclonais contra receptores de membrana específicos (Rituximab (anti CD120), Trastuzumab (anti Her-2), Cetuximab (anti EGFR)), inibidores de domínios tirosina cinase intracelular em receptores ou proteínas acopladas a receptores (Imatinib, inibidor de bcr/abl); inibidores de proteassoma (bortezomib), inibidores da angiogênese (talidomida e bevacizumab, e inibidores da sinalização de VEGF) são alguns exemplos desses novos fármacos (Mercer et al., 2009; Sathornsumetee et al., 2009; Dancey et al., 2002; Hurley et al., 2002; Xiong-Zhi et al., 2006; Baker e Reddy, 2010). Estas moléculas são desenvolvidas e validadas através da elucidação das rotas de promoção/sinalização tumorais envolvidas nos diferentes eventos neoplásicos, não atuando, diretamente, na síntese de DNA e duplicação celular, como os quimioterápicos clássicos descritos no parágrafo anterior. Estes novos agentes são também conhecidos como "*Inibidores da Transdução de Sinal".*

A caracterização de vias de sinalização seletivamente alteradas em células tumorais, e a validação de fármacos inibidores da transdução de sinal que interajam com as mesmas de modo a atuar como terapia principal ou adjuvante no tratamento de neoplasias sólidas e hematopoiéticas é um campo em amplo crescimento entre as publicações na área de oncologia. De fato, o surgimento de novas moléculas e protocolos terapêuticos envolvendo inibidores da transdução de sinal tem crescido nos últimos anos (Dancey et al., 2002; Orlowsky e Baldwin, 2002; Tentori e Graziani, 2009). Tal demanda é

consequência do considerável número de pacientes refratários às terapias convencionais, dos efeitos adversos associados, e do surgimento de resistência ao longo do tratamento, fatores que frequentemente levam à falha terapêutica. Inevitavelmente, em muitos pacientes, principalmente naqueles cujos tumores são diagnosticados em estágios avançados, o prognóstico do câncer ainda permanece bastante reservado (Orlowsky e Baldwin, 2002; Morotti et al., 2006). É na perspectiva da interferência farmacológica em vias de sinalização tumor-específicas e na falha de terapias convencionais que se baseia a pesquisa com inibidores de transdução de sinal como tentativa de aumentar a variedade e eficácia do arsenal anticâncer. Assim, a utilização de protocolos quimioterápicos baseados na combinação de dois ou mais fármacos pertencentes a diferentes classes, e com mecanismos de ação distintos, a fim de atacar as células malignas por vias diversas, poderia aumentar a eficácia, diminuir as altas doses requeridas para atividade farmacológica e, consequentemente, os efeitos adversos em tecidos sadios em pacientes refratários (Orlowsky e Baldwin, 2002; Morotti et al., 2006; Tentori e Graziani, 2009; Kandel et al., 2009).

### I.2 - A via de transdução de sinal do fator de transcrição NFκB

NFκB (Nuclear factor kappa-B) é um fator de transcrição descoberto, inicialmente, devido a sua atividade ligante à região promotora do gene codificador das cadeias kappa (κ) de imunoglobulinas em linfócitos B (Sen e Baltimore, 1986). Desde sua descoberta em 1986, o papel de NFκB na modulação da resposta inflamatória tem sido extensivamente estudado. Em mamíferos, NFκB é um fator de transcrição formado por uma família de

proteínas (RelA/p65, p50, RelB, cRel, NF-κB1 (p50; p105) e NF-κB2 (p52; p100) combinadas em diferentes homo e heterodímeros. Essas proteínas têm em comum uma região conservada de 300 aminoácidos chamada “domínio REL”, o qual contém os domínios de dimerização, localização nuclear e ligação ao DNA. As proteínas RelA/p65, c-Rel e RelB possuem domínio de transativação na região C-terminal ao passo que NF-κB1/p105 e NF-κB2/p100 são os precursores inativos das proteínas p50 e p52, respectivamente. Em um estado não estimulado, estas proteínas ficam localizadas no citoplasma em estado inativo. Sob estimulação, o processamento proteolítico remove parte do domínio inibitório da região C-terminal de NF-κB1 e NF-κB2, formando p50 e p52, e permitindo a translocação nuclear das mesmas. Rel A e p50 existem em uma ampla variedade de tipos celulares ao passo que a expressão de c-Rel é restrita a linhagens hematopoiéticas e linfócitos. Por outro lado, a expressão de RelB é limitada a sítios específicos, como o timo, linfonodos e Placas de Peyer (Li e Verma, 2002)

Embora cada dímero de NFκB tenha uma atividade ligante de DNA diferente para a sequencia consenso kB (GGGRNNYYCC (R, purina : Y, pirimidina : N, any base) (Hayden e Ghosh, 2004), as funções destes frequentemente se sobrepõem. Dímeros de NFκB formados unicamente por membros sem domínio de ativação, como homodímeros de p50, são capazes de promover repressão transcricional (May e Ghosh, 1997).

NFκB é expresso no citoplasma da maioria dos tipos celulares, não qual sua atividade é controlada por uma família de proteínas regulatórias, chamadas inibidoras de NFκB. IκB-α, IκB-β, IκB-ξ e Bcl3 são os membros da família IκB, os quais possuem um domínio em comum formado por 33 aminoácidos, os

quais ligam e inibem os dímeros de NFκB. As proteínas IκB são conhecidas por inibirem os dímeros de NFκB no citoplasma através do mascaramento das suas sequencias de reconhecimento para internalização nuclear (Silverman e Maniatis, 2001; Li e Verma, 2002; Hayden e Ghosh, 2004).

Por outro lado, estudos demonstraram que tanto IκB-α quanto IκB-ξ são transportadas junto com os complexos de NFκB-IκB; tais complexos são envolvidos no desligamento do NFκB ativo do DNA e retorno ao citoplasma (Huang e Miyamoto, 2001; Birbach et al., 2002). Em um mecanismo de feedback negativo para desligamento de sinal, sabe-se que, uma vez no núcleo e ativo, os dímeros de NFκB regulam positivamente a expressão das proteínas IκB-α e IκB-ξ. Entretanto, a expressão de IκB-β não segue o mesmo padrão. Ao contrário, IκB-β é constituivamente retida no citoplasma, e não está envolvida no loop auto-regulatório da terminação da sinalização por NFκB (Huang e Miyamoto, 2001; Birbach et al., 2002). Recentemente foi descrita a regulação do conteúdo celular de IκB-α pela ação de micro-RNA (Jiang et al., 2012). Aparentemente, cada membro da família IκB tem funções tanto distintas quanto redundantes.

A ativação de NFκB é regulada por sinais que degradam IκB (Figura 1). Existem, basicamente, duas vias de ativação: Via Clássica e Via Alternativa. Na via clássica, proteínas de família IκB são fosforiladas por proteínas do complexo IκB cinases (também conhecidas como IKK) em sítios específicos de Ser32 e Ser36 de IκB-α. Fosforilação de IκB-α induz a poliubiquitinação dos sítios Lys21 e Lys22 e subsequente degradação pela subunidade 26S do proteassoma, e liberando a forma dimérica ativa de NFκB. Na via clássica, o

dímero p65/p50 é o mais comumente encontrado (Dalhase et al.,1999; Li e Verma, 1999; Karin e Bem-Neriah, 2000).

O complexo IKK é formado pelas subunidades catalíticas (IKK-α e IKK-β) e a subunidade regulatória IKKγ, também conhecida como “NFκB essential modulator (NEMO). IKKα e IKK-β são 52 % idênticas em sua sequencia de aminoácidos, formam tanto homo quanto heterodímeros que, embora ambas cooperem na fosforilação de IκB, elas diferem no sinal que elas medeiam (Senftleben et al., 2001). O componente IKK-β é essencial na ativação da via clássica, entretanto estímulos como UV, radiação gama e ERO podem promover a ativação de proteínas tirosina cinases intracelulares e MAP cinases como p38 e JNK as quais podem promover a ativação da via clássica diretamente em nível de fosforilação de IkB (Dalhase et al.,1999; Li e Verma, 1999; Karin e Bem-Neriah, 2000).

Diferente da via clássica, a via alternativa de ativação de NFκB foi recentemente descrita. No mecanismo alternativo, a cinase indutora de NFκB (NIK, NFκB-inducing kinase) ativa um homodímero de IKK-α, a qual fosforila dois sítios C-terminais de NF-κB2/p100, a qual está ligada a RelB, e subsequentemente NF-KB2/p100 é ubiquitinado. IKK-β e IKKγ são dispensáveis para esse mecanismo (Senftleben et al., 2001; Nishikori, 2004). Tal modificação induz a clivagem proteassomal deste domínio produzindo p52. Após a formação de p52, o dímero p52/RelB transloca para o núcleo onde regula a expressão gênica (figura 1).

Ativação das duas vias pode ocorrer simultaneamente, entretanto elas parecem ter indutores de ativação e atividades diferentes em órgãos específicos, as quais decorrem da expressão diferencial dos membros de cada

uma das vias entre os diferentes tecidos, (Shishodia e Aggarwal, 2002; Pikarsky et al., 2004; Baud e Karin, 2009) . Na via clássica de ativação, uma variedade estímulos ligantes de receptor como, por exemplo, Lipopolissacarídeo (LPS) em receptores TLR4, citocinas inflamatórias (interleucinas), fator de necrose tumoral alfa (TNF-α) em receptores TNFR1/2, além de estímulos independentes de receptor como radiação, agentes antitumorais e oxidantes/ERO (Pikarsky et al., 2004; Baud e Karin, 2009). Nessas condições a forma ativa de NFκB (p65/p50; via clássica) migrará para o núcleo, ligará em regiões promotoras, e participará da regulação de diversos genes como, por exemplo:

- Mediadores inflamatórios: TNF-α, diversas interleucinas como IL1-β, IL-8, MCP-1, COX2 (ciclooxigenase 2).
- Controladores antiapoptóticos: (c-IAP1/2, XIAP, FLICE, Bcl-xL, A20, survivina)
- Proteínas de invasão tecidual: matriz metaloproteinases (MMP2 e MMP9).
- Proteínas de imortalização celular: Telomerase
- Reguladores do ciclo celular: ciclinas D1, D2, c-MYC
- Resposta a estresse oxidativo: SOD2 (Superóxido dismutase mitocondrial), FHC (cadeia pesada da ferritina), NOS2A (oxido nítrico sintase induzível, iNOS).
- Promotores de vascularização: VEGF, TNF, IL-1, IL-8
- Fatores de adesão: VCAM, ICAM, SELE (selectina E), ELAM

Importante enfatizar que praticamente todos os genes acima mencionados são descritos como importantes nos mecanismos de crescimento

de tumores (Barket and Gilmore, 1999; Baud and Karin, 2009; Orlowski e Baldwin, 2009; Shen e Tergaonkar, 2009). Esse espectro de modulação anti-apoptótica, proliferativa, pró-invasiva, inflamatória e antioxidante gerou a hipótese de que o NFκB poderia estar diretamente ligado aos eventos de proliferação, metástase e resistência tumoral aos quimioterápicos e ao sistema imune (Pickering et al., 2007; Baud e Karin, 2009). Portanto, a inibição de NFκB poderia ser um mecanismo de sensibilização e/ou inativação de células e processos tumorais (Orlowski e Baldwin, 2002; Jost e Ruland, 2007).

Diferentemente, a via alternativa é estimulada pela ativação de certas proteínas membros da família de receptores de TNF, incluindo o receptor para linfotoxina B (LTBr), receptor do fator ativador de células B (BAFF-R), CD40, e CD30. Devido a expressão tecido-específica de RelB, acima descrito, a ativação da via alternativa regula o desenvolvimento de órgãos linfoides e sistema imune, sendo sua relevância em processos tumorais ainda desconhecida (Nishikori, 2004). Além disso, o grupo de genes regulados por cada uma das vias de ativação é bastante diferente.

**VIA ALTERNATIVA** **VIA CLÁSSICA**

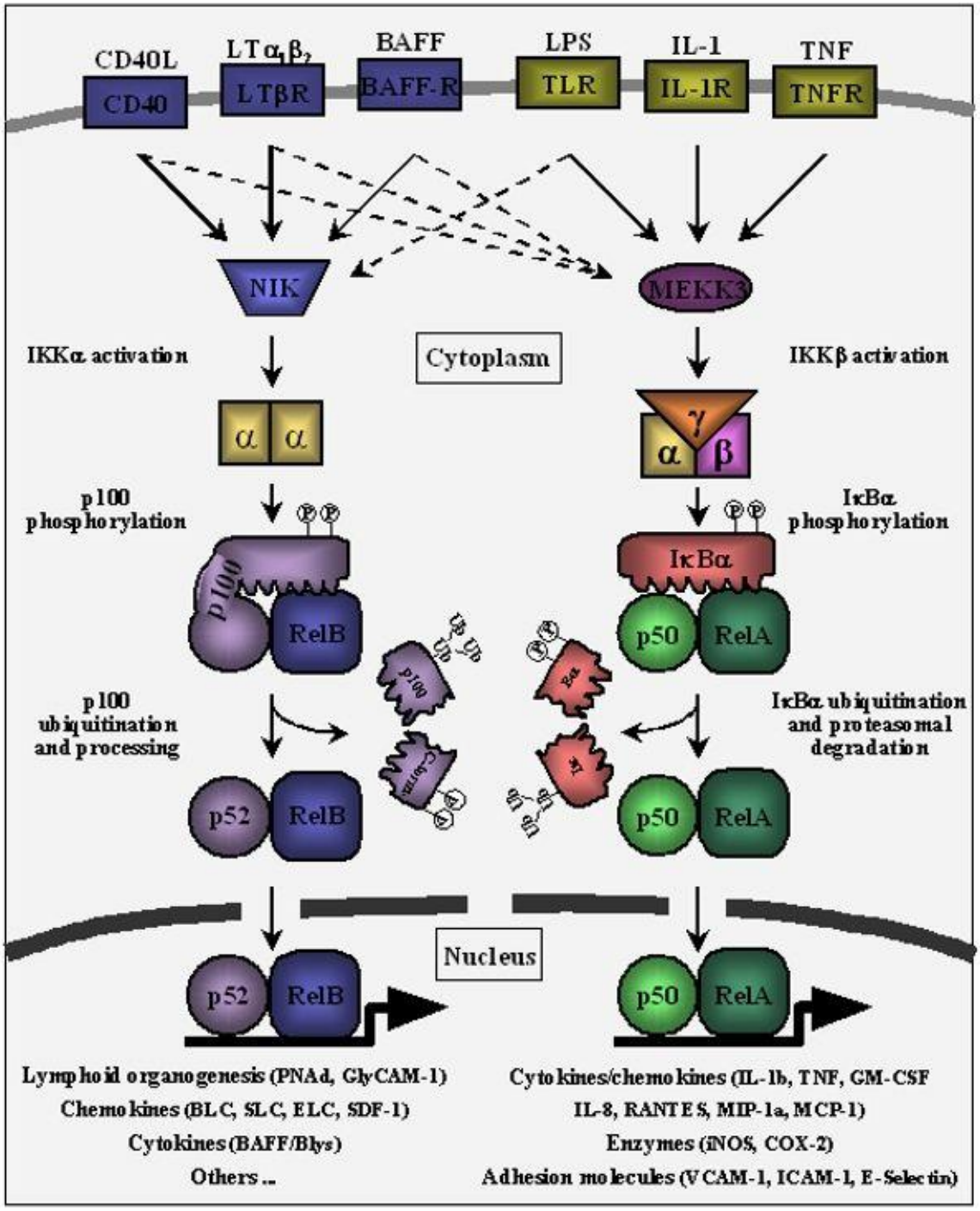


Figura 1: Via Clássica e Alternativa de ativação de NFκB (AbCam website e http://www.stat.rice.edu/~siefert/Research/NfKB.html**)**

**I.3 - Inibidores de NFκB**

Existem, atualmente, diversas moléculas inibidoras da via de NFκB (figura 2B a 2F), as quais atuam em diferentes pontos da via (figura 2A):

1) Inibidores da fosforilação da subunidade inibitória IκB.

i) BAY117082 ((E)-3-(4-Methylphenylsulfonyl)-2-propenenitrile): inibidor específico de IKK-β; IC50: 10 μM (Pierce et al., 1997):

ii) PS1145: N-(6-Cloro-9H-pirido[3,4-b]indol-8-yl)-3-piridinocarboxamida dihidrocloridrato; inibidor de IKKs (10–20 μM).

iii) Partenolideo: lactona sesquiterpênica; inibe IKK-β na Cys179. Além disso, inibe p65 por ligação em resíduos de cisteína no loop de ativação; IC50: 10 μM (Hehner et al., 1999; Kwok et al., 2001).

iv) Curcumina: pigmento extraído da *Curcuma longa*; inibidor de IKKs; IC50: 13 μM (Dhandapani et al., 2007).

2) Inibidores da degradação proteassômica de IκB-α.

v) Inibidores de proteassoma: PS341 (bortezomib), MG132 (Z-leu-leu-leu-CHO) e lactacistina. Por exemplo, MG132 inibe proteassoma com IC50: 0.1 μM, e a degradação proteassômica de IκB-α em IC50: 3 μM.

vi) Trióxido de arsênico: inibe degradação proteassômica de IκB-α e aumenta a expressão de NFKBIA (gene da IκB-α) (Han et al., 2005).

Apesar da utilização dos inibidores de NFκB como ferramenta em pesquisa básica, a descoberta do papel de NFκB como um fator importante na resistência e na modulação da morte e vida celular, e a utilização dos inibidores farmacológicos deste fator de transcrição como potenciais antitumorais é recente, embora cresça nos últimos anos. Consequentemente, poucos estudos

têm avaliado a eficácia e a toxicidade dessas substâncias em modelos tumorais in vitro e pré-clínicos (Zhang et al., 2004; García et al., 2005; Piva et al., 2005; Cilloni et al., 2006 e 2007).

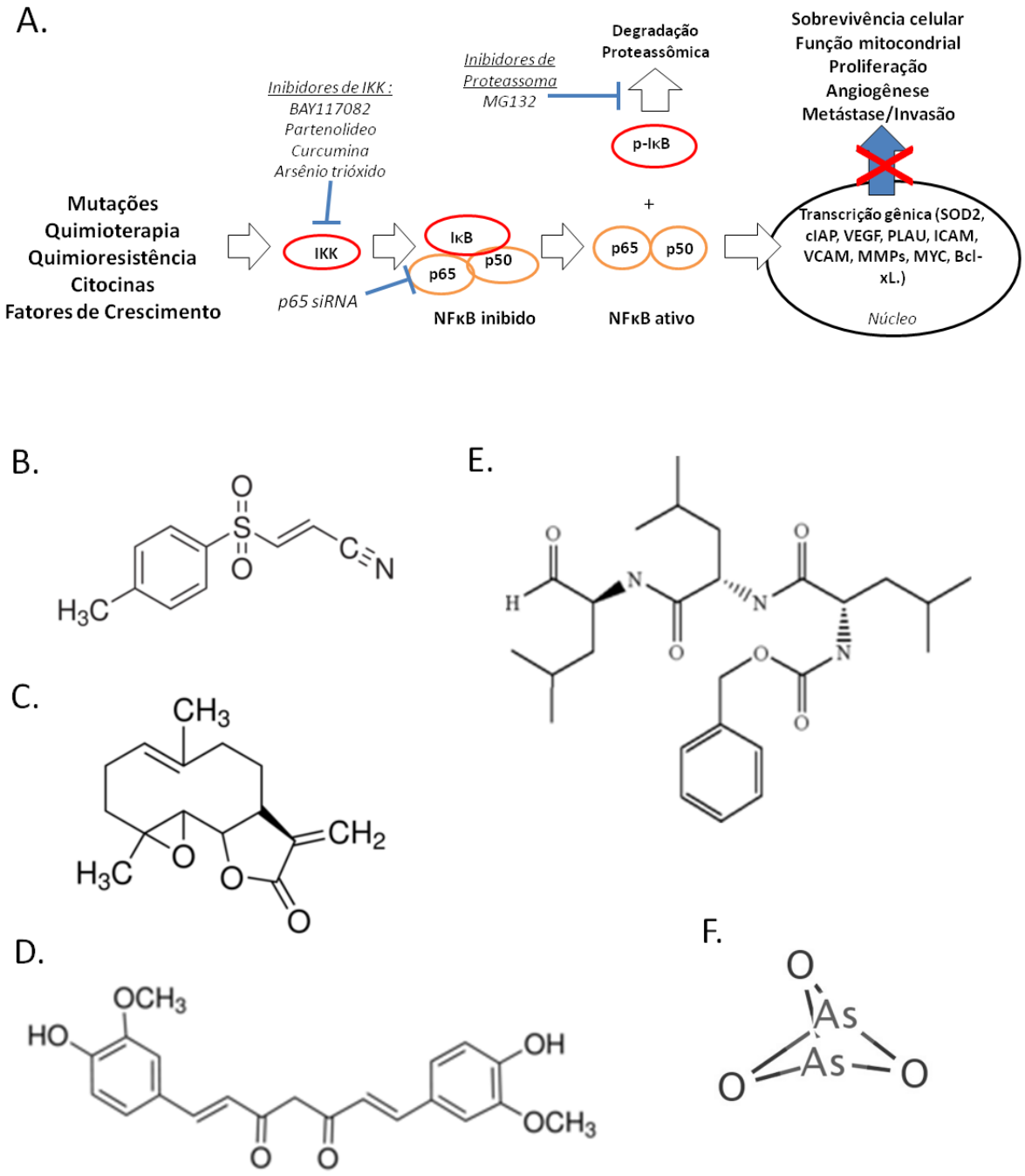


Figura 2: (A) Pontos de inibição da via de NFκB pelos inibidores utilizados neste estudo. (B-F) Estruturas moleculares dos inibidores de NFκB: (B)

BAY117082; (C) Partenolideo; (D) Curcumina; (E) MG132; (F) Trióxido de arsênio. Figuras desenhadas com o software BKChem®.

**Modelos de neoplasias estudados nesta tese:**

**I.4 - Glioblastomas:**

Os glioblastomas (astrocitoma grau IV) são tumores sólidos originários de transformações neoplásicas em células precursoras neurais, constituindo o tipo de tumor encefálico maligno mais comum em adultos, sendo altamente agressivos, invasivos, e sem tratamento curativo até o momento (Friedman et al., 2000; Mercer et al., 2009; Koukourakis et al., 2009; Sathornsumetee e Reardon, 2009). Ao contrário de outros tipos de câncer, as alternativas terapêuticas para o tratamento deste tipo de tumor são bastante restritas. As modalidades terapêuticas que demonstram benefício no prolongamento da sobrevida dos pacientes são a cirurgia para ressecção tumoral, a radioterapia craniana total e a quimioterapia, sendo que o agente quimioterápico com maior evidência de eficácia e mais utilizado é o alquilante temozolomida (Mercer et al., 2009). Entretanto, mesmo com a combinação dos tratamentos supracitados, a sobrevida média após o diagnóstico não costuma ultrapassar a marca de 12 a 18 meses, sendo o tratamento, assim, muitas vezes paliativo.

A literatura científica tem apontado os glioblastomas como “modelos de tumores refratários” devido aos mais variados mecanismos de invasão tecidual, infiltração e resistência quimioterápica, além da capacidade de proliferação celular extremamente alta que se verifica em pacientes e nas linhagens de glioblastoma in vitro (Friedman et al., 2000; Mercer et al., 2009; Koukourakis et

al., 2009). Devido a essa lista de fatores negativos, o prognóstico reservado do glioblastoma tem estimulado a pesquisa de novas modalidades terapêuticas, que têm focado tanto na busca de novos alvos celulares (utilizando inibidores farmacológicos de vias de transdução de sinal alteradas) e terapias adjuvantes quanto no desenvolvimento de estratégias tecnológicas de vetorização de fármacos como, por exemplo, a produção de nanopartículas carreadoras (Koukourakis et al., 2009; Anand et al., 2010; Sun et al., 2010; Tsai et al., 2011).

O crescimento dos glioblastomas é um processo multifatorial e, até o momento, alterações (mutações, amplificações e/ou deleções) em genes como o supressor tumoral p53, PTEN, EGFR (receptor para o fator de crescimento endotelial) e PDGF (fator de crescimento derivado de plaquetas) consistem as alterações genéticas mais comuns encontradas em transcriptomas de biópsias de glioblastomas humanos (Desbaillets et al., 1999; Demuth e Berens, 2004; de I et al., 2008). Essas alterações levam à ativação exacerbada de diferentes vias de sinalização celular como Ras/MEK/ERK, EGFR/PI3K/Akt, AP-1 (activator protein 1), PKC (proteína cinase C) e JAK/Stat (de I et al., 2008; Sathornsumetee e Reardon, 2009; Mao et al., 2012). Além disso, elevada angiogênese e o desencadeamento de um processo inflamatório que beneficiam o crescimento tumoral são descritos. Embora anticorpos monoclonais contra receptores de membrana específicos (Rituximab (anti CD120); Trastuzumab (anti Her-2); Cetuximab (anti EGFR), inibidores da angiogênese (talidomida e bevacizumab) e anticorpos contra o fator de crescimento endotelial (VEGF) estejam em pleno desenvolvimento e testes para diversos tipos de cânceres, no caso dos gliomas a terapia farmacológica

continua utilizando o alquilante temozolomide, uma vez que os inibidores de EGFR, PDGF e VEGF têm demonstrado eficácia clínica limitada (Mercer et al., 2009; Sathornsumetee e Reardon, 2009; Mellinghoff et al., 2011), o que sugere que processos celulares altamente adaptáveis colaboram nos mecanismos de fuga celular, resistência e consequente evolução da patologia.

Em um estudo pioneiro, Gill e colaboradores demonstraram que o tratamento com oligonucleotídeos *decoy* para NFκB induziu morte celular em linhagens de glioma, sem efeitos significantes nas células não-tumorais (astrócitos) (Gill et al., 2002). Outros pesquisadores observaram, através de modelos de resistência celular induzidas por temozolomida em cultivos primários de células de glioma humano, que um conjunto de genes intimamente ligados à sinalização de NFκB estavam aumentando em células resistentes à quimioterapia quando comparado a células de tumorais sensíveis. Neste contexto, foi identificado que o gene TNFAIP3 (tumor necrosis factor-induced protein 3), uma proteína com atividade inibidora de NFκB estava reduzido em células resistentes a agentes alquilantes (Bredel et al., 2006). Entretanto, o papel específico de NFκB no controle do crescimento de células de glioma e o potencial de inibidores de NFκB não foi avaliado.

### I.5 - Leucemias

A leucemias são tumores não-sólidos originários de transformações em células precursoras da linhagem hematopoiética, se caracterizando pelo acúmulo destas na medula óssea, interferindo, assim, com a produção de hemácias, linfócitos, neutrófilos e plaquetas (Cramer e Hallek, 2012). Embora originário na medula óssea, as células tem um significante poder metastático,

sendo as metástases hepáticas, renais, linfonodais e cerebrais as mais frequentes. Dividem-se em dois grupos principais, dependendo dos precursores hematopoiéticos afetados: Linfocítica ou Mielóide. Além disso, podem se apresentar de forma aguda ou crônica: Leucemia linfoide Aguda (LLA); Leucemia Linfóide crônica (LLC); Leucemia Mielóide Aguda (LMA); Leucemia Mielóide Crônica (LMC); cada uma com alterações genéticas (mutações e aberrações cromossômicas) bastante particulares (Sison e Brown, 2011; Cramer e Hallek, 2012).

Três maiores formas de tratamento (excluindo a terapia celular) estão correntemente disponíveis em onco-hematologia: quimioterpia convencional, inibidores da transdução de sinal, e anticorpos monoclonais (Cramer e Hallek, 2012). Enquanto a terapia com quimioterápicos clássicos se utiliza das combinações entre diferentes fármacos na tentativa de aumentar a sobrevida, os tratamentos com inibidores de transdução de sinal são direcionados pelos resultados citogenéticos e caracterização molecular das hemopatias (Cramer e Hallek, 2012; Skorski, 2012). Diferente dos gliomas, as leucemias são um dos melhores exemplos da terapia com inibidores de transdução de sinal. Em LMC e LLA Ph+, a translocação t(9;22)(q34;q11), que forma o conhecido cromossomo Philadelphia (Ph), a proteína oncogênica de fusão Brc-Abl têm sido tratados com grande eficácia por inibidores tirosina cinases (TKI) como o Imatinib (Gleevec®, STI571), com resultados extremamente satisfatórios (Orlowsky et al, 2002; Skorski, 2012).

Células hematopoiéticas malignas são também caracterizadas pela expressão diferencial de clusters de diferenciação (CD) na superfície celular. Anticorpos monoclonais contra diferentes CD, como o Rituximab (anti-CD20),

estão sendo desenvolvidos para tratamentos de leucemias e encontram-se em estudos clínicos de fase I/II, assim como novos TKI (Cramer e Hallek, 2012). Em LLA de células T, mutações ativadoras da via de sinalização NOTCH1 constituem-se a anormalidade genética mais frequente. Consequentemente, tais células são resistentes aos tratamentos com inibidores de γ-secretase, os quais deveriam bloquear NOTCH1 (ex: MRK-003). Alternativamente, a utilização de inibidores da via PI3K/Akt/mTOR tem sido considerada, uma vez que a via é ativa em diversos tumores (Nefedova, 2003; Skorski, 2012). Entretanto, os resultados ainda são bastante insipientes.

Em LLC tem sido demonstrado um crescente número de evidências apontando para a via de sinalização das proteínas Wnt, as quais, assim como NOTCH1 e mTOR ,colaboram em alguns tipos de câncer e também parecem ter um papel em neoplasias de linfócitos B (Nishikori, 2003). Wnt aparece super-expressa nesse tipo de neoplasia e colabora com a ativação downstream da via de Beta-catenina, a qual coopera com a ativação de LEF-1 (lymphoid enhancer binding factor-1). LEF-1 é conhecido por estar até 3000 vezes aumentado em LLC. Entretanto, o uso de inibidores da via de β-catenina, embora afete a proliferação de células tumorais, tem sido questionada tanto na sua eficácia quanto na segurança (Nishikori, 2003).

Alguns membros da família NFκB já foram identificados em translocações cromossomais em neoplasias linfoides. Bcl3 foi identificado em uma translocação recorrente de LLC de células B (B-LLC) (Ohno et al., 1990 e 1993; MacKeithan et al., 1997). Bcl3 também está superexpresso em translocações t(2 ; 5)+ de linfomas anaplásicos de células T (Nishikori, 2003). Por outro lado, anormalidades em RelA são raras (Reyet e Gelinas, 1999) ao

passo que amplificações no gene de C-REL são frequentes em linfomas (Houldsworth et al., 1996; Goff et al., 2000; Martin-Subero et al., 2002).

Linfoma Hodgkin (LH) foi primeira neoplasia caracterizada pela ativação aberrante da via de NFκB, servindo como modelo para muitos estudos que analisaram as desregulações nesta via de sinalização (Bargou et al., 1996). Enquanto c-REL é a forma de NFκB ativada em linfomas de células B, LH apresentam desregulação no complexo RelA/p50. Expressão de LMP-1 (EBV-encoded latent protein) em células infectadas com o vírus Epstein-Barr (EBV) aumenta atividade de IKK (Krappman et al., 1999), e induz expressão funcional do receptor ativador de NFκB, RANK (Fiumara et al., 2001). Além disso, estima-se que 10-25% dos casos de LH sejam atribuídos a mutações em IκB-α (Cabannes et al., 1999); mutações em IκBe também foram descritas em alguns sub-grupos de pacientes (Emmerich et al., 2003).

Em mielomas, ativação de NFκB é mediada pela interação com outros elementos do microambiente da medula óssea. Interação com osteoclastos, citocinas, fatores de crescimento (IL-6, IGFs, IL-1 α, IL-1 β, IGF, VEGF, Stromal-derived growth factor (SDF-1), além do TNF-α e membros da família NOTCH liberados pelas células-tronco de medula e células do próprio mieloma, ativam NFκB (Chauhan et al., 1996; Mitsiades et al., 2004; Nefedova et al., 2004).

### I.6 - Estudos clínicos com inibidores de NFκB

Considerando que o crescimento de dados sobre a relação entre NFκB e câncer é recente, a primeira e única droga com ação inibitória de NFκB a ser testada e aprovada pelo FDA em estudos clínicos foi o bortezomib (ácido

borônico-*N*-pirazinacarbonil-L-fenilalanina-L-leucina). O Bortezomib inibe a degradação proteassomal de IκB ubiquitinada através do bloqueio da subunidade 20S do proteassoma. Em estudos multicêntricos de fase 2, aproximadamente 1/3 dos pacientes com mieloma avançado responderam positivamente (completamente ou parcialmente) ao bortezomib. Além disso, os efeitos adversos relatados foram gastrointestinais, fadiga, trombocitopenia e neuropatia sensorial, as quais foram bem toleradas. Outros estudos têm avaliado o efeito do bortezomib tanto em neoplasias sólidas e hematológicas em pacientes refratários ou que desenvolveram resistência ao longo do tratamento (Adams et al., 1999).

A utilidade clínica da inibição de NFκB em pacientes resistentes tem sido amparada pelos experimentos in vitro, uma vez que o tratamento de linhagens celulares de leucemia mielóide crônica (LMC) com PS1145, um inibidor de IKK (IκB cinase), quebrou a resistência celular e induziu apoptose em linhagens resistentes ao fármaco de escolha ao Imatinib (Cilloni et al., 2006 e 2007).

# II - OBJETIVOS

## II. OBJETIVOS

### Objetivo geral

O objetivo geral desta tese foi determinar o papel do fator de transcrição NFκB nos processos de sobrevivência celular, e avaliar o potencial terapêutico da inibição desta via de sinalização em modelos tumorais e de estresse celular.

### Objetivos específicos:

1) Determinar o papel de NFκB como modulador da resposta celular anti-apoptótica e proliferativa através do controle da produção de espécies reativas de oxigênio (ERO) e da ativação de vias de sinalização redox-sensíveis.

2) Determinar os imunoconteúdos e os níveis de ativação basal de NFκB em células tumorais e em células-não transformadas de mesma origem histológica.

3) Avaliar os efeitos citotóxicos e os mecanismos de ação dos inibidores farmacológicos de NFκB em células tumorais comparado às células sadias.

4) Avaliar a potencial de utilização dos inibidores de NFκB em terapia adjuvante com antitumorais clássicos.

5) Determinar o papel de NFκB na quimiorresistência, e avaliar a utilização dos seus inibidores na reversão de tal fenômeno.

6) Avaliar possíveis mecanismos envolvidos na resposta celular à inibição de NFκB.

7) Determinar o potencial in vivo da inibição farmacológica de NFκB em modelo animal de glioma.

# III – ARTIGOS CIENTÍFICOS

II.1 – Artigo 1

# The NF kappa B-mediated control of RS and JNK signaling in vitamin A-treated cells: duration of JNK-AP-1 pathway activation may determine cell death or proliferation.

Biochemical Pharmacology 2009; 77(7): 1291-1301.

doi:10.1016/j.bcp.2008.12.010

BIOCHEMICAL PHARMACOLOGY 77 (2009) 1291–1301

available at www.sciencedirect.com

ScienceDirect

journal homepage: www.elsevier.com/locate/biochempharm

# The NFκB-mediated control of RS and JNK signaling in vitamin A-treated cells: Duration of JNK–AP-1 pathway activation may determine cell death or proliferation

*Alfeu Zanotto-Filho*, Daniel P. Gelain, Rafael Schröder, Luís F. Souza, Matheus A.B. Pasquali, Fábio Klamt, José Cláudio F. Moreira*

*Centro de Estudos em Estresse Oxidativo, Departamento de Bioquímica, Instituto de Ciências Básicas da Saúde, Universidade Federal do Rio Grande do Sul, Porto Alegre, Rio Grande do Sul, Brazil*

ARTICLE INFO

*Article history:*
Received 2 December 2008
Accepted 22 December 2008

*Keywords:*
Retinol
NFκB
Oxidative stress
JNK1/2
AP-1

ABSTRACT

Nuclear factor kappa B (NFκB) has emerged as a crucial regulator of cell survival, playing important functions in cellular resistance to oxidants and chemotherapeutic agents. Recent studies showed that NFκB mediates cell survival through suppression of the accumulation of reactive species (RS) and a control of sustained activation of the Jun-N-terminal kinase (JNK) cascade. This work was undertaken in order to evaluate the role of NFκB in modulating the pro-oxidant effects of supplementation with vitamin A (retinol, ROH) in Sertoli cells, a major ROH physiological target. In this work, we reported that ROH treatment increases mitochondrial RS formation leading to a redox-dependent activation of NFκB. NFκB activation played a pivotal role in counteract RS accumulation in ROH-treated cells, since NFκB inhibition with DNA decoy oligonucleotides or pharmacological inhibitors (BAY-117082) potentiated ROH-induced RS accumulation and oxidative damage. In the presence of NFκB inhibition, ROH-induced oxidative stress promoted a prolonged activation of the JNK–activator protein 1 (AP-1) pathway and induced significant decreases in cell viability. Inhibition of JNK–AP-1 with decoy oligonucleotides to AP-1 or JNK inhibitor SP600125 prevented the decreases in cell viability. Antioxidants blocked the persistent JNK–AP-1 activation, cell oxidative damage, and the decreases in cell viability induced by NFκB inhibition. Finally, our data point superoxide dismutase (SOD)2 as a potential antioxidant factor involved in NFκB protective effects against ROH-induced oxidative stress. Taken together, data presented here show that NFκB mediates cellular resistance to the pro-oxidant effects of vitamin A by inhibiting RS accumulation and the persistent and redox-dependent activation of JNK–AP-1 cascade.



## 1. Introduction

Reactive species (RS) are implicated on the modulation of both proliferation and apoptosis events depending on stimuli and on cell type [1]. High and persistent RS production is frequently related to cell death by inducing extensive oxidative damage to cellular components, whereas low oxidant levels are associated with proliferative events [1]. In this way, several studies have suggested a dualistic effect of mitogen-activated protein kinases (MAPKs) and transcription

* *Corresponding author*. Departamento de Bioquímica (ICBS-UFRGS), Rua Ramiro Barcelos, 2600/Anexo, CEP 90035-003, Porto Alegre, Rio Grande do Sul, Brazil Tel.: +55 51 3316 5578; fax: +55 51 3316 5535.
E-mail address: ohalceu@yahoo.com.br (A. Zanotto-Filho).
0006-2952/$ – see front matter 
doi:10.1016/j.bcp.2008.12.010

factors as nuclear factor kappa B (NFκB) and activator protein 1 (AP-1) in oxidative stress environments, since they may induce both proliferation or death depending on persistence of their activation, and this transient or persistent activation is directly related to duration of oxidative insult [2–4]. In pro-oxidant environments, rapid and transient activation of MAPKs as Jun-N-terminal kinase (JNK)1/2 and extra cellular signal-regulated kinase (ERK)1/2 are frequently reported mediating proliferative events [1,4,5], whereas a prolonged activation may promote cell death [2–4]. Thus, cells need to orchestrate the balance between its pro-oxidant and anti-oxidant factors in order to counteract RS production and oxidative damage, avoiding the persistent activation of some redox-sensitive pathways, and finally promoting resistance/adaptation to pro-oxidant environments [5–7]. In this context, activation and/or expression of antioxidant enzymes as superoxide dismutases (SOD1/2), catalase and glutathione peroxidases, and the synthesis of non-enzymatic antioxidants as glutathione play important roles in keeping the intracellular redox balance thus preventing the persistence of oxidative stress and the extensive cell damage [6,7]. The ability of transcription factors as NFκB in modulating anti-apoptotic and antioxidant genes as SOD2 (mitochondrial SOD), ferritin heavy chain, glutathione S-transferase, inhibitor of apoptosis proteins (IAPs), and caspase 8 homologue FLICE-inhibitory protein (c-FLIP) [6,8–10], which ultimately lead to cellular resistance to oxidative stress and death inductors agents, have addressed NFκB as a important factor involved on cellular resistance to oxidants and chemotherapeutic drugs [8–10].

Our previous studies have demonstrated the pro-oxidant effects of vitamin A supplementation in rats and in cultured cells [11–15]. In Sertoli cells, a major physiological target of ROH in mammalian, treatment with ROH induces an interesting effect; incubation of Sertoli cells with ROH increases RS production and stimulates proliferation through a transient and redox-dependent activation of the JNK1/2 pathway [15]. Antioxidant treatment blocks ROH-induced RS production, JNK1/2 activation, and proliferation, suggesting a mechanism mediated by oxidants. The investigation of potential sites of RS indicates that ROH leads to impairment on electron transfer system causing a significant increase in mitochondrial superoxide production [15]. Thus, it is comprehensible that attenuation of the intracellular RS accumulation, significantly in mitochondria, was involved in the control of RS levels and in triggering Sertoli cells to a redox-mediated proliferation and not to a cell death pathway following ROH treatment in our experimental model.

Since NFκB is an important factor in resistance to oxidative stress [6,8–10], this work was undertaken in order to evaluate the involvement of this transcription factor in modulating ROH pro-oxidant effects in cultured Sertoli cells. The results show that a redox-dependent activation of NFκB lead to increases in manganese SOD (SOD2) activity and reduction of RS accumulation in ROH treatment. Inhibition of NFκB increased ROH-induced RS accumulation at later time points of incubation (6–24 h), and it induced extensive oxidative damage and persistent activation of JNK1/2–AP-1 cascade, which promoted significant decreases in cell viability. Data suggest that NFκB modulates the levels of RS, the duration of the JNK1/2-AP1 pathway activation, and the cell fates during a vitamin A-induced oxidative stress.

## 2. Methods and materials

### 2.1. Materials

All-*trans* retinol alcohol (retinol, ROH), 2′,7′-dichlorohydrofluorescein diacetate (DCFH-DA), 3-(4,5-dimethyl)-2,5-diphenyl tetrazolium bromide (MTT), *N*-acetyl-L-cysteine (NAC), (E)-3-(4-methylphenylsulfonyl)-2-propenenitrile) (BAY-117082), (±)-6-hydroxy-2,5,7,8-tetramethylchromane-2-carboxylic acid (Trolox), rotenone, Nonidet P-40, dithiothreitol, 2-thiobarbituric acid (TBA), anti-phospho-JNK1/2 (Thr 183/ Tyr 185), anti-JNK2, anti-β-actin, anti-β-tubulin antibodies, and culture analytical grade reagents were from Sigma Chemical Co. (St. Louis, MO, USA). Anti-SOD2, anti-p65, and anti-lamin B antibodies were from Santa Cruz Biotechnologies (Santa Cruz, CA, USA). SP600125 was from Promega Corporation (Madison, WI, USA), anti-c-Fos antibody was from Calbiochem (San Diego, CA, USA), and electrophoresis/immunoblotting reagents were from Bio-Rad Laboratories (Hercules, CA, USA). DNA oligonucleotides were synthesized by The Midland Certified Reagent Company, Inc. (Midland, TX, USA).

### 2.2. Sertoli cells cultures

Sertoli cells were isolated as previously described [15]. Briefly, testes of 15-day-old rats were removed, decapsulated, and digested enzymatically with trypsin for 30 min at 37 °C, and centrifuged at 750 × *g* for 5 min. The pellet was mixed with soybean trypsin inhibitor, then centrifuged and incubated with collagenase, hyaluronidase and deoxyribonuclease for 30 min at 37 °C. After centrifugation (10 min at 40 × *g*), the pellet was taken to isolate Sertoli cells. Cells were plated in multi-well plates ($2.1 \times 10^5$ cells/cm$^2$, 80% confluence) in Medium 199, pH 7.4, 1% FBS, and maintained in a humidified atmosphere at 34 °C for 24 h to attach. The medium was then changed to serum-free medium and cells were taken for assays after 48 h of culture. ROH and inhibitors were dissolved in dimethylsulphoxide (DMSO), and solvent controls were performed for each condition.

### 2.3. Sodium dodecyl sulfate polyacrylamide gel electrophoresis (SDS-PAGE) and immunoblot

Proteins (20 μg) were separated by SDS-PAGE on 10% (w/v) acrylamide, 0.275% (w/v) bisacrylamide gels and electrotransferred onto nitrocellulose membranes. Membranes were then incubated in Tris-buffered saline Tween-20 [TBS-T; 20 mM Tris–HCl, pH 7.5, 137 mM NaCl, 0.05% (v/v) Tween 20] containing 1% (w/v) non-fat milk powder for 1 h at room temperature. Subsequently, the membranes were incubated for 12 h with the appropriate primary antibody. After washing in TBS-T, blots were incubated with horseradish peroxidase-linked anti-immunoglobulin G (IgG) antibodies for 1.5 h at room temperature. Chemiluminescent bands were detected, and densitometric analysis was performed by Image-J® software.

### 2.4. Nuclear and cytoplasmic extracts preparation

To prepare nuclear extracts, $2.7 \times 10^6$ cells were collected by centrifugation 750 × *g* for 5 min, and resuspended in 300 μl of hypotonic buffer consisting of 10 mM HEPES (pH 7.9), 1.5 mM $MgCl_2$, 10 mM KCl, 0.2 mM phenylmethylsulfonyl fluoride, 0.5 mM dithiothreitol, 1 μg/ml pepstatin A, 1 μg/ml leupeptin and incubated in ice for 15 min. Later, 12 μl of 10% Nonidet P-40 was added and the swollen cells were disrupted by vortexing (15 seg). Nuclei were isolated by centrifugation 14,000 × *g* for 30 s, and pellet (intact nuclei) and supernatant (cytoplasmic) fractions were separated. Nuclear fraction was resuspended in 70 μl of high salt buffer [10 mM HEPES (pH 7.9), 0.42 M NaCl, 1.5 mM $MgCl_2$, 10 mM KCl, 1 mM phenylmethylsulfonyl fluoride, 1 mM dithiothreitol, 1 μg/ml pepstatin A, 1 μg/ml leupeptin], and incubated for 40 min in ice bath releasing soluble proteins from the nuclei. After extraction, the nuclei debris (insoluble fraction) was removed by centrifugation 14,000 × *g* for 10 min, and supernatant containing soluble nuclear proteins was stored at −80 °C until experiments.

### 2.5. Electro-mobility shift assay (EMSA)

To determine NFκB and AP-1 DNA-binding activity, biotin 3'end-labeled AP-1 and NFκB oligonucleotide consensus sequence were carried out by EMSA. Briefly, oligonucleotide consensus sequences were labeled with biotin-ddUTP in accordance with manufacturer instructions (LightShift Chemiluminescent EMSA kit, Pierce, Rockford, IL, USA). In binding reactions, 20 μl of reaction mixture comprising 15 mM HEPES (pH 7.9), 1 mM dithiothreitol, 2.5 mM ethylenediaminetetraacetic acid (EDTA), 5 mM $MgCl_2$, 2.5% glycerol and 50 ng/μl poly (dI·dC), 5 μg of nuclear extracts, and 30 fmol of biotin-3'end-labeled DNA probes were incubated for 30 min in ice bath. Nucleo-protein complexes were loaded onto the pre-electrophoresis 5.5 % non-denaturing polyacrylamide gels in 0.5× Tris–boric acid–EDTA buffer (TBE) and run at 120 V. The electrophoresed binding reactions were electrotransferred (100 mA for 3 h) in 0.5× TBE to a nylon membrane positively charged in ice-cold bath. The biotin-ddUTP 3'end-labeled DNA probe was cross-linked with ultraviolet-C (UVC) exposure for 15 min and detected using streptavidin–horseradish peroxidase conjugated. The membranes were exposed to X-ray film for 1–5 min to obtain the adequate signal.

### 2.6. Determination of intracellular RS production [real-time dichlorofluorescein (DCF) assay]

Intracellular RS production was detected using DCFH-DA [16]. This reagent enters the cells and reacts predominantly with highly oxidizing species of RS such as hydroxyl radicals (•OH), hydroperoxides, and peroxynitrite, thus producing the fluorophore DCF. Briefly, cells were seeded in 96-well plates and 25 μM DCFH-DA dissolved in medium containing 1% fetal bovine serum (FBS) was added to the cell culture 30 min before ROH/RA incubation to allow cellular incorporation. Then, the medium was discarded and cells were treated in complete medium. The DCFH oxidation was monitored with 5 min interval at 37 °C in a 96-well plate fluorescence reader with an emission wavelength set at 535 nm and an excitation wavelength set at 485 nm.

### 2.7. Decoy targeting to NFκB and AP-1

To decoy experiments, double-stranded oligonucleotide decoy (dsODN) to NFκB and AP-1were prepared by annealing of sense and antisense oligonucleotides in vitro in 1× annealing buffer (20 mM Tris–HCl, pH 7.5, 20 mM $MgCl_2$, and 50 mM NaCl). The mixture was heated at 95 °C for 2 min and allowed to cool to room temperature slowly over 6 h [17]. These oligonucleotides are specifically designed to bind NFκB and AP-1 factors and are used to dampen the content of these factors within the cell. Cells were transfected with dsODN–liposome complexes containing 2 μg/ml dsDNA and 8.3 μl/ml lipofectamine for 6 h at 37 °C, 5% $CO_2$ before exposing them to the different treatments. The sequence oligonucleotide decoy to NFκB and AP-1 used was (1) NFκB consensus sequence: 5'-CGACACCCCTCGGGAATTCCCCCACTGGGCC-3', 3'-GCTGTGGGGAGCCCTTAAGGGGGTGACCCGG-5' and (2) AP-1 consensus sequence: 5'-TGACACACATTAGTCACATATTAAT-3', 3'-ACTGTGTGTAATCAGTGTATAATTA-5'. A non-related oligonucleotide sequence Oct2A (5'-AGCTTAGGGCTCGTTGACGTCTCCAAG-3') was used as control. In preliminary experiments, we confirmed the ability of NFκB or AP-1 decoy ODNs to block, respectively, NF(B or AP-1DNA binding activities. Oct2A did not alter NFκB or AP-1 pathways.

### 2.8. MTT assay

Cell viability was estimated by the quantification of the MTT reduction to a blue formazan product by cellular dehydrogenases [15]. At the end of treatments, the medium was discarded and a new medium containing 0.5 mg/ml MTT was added. The cells were incubated for additional 30 min at 37 °C. After the medium was removed, cells were washed three times with phosphate buffered saline, and DMSO was added for 10 min. Formazan salt formation was determined at 560 nm. Data were expressed as percentage of formazan formation in untreated cells.

### 2.9. Thiobarbituric acid reactive species (TBARS)

As an index of lipid peroxidation, we used the formation of TBARS during an acid-heating reaction, which is widely adopted for measurement of lipid redox state, as previously described [18]. Briefly, 300 μl cell extracts were mixed with 600 μl of 10% trichloroacetic acid (TCA) and 0.5 ml of 0.67% TBA, and then heated in a boiling water bath for 25 min. TBARS were determined in spectrophotometer at 532 nm. Results are expressed as TBARS/mg protein.

### 2.10. SOD2 activity

To measure manganese SOD2 activity, NaCN was added to the reaction mix at a final concentration of 2 mM and incubated for 30 min. High concentrations of cyanide (1–2 mM) were reported to inhibit SOD1 up to 97–99% at pH 10.00 [19]. SOD2 activity was assessed by quantifying the inhibition of the superoxide-dependent adrenaline auto-oxidation at pH 10.2 in

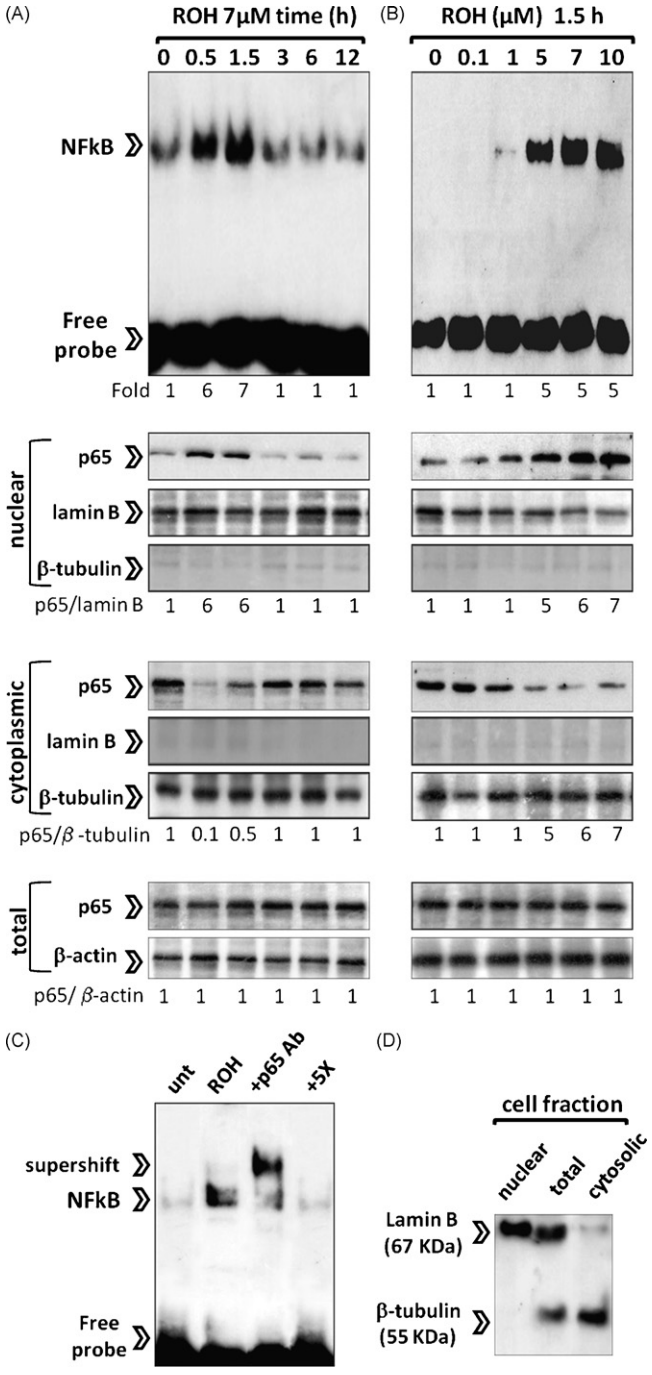


**Fig. 1 – NFκB activation in ROH-treated Sertoli cells. Cells were treated with 7 μM ROH for different times and NFκB DNA-binding activity or p65 immunocontent in cell subfractions was determined. (A) Time-course effect of 7 μM ROH in NFκB DNA-binding activity and p65 protein translocation. (B) Effect of different ROH concentrations (μM) on NFκB binding and p65 translocation. Cells were treated for 1.5 h, and cell extracts were isolated for EMSA or immunoblotting. (C) Supershift and competition assays for NFκB. In binding reactions, nuclear extracts of 7 μM ROH-treated cells were pre-incubated with 0.01 μg anti-p65 NFκB antibody (+p65 Ab lane) or 5× excess of an unlabeled NFκB oligonucleotide (+5× lane) for 15 min prior labeled oligonucleotide addition. Later, EMSA were performed. (D) For control of the purity of nuclear and cytoplasmic fractions, proteins were separated by SDS/PAGE and blots were incubated with a solution containing anti-lamin B (1:1000) and anti-β-tubulin (1:1000) antibodies. Legends: unt, untreated; ROH, retinol; +5×, nuclear extracts of ROH-treated cells plus five-fold excess of unlabeled NFκB oligonucleotides; +p65 Ab, ROH-treated extracts +p65 Ab, supershift. Representative of four independent experiments ($n = 4$).**

a 0.1 M glycine–NaOH buffer in spectrophotometer at 480 nm, as previously described [20]. The results are expressed as U SOD2/mg protein.

### 2.11. Cell proliferation assay

[Methyl-$^3$H] thymidine incorporation was assessed as indicative of the DNA synthesis and proliferation rate in Sertoli cells [15]. At 24 h prior ROH treatment, cells were pre-warmed with 0.5 μCi/ml [methyl-$^3$H] thymidine (248 GBq/mmol; Amersham, UK). After the medium was removed and cells were treated. After treatments, 1 μCi/ml of [methyl-$^3$H] thymidine diluted in medium was added for additional 18 h. After DNA precipitation, scintillant liquid was added, and incorporated radionucleotide was measured using a Packard Tri-Carb Model 3320 scintillation counter.

### 2.12. Protein quantification

Protein contents of each sample were measured by Lowry method [21].

### 2.13. Statistical analysis

Data are expressed as means ± SD and were analyzed by one-way analysis of variance (ANOVA) followed by Duncan's post-hoc test. Differences were considered significant at $p < 0.05$.

## 3. Results

### 3.1. ROH induces redox-dependent NFκB activation

Cells were incubated for different times (h) with 7 μM ROH, and NFκB-binding activity was evaluated by EMSA. Fig. 1A shows that ROH induced a transient increase in NFκB DNA-binding activity. NFκB activation occurred as early as 0.5 h after ROH incubation, continued for up to 1.5 h, and decreased at 3 h. The increase in NFκB activity was accompanied by a time-related translocation of the NFκB subunit p65 from cytoplasm to nucleus of 7 μM ROH-treated cells (Fig. 1A). Total p65 protein immunocontent was unaltered by 7 μM ROH treatment. Thus, a 1.5 h incubation period was used for subsequent experiments. We also tested the effect of different ROH concentrations on NFκB-binding activity and p65 translocation (Fig. 1B). Data show that NFκB activity and p65 translocation from cytoplasm to nuclear compartment were stimulated from 5 μM ROH; total p65 immunocontent remained unaltered (Fig. 2B). To give assay specificity, supershift analyses were performed by pre-incubating nuclear extracts from ROH-treated cells with

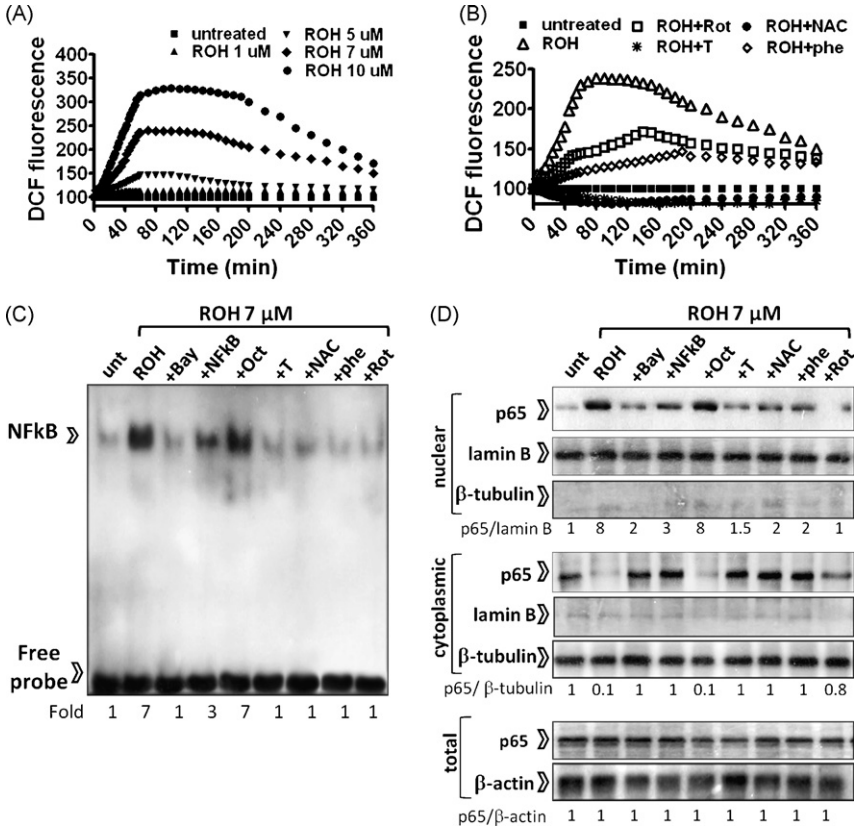


**Fig. 2 – ROH induces redox-dependent NFκB activation. (A) Representative experiment showing the time-course effect of different ROH concentrations on RS production in Sertoli cells. (B) Mitochondrial electron transfer inhibitor (rotenone) and RS scavengers inhibit RS-dependent DCFH oxidation. Cells were pre-incubated for 30 min with 5 μM rotenone, 100 μM phenantroline (iron chelator), N-acetylcysteine (NAC 1 mM), or 50 μM Trolox (general antioxidant) prior 7 μM ROH addition, and DCF formation was monitored. (C and D) Effect of different antioxidants and classical NFκB inhibitors on (C) NFκB-binding activity and (D) p65 immunocontent in subcellular fractions. For experiments presented in (C) and (D), cells were pre-treated with antioxidants and NFκB inhibitors for 30 min prior 7 μM ROH addition, and cellular extracts were isolated after 1.5 h of incubation with ROH. Legends: ROH, retinol (7 μM); Rot, rotenone; NAC, N-acetylcysteine; T, Trolox; Bay, BAY-117082 (10 μM); +NFκB, NFκB decoy; +Oct, Oct2A decoy; phe, phenantroline. Representative of three independent experiments (*n* = 3).**

purified anti-p65 NFκB antibody. The presence of supershift following p65 antibody incubation (+p65 Ab lane), and the absence of shift in competition assays with five-fold excess of unlabeled NFκB oligonucleotides (+5× lane) confirmed that shifted band visualized on EMSA are indeed due to the binding of NFκB proteins (Fig. 1C). The purity of cytoplasmic and nuclear lysates was confirmed by the absence of β-tubulin immunoreactivity in the soluble nuclear proteins isolated for EMSA, and the absence of lamin-B in cytoplasmic extracts. In whole lysates, immunoreactivity for both β-tubulin and lamin-B was observed (Fig. 1D). β-Actin was used as loading control to total cell lysates.

Next, we evaluated whether ROH-induced NFκB activation involved alterations in intracellular redox state. ROH induced a rapid (within 15 min) and dose-dependent (5–10 μM) increase in RS production as assessed by DCF assay (Fig. 2A). Pre-incubation of cells with RS scavengers as NAC (1 mM), Trolox (50 μM), phenantroline (50 μM) attenuated 7 μM ROH-induced RS production (Fig. 2B), NFκB-binding activity (Fig. 2C) and p65 nuclear translocation (Fig. 2D). We also tested the effect of the mitochondrial electron transport inhibitor rotenone (5 μM), which we previously showed to inhibit RS production and MAPKs activation in ROH treatment [11]. Rotenone pre-treatment not only blocked RS formation (Fig. 2B), but also prevented NFκB activation and p65 translocation into nucleus (Fig. 2C and D).

Finally, we use decoy ODNs to NFκB, and the IκB kinase (IKK) inhibitor BAY-117082 (10 μM) in order to specifically inhibit NFκB. DNA decoy and BAY-117082 inhibited 7 μM ROH-induced NFκB-binding activity (Fig. 2C) and p65 translocation from cytoplasm to nucleus (Fig. 2D). Decoy with a non-related sequence Oct2A did not alter the pattern of ROH induced NFκB.

### 3.2. *NFκB inhibition induces persistent RS production, potentiates oxidative damage, and promotes decreases cell viability in ROH-treated cells*

Incubation of Sertoli cells with 7 μM ROH increased RS formation as showed in Fig. 2A. The increase in RS started at early time points (10 min), reached a plateau between 1 and

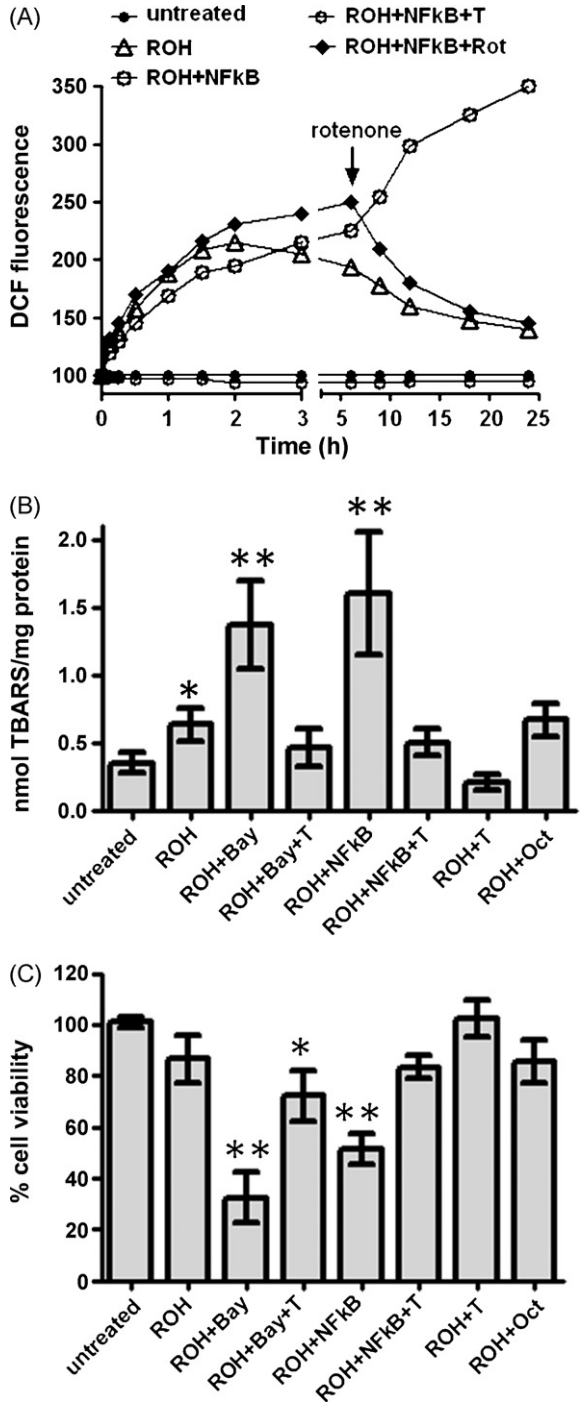


**Fig. 3 – NFκB inhibition potentiates ROH-induced oxidative stress leading to decreases in cell viability. (A) Representative experiment showing the time-course effect of NFκB inhibition on 7 μM ROH-induced RS formation in Sertoli cells. Cells were pre-incubated with NFκB inhibitors prior ROH addition and DCF fluorescence was monitored at different times. (B) NFκB inhibition potentiates ROH-induced lipoperoxidation. Damage to lipids was assessed by TBARS assay at 24 h after 7 μM ROH addition. (C) NFκB inhibition induces decreases in cell viability following 7 μM ROH treatment. Legends: ROH, retinol (7 μM); T, Trolox; Bay, BAY-117082 (10 μM); NFκB, NFκB decoy; Oct, Oct2A decoy. *Different from untreated cells, **different from untreated and from ROH-treated cells. Representative of three experiments ($n = 3$).**

3 h treatment, and decreased after 6 h to levels approximately 1.4-fold higher than that observed in untreated cells (Fig. 2A). Pre-treatment of cells with NFκB decoy ODNs – which ultimately lead to NFκB inhibition as showed in Fig. 2C – or BAY-117082 induced a prolonged increase in RS formation following 7 μM ROH treatment (Fig. 3A). At 6–24 h ROH treatment, RS production was approximately 3.5-fold higher in the presence of NFκB inhibitors. In some experiments, the addition of the electron transfer chain inhibitor rotenone (5 μM) at 6 h attenuated ROH-induced RS accumulation in the presence of decoy ODNs to NFκB, suggesting an involvement of mitochondria on RS accumulation. The NFκB inhibitors BAY-117082 and decoy ODNs alone did not present effects on RS production and oxidative damage (not shown).

In agreement, NFκB inhibition with BAY-117082 or DNA decoy potentiated 7 μM ROH-induced lipoperoxidation at 24 h as assessed by TBARS assay (Fig. 3B). Pre-treatment with the RS scavenger Trolox, besides to block RS formation (Fig. 2B), blocked the increase in TBARS levels in both ROH and ROH plus NFκB inhibitor groups, confirming a redox mechanism (Fig. 3B). Data obtained from MTT assay show that 7 μM ROH alone did not decrease cell viability at 24 h treatment, but the presence of NFκB inhibition with BAY-117082 or NFκB decoy induced significant decreases in cell viability following ROH treatment (Fig. 3C). BAY-117082 (10 μM) or DNA decoy ODNs alone did not alter cell viability or lipoperoxidation (not shown). Again, pre-treatment with Trolox prevented the decrease in viability. Taken together, these data suggest a protective role of NFκB against ROH-induced oxidative stress.

### 3.3. *NFκB inhibition induces persistent activation of JNK1/2–AP1*

In previous studies, we reported that a transient and redox-dependent activation of JNK1/2 mediates the proliferative effects of ROH in Sertoli cells [15]. The aforementioned data showed that NFκB inhibition potentiates RS production and oxidative damage in ROH-treated cells. In addition, NFκB inhibition decreased cell viability in ROH treatment. Thus, we decided to test whether the decreases in cell viability could be related to a prolonged stimulation of JNK1/2 pathway during the persistent oxidative stress observed in presence of NFκB inhibitors as previously reported in other studies [2,22]. Treatment with 7 μM ROH alone induced a rapid and transient increase in JNK1/2 phosphorylation (Fig. 4A). JNK1/2 phosphorylation (i.e. activation) increased at 15 min, continued up to 2 h, and decreased to basal levels at 3 h up to 24 h treatment. In agreement, 7 μM ROH induced a transient increase in DNA-binding activity of transcription factor AP-1. AP-1 activation occurred as early as 1.5 h, continued up to 3 h, and decreased to basal levels at 6 h treatment (Fig. 4B).

NFκB inhibition changed the pattern of JNK1/2 and AP-1 activation from a transient to a prolonged time profile in 7 μM ROH-treated cells (Fig. 4A and B, respectively). JNK1/2 phosphorylation and AP-1-binding activity remained

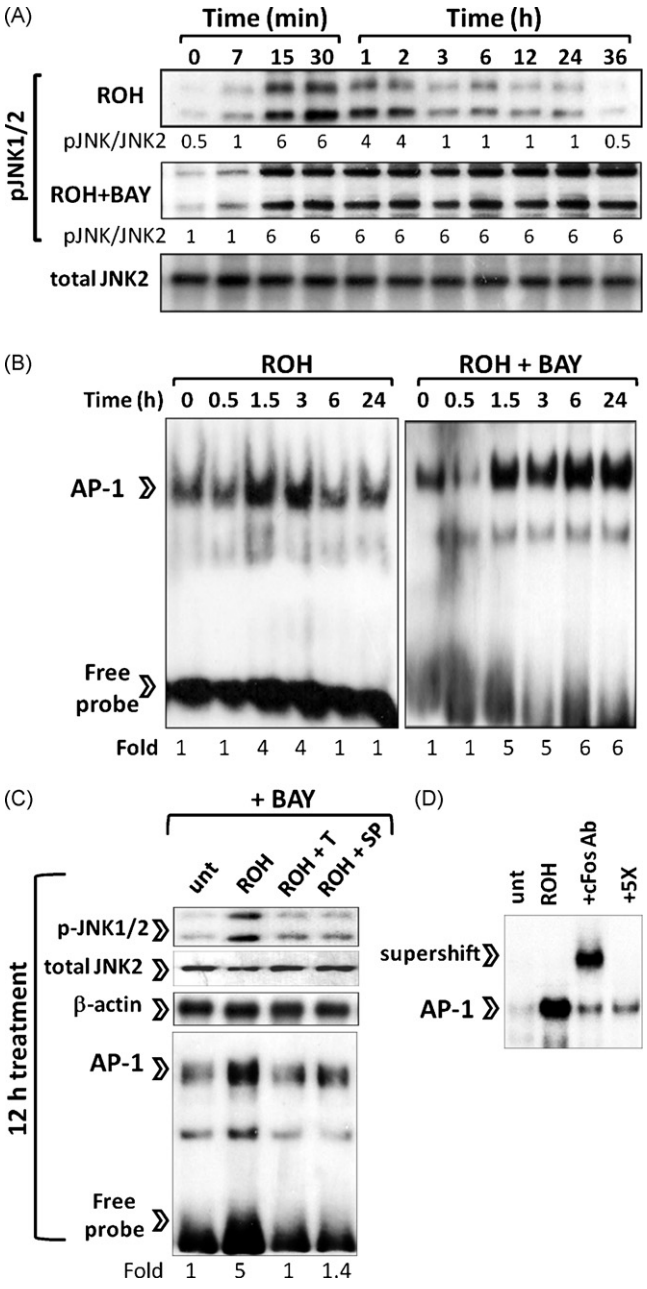


**Fig. 4 – NFκB inhibition induces persistent activation of JNK–AP-1 in ROH treatment. (A) Time-course effect of 7 μM ROH on JNK1/2 phosphorylation in Sertoli cells in the presence or absence of the NFκB inhibitor BAY-117082 10 μM. (B) Time-course effect of 7 μM ROH on AP-1 DNA-binding activity in the presence of absence of NFκB inhibition. (C) Effect of 50 μM Trolox and JNK1/2 inhibitor SP600125 (10 μM) on 7 μM ROH plus 10 μM BAY-117082-induced persistent AP-1 activation. Cells were pre-treated with BAY-117082 for 30 min, after 7 μM ROH plus Trolox or SP600125 was added, and cells were incubated for additional 12 h. Nuclear extracts were isolated and EMSA were performed. (D) Supershift and competition assays for AP-1. In binding reactions, nuclear extracts of 7 μM ROH-treated cells were pre-incubated with 0.01 μg anti-cFos AP-1 subunit antibody (+cFos Ab lane) or 5× excess of an unlabeled AP-1 oligonucleotide sequence (+5× lane) for 15 min prior labeled AP-1 oligonucleotide addition. Legends: ROH, 7 μM retinol; T lanes, Trolox; SP lanes, 10 μM SP600125; BAY, 10 μM BAY-117082; +5×, five-fold excess of unlabeled AP-1 oligonucleotides; +cFos Ab, ROH + cFos antibody, supershift. Representative of three experiments (*n* = 3).**

increased up to 24 h treatment with ROH in the presence of DNA decoy to NFκB (not shown). The same pattern was observed with 10 μM BAY-117082 as NFκB inhibitor (Fig. 4A and B). Pre-treatment with a pharmacological JNK1/2 inhibitor (SP600125, 10 μM) inhibited AP-1 activation as assessed at 12 h incubation, suggesting that JNK1/2 mediates AP-1 activation (Fig. 4C). The presence of the antioxidant Trolox (50 μM) prevented the prolonged activation of JNK1/2 and AP-1 suggesting that the persistent activation of this pathway is mediated by RS (Fig. 4C). To confirm the specificity of EMSA to AP-1, we performed supershift to c-Fos (a major AP-1 subunit) and competition assays. The presence of a total shift following c-Fos antibody incubation (+cFos Ab lane), and the significant reduction of shifted band in competition assays with five-fold excess of unlabeled AP-1 oligonucleotide (+5× lane) confirmed that band on EMSA was indeed due to the binding of AP-1complexes (Fig. 4D).

### 3.4. *Persistent JNK–AP-1 pathway activation mediates the decreases in cell viability following treatment with ROH plus NFκB inhibitors*

The evaluation of cell viability showed that cytotoxic effects of treatment with NFκB inhibitors in combination with ROH were prevented by inhibiting JNK1/2–AP1 pathway activation with SP600125 or DNA decoy ODNs to AP-1 (Fig. 5A, see ROH + NFκ‴ B + AP-1 and ROH + NFκB + SP lanes), suggesting that the persistent JNK–AP-1 pathway activation observed in ROH plus NFκB inhibitors induce decreases in cell viability. DNA decoy to AP-1 in absence of NFκB inhibition (ROH + AP-1 lane) did not alter cell viability (Fig. 5A).

Finally, in absence of NFκB inhibitors, Sertoli cells proliferate following 7 μM ROH treatment (Fig. 5B), and DNA decoy to AP-1 or JNK1/2 inhibition with SP600125 attenuated ROH-induced proliferation. Thus, these data altogether suggest that a transient activation of the JNK–AP-1 pathway induces cell proliferation, whereas its prolonged activation induces cell death, and NFκB activation plays a key role in inhibiting persistent activation of JNK–AP-1 by attenuating RS accumulation and oxidative stress in ROH-treated cells.

### 3.5. *ROH induces NFκB dependent increases in mitochondrial SOD*

In our previous studies and here, we showed that mitochondria act as a primary source of RS in ROH-treated Sertoli cells [15]. Thus, it is plausible that the effects of NFκB in inhibiting prolonged RS formation and oxidative damage in our model could be related to modulation of mitochondrial oxidative stress. SOD2 (mitochondrial SOD) is a major mitochondrial antioxidant enzyme regulated through NFκB [8,9,23], and authors showed that retinoids could increase SOD2 in an

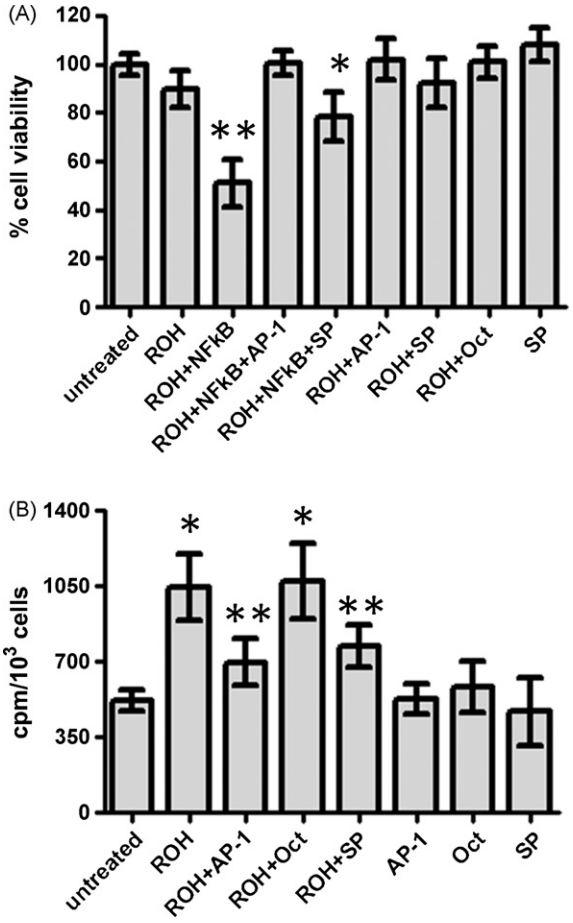


**Fig. 5 – Persistent JNK–AP-1 pathway activation mediates the decreases in cell viability following treatment with ROH plus NFκB inhibitors. (A) AP-1 DNA decoy and the JNK1/2 inhibitor SP600125 pre-treatment prevented the decrease in cell viability promoted by NFκB inhibition (NFκB decoy) in 7 μM ROH treatment. (B) ROH induces proliferation through of JNK–AP-1 pathway activation in the presence of NFκB signaling. Cell proliferation was assessed by radiolabeled thymidine incorporation after 24 h of 7 μM ROH incubation. Legends: ROH, retinol 7 μM; NFκB lanes, NFκB decoy; AP-1 lanes, AP-1 decoy; Oct, Oct2A decoy; SP lanes, SP600125 (10 μM). *Different from untreated cells, **different from untreated and from ROH-treated cells. Representative of three experiments ($n$ = 3).**

NFκB-dependent manner [8]. In our model, 7 μM ROH induced a dose-dependent increase in SOD2 activity and immunocontent as assessed after 24 h treatment (Fig. 6A). The evaluation of time-course effect of retinol upon SOD2 levels showed that treatment with 7 μM retinol increased SOD2 protein and activity as early as 6 h after retinol addition to Sertoli cells (not shown). Inhibition of NFκB with 10 μM BAY-117082 or DNA decoy ODNs blocked the increase in SOD2 activity and protein (Fig. 6B). Decoy to a non-related sequence Oct2A did not present any effect on ROH-induced SOD2 protein and activity. Pre-incubation with 50 μM Trolox or 1 mM NAC prevented ROH-induced SOD2.

## 4. Discussion

NFκB is a transcription factor consisting of a heterodimer of p65/p50 retained in the cytoplasm as an inactive tertiary complex associated with inhibitory proteins known as IκBs. After specific stimuli as for example tumor necrosis factor alpha (TNFα), IκB phosphorylation by IKKs leads to proteasome degradation of IκB, releasing NFκB to the nucleus [24]. Diverse stimuli as plasma membrane receptor-mediated mechanisms and alterations in the intracellular redox state may induce NFκB activation [24,25]. Once in nucleus, the mechanisms by which NFκB controls cell survival in pro-oxidant environments is to enhance transcription of anti-apoptotic and antioxidant genes, including Bcl-xL c-FLIP, XIAP, SOD2, glutathione S-transferase, and ferritin heavy chain [9,10]. The modulation of the intracellular redox status seems to play an important role in understanding the protective functions of NFκB in our model. ROH alone increased RS production and lipoperoxidation. However, inhibition of NFκB with the pharmacological IKK inhibitor BAY-117082 or DNA decoy ODNs potentiated ROH-induced RS, TBARS formation, and it induced decreases in cell viability. The decrease in cell viability was mediated by a prolonged activation of JNK–AP-1 pathway, since ROH in the presence of NFκB inhibitors, besides to promote persistent RS, induced persistent activation of JNK–AP-1, and pre-treatment with JNK1/2 inhibitor or DNA decoy to AP-1 blocked the decrease in viability. In addition, antioxidant pre-treatment inhibited the persistent activation of JNK1/2 and AP-1 suggesting that NFκB controls JNK–AP-1 activation by modulating intracellular redox state. It is important to note that NFκB was activated through alterations in intracellular redox state, since ROH increased RS and NFκB activation, and pre-treatment with antioxidants inhibited both RS production and NFκB activation. Taken in consideration that NFκB was activated by RS-dependent mechanisms, and its activation was pivotal to counteract oxidative stress at later time points of ROH treatment, data suggest that NFκB mediates adaptative responses to pro-oxidant effects of ROH.

In Sertoli cells, we have characterized that ROH at concentrations higher than physiological (ROH $\geq$ 5 μM) induces dysfunction in mitochondrial electron transfer system leading to increases in the rate of mitochondrial superoxide formation [15,26,27]. The effect of ROH on mitochondrial superoxide formation was also evidenced in brain mitochondria isolated from ROH supplemented rats [28], and in liver isolated mitochondria incubated with ROH in vitro [29]. In previous studies, we reported that incubation with electron transfer inhibitors as rotenone blocked ROH-induced RS formation and JNK1/2 activation in Sertoli cells [15]. In the presence of NFκB inhibition, the potentiating of RS formation in ROH-treated cells was attenuated by rotenone addition (Fig. 3A), suggesting that mitochondria act as a primary source of RS. Mitochondria-generated RS, including superoxide anions and hydrogen peroxide, may act as signaling intermediates or damaging agents depending on their intracellular concentrations [1]. In mitochondria, the formed superoxide anions are significantly eliminated by manganese SOD2 in order to avoid its accumulation [23,30,31]. It has been well established that decreases in, or SOD2 knockout/knockdown,

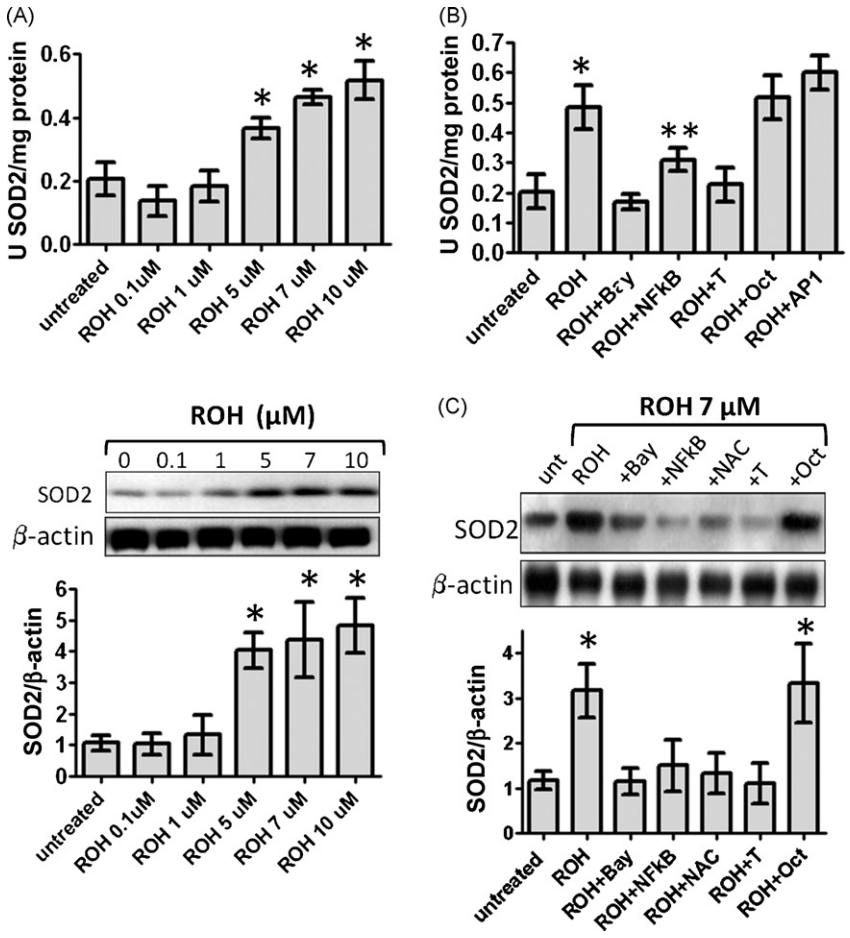


**Fig. 6 – ROH increases SOD2 activity and protein through an NFκB-dependent mechanism. (A) Effect of different ROH concentrations (μM) on SOD2 activity and immunocontent at 24 h. (B) Effect of pre-treatment with 50 μM Trolox, 10 μM BAY-117082, or NFκB decoy on SOD2 protein and activity at 24 h of treatment. Legends: ROH, retinol 7 μM; NFκB lanes, NFκB decoy; Oct, Oct2A decoy; NAC lanes, N-acetylcystein (1 mM); AP-1 lanes, AP-1 decoy; Bay, BAY-117082 (10 μM). *Different from untreated cells, **different from untreated and from ROH treated cells. Representative of three experiments (*n* = 3).**

increase oxidative stress, biomolecules damage and cellular sensitivity to oxidants [32]. In our model, ROH increased SOD2 protein and activity through an NFκB-dependent mechanism. Considering that ROH-induced RS are formed significantly in mitochondria, and that SOD2 play a role in mitochondrial RS detoxification, its plausible that NFκB dependent increases in SOD2 play a function in inhibiting ROH-induced RS accumulation and the persistent JNK–AP-1 pathway activation [9,23]. Corroborating, a recent study demonstrated that retinoic acid increases SOD2 through NFκB-dependent mechanisms in neuroblastoma cells [8]. Besides upregulating SOD2, it was recently reported that NFκB may suppress RS accumulation and downregulate the activation of JNK pathway by increasing ferritin heavy chain expression – a primary iron storage factor – as a mediator of antioxidant and protective activities of NFκB [9,10].

MAPK cascades are activated by several cellular stresses, and are involved in various biological responses such as differentiation, proliferation, and cell death [25,33,34]. Several lines of evidence suggested that transient MAPK activation is associated with cell proliferation or differentiation, whereas prolonged MAPK activation may promote cell death [2–4,35]. The relation between persistent or transient activation of MAPKs and its consequences on cell death/proliferation are well characterized on prolonged JNK activation observed during TNFα-induced cell death in cell types lacking NFκB signaling [2,9,36–38]. Cells lacking p65 and IKKb show increased sensitivity to TNF-induced cell death. In the absence of NFκB signaling, TNF promotes persistent mitochondrial RS formation and sustained stimulation of JNK1/2, which mediates necrosis. Treatment with antioxidants prevented both persistent JNK activation and cell death [2].

Corroborating with these studies, data presented here show that ROH could induce different cell fates depending on presence or absence of NFκB signaling, and duration of JNK pathway activation plays a role in these events. Upon NFκB inhibition, we determined a persistent (up to 24 h) increase in RS formation, which induced a prolonged stimulation of JNK–AP-1 pathway and JNK–AP-1-dependent decreases in cell viability. In these conditions, treatment with the antioxidant Trolox, JNK1/2 inhibitor, and DNA decoy to AP-1 attenuated both ROH-induced JNK–AP-1 pathway activation and decreases in cell viability. In contrast, upon normal conditions (i.e. with active NFκB signaling) ROH induced a transient

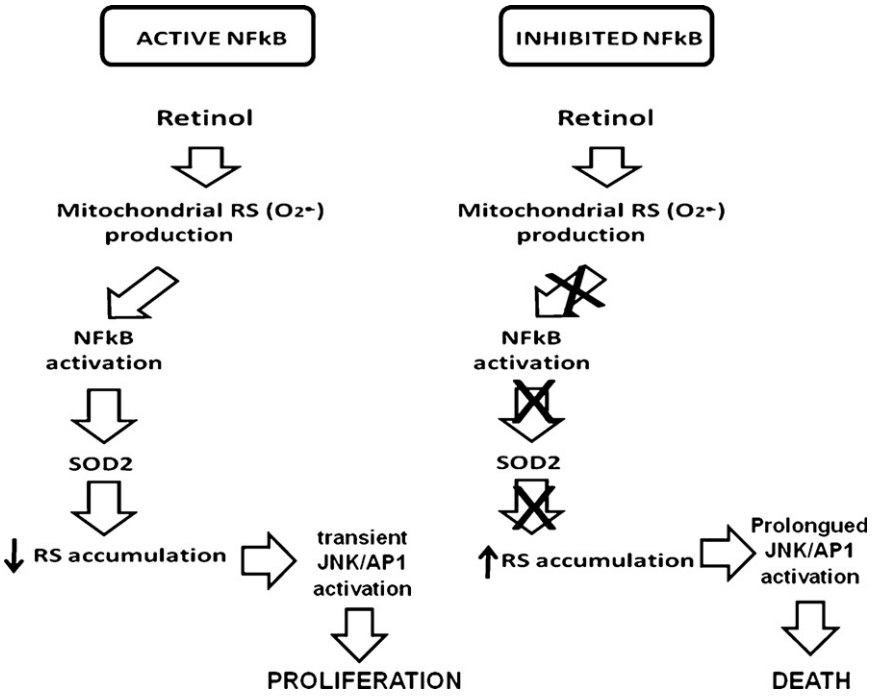


**Fig. 7 – Schematic representation of ROH pro-oxidant effects in the presence or absence of NFκB signaling in Sertoli cells.**

increase in RS formation, lower levels of oxidative damage, and no significant alterations in cell viability compared to that observed upon NFκB inhibition. In presence of NFκB, signaling was also observed that a transient activation of JNK–AP-1 pathway mediates proliferation, since inhibition with SP600125 or DNA decoy to AP-1-inhibited ROH-induced proliferation (Fig. 7). Thus, data indicate that a prolonged activation of JNK–AP-1 induces decreases in cell viability, while a transient activation leads to proliferation, and NFκB play a role in modulating these differential effects. This dual effect of JNK1/2 modulating proliferation and apoptosis also has been demonstrated during UVC-induced oxidative stress [4]. Data from others [2,4,22,39,40] and data presented here suggest that NFκB-mediated control of JNK1/2 signaling, and the consequences of prolonged/transient JNK activation on cell proliferation/apoptosis seems to represent a common mechanism among different pro-oxidant agents as UVC, TNF, and vitamin A.

Taken together, data suggest that NFκB plays important functions in modulating the duration of an oxidative insult, the duration of activation of redox-sensitive pathways as JNK–AP-1 and, consequently, the cellular fates in stressor environments. The events observed in this work could be useful not only to understanding vitamin A actions in biological systems but also to understand the NFκB function as an important factor involved in cellular resistance to oxidants and other cytotoxic agents [37,38,41], and show the inhibition of NFκB as mechanism to enhance cytotoxicity of oxidant agents.

## Acknowledgements

We acknowledge the Brazilian funds CAPES, CNPq, FAPERGS, and PPG-Bioquímica/UFRGS

## REFERENCES

[1] Stone JR, Yang S. Hydrogen peroxide: a signaling messenger. Antioxid Redox Signal 2006;8:244–62.
[2] Sakon S, Xue X, Takekawa M, Sasazuki T, Okazaki T, Okumura K, et al. NF-κB inhibits TNF-induced accumulation of ROS that mediate prolonged MAPK activation and necrotic cell death. EMBO J 2003;22:3898–909.
[3] Choi B, Hur E-M, Lee J-H, Jun D-J, Kim K-T. Protein kinase C-mediated proteasomal degradation of MAP kinase phosphatase-1 contributes to glutamate-induced neuronal cell death. J Cell Sci 2006;119:1329–40.
[4] Chen YR, Wang X, Templeton D, Davis RJ, Tan TH. The role of c-Jun N-terminal kinase (JNK) in apoptosis induced by ultraviolet C and gamma radiation. Duration of JNK activation may determine cell death and proliferation. J Biol Chem 1996;271:31929–36.
[5] Gelain DP, Cammarota M, Zanotto-Filho A, de Oliveira RB, Dal-Pizzol F, Moreira JC, et al. Retinol induces the ERK1/2-dependent phosphorylation of CREB through a pathway involving the generation of reactive oxygen species in cultured Sertoli cells. Cell Signal 2006;18:1685–94.
[6] Ji LL, Gomez-Cabrera MC, Vina J. Role of nuclear factor kappaB and mitogen-activated protein kinase signaling in exercise-induced antioxidant enzyme adaptation. J Appl Physiol Nutr Metab 2007;32:930–5.
[7] Matés JM, Segura JA, Alonso FJ, Márquez J. Intracellular redox status and oxidative stress: implications for cell proliferation, apoptosis, and carcinogenesis. Arch Toxicol 2008;82(5):273–99.
[8] Kiningham K, Cardozo Z, Cook C, Cole MP, Stewart JC, Spitz DR, et al. All-trans-retinoic acid induces manganese superoxide dismutase in human neuroblastoma through NF-κB. Free Radic Biol Med 2008;44:1610–6.
[9] Nakano H, Nakajima A, Sakon-Komazawa S, Piao J-H, Xue X, Okumura K. Reactive oxygen species mediate crosstalk between NF-κB and JNK. Cell Death Differ 2006;13:730–7.

[10] Pham CG, Bubici C, Zazzeroni F, Papa S, Jones J, Alvarez K, et al. Ferritin heavy chain upregulation by NF-kappaB inhibits TNFalpha-induced apoptosis by suppressing reactive oxygen species. Cell 2004;119:529–42.
[11] Klamt F, Dal-Pizzol F, Rohers R, Oliveira RB, Dalmolin RJS, Henriques JAP, et al. Genotoxicity, recombinogenicity and preneoplasic transformation induced by vitamin A supplementation. Mutat Res 2003;539:117–25.
[12] Dalmolin RJ, Zanotto-Filho A, De Oliveira RB, Duarte RF, Pasquali MA, Moreira JC. Retinol and retinoic acid increase MMP-2 activity by different pathways in cultured Sertoli cells. Free Radic Res 2007;41:1338–47.
[13] De Oliveira MR, Silvestrin RB, Mello e Souza T, Moreira JCF. Oxidative stress in the hippocampus, anxiety-like behavior and decreased locomotory and exploratory activity of adult rats: effects of sub acute vitamin A supplementation at therapeutic doses. Neurotoxicology 2007;28:1191–9.
[14] De Oliveira MR, Silvestrin RB, Mello e Souza T, Moreira JCF. Therapeutic vitamin A doses increase the levels of markers of oxidative insult in substantia nigra and decrease locomotory and exploratory activity in rats after acute and chronic supplementation. Neurochem Res 2008;33:378–83.
[15] Zanotto-Filho A, Schröder R, Moreira JCF. Differential effects of retinol and retinoic acid on cell proliferation: a role for reactive species and redox-dependent mechanisms in retinol supplementation. Free Radic Res 2008;42(9): 778–88.
[16] Wang H, Joseph JA. Quantifying cellular oxidative stress by dichlorofluorescein assay using microplate reader. Free Radic Biol Med 1999;27:612–6.
[17] Igaz LM, Refojo D, Costas MA, Holsboer F, Arzt E. CRE-Mediated transcriptional activation is involved in cAMP protection of T-cell receptor-induced apoptosis but not in cAMP potentiation of glucocorticoid-mediated programmed cell death. Biochim Biophys Acta 2002;1542:139–48.
[18] Draper HH, Hadley M. Malondialdehyde determination as index of lipid peroxidation. Methods Enzymol 1990;186:421–31.
[19] Strassburger M, Bloch W, Sulyok S, Schuller J, Keist AF, Schmidt A, et al. Heterozygous deficiency of manganese superoxide dismutase results in severe lipid peroxidation and spontaneous apoptosis in murine myocardium in vivo. Free Radic Biol Med 2005;38:1458–70.
[20] Misra HP, Fridovich I. The role of superoxide anion in the autoxidation of epinephrine and a simple assay for superoxide dismutase. J Biol Chem 1972;247:3170–5.
[21] Lowry OH, Rosebrough AL, Farr AL, Randal RJ. Protein measurement with the Folin phenol reagent. J Biol Chem 1951;193:265–75.
[22] Bubici C, Papa S, Pham CG, Zazzeroni F, Franzoso G. The NF-kappaB-mediated control of ROS and JNK signaling. Histol Histopathol 2006;21:69–80.
[23] Sasazuki T, Okazaki T, Tada K, Sakon-Komazawa S, Katano M, Tanaka M, et al. Genome wide analysis of TNF-inducible genes reveals that antioxidant enzymes are induced by TNF and responsible for elimination of ROS. Mol Immunol 2004;41:547–51.
[24] Bowie A, O'Neill LA. Oxidative stress and nuclear factor-kappaB activation: a reassessment of the evidence in the light of recent discoveries. Biochem Pharmacol 2000;59: 13–23.
[25] Kefaloyianni E, Gaitanaki C, Beis I. ERK1/2 and p38-MAPK signalling pathways, through MSK1, are involved in NF-kB transactivation during oxidative stress in skeletal myoblasts. Cell Signal 2006;18:2238–51.
[26] Dal-Pizzol F, Klamt F, Benfato MS, Bernard EA, Moreira JC. Retinol supplementation induces oxidative stress and modulates antioxidant enzyme activities in rat Sertoli cells. Free Radic Res 2001;34:395–404.
[27] Klamt F, Dal-Pizzol F, Bernard EA, Moreira JC. Enhanced UV-mediated free radical generation. DNA and mitochondrial damage caused by retinol supplementation. Photochem Photobiol 2003;2:856–60.
[28] De Oliveira MR, Moreira JCF. Acute and chronic vitamin A supplementation at therapeutic doses induces oxidative stress in submitochondrial particles isolated from cerebral cortex and cerebellum of adult rats. Toxicol Lett 2007;173:145–50.
[29] Klamt F, Roberto de Oliveira M, Moreira JC. Retinol induces permeability transition and cytochrome c release from rat liver mitochondria. Biochim Biophys Acta 2005;1726:14–20.
[30] Nelson KK, Melendez JA. Mitochondrial redox control of matrix metalloproteinases. Free Radic Biol Med 2004;15:768–84.
[31] Giorgio M, Trinei M, Migliaccio E, Pelicci PG. Hydrogen peroxide: a metabolic by-product or a common mediator of ageing signals? Nat Rev 2007;8:722–8.
[32] Macmillan-Crow LA, Cruthirds DL. Manganese superoxide dismutase in disease. Free Radic Res 2001;34:325–36.
[33] Ichijo H. From receptors to stress-activated MAP kinases. Oncogene 1999;18:6087–93.
[34] Davis RJ. Signal transduction by the JNK group of MAP kinases. Cell 2000;103:239–52.
[35] Xia Z, Dickens M, Raingeaud J, Davis RJ, Greenberg ME. Opposing effects of ERK and JNK-p38 MAP kinases on apoptosis. Science 1995;270:1326–31.
[36] Guo YL, Baysal K, Kang B, Yang LJ, Williamson JR. Correlation between sustained c-Jun N-terminal protein kinase activation and apoptosis induced by tumor necrosis factor-alpha in rat mesangial cells. J Biol Chem 1998;273:4027–34.
[37] Barkett M, Gilmore TD. Control of apoptosis by Rel/NF-κB transcription factors. Oncogene 1999;18:6910–24.
[38] Karin M, Lin A. NF-κB at the crossroads of life and death. Nat Immunol 2002;3:221–7.
[39] Smaele E, Zazzeroni F, Papa S, Nguyen DU, Jin R, Jones J, et al. Induction of gadd45b by NF-κB downregulates pro-apoptotic JNK signaling. Nature 2001;414:308–13.
[40] Bubici C, Papa S, Pham CG, Zazzeroni F, Franzoso G. NF-κB and JNK: an intricate affair. Cell Cycle 2004;12: 1524–9.
[41] Papa S, Bubici C, Zazzeroni F, Pham CG, Kuntzen C, Knabb JR, et al. The NF-κB-mediated control of the JNK cascade in the antagonism of programmed cell death in health and disease. Cell Death Differ 2006;13:712–29.

III.1 – Artigo 2

# The pharmacological NFκB inhibitors BAY117082 and MG132 induce cell arrest and apoptosis in leukemia cells through ROS-mitochondria pathway activation.

Cancer Letters, 2010; 288(2):192-203.

doi:10.1016/j.canlet.2009.06.038

Cancer Letters 288 (2010) 192–203

Contents lists available at ScienceDirect

Cancer Letters

journal homepage: www.elsevier.com/locate/canlet

# The pharmacological NFκB inhibitors BAY117082 and MG132 induce cell arrest and apoptosis in leukemia cells through ROS-mitochondria pathway activation

Alfeu Zanotto-Filho [a,*], Andrés Delgado-Cañedo [b], Rafael Schröder [a], Matheus Becker [b,c], Fábio Klamt [a], José Cláudio Fonseca Moreira [a]

[a] Centro de Estudos em Estresse Oxidativo, Departamento de Bioquímica, UFRGS, Rio Grande do Sul, Brazil
[b] Instituto de Cardiologia de Porto Alegre, Rio Grande do Sul, Brazil
[c] Laboratório de Imunogenética, Departamento de Genética, UFRGS, Rio Grande do Sul, Brazil

ARTICLE INFO

*Article history:*
Received 25 March 2009
Received in revised form 28 June 2009
Accepted 30 June 2009

*Keywords:*
MG132
BAY117082
Apoptosis
ROS
Leukemia cells

ABSTRACT

A growing body of evidence suggests the inhibition of NFκB as a strategy to induce cell death in tumor cells. In this work, we evaluated the effects of the pharmacological NFκB inhibitors BAY117082 and MG132 on leukemia cells apoptosis. BAY117082 and MG132 presented potent apoptotic effects compared to inhibitors of MAPKs, EGFR, PI3K/Akt, PKC and PKA signaling pathways. Non-tumor peripheral blood cells were insensitive to BAY117082 and MG132 apoptotic effects. BAY117082 and MG132-induced apoptosis was dependent on their ability to increase ROS as a prelude to mitochondria membrane potential (MMP) depolarization, permeability transition pore opening and cytochrome *c* release. Antioxidants blocked MG132 and BAY117082 effects on ROS, MMP and cell death. Although apoptotic markers as phosphatidylserine externalization, chromatin condensation and sub-G1 were detected in BAY117082-treated cells, caspases activation did not occur and apoptosis was insensitive to caspase inhibitors, suggesting a caspase-independent mechanism. In contrast, MG132 induced classical apoptosis through ROS-mitochondria and subsequent caspase-9/caspase-3 activation. At sub-apoptotic concentrations, BAY117082 and MG132 arrested cells in G2/M phase of the cell cycle and blocked doxorubicin-induced NFκB, which sensitized doxorubicin-resistant cells. Data suggest that the NFκB inhibitors MG132 and BAY117082 are potential anti-leukemia agents.



## 1. Introduction

The transcription factor NFκB (nuclear factor kappa B) has emerged as a crucial regulator of cell survival, playing important functions in cellular resistance to oxidants and anticancer agents [1–3]. Substantial evidence associates NFκB to the regulation of oncogenesis and tumor progression, attributing to NFκB a role as a survival factor in tumor cells and thus a potential target to therapy [1–3]. The NFκB family comprises p50/p105, p52/p100, p65, c-Rel and RelB proteins which exist in an inactive state as homodimers or heterodimers bound to inhibitory IκB proteins in the cytoplasm [1]. The most common form of NFκB is the p65/p50 heterodimer. Diverse stimuli, including tumor necrosis factor alpha and oxidants, activate the IκB kinase (IKK) complex, which phosphorylates and triggers proteasome-dependent degradation of IκB-alpha, the predominant NFκB inhibitory molecule. NFκB then translocates to the nucleus and modulates transcription by binding to specific DNA sequences in target promoters [4–6]. There are multiple mechanisms by which NFκB promotes cell

* Corresponding author. Address: Depto. Bioquímica (ICBS-UFRGS), Rua Ramiro Barcelos, 2600/Anexo, CEP 90035-003, Porto Alegre, Rio Grande do Sul, Brazil. Tel.: +55 51 3308 5578; fax: +55 51 3308 5535.
*E-mail address:* ohalceu@yahoo.com.br (A. Zanotto-Filho).

0304-3835/$ - see front matter © 2009 Elsevier Ireland Ltd. All rights reserved.
doi:10.1016/j.canlet.2009.06.038

survival [7–9]. Target genes induced by NFκB that are important for the control of cell survival include the anti-apoptotics bcl-xL, cFLIP, cIAP1/2 and Bcl-2, and the antioxidants SOD2 [4–6] and ferritin heavy chain [7], which act to prevent the pro-apoptotic machinery activation [8,9].

Several studies have provided compelling evidence that aberrant NFκB activation contributes to inappropriate cell survival in a wide range of solid and hematopoietic malignances [10–16]. In this intent, researchers have interfered with NFκB activity via proteasome and IKK inhibitors in order to induce cell arrest and apoptosis of myeloma [3], sarcoma [17], lymphoma [18] and leukemia cells [2]. For example, chronic lymphocytic leukemia (CLL) cells express abundant levels of nuclear NFκB activity compared to normal B cells [12–16], and an in vitro treatment of CLL cells with the pharmacological NFκB inhibitors Kamebakaurin and BAY117082 induced apoptosis in almost 70% of cases [2]. Clinically, the therapeutic potential of NFκB inhibitors has been demonstrated in myeloma patients treated with the proteasome-dependent NFκB inhibitor PS341 (bortezomib) [3].

In addition to the aforementioned, NFκB overstimulation has been associated with cellular resistance to classical chemotherapeutic agents as doxorubicin, etoposide and imatinib [19–22], and it has been correlated with chemotherapy resistance and therapy failure in vivo [21,22]. In this context, the combined use of NFκB inhibitors with classical anticancer drugs could be useful to abolish cellular resistance [21–23]. For example, in chronic myelocytic leukemia (CML) cells as K562, NFκB has been identified as a downstream component of the Bcr-Abl-initiated signaling pathway, and has been associated with cellular resistance to imatinib [23]. Treatment with PS341 [23] or the IKK inhibitor PS1145 [22] overcame imatinib resistance and induced apoptosis in imatinib-resistant K562 cells. Based on these findings, clinical phase I/II studies are ongoing to evaluate the usefulness of PS1145 combined with imatinib in CML patients [20]. Thus, the validation of compounds targeting NFκB pathway as potential chemotherapeutic agents may provide novel and selective therapeutic opportunities [3].

Recently, anticancer activity of novel NFκB pathway inhibitors has been evaluated. Studies showed that the proteasome inhibitor peptide MG132 (Z-Leu-Leu-Leu-CHO) acts as a powerful apoptotic agent in several tumor cell lines, and much of the MG132 activity has been attributed to NFκB inhibition through inhibition of IκB degradation [24,25]. On the other hand, few studies have directly assessed the apoptotic potential of inhibitors of other checkpoints of the NFκB pathway as the IκB phosphorylation inhibitor BAY117082 [2,17,21]. Moreover, the mechanisms underlying MG132 and, principally, BAY117082 apoptotic effects remain to be better understood since nonclassical effects – as for example reactive oxygen species (ROS)-dependent mechanisms – were indicated in previous studies [17,25].

Thus, the aim of this study was to investigate the mechanisms underlying the apoptotic activity of the NFκB pathway inhibitors BAY117082 and MG132 in K562 (human chronic myelocytic leukemia), U937 (human monocytic leukemia), and Jurkat T (human T cell lymphoblast) leukemia cell lines. We investigated the role of ROS and mitochondrial apoptotic pathway activation, the selectivity to tumor cells, and the effect of combined treatment of NFκB inhibitors plus doxorubicin in doxorubicin-resistant cells.

## 2. Materials and methods

### 2.1. Reagents

BAY117082 ((E)-3-(4-methylphenylsulfonyl)-2-propenenitrile), MG132 (Z-Leu-Leu-Leu-al), propidium iodide, MTT (3-(4,5-dimethyl)-2,5-diphenyl tetrazolium bromide), Bongkrekic acid, BAPTA-AM, allopurinol, diphenylene iodonium (DPI), Trolox ((±)-6-hydroxy-2,5,7,8-tetramethylchromane-2-carboxylic acid), dithiothreitol (DTT), doxorubicin, anti-beta-actin, anti-beta tubulin, anti-SOD1 antibodies, and culture analytical grade reagents were purchased from Sigma Chemical Co. (St. Louis, MO, USA). YO-PRO-1 was from Invitrogen-Molecular Probes. SP600125 was from Promega Corporation (Madison, USA). SB203580 were from Merck Biosciences (Darmstadt, Germany). UO126, H89 and Gö 6983 were from Biomol Research Laboratories (Plymouth Meeting, PA). The caspase inhibitors Z-VAD-fmk, Z-IETD-fmk and Z-LEHD-fmk were from B&D Systems. TCEP (tris(2-carboxyethyl)-phosphine) was from Pierce (Rockford, IL, USA). Anti-cytochrome *c*, anti-lamin B, anti-Bcl-xL, anti-hsp70 and anti-p65 antibodies were from Santa Cruz Biotechnologies (Santa Cruz, CA, USA). Electrophoresis/immunoblotting reagents were from Bio-Rad Laboratories (Hercules, CA, USA). DNA oligonucleotides were synthesized by The Midland Certified Reagent Company, Inc. (Midland, TX, USA).

### 2.2. Cell cultures

K562, U937 and Jurkat cell lines were seeded at $1 \times 10^5$ cells/ml in 75 $cm^2$ tissue culture flasks, grown in RPMI 1640 medium (Gibco BRL, Cergy-Pontoise, France) supplemented with 10% fetal calf serum, 100 U/ml penicillin and 100 μg/ml streptomycin (Gibco, BRL). Cultures were maintained in a humidified atmosphere with 5% $CO_2$ at 37 °C. Cells were allowed to grow for 24 h in culture medium prior to exposure to treatments. Inhibitors stock solutions were dissolved in dimethylsulphoxide (DMSO), and solvent controls (DMSO < 0.4%) were performed for each condition. Peripheral blood mononuclear cells (PBMC) were isolated from healthy individuals using Ficoll-Paque centrifugation, and cultured at $10^5$ cells/ml in RPMI supplemented with 10% fetal calf serum during 2 days before experiments [2].

### 2.3. MTT assay

Cell viability was estimated by the quantification of the MTT reduction to a blue formazan product by cellular dehydrogenases as previously described [26].

### 2.4. Assessment of cell death

Treated cells ($10^5$ cells/ml) were incubated for 15 min at 37 °C with YOPRO-1 dye (1 μM final concentration) plus

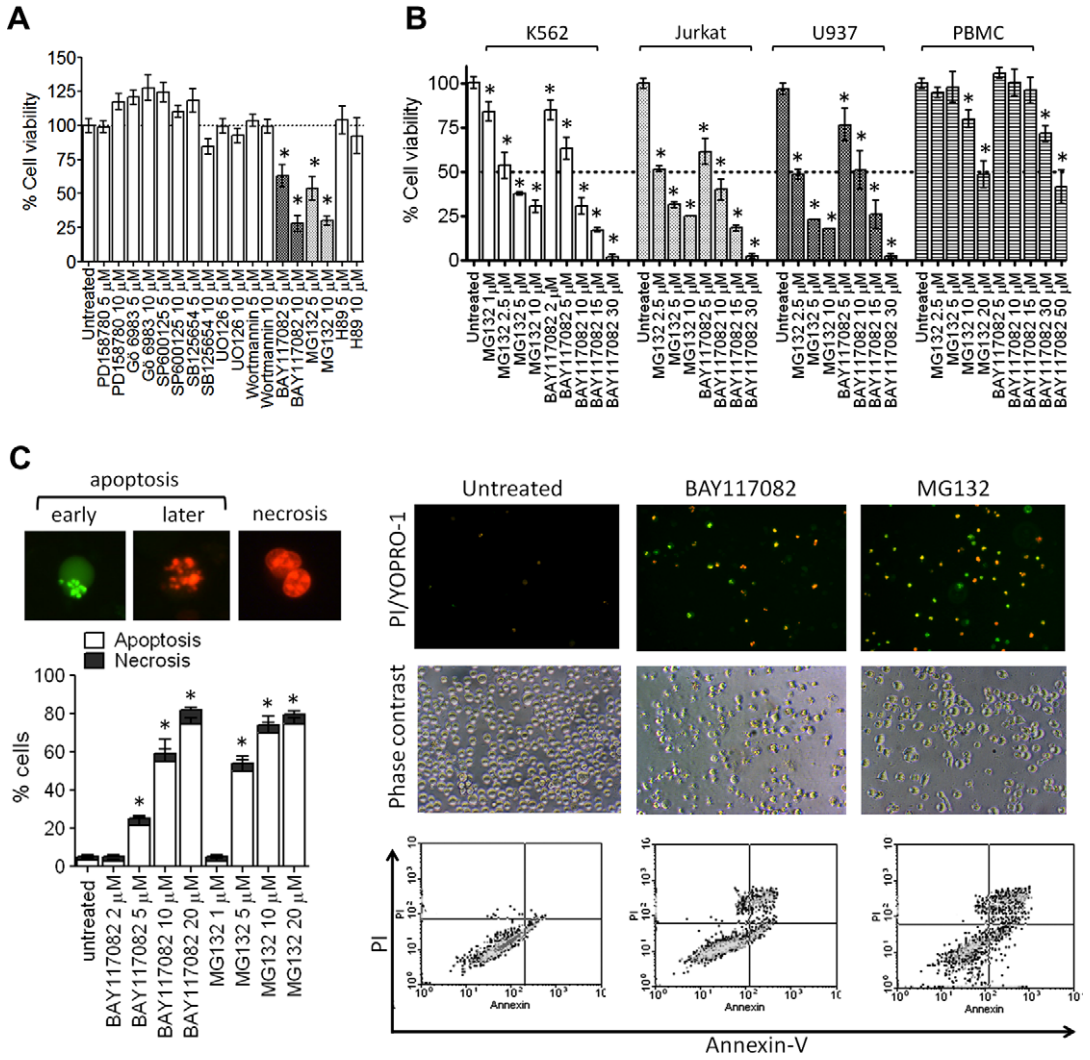


**Fig. 1.** BAY117082 and MG132 induce selective leukemia cells apoptosis. (A) MTT assay showing the effect of pharmacological inhibitors of classical signaling pathways on K562 cells viability. (B) BAY117082 and MG132 induced decreases in cell viability of K562, Jurkat T and U937 cell lines with minor effects on PBMC as assessed by MTT. (C) Nuclear morphological characteristics used to differentiate apoptotic and necrotic cells in PI/YOPRO-1 staining assays. In Fig. 1C are also showed microphotographs (20× magnifications) of PI/YOPRO-1 staining, flow cytometry graphs for phosphatidylserine exposure (right panel) and quantification of the apoptosis by PI/YOPRO-1 assay. *Different from untreated cells ($p < 0.01$).

propidium iodide (PI, 50 μg/ml), centrifuged, washed with PBS, and then resuspended at ~$2 \times 10^7$cells/ml. The cells were visualized using fluorescence microscopy (10× magnification) and a minimum of 200 cells was counted. Cell morphology was classified as follows: (A) live cells (non-fluorescent, normal nuclei, with organized structure); (B) apoptotic cells (early apoptotic are bright green/yellow chromatin, which is highly condensed or fragmented; late apoptotic are bright red/orange chromatin, condensed or fragmented); and (C) necrotic (red,[1] enlarged nuclei with normal structure) [27] (see Fig. 1C).

For annexin-V/PI staining, $2 \times 10^5$ cells were incubated with 3 μl FITC-conjugated annexin-V in 100 μl binding buffer (10 mM HEPES pH 7.4, 145 mM NaCl, 5 mM KCl, 1.0 mM $MgCl_2 \cdot 6H_2O$, 1.8 mM $CaCl_2 \cdot 2H_2O$) for 30 min in ice bath. After 2 μM propidium iodide was added and externalized phosphatidylserine was determined using a FACS Calibur cytometer (FACS Calibur System, BD Biosciences, San Jose, CA) [17].

### 2.5. Cell cycle analysis

After treatments, cells were immediately centrifuged and resuspended in a PBS containing 5 mM EDTA, 50 μg/ml RNAse A, 0.1% Triton X-100 and 50 μg/ml propidium iodide, and incubated for at least 10 min on ice. Stained and single cells were analyzed by flow cytometry. Ten thousand events were counted per sample [28].

[1] For interpretation of color in Figs. 1, 5 and 6, the reader is referred to the web version of this article.

### 2.6. Determination of intracellular ROS production in living cells [real-time DCF assay]

ROS production was detected using 2,7-dichlorodihydrofluorescein diacetate, DCFH-DA (Sigma, St. Louis, USA) [29]. This reagent enters the cells and reacts with ROS, producing the fluorophore dichlorofluorescein (DCF). Briefly, $0.5 \times 10^6$ cells were incubated with 50 μM DCFH-DA in complete medium for 30 min at 37 °C to allow cellular incorporation. After, cells were centrifuged and resuspended in 200 μL of a new medium containing treatments. ROS-dependent DCF fluorescence was monitored at 37 °C with an emission wavelength set at 535 nm and an excitation wavelength set at 485 nm in a 96-well plate fluorescence reader (Spectra Max M2, Molecular Devices, USA). Hydrogen peroxide was used as positive control for ROS.

### 2.7. Cellular fractionation and immunoblotting

To prepare nuclear extracts, $2 \times 10^6$ cells were collected by centrifugation 750*g* for 5 min, and resuspended in 200 μl of hypotonic buffer (buffer A) containing 10 mM HEPES (pH 7.9), 1.5 mM $MgCl_2$, 10 mM KCl, 0.2 mM phenylmethylsulfonyl fluoride, 0.5 mM DTT, proteases inhibitor cocktail (Roche). After, samples were incubated in ice for 15 min. After, 12 μl of 10% Nonidet P-40 was added and cells were disrupted by vortexing (15 seg). Nuclei were isolated by centrifugation (14,000*g*, 30 seg) and resuspended in 100 μl of high salt buffer (Buffer A plus 0.42 M NaCl) followed by incubation (40 min) in ice for releasing soluble proteins from the nuclei. After extraction, the nuclei were removed by centrifugation (14,000*g*, 15 min), and supernatant containing soluble nuclear proteins was stored at −80 °C.

To detect cytochrome *c* release from mitochondria, cells were incubated with ice-cold digitonin lyses buffer (75 mM KCl, 1 mM $NaH_2PO_4$, 8 mM $Na_2HPO_4$, 250 mM sucrose, 190 μg/ml digitonin, pH 7.4) for 5 min, and centrifuged for 15 min at 14,000*g*. The supernatant (cytosolic proteins) and mitochondrial pellet were stored at −80 °C [30].

Isolated nuclear, cytoplasmic, and mitochondrial (25 μg) proteins were fractionated by SDS/PAGE and transferred onto nitrocellulose membranes. After blocking with 5% non-fat dry milk, membranes were incubated with primary antibodies for 18 h at 4 °C, washed, and followed by

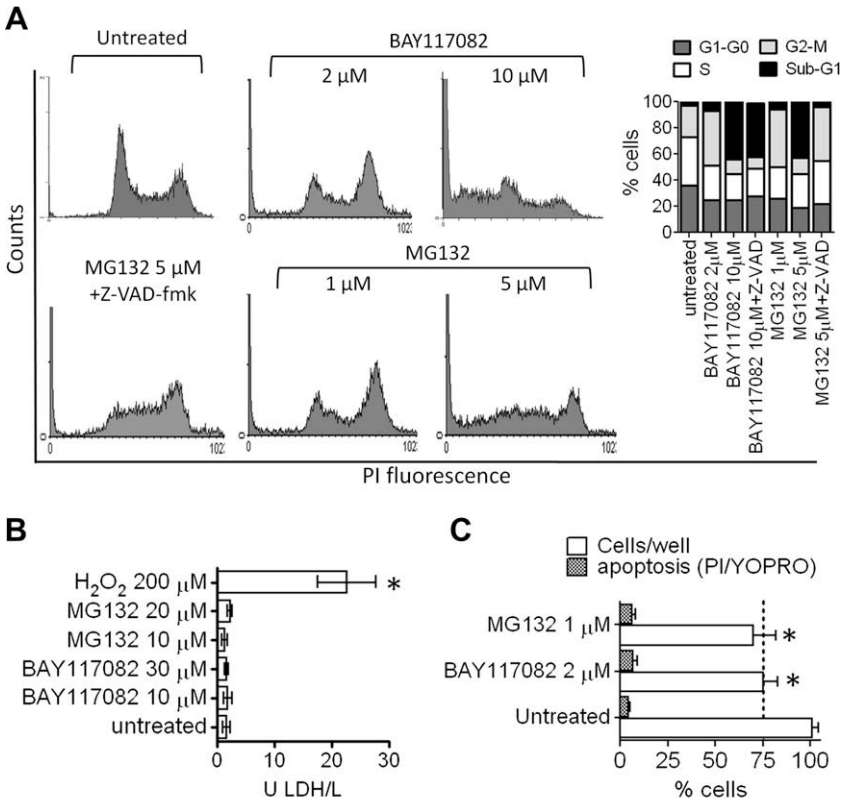


**Fig. 2.** Cell cycle analyses, LDH release and cell number in BAY117082 and MG132-treated cells. (A) Representative flow cytometry graphs with respective quantification showing the effect of apoptotic and sub-apoptotic concentrations of MG132 and BAY117082 on cell cycle distribution in K562 cells. The effect of the broad spectrum caspase inhibitor Z-VAD-fmk (50 μM) on 5 μM MG132-induced apoptosis is also showed. (B) LDH release in culture medium after 24 h treatment with different concentrations of BAY117082 and MG132. (C) Sub-apoptotic concentrations of BAY117082 and MG132 decreased cell number without affect the apoptotic rate. Cells were treated for 24 h with 2 μM BAY117082 or 1 μM MG132. After, cell number and PI/YOPRO-1 stained cells were determined. *Different from untreated cells ($p < 0.01$).

incubation horseradish peroxidase-conjugated secondary antibodies (1:5000) for additional 1 h at 25 °C. Bands were detected by X-ray film exposure.

### 2.8. Electro-mobility shift assay (EMSA)

To determine NFκB DNA-binding activity, biotin 3-end labeled NFκB oligonucleotide consensus sequence was carried out by EMSA [4]. Briefly, the NFκB sequence 5′-CGACACCCCTCGGGAATTCCCCCACTGGGCC-3′ was labeled with biotin-ddUTP in accordance with manufacturer instructions (LightShift Chemiluminescent EMSA Kit, Pierce). In binding reactions, 20 μl of reaction mixture containing 15 mM Hepes pH 7.9, 1 mM DTT, 2.5 mM EDTA, 5 mM $MgCl_2$, 2.5% glycerol and 50 ng/μl poly (dI–dC), 5 μg of nuclear proteins, and 30 fmol of biotin-labeled DNA probes were incubated for 30 min in ice bath. Nucleo-protein complexes were loaded onto 5.5% non-denaturing polyacrylamide gels in 0.5× Tris–boric acid–EDTA buffer (TBE) and run at 130 V. The electrophoresed binding reactions were electrotransferred in 0.5× TBE to nylon membranes. The biotin-ddUTP-labeled DNA probe was detected using streptavidin-horseradish peroxidase-conjugated.

### 2.9. Caspase and LDH activities

Caspase-3 and caspase-9 activities were determined in accordance with CASP3F (Sigma/Aldrich, St. Louis), and Caspase-9 colorimetric assay kits (Biovision Incorporated), respectively, in accordance with manufacturer instructions. LDH activity was quantified in culture medium using The Promega CytoTox 96® Non-Radioactive Cytotoxicity Assay (Madison, USA).

### 2.10. Mitochondrial membrane potential ($\Delta\Psi m$)

After treatments, cells ($2 \times 10^5$ cells/ml) were incubated for 20 min at 37 °C with the lipophilic cationic probe JC-1 (5,5′,6,6′-tetrachloro-1,1′,3,3′-tetraethylbenzimidazolcarbocyanine iodide, 2 μg/ml in medium), centrifuged, washed once with medium, transferred to a 96-well plate ($10^5$ cells/well), and assayed in a fluorescence plate reader with the following settings: excitation at 485 nm, emission at 540 and 590 nm, and cutoff at 530 nm (SpectraMax M2, Molecular Devices, USA). In some experiments, emission spectra between 510 and 610 nm were obtained. $\Delta\Psi m$ was calculated using the ratio of 590 nm (J-aggregates)/540 nm (monomeric form) [31]. For confocal microscopy

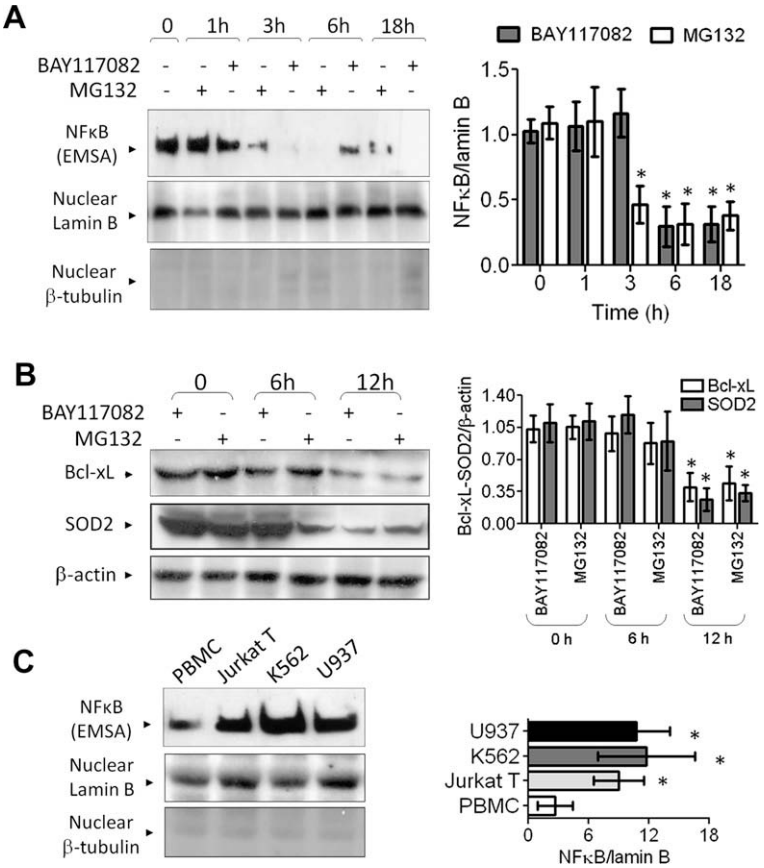


**Fig. 3.** BAY117082 and MG132 induce NFκB pathway inhibition. (A) Effect of BAY117082 and MG132 on NFκB DNA-binding activity (EMSA). (B) Bcl-xL and SOD2 protein immunocontent. In Fig. 3A and 3B, K562 cells were treated for different times (*h*) with 5 μM MG132 or 10 μM BAY117082. Nuclear and total cellular extracts were collected and analyzed by EMSA or western blotting. (C) Comparison between basal levels of NFκB activity in K562, Jurkat T, U937 and PBMC. *Different from untreated cells (3A and 3B) or from PBMC (3C) ($p < 0.01$).

for $\Delta\Psi m$, cells were transferred to microscope slides and examined immediately. The samples were viewed at room temperature in a darkened room with an Axiovert 40 CFl – Zeiss.

### 2.11. Measurement of protein carbonyl groups

Oxidative damage to proteins was assessed by the quantification of carbonyl groups based on the reaction with dinitrophenylhydrazine (DNPH) as previously described [26]. Cells ($2 \times 10^6$) were treated, collected, and protein carbonyl groups were labeled by incubating samples with 10 mM DNPH for 1 h at room temperature. The absorbance was read in a spectrophotometer at 370 nm. Results were calculated using an absorption coefficient of 22 $mM^{-1}cm^{-1}$, and data were expressed as nmol/mg protein.

### 2.12. Protein quantification

Sample protein contents were quantified as described by Lowry et al. [32].

### 2.13. Statistical analysis

Data are expressed as means plus standard deviations (SD) and were analyzed by one-way ANOVA followed by Duncan's post-hoc test. Differences were considered significant at $p < 0.01$.

## 3. Results

### 3.1. NFkB inhibitors induce selective cell death to leukemia cells

First, K562 cells were treated with well-known inhibitors of some classical signaling pathways involved on cell cycle regulation. The effect of a 24 h treatment with MAPK inhibitors (UO126 – MEK1/2-dependent ERK activation inhibitor; SP600125 – JNK1/2 inhibitor; SB125654 – p38 inhibitor), PI3K/Akt pathway inhibitor (wortmannin), PKC inhibitor (Gö 6983), EGFR (epidermal growth factor receptor) kinase inhibitor (PD158780), IKK/NFκB inhibitor (BAY117082), proteasome/NFκB inhibitor (MG132) and PKA inhibitor (H89) on cell viability was evaluated (Fig. 1A). Interestingly, only the pharmacological inhibitors of NFκB signaling BAY117082 and MG132 promoted significant decreases in cell viability. Thus, they were chosen for subsequent experiments. To test whether BAY117082 and MG132 effects are exclusive to K562 cells or they could be extended to other leukemia cell lines and to control normal peripheral blood mononuclear cells (PBMC), we tested BAY117082 and MG132 cytotoxicity in Jurkat T, U937 and PBMC (Fig. 1B). Fig. 1B shows that BAY117082 and MG132 induced significant decreases in cell viability of K562 (IC50, MG132 = 3.5 μM; BAY117082 = 8 μM), Jurkat T (IC50, MG132 = 2.8 μM; BAY117082 = 7.1 μM) and U937 (IC50, MG132 = 2.5 μM; BAY117082 = 10.5 μM) leukemia cells whereas normal PBMC were less sensitive to NFκB inhibitors (IC50, MG132 = 21 μM; BAY117082 = 40.2 μM).

### 3.2. Characterization of the cell death in MG132 and BAY117082-treated cells

To characterize the mechanisms by which MG132 and BAY117082-induced cell death we used K562 cells. MG132 at 5 μM and BAY117082 at 10 μM were chosen for experiments. Fig. 1C shows the morphological criteria used to differentiate apoptotic and necrotic cells by PI/YOPRO-1 staining assay (additional information are provided in Materials and methods section). In agreement with MTT assay, quantification of cell death by PI/YOPRO-1 staining shows a dose-dependent induction of apoptosis in K562 cells following treatment with NFκB inhibitors (Fig. 1C, column graph). YOPRO-1/PI assays showed that incubation with BAY117082 or MG132 for 24 h induced nuclear shrinkage, chromatin condensation and a high percentage of apoptotic cells (green/yellow or red cells with nuclear chromatin condensation). Necrotic morphological features were rarely observed.

In addition, treatment with 5 μM MG132 or 10 μM BAY117082 for 24 h increased externalization of phosphatidylserine as an indicative of apoptosis (Fig. 1C). Corroborating, cell cycle analysis detected formation of a sub-G1 cell population (cells with hypodiploid DNA content) comprising approximately 35% and 42% cells, respectively, confirming DNA fragmentation (Fig. 2A). To exclude the possibility of cell rupture by necrosis, we quantified the levels of LDH released in the culture medium. At the end of 24 h treatment with BAY117082 or MG132, no alterations on LDH activity were observed, thus excluding necrotic cell death. In LDH assays, hydrogen peroxide was used as positive control (Fig. 2B).

Interestingly, low concentrations of MG132 (1 μM) and BAY117082 (2 μM) caused G2/M arrest as assessed by flow cytometry (Fig. 2A). At the end of 24 h, these low concentrations induced decreases in cell number although they did not elicit cell death as assessed by PI/YOPRO-1 assay (Fig. 2C), suggesting that sub-apoptotic concentrations of BAY117082 and MG132 induced inhibition of proliferation.

We also performed control experiments to confirm that BAY117082 and MG132 were effective to affect NFκB pathway (Fig. 3). Treatment with 10 μM BAY117082 or 5 μM MG132 decreased NFκB DNA-binding activity from 3 h incubation (Fig. 3A). As a consequence of NFκB inhibition, decreases in Bcl-xL and SOD2 (two NFκB-induced anti-apoptotic and antioxidant genes, respectively) protein levels occurred after 12 h incubation with BAY117082 and MG132 (Fig. 3B). Last, we determined that K562, U937 and Jurkat T cells presented higher levels (approximately

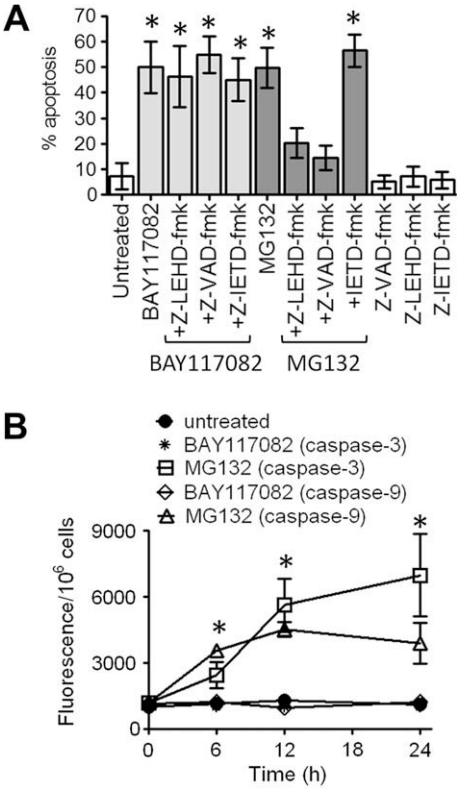


**Fig. 4.** Effect of caspase inhibitors and caspase activity in MG132 and BAY117082-induced apoptosis. (A) Cells were treated for 24 h with 10 μM BAY117082 or 5 μM MG132 in the presence or absence of specific (Z-LEHD-fmk, Z-IETD-fmk) or broad spectrum (Z-VAD-fmk) caspase inhibitors (50 μM). Apoptosis was quantified by PI/YOPRO-1 staining assay. (B) Caspase-9 and caspase-3 activity quantification. Cells were treated for different times (*h*) with 5 μM MG132 or 10 μM BAY117082, and cellular homogenates were collected for caspase activity quantification. *Different from untreated cells ($p < 0.01$).

4-fold) of constitutive NFκB DNA-binding activity compared to PBMC (Fig. 3C). Immunoreactivity against lamin B and β-tubulin were tested to evaluate the purity of nuclear extracts; β-actin was used as a loading control to total cellular extracts.

### 3.3. Differential apoptotic mechanisms in BAY117082 and MG132-treated cells

In order to determine the apoptotic pathways involved in BAY117082 or MG132-induced apoptosis, we pre-treated cells with selective cell-permeable caspase-8 (Z-IETD-fmk 50 μM – extrinsic pathway), caspase-9 (Z-LEHD-fmk 50 μM – mitochondria pathway) and pan caspase (Z-VAD-fmk 50 μM) inhibitors for 1 h before 10 μM BAY117082 or 5 μM MG132 treatment. At the end of 24 h incubation with NFκB inhibitors, both caspase-9 and pan caspase inhibitors blocked MG132-induced apoptosis. Caspase-8 inhibitor had no effect (Fig. 4A). Corroborating, MG132 increased caspase-9 (peaked 6–12 h) and caspase-3 (peaked 12–24 h treatment) activities (Fig. 4B), and caspase-8 was not stimulated (data not shown). Moreover, inhibition of caspases with Z-VAD-fmk inhibited formation of the sub-G1 cell population in 5 μM MG132 treatment, although cells remained arrested in G2/M phase of the cell cycle (Fig. 2A).

On the other hand, BAY117082-induced cell death was insensitive to caspase inhibitors including the broad spectrum inhibitor Z-VAD-fmk (Fig. 4A). Evaluation of initiator caspase-9 and effector caspase-3 activities showed that 10 μM BAY117082 did not stimulate caspases over the 24 h of incubation (Fig. 4B). In addition, Z-VAD-fmk pre-treatment did not inhibit formation of sub-G1 in BAY117082-treated cells (Fig. 2A, right graph), suggesting a caspase-independent mechanism of cell death.

### 3.4. MG132 and BAY117082-induced ROS-dependent cell death

Pre-treatment of K562 cells with the antioxidant agents Trolox (a Vitamin E analogue) and TCEP (a cysteine reductor) at 50 μM prevented BAY117082 and MG132-induced apoptosis as assessed after 24 h treatment, suggesting a role for ROS in MG132 and BAY117082-induced cell death (Fig. 5B). In fact, BAY117082 and MG132 increased ROS production in K562 cells as assessed by DCF assay. The effect of BAY117082 occurred as early as 3 h incubation whereas MG132-induced ROS was clearly observed after 6 h incubation (Fig. 5A). NFκB inhibitors also increased ROS production in U937 and Jurkat T cells (data not shown). Thus, the increase in the level of ROS anticipated the onset of apoptosis triggered by NFκB inhibitors. Fig. 5C shows representative microphotographs of the DCF and PI/YOPRO-1 staining assays to illustrate the effect of the antioxidant TCEP on NFκB inhibitors-induced cell death and ROS production. As an index of oxidative damage, we observed that protein carbonyl groups increased from 0.12 ± 0.04 (untreated cells) to 0.22 ± 0.03 and 0.43 ± 0.06 nmol/mg of protein after 24 h treatment with BAY117082 and MG132, respectively ($p < 0.01$), confirming that NFκB inhibitors damaged cellular structures.

### 3.5. BAY117082 and MG132-induced ROS-dependent mitochondrial depolarization and cytochrome c release in K562 cells

By JC-1 assay, we observed that 10 μM BAY117082 or 5 μM MG132 induced a time-dependent decrease in mitochondrial membrane potential (MMP), which was clearly observed after 6 h incubation (Fig. 6A). Fig. 6C shows a representative fluorescence microscopy for JC-1 staining in K562 cells. After 12 h incubation with BAY117082 or MG132, significant mitochondrial depolarization was observed (decrease in red points (J-aggregates)). Pre-treatment with 200 μM TCEP blocked NFκB inhibitors-induced MMP collapse (Fig. 6C). In Fig. 6B and D are shown representative JC-1 spectra and 590/540 nm ratio, respectively, as assessed at 12 h incubation. The decrease in fluorescence emission at 590 nm (indicating decreased formation of J-aggregates) induced by BAY117082 and MG132 suggests losses in MMP ($\Delta\Psi m$), which were prevented by TCEP. Western blotting showed that BAY117082 and MG132 induced cytochrome *c* translocation from mitochondrial to cytosolic fraction, which was blocked by pre-incubation with TCEP (Fig. 6E). Taken together, these data suggest that MMP depolarization and cytochrome *c* release are

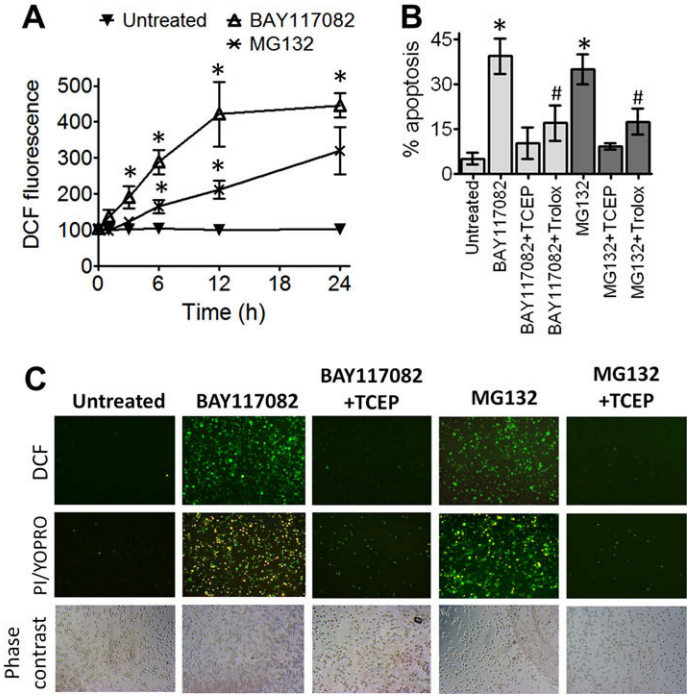


**Fig. 5.** BAY117082 and MG132 induce ROS-dependent cell death. (A) DCF assay showing the time course effect of 10 μM BAY117082 and 5 μM MG132 on ROS production in K562 cells. (B) Pre-treatment with antioxidant agents (TCEP and Trolox, 50 μM) for 1 h blocked NFκB inhibitors-induced apoptosis. Cells were treated with 10 μM BAY117082 and 5 μM MG132 for 24 h, and apoptosis was quantified by PI/YOPRO-1 staining. (C) Representative microphotographs (10× magnification) showing the effect of 50 μM TCEP on 10 μM BAY117082 or 5 μM MG132-elicited ROS production (DCF green fluorescence) and cell death (PI/YOPRO-1 fluorescence). *Different from untreated cells; #different from untreated and from its respective NFκB inhibitor-treated cells ($p < 0.01$).

consequences of the increased generation of ROS in BAY117082 and MG132-treated cells. SOD1 (cytoplasmic superoxide-dismutase) and ANT (adenine nucleotide translocase, mitochondrial) immunocontents were determined to assure the purity of cytoplasmic and mitochondrial fractions, respectively (Fig. 6E).

### 3.6. ROS sources and ROS-dependent PTP opening in BAY117082 and MG132-treated cells

In order to determine the mechanisms of ROS production, cells were pre-treated with inhibitors of diverse ROS sources. Cells were pre-incubated with inhibitors of NADPH oxidase (diphenylene iodonium (DPI), 10 μM), xanthine oxidase (allopurinol, 100 μM), intracellular calcium specific chelator (BAPTA-AM, 20 μM), extracellular calcium chelator (EGTA 4 mM) and inhibitor of the PTP/ANT (permeability transition pore/adenine nucleotide translocase) opening (bongkrekic acid, 50 μM) for 1 h. ROS, MMP and apoptosis were evaluated. Results showed that BAY117082-induced ROS was abolished by the intracellular calcium chelator BAPTA-AM (Fig. 7A). Pre-treatment with BAPTA-AM besides to inhibit ROS production also prevented MMP depolarization (Fig. 7B) and apoptosis (Fig. 7C), suggesting that mitochondria-calcium pathway is involved in apoptotic effects of BAY117082. As control, the extracellular calcium chelator EGTA did not alter BAY117082-induced ROS, MMP depolarization and apoptosis, suggesting that BAY117082 effects are attributed to intracellular calcium. Inhibitors of xanthine oxidase and NADPH oxidase had no effect. The PTP opening inhibitor bongkrekic acid

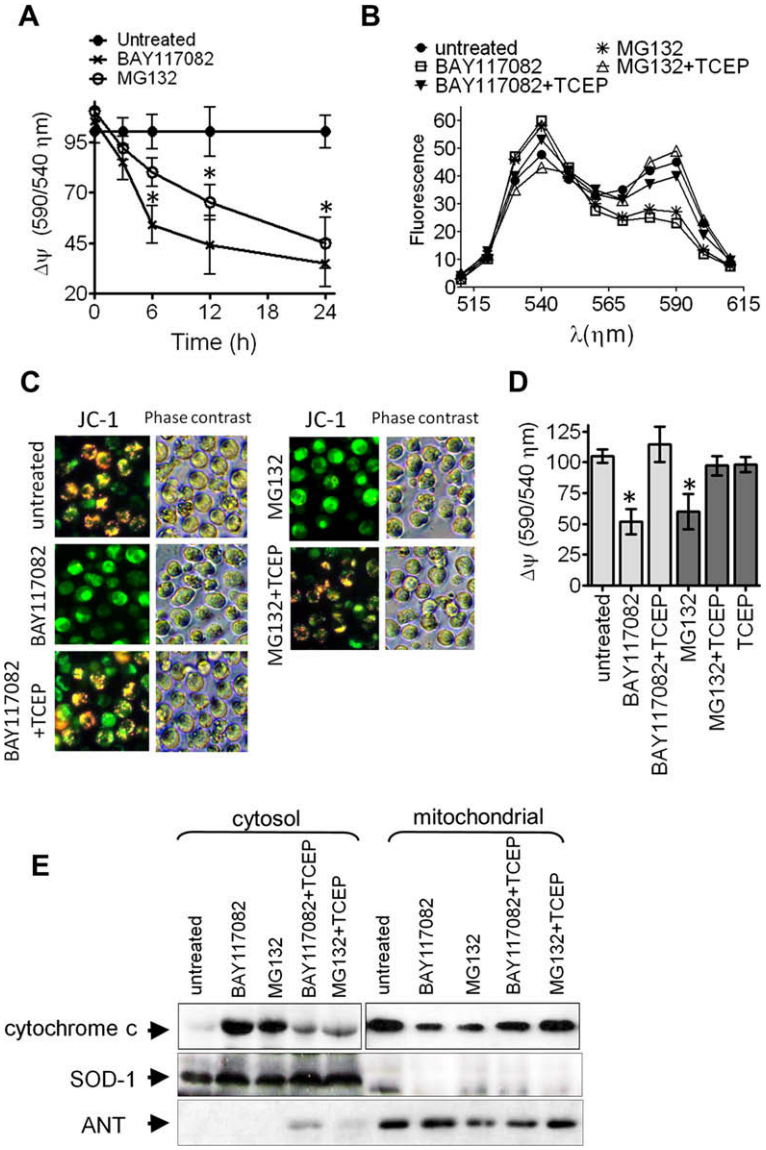


**Fig. 6.** NFκB inhibitors induce ROS-dependent mitochondrial depolarization and cytochrome *c* release. (A) Time-course of the loss of MMP. K562 cells were treated for different times with 10 μM BAY117082 or 5 μM MG132, and MMP was determined by JC-1 590/540 nm fluorescence ratio. (B) Representative JC-1 fluorescence emission spectra (510–610 nm) were taken to show that MG132 and BAY117082 treatments for 12 h decreased MMP, and antioxidant treatment with 50 μM TCEP blocked MMP depolarization. (C) Representative JC-1 confocal microscopy (20X magnification) showing the effect of 50 μM TCEP on BAY117082 or MG132-induced MMP collapse. (D) The ratio between 590 and 540 nm emission intensities gives the MMP after 12 h treatment with NFκB inhibitors plus 50 μM TCEP. (E) BAY117082 and MG132 induce cytochrome *c* release from mitochondria through redox-dependent mechanisms. Cells were treated for 12 h with 10 μM BAY117082 or 5 μM MG13210. *Different from untreated cells ($p < 0.01$).

attenuated BAY117082-induced MMP collapse and apoptosis, although no effects were observed on ROS production (Fig. 7A–C), suggesting that ROS are a prelude to PTP opening and MMP depolarization.

MG132-induced ROS only was attenuated by the cysteine reductor TCEP as assessed at 12 h incubation (Fig. 7A). Blockers of other ROS sources as NADPH oxidase, xanthine oxidase or calcium had no effects on MG132-induced ROS. As observed in BAY117082-treated cells, MG132-induced MMP depolarization and apoptosis, but not ROS production, were blocked by bongkrekic acid, suggesting that MMP collapse and apoptosis were dependent on PTP opening (Fig. 7B and C).

### 3.7. Sub-apoptotic concentrations of BAY117082 and MG132 sensitized K562 cells to doxorubicin

NFκB activation has been associated with cellular resistance of cancer cells to chemotherapeutic agents. Thus, we decided to investigate whether sub-apoptotic concentrations of the NFκB inhibitors could sensitize doxorubicin-resistant K562 cells to doxorubicin. Dox-resistant cells were selected by incubating 40 nM doxorubicin (IC50) for 24 h, followed by additional 48 h in a doxorubicin free medium to allow resistant cells growth. This protocol was repeated three times. After, cells were collected and resistance to doxorubicin was evaluated. As expected, IC50 values to doxorubicin were higher in doxorubicin-resistant cells (Fig. 8A). EMSA showed that doxorubicin-resistant cells presented increased levels of NFκB DNA-binding activity and nuclear/total p65 NFκB subunit immunocontent. In addition, Bcl-xL (an anti-apoptotic NFκB-inducible gene) protein levels were increased in doxorubicin-resistant cells compared to normal K562 cells (Fig. 8B). Doxorubicin-resistant cells also presented high levels of heat shock protein 70 (hsp70), which has been identified as a marker of cell resistance in K562 cells [33] and CML patients [34]. Incubation of doxorubicin-resistant K562 cells with 850 nM doxorubicin (~IC50) for 12 h activated NFκB, and pre-treatment with sub-apoptotic concentrations of BAY117082 (2 μM) or MG132 (1 μM) for 1 h blocked doxorubicin-induced NFκB activation (Fig. 8C) sensitizing doxorubicin-resistant cells to doxorubicin (Fig. 8D).

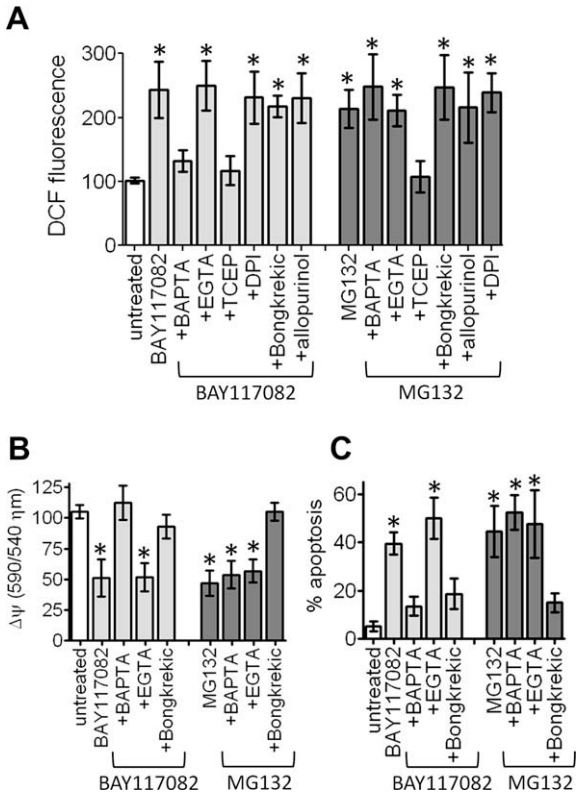


**Fig. 7.** BAY117082 and MG132-induced MMP depolarization and apoptosis are dependent on ROS-mediated PTP opening. (A) Effect of inhibitors of NADPH oxidase (DPI, 10 μM), xanthine oxidase (allopurinol, 100 μM)), calcium chelators (BAPTA-AM and EGTA) and PTP opening inhibitor (bongkrekic acid, 50 μM) on BAY117082 and MG132-induced ROS formation (DCF assay), (B) MMP depolarization and (C) apoptosis. DCF and JC-1 assays were taken after 12 h incubation. Apoptosis was assessed after 24 h treatment by PI/YOPRO-1 staining. *Different from untreated cells ($p < 0.01$).

## 4. Discussion

This work was undertaken in order to determine the potential of the NFκB inhibitors BAY117082 and MG132 as anti-proliferative and apoptotic agents in leukemia. First, we determined that the NFκB pathway inhibitors BAY117082 and MG132 were effective to decrease cell viability in leukemia cell lines (K562, Jurkat T and U937) whereas inhibitors of other classical signaling pathways as ERK, JNK, p38, PKA, PI3K/Akt, PKC and EGFR had no cytotoxic effects. Interestingly, MG132 and BAY117082 presented low toxicity to normal PBMC indicating a pattern of selectivity to tumor cells. These data altogether suggest that NFκB pathway is a potential and selective target to induce cell death in leukemia cells. In a previous work, we used BAY117082 to inhibit oxidant-induced NFκB activation in cultured Sertoli cells (non-tumoral) and, at least up to 20 μM, no cytotoxicity occurred [4]. Corroborating, treatment of normal adipose and skeletal muscle cells obtained from pregnant women with up to 100 μM BAY117082 decreased NFκB activity without effects on cell viability [35]. The higher constitutive NFκB activity in leukemia cells compared to PBMC (Fig. 3C) could explain the selectivity of BAY117082 and MG132, and possibly other NFκB inhibitors, to tumor cells [2,3,12,14–16].

BAY117082 and MG132-induced cell death occurred through mechanisms involving ROS-mitochondria pathway activation. BAY117082 caused increases in ROS, which lead to MMP depolarization and cytochrome *c* translocation. ROS production and apoptosis were mediated by alterations in intracellular calcium, since the specific intracellular calcium chelator BAPTA-AM decreased BAY117082-induced ROS, MMP depolarization and apoptosis. Inhibition of the PTP opening with bongkrekic acid attenuated MMP collapse and apoptosis, but not ROS production, suggesting that the calcium mechanism induced ROS production leading to PTP opening and MMP collapse. As consequence of the mitochondrial dysfunction, cytochrome *c* was found in the cytosol of BAY117082-treated cells. In addition, apoptotic markers as phosphatidylserine externalization, chromatin condensation and formation of sub-G1 cells were observed after BAY117082 treatment. However, neither the initiator caspase-9 nor the effector caspase-3 was stimulated, and caspase inhibitors – including the broad spectrum inhibitor Z-VAD-fmk – failed to abolish apoptosis, implying that apoptogenic activity of BAY117082 was caspase-independent. Caspase-independent/ROS-dependent apoptosis could occurs through a calcium-mediated MMP depolarization leading to translocation of apoptotic factors as AIF from mitochondria into the nucleus, which could preserve an apoptotic phenotype in absence of caspases activation [36].

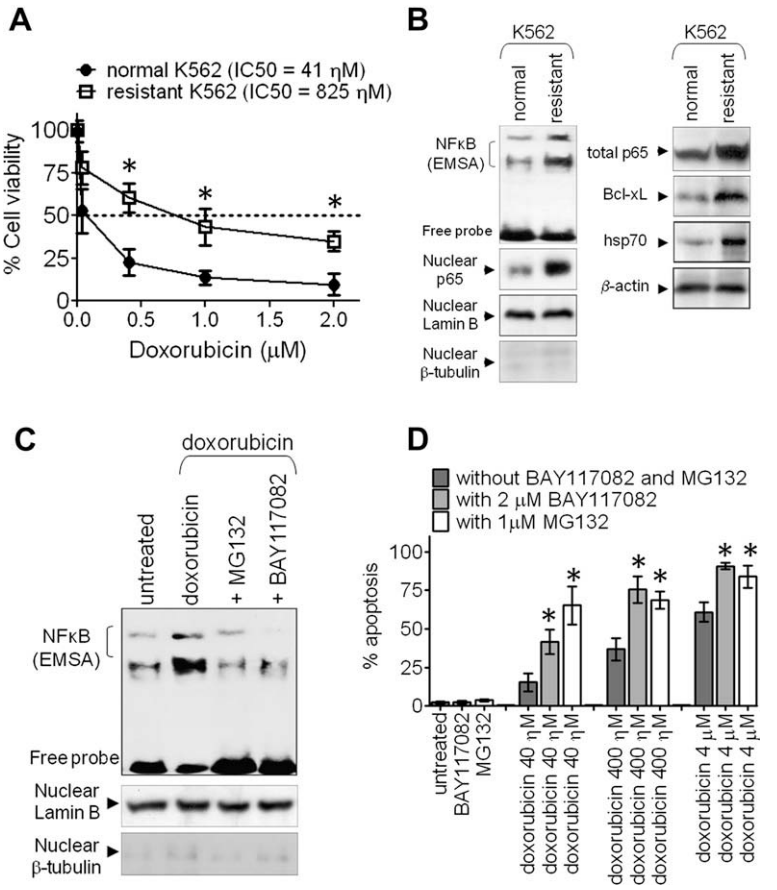


**Fig. 8.** Sub-apoptotic concentrations of NFκB inhibitors sensitized doxorubicin-resistant K562 cells. (A) MTT assay showing the resistance to doxorubicin in K562 cells. K562 and doxorubicin-resistant K562 cells were treated for 24 h with different doxorubicin concentrations. (B) NFκB DNA-binding activity, p65 immunocontent in nuclear and total cellular extracts, and total Bcl-xL and hsp70 protein levels in normal and doxorubicin-resistant K562 cells. (C) Effect of the pre-treatment with 2 μM BAY117082 or 1 μM MG132 on doxorubicin-induced NFκB activation in doxo-resistant K562 cells. Cells were treated for 12 h with 850 nM doxorubicin, and NFκB activity was assessed by EMSA. (D) Pre-treatment with 2 μM BAY117082 or 1 μM MG132 abolished doxorubicin resistance in K562 cells. Cells were treated with different concentrations of doxorubicin in the presence or absence of sub-apoptotic concentrations of NFκB inhibitors and cell death was evaluated by PI/YOPRO-1 staining. *Different from untreated cells ($p < 0.01$).

Until now, there are few studies showing the apoptotic effects of the IκB phosphorylation inhibitor BAY117082. BAY117082-induced apoptosis was yet related in Ewing's sarcoma tumors [17] and in lymphocytes isolated from CLL patients. In CLL cells, apoptosis was dependent on MMP depolarization and caspase-9 activation and, in agreement with data presented here, normal PBMC were resistant to apoptotic effects of BAY117082 [2]. In Ewing's cells, the apoptotic effects of BAY117082 were attributed to ROS, although the mechanisms of ROS production were not determined [17]. Here, we added information that a calcium-dependent mechanism of ROS production, MMP collapse and PTP opening mediated the apoptotic effects of BAY117082 in leukemia cells. The aforementioned data [2,17] and data presented in this work concern that ROS-mitochondria pathway activation plays a key role in BAY117082-induced cell death.

On the other hand, MG132 induced caspase-dependent apoptosis, which was mediated by MMP depolarization, cytochrome *c* release and caspase-9/caspase-3 activation. Such as BAY117082, MG132 increased the rate of ROS production, and antioxidant treatment blocked MMP depolarization, cytochrome *c* release and cell death. PTP inhibition blocked MMP depolarization and apoptosis, but not ROS, suggesting that ROS production was a prelude to PTP opening, MMP collapse, cytochrome *c* release, and caspase-9-dependent apoptosis. In spite of MG132 apoptotic effects have been demonstrated in diverse cell lines, this work provides new insights which are centered in the role of ROS-mitochondria apoptotic pathway activation. An explanation for MG132 (and possibly other proteasome inhibitors) pro-oxidant effects is the well-known role of proteasome in removal of oxidized proteins [37]. Since basal ROS induce oxidation of intracellular proteins, proteasome inhibitors can lead to accumulation of its oxidized proteins (as determined by carbonyl groups formation in MG132-treated cells), which are suitable to propagate ROS chain reactions leading to dysfunctions in cellular structures as mitochondria [38,39].

Important to note that, in spite of BAY117082 and MG132 have inhibited NFκB binding activity after 3 h incubation, their effects on ROS induction were rapid (<6 h), implying the time frame is too short to be primarily attributed to a down-regulation of NFκB target genes. BAY117082 and MG132 only decreased the NFκB-regulated gene products Bcl-xL and SOD2 after 12 h, suggesting that ROS formation preceded the genomic effects of the NFκB inhibition. Thus, BAY117082 and MG132 besides increasing ROS, they are preventing NFκB anti-apoptotic responses (as Bcl-xL and SOD2) due to their intrinsic NFκB inhibitory properties [6,7,9]. In this context, we previously demonstrated that NFκB inhibition potentiates cell death in pro-oxidant environments by preventing NFκB-dependent SOD2 up-regulation [4].

BAY117082 and MG132 were anti-proliferative at low concentrations. This anti-proliferative action was characterized by arrest in G2/M phase of the cell cycle. Moreover, sub-apoptotic concentrations of BAY117082 and MG132 sensitized doxorubicin-resistant K562 cells. Combination of doxorubicin with sub-apoptotic concentrations of NFκB inhibitors blocked doxorubicin-induced NFκB activation and increased doxorubicin-induced cell death, suggesting a role for NFκB in the resistance to doxorubicin. In fact, doxorubicin-resistant cells showed increased nuclear/total p65 protein, NFκB binding activity, and Bcl-xL levels consistent with the evidence that NFκB is overstimulated in resistant tumor cells [2,3,10,12,16]. In agreement with data presented here, previous studies reported that sub-apoptotic concentrations of BAY117082 and MG132 enhanced etoposide-induced apoptosis in K562 cells by inhibiting etoposide-induced NFκB activation [19]. Others reported that LBR-V160 and LBR-D160 leukemia cells (resistant to vincristine and doxorubicin) presented higher constitutive NFκB activity than the sensitive LBR-cells, and treatment with 3.5 μM BAY117082 induced a high percentage of apoptosis [21]. Taken together, data concern that combination of anticancer agents plus NFκB inhibitors could be useful to abolish cellular resistance to anticancer drugs [21,22,40]. These combinations have yet proved beneficial in pre-clinical studies with the NFκB inhibitors bortezomib and parthenolide [3,40]. Besides combination of NFκB inhibitors with classical anticancer drugs, the apoptotic and anti-proliferative properties of BAY117082 and MG132 alone also sound attractive and may be exploited for therapeutic advantage [2,17,19,21,22].

In conclusion, data presented here support the hypothesis that MG132 and BAY117082 are potential and selective anti-leukemia agents by modulating apoptosis, proliferation and drug resistance in leukemia cells. Further studies should test the usefulness (efficacy and toxicity) of these compounds in other cell lines and in models of tumor implantation.

## Conflict of interest

The authors report no conflicts of interest. The authors alone are responsible for the content and writing of the paper.

## Acknowledgements

We acknowledge the Brazilian funds CAPES, CNPq, FAURGS, and Instituto de Cardiologia de Porto Alegre for financial support.

## References

[1] M. Barkett, T.D. Gilmore, Control of apoptosis by Rel/NFκB transcription factors, Oncogene 18 (1999) 6910–6924.
[2] B.M. Pickering, S. de Mel, M. Lee, M. Howell, F. Habens, C.L. Dallman, L.A. Neville, K.N. Potter, J. Mann, D.A. Mann, P.W.M. Johnson, F.K. Stevenson, G. Packham, Pharmacological inhibitors of NF-κB accelerate apoptosis in chronic lymphocytic leukemia cells, Oncogene 26 (2007) 1166–1177.
[3] V. Baud, M. Karin, Is NF-κB a good target for cancer therapy? Hopes and pitfalls, Nat. Rev. Drug Disc. 8 (2009) 33–40.
[4] A. Zanotto-Filho, D.P. Gelain, R. Schröder, L.F. Souza, M.A. Pasquali, F. Klamt, J.C.F. Moreira, The NFkappaB-mediated control of RS and JNK signaling in vitamin A-treated cells: duration of JNK-AP-1 pathway activation may determine cell death or proliferation, Biochem. Pharmacol. 77 (2009) 1291–1301.
[5] A. Bowie, L.A. O'Neill, Oxidative stress and nuclear factor-kappaB activation: a reassessment of the evidence in the light of recent discoveries, Biochem. Pharmacol. 59 (2000) 13–23.
[6] H. Nakano, A. Nakajima, S. Sakon-Komazawa, J-H Piao, X. Xue, K. Okumura, Reactive oxygen species mediate crosstalk between NF-κB and JNK, Cell Death. Differ. 13 (2006) 730–737.
[7] C.G. Pham, C. Bubici, F. Zazzeroni, S. Papa, J. Jones, K. Alvarez, S. Jayawardena, E. De Smaele, R. Cong, C. Beaumont, F.M. Torti, S.V. Torti, G. Franzoso, Ferritin heavy chain upregulation by NF-kappaB inhibits TNF alpha-induced apoptosis by suppressing reactive oxygen species, Cell 119 (2004) 529–542.
[8] E. Smaele, F. Zazzeroni, S. Papa, D.U. Nguyen, R. Jin, J. Jones, R. Cong, G. Franzoso, Induction of gadd45b by NF-κB downregulates pro-apoptotic JNK signaling, Nature 414 (2001) 308–313.
[9] C. Bubici, S. Papa, C.G. Pham, F. Zazzeroni, G. Franzoso, NF-κB and JNK: an intricate affair, Cell Cycle 12 (2004) 1524–1529.
[10] R.Z. Orlowski, A.S. Baldwin Jr, NF-kappa B as a therapeutic target in cancer, Trends Mol. Med. 8 (2002) 385–389.
[11] N.D. Perkins, NF-kappa B: tumour promoter or suppressor?, Trends Cell Biol. 14 (2004) 64–69.
[12] J. Philipp, J. Ruland, Aberrant NF-κB signaling in lymphoma: mechanisms, consequences, and therapeutic implications, Blood 109 (2007) 2700–2707.
[13] M. Karin, Y. Cao, F.R. Greten, Z.W. Li, NF-κB in cancer: from innocent bystander to major culprit, Nat. Rev. Cancer 2 (2002) 301–310.
[14] R.R. Furman, Z. Asgary, J.O. Mascarenhas, H.C. Liou, E.J. Schattner, Modulation of NF-kappa B activity and apoptosis in chronic lymphocytic leukemia B cells, J. Immunol. 164 (2000) 2200–2206.
[15] G. Munzert, D. Kirchner, H. Stobbe, L. Bergmann, R.M. Schmid, H. Dohner, Tumour necrosis factor receptor associated factor 1 gene overexpression in B-cell chronic lymphocytic leukemia: analysis of NF-kappa B/Rel regulated inhibitors of apoptosis, Blood 100 (2002) 3749–3756.
[16] S. Cuni, P. Perez-Aciego, G. Perez-Chacon, J.A. Vargas, A. Sanchez, F.M. Martin-Saavedra, A sustained activation of PI3K/NF-kappaB pathway is critical for the survival of chronic lymphocytic leukemia B cells, Leukemia 18 (2004) 1391–1400.
[17] D.E. White, S.A. Burchill, BAY 11-7082 induces cell death through NF-κB-independent mechanisms in the Ewing's sarcoma family of tumours, Cancer Lett. 18 (2008) 212–224.
[18] R. Piva, P. Gianferretti, A. Ciucci, R. Taulli, G. Belardo, M. Gabriella Santoro, 15-Deoxy-delta12, 14-prostaglandin J2 induces apoptosis in human malignant B cells: an effect associated with inhibition of NF-κB activity and down-regulation of anti-apoptotic proteins, Blood 105 (2005) 1750–1758.
[19] A. Morotti, D. Cilloni, M. Pautasso, F. Messa, F. Arruga, I. Defilippi, S. Carturan, R. Catalano, V. Rosso, A. Chiarenza, R. Taulli, E. Bracco, G. Rege-Cambrin, E. Gottardi, G. Saglio, NF-κB inhibition as a strategy to enhance etoposide-induced apoptosis in K562 cell line, Am. J. Hematol. 81 (2006) 938–945.
[20] D. Cilloni, G. Martinelli, F. Messa, M. Baccarani, G. Saglio, NF-kappa B as a target for new drug development in myeloid malignancies, Haematologica 92 (2007) 1224–1229.
[21] M.G. García, L. Alaniz, E.C. Lopes, G. Blanco, S.E. Hajos, E. Alvarez, Inhibition of NF-κB activity by BAY 11-7082 increases apoptosis in

multidrug resistant leukemic T-cell lines, Leukemia Res. 29 (2005) 1425–1434.
[22] D. Cilloni, F. Messa, F. Arruga, I. Defilippi, A. Morotti, E. Messa, S. Carturan, E. Giugliano, M. Pautasso, E. Bracco, V. Rosso, A. Sen, G. Martinelli, M. Baccarani, G. Saglio, The NF-kappaB pathway blockade by the IKK inhibitor PS1145 can overcome imatinib resistance, Leukemia 20 (2006) 61–67.
[23] S. Gatto, B. Scappini, L. Pham, F. Onida, M. Milella, G. Ball, The proteasome inhibitor PS-341 inhibits growth and induces apoptosis in Bcr-Abl positive cell lines sensitive and resistant to imatinib mesylate, Haematologica 88 (2003) 853–863.
[24] A.P. MacLaren, R.S. Chapman, A.H. Wyllie, C.J. Watson, P53-dependent apoptosis induced by proteasome inhibition in mammary epithelial cells, Cell Death. Differ. 8 (2001) 210–218.
[25] S. Emanuele, G. Calvaruso, M. Lauricella, M. Giuliano, G. Bellavia, A. D'Anneo, R. Vento, G. Tesoriere, Apoptosis induced in hepatoblastoma HepG2 cells by the proteasome inhibitor MG132 is associated with hydrogen peroxide production, expression of Bcl-XS and activation of caspase-3, Int. J. Oncol. 21 (2002) 857–865.
[26] A. Zanotto-Filho, R. Schröder, J.C. Moreira, Xanthine oxidase-dependent ROS production mediates vitamin A pro-oxidant effects in cultured Sertoli cells, Free Radic. Res. 42 (2008) 593–601.
[27] D. Gawlitta, C.W. Oomens, F.P. Baaijens, C.V. Bouten, Evaluation of a continuous quantification method of apoptosis and necrosis in tissue cultures, Cytotechnology 46 (2004) 139–150.
[28] A. Zanotto-Filho, R. Schröder, J.C.F. Moreira, Differential effects of retinol and retinoic acid on cell proliferation: a role for reactive species and redox-dependent mechanisms in retinol supplementation, Free Radic. Res. 42 (2008) 778–788.
[29] H. Wang, J.A. Joseph, Quantifying cellular oxidative stress by dichlorofluorescein assay using microplate reader, Free Radic. Biol. Med. 27 (1999) 612–616.
[30] R.A. Gottlieb, D.J. Granville, Analyzing mitochondrial changes during apoptosis, Methods 26 (2002) 341–347.
[31] F. Klamt, E. Shacter, Taurine chloramine, an oxidant derived from neutrophils, induces apoptosis in human B lymphoma cells through mitochondrial damage, J. Biol. Chem. 280 (2005) 21346–21352.
[32] O.H. Lowry, A.L. Rosebrough, A.L. Farr, R.J. Randal, Protein measurement with the Folin phenol reagent, J. Biol. Chem. 193 (1951) 265–275.
[33] M. Pocaly, V. Lagarde, G. Etienne, M. Dupouy, D. Lapaillerie, S. Claverol, S. Vilain, M. Bonneu, B. Turcq, F.X. Mahon, J.M. Pasquet, Proteomic analysis of an imatinib resistant K562 cell line highlights opposing roles of heat shock cognate 70 and heat shock 70 proteins in resistance, Proteomics 8 (2008) 2394–2406.
[34] M. Pocaly, V. Lagarde, G. Etienne, J.A. Ribeil, S. Claverol, M. Bonneu, F. Moreau-Gaudry, V. Guyonnet-Duperat, O. Hermine, J.V. Melo, M. Dupouy, B. Turcq, F.X. Mahon, J.M. Pasquet, Overexpression of the heat-shock protein 70 is associated to imatinib resistance in chronic myeloid leukemia, Leukemia 21 (2007) 93–101.
[35] M. Lappas, K. Yee, M. Permezel, G.E. Rice, Sulfasalazine and BAY 11-7082 interfere with the nuclear factor-kB and IkB kinase pathway to regulate the release of pro-inflammatory cytokines from human adipose tissue and skeletal muscle in vitro, Endocrinology 146 (2006) 1491–1497.
[36] C. M Shih, J.S. Wu, W. C Ko, L.F. Wang, Y.H. Wei, H.F. Liang, Y.C. Chen, C.T. Chen, Mitochondria-mediated caspase-independent apoptosis induced by cadmium in normal human lung cells, J. Cell. Biochem. 89 (2003) 335–347.
[37] M. Lauricella, A. D'Anneo, M. Giuliano, G. Calvaruso, S. Emanuele, R. Vento, G. Tesoriere, Induction of apoptosis in human osteosarcoma Saos-2 cells by the proteasome inhibitor MG132 and the protective effect of pRb, Cell Death. Differ. 10 (2003) 930–932.
[38] C. C Winterbourn, I.H. Buss, T.P. Chan, L.D. Plank, M.A. Clark, J.A. Windsor, Protein carbonyl measurements show evidence of early oxidative stress in critically ill patients, Crit. Care Med. 28 (2000) 43–149.
[39] A.S. Baldwin, Control of oncogenesis and cancer therapy resistance by the transcription factor NF-kappaB, J. Clin. Invest. 107 (2001) 241–246.
[40] J. Adams, V.J. Palombella, E.A. Sausville, J. Johnson, A. Destree, D.D. Lazarus, J. Maas, C.S. Pien, S. Prakash, P.J. Elliott, Proteasome inhibitors: a novel class of potent and effective anti-tumor agents, Cancer Res. 59 (1999) 2615–2622.

III.1 – Artigo 3

# NFκB inhibitors induce cell death in glioblastomas.

Biochemical Pharmacology, 2011; 81(3): 412-424.

doi:10.1016/j.bcp.2010.10.014

Biochemical Pharmacology 81 (2011) 412–424

Contents lists available at ScienceDirect

Biochemical Pharmacology

journal homepage: www.elsevier.com/locate/biochempharm

# NFκB inhibitors induce cell death in glioblastomas

Alfeu Zanotto-Filho [a,*], Elizandra Braganhol [b], Rafael Schröder [a], Luís Henrique T. de Souza [a], Rodrigo J.S. Dalmolin [a], Matheus A. Bittencourt Pasquali [a], Daniel Pens Gelain [a], Ana Maria Oliveira Battastini [b], José Cláudio Fonseca Moreira [a]

[a] Centro de Estudos em Estresse Oxidativo, Departamento de Bioquímica, Universidade Federal do Rio Grande do Sul (UFRGS), Porto Alegre, Rio Grande do Sul, Brazil
[b] Laboratório de Enzimologia, Departamento de Bioquímica, Universidade Federal do Rio Grande do Sul (UFRGS), Porto Alegre, Rio Grande do Sul, Brazil

ARTICLE INFO

*Article history:*
Received 14 August 2010
Accepted 21 October 2010

*Keywords:*
NFκB
Glioblastoma
NFκB inhibitors
Apoptosis
Chemotherapy

ABSTRACT

Identification of novel target pathways in glioblastoma (GBM) remains critical due to poor prognosis, inefficient therapies and recurrence associated with these tumors. In this work, we evaluated the role of nuclear-factor-kappa-B (NFκB) in the growth of GBM cells, and the potential of NFκB inhibitors as antiglioma agents. NFκB pathway was found overstimulated in GBM cell lines and in tumor specimens compared to normal astrocytes and healthy brain tissues, respectively. Treatment of a panel of established GBM cell lines (U138MG, U87, U373 and C6) with pharmacological NFκB inhibitors (BAY117082, parthenolide, MG132, curcumin and arsenic trioxide) and NFκB-p65 siRNA markedly decreased the viability of GBMs as compared to inhibitors of other signaling pathways such as MAPKs (ERK, JNK and p38), PKC, EGFR and PI3K/Akt. In addition, NFκB inhibitors presented a low toxicity to normal astrocytes, indicating selectivity to cancerous cells. In GBMs, mitochondrial dysfunction (membrane depolarization, bcl-xL downregulation and cytochrome c release) and arrest in the G2/M phase were observed at the early steps of NFκB inhibitors treatment. These events preceded sub-G1 detection, apoptotic body formation and caspase-3 activation. Also, NFκB was found overstimulated in cisplatin-resistant C6 cells, and treatment of GBMs with NFκB inhibitors overcame cisplatin resistance besides potentiating the effects of the chemotherapeutics, cisplatin and doxorubicin. These findings support NFκB as a potential target to cell death induction in GBMs, and that the NFκB inhibitors may be considered for in vivo testing on animal models and possibly on GBM therapy.



## 1. Introduction

Glioblastoma (GBM) is an aggressive, invasive, and difficult to treat primary brain tumor. Standard therapy includes surgical resection, external beam radiation and chemotherapy, with no known curative therapy [1]. A number of dysregulated signaling cascades have been described in GBMs, including the MEK/ERK pathway, PLC/PKC pathway, and the PI3K/Akt pathway. Dysregulation of these pathways is driven by mutation, amplification, or overexpression of multiple genes such as PTEN, EGFR, PDGFR-a, p53, and mTOR [2–4]. Understanding these dysregulated pathways has provideded the basis for designing molecular targeted therapies as monoclonal antibodies against EGF, VEGF and PDGF receptors, as well as new combination therapies and drug delivery systems [4–6]. Despite these new treatment strategies, median survival has remained approximately 1 year for decades [1]. Thus, it is urgent to determine novel molecular targets in GBMs in order to develop more effective therapies and new therapeutic opportunities to patients.

Studies have compelling evidence that the transcription factor NFκB (Nuclear factor κB) plays a role in the control of oncogenesis, tumor progression and chemotherapy resistance of diverse types of malignances as lymphoma, leukemia, breast and ovarian cancers [7–11]. NFκB is formed by homo or heterodimers comprising members of the Rel family of proteins (p50/p105, p52/p100, p65, c-Rel and RelB) which form, upon non-stimulated conditions, a ternary and inactive cytoplasmic complex by interacting with inhibitory proteins of the IκB family. Upon stimulation by cytokines (TNF-alpha and IL1-beta), growth factors (EGF and PDGF), anticancer drugs (cisplatin, doxorubicin and vincristine) and other stressor stimuli, IκBs are phosphorylated by IKK (IκB kinase) proteins thus releasing the active NFκB, which translocates into nucleus and binds to DNA sequences in gene promoters. NFκB binding to DNA modulates the expression of a wide range of genes as that involved in inflammation (IL1-beta, IL-6, COX2, and TNF), apoptosis resistance (bcl-xL, cIAP1/2, XIAP, FLICE and survivin), cell

* Corresponding author at: Depto. Bioquímica (ICBS-UFRGS), Rua Ramiro Barcelos, 2600/Anexo, Porto Alegre CEP 90035-003, Rio Grande do Sul, Brazil. Tel.: +55 51 3308 5578; fax: +55 51 3308 5535.
*E-mail address:* alfeuzanotto@hotmail.com (A. Zanotto-Filho).

0006-2952/$ – see front matter © 2010 Elsevier Inc. All rights reserved.
doi:10.1016/j.bcp.2010.10.014

invasion (ICAM-1, VCAM-1, MMP2, MMP9), angiogenesis (VEGF), proliferation (cyclin D1, MYC) and metastasis (CXCR4 and TWIST) [7–12]. These groups of genes are directly related to tumor-associated phenomena suggesting NFκB as a potential target to cell death induction and chemosensitization in cancer [9,13–15].

Aberrant NFκB activity has been described in some types of cancer cells upon basal and following anticancer drugs treatments. Besides, constitutive NFκB up-regulation has been found in chemotherapy-resistant cell lines, which correlates with therapy failure [9,13,15–17]. In this context, studies have suggested that molecules with NFκB inhibitory properties are potential anticancer agents [9,15,17,18]. In this intent, researchers have blocking NFκB activity via IKK/NFκB inhibitors (as BAY117082, BAY117085, parthenolide, curcumin, arsenic trioxide and PDTC) or proteasome/NFκB inhibitors (PS-341 and MG132) in order to inhibit the growth of myeloma [10], leukemia [17,19], esophageal [14] and breast cancer cells [20]. Recently, analysis of brain tumor biopsies identified that NFκB and its target genes are overexpressed in GBM and astrocytoma tumors compared to normal brain tissues [21,22]. In addition, a positive correlation between NFκB activation and poor GBM prognosis was reported, suggesting that the known role of NFκB as a survival factor in other cancers could also be considered in GBMs [23]. Taken into account the aforementioned, this study was undertaken in order to determine the role of NFκB in GBM growth, and the selectivity, apoptotic potential and chemosensitizing activity of the NFκB inhibitors BAY117082, parthenolide, curcumin, arsenic trioxide, MG132, and p65 small-interfering RNA in GBM cell lines.

## 2. Materials and methods

### 2.1. Reagents and antibodies

BAY117082 ((E)3-[(4-methylphenyl)-sulfonyl]-2-propenenitrile); MG132 (Z-Leu-Leu-Leu-CHO), curcumin, arsenic trioxide, propidium iodide, Hepes, CHAPS, dithiothreitol, EDTA, trypsin, MTT (3-(4,5-dimethyl)-2,5-diphenyl tetrazolium bromide), Nonidet-P40, spermin tetrahydrochloride, RNAse A and culture analytical grade reagents were purchased from Sigma Chemical Co. (St. Louis, MO, USA). Anti-NFκB p65 rabbit polyclonal antibody and anti-Lamin B were from Santa Cruz Biotechnologies; anti-β-actin was from Cell Signaling Technology; SP600129 was from Promega Corporation (Madison, USA). SB203580 were from Merck Biosciences (Darmstadt, Germany). Anti-cytochrome c antibody was from BD PharMingen (San Diego, USA). Parthenolide, LY294002, UO126 and Gö6983 were from Biomol International (Plymouth Meeting, PA). PD158780 was from Tocris Bioscience (MO, USA). Electrophoresis/immunoblotting reagents were from Bio-Rad Laboratories (Hercules, CA, USA).

### 2.2. Cell cultures

The rat (C6) and human (U138MG, U87 and U373) malignant GBM cell lines were obtained from American Type Culture Collection (Rockville, MD, USA). Cells were grown and maintained in low glucose Dulbecco's modified Eagle's medium (DMEM; Gibco BRL, Carlsbad, USA), containing 0.1% Fungizone, 100 U/l gentamicin and supplemented with 10% fetal bovine serum. Cells were kept at 37 °C in a humidified atmosphere with 5% $CO_2$. Primary astrocyte cultures were prepared as previously described [24]. Briefly, cortex of newborn Wistar rats (1–2 days old) was removed and mechanically dissociated in a $Ca^{2+}$ and $Mg^{2+}$ free balanced salt solution (137 mmol/L NaCl, 5.36 mmol/L KCl, 0.27 mmol/L $Na_2HPO_4$, 1.1 mmol/L $KH_2PO_4$, 6.1 mmol/L glucose; pH 7.4). After centrifugation at 1000 rpm (5 min), the pellet was resuspended in DMEM supplemented with 10% FBS. The cells ($2 \times 10^5$) were plated in 48 multi-well plates pretreated with poly-L-lysine. After 4 h platting, plates were gently shaken, cells were washed with PBS, and medium was changed to remove neuron and microglia contaminants. Cultures were allowed to grow by 20–25 days (100% confluence). Medium was replaced every 4 days.

### 2.3. MTT and LDH assays

Dehydrogenase-dependent MTT reduction (MTT assay) and lactate dehydrogenase release into culture medium from cells with losses in membrane integrity (LDH assay) were used as an estimative of cell viability [15,17]. Cells were plated in 96-well plates ($10^4$/well) and treated after to reach 60–70% confluence as detailed in Section 3. At the end of incubation, MTT and LDH assays were performed. Lactate dehydrogenase (LDH) release into culture medium was determined by fluorescent assay kit (CytoTox 96-NonRadioactive Cytotoxicity Assay, Promega) as recommended by the manufacturer. Qualitative morphology of the cell cultures was also evaluated by light microscopy (Nikon Eclipse TE 300), and the cell cultures were classified as: normal (cells with unaltered morphology and normal density); low-density (cell with normal morphology and low-density/lower number in plates); and dead cells (altered cellular/nuclear morphology, cytoplasm vacuolization, and presence of detached cells).

### 2.4. Propidium iodide incorporation and staining of chromatin

For the determination of propidium iodide (PI) uptake in cells with losses in membrane integrity, treated cells were incubated with 2 μg/mL PI in complete medium for 1 h. PI fluorescence was excited at 515–560 nm using an inverted microscope (Nikon Eclipse TE 300) fitted with a standard rhodamine filter. Representative microphotographs (at least 5/well) were collected [25]. For the detection of the morphological alterations in chromatin (condensation and fragmentation) and apoptotic body formation, cells were fixed in methanol/acetone (1:1) for 5 min and washed with PBS (3 times). Then, chromatin was stained with PI (0.5 μg/mL, 10 min) followed by fluorescent microscopy (Nikon Eclipse TE 300).

### 2.5. Cell cycle analysis

For cell cycle analysis, cells were trypsinized, centrifuged and resuspended in a lysis buffer (3.5 mmol/L trisodium citrate, 0.1% (v/v) Nonidet P-40, 0.5 mmol/L Tris–HCl, 1.2 mg/mL spermine tetrahydrochloride, 5 μg/mL RNAse, 5 mmol/L EDTA, 1 μg/mL propidium iodide, pH 7.6), vortexed and incubated for at least 10 min on ice for cell lysis. DNA content was determined by flow cytometry. Ten thousand events were counted per sample. FACS analyses were performed in the CellQuest Pro software (BD Biosciences, CA) [17].

### 2.6. Caspase-3 activity

Caspase-3 activity was assessed in agreement with CASP3F Fluorimetric kit (Sigma, St. Louis/MI). Treated cells were harvested and incubated in a lysis buffer (50 mmol/L Hepes, 5 mmol/L CHAPS and 5 mmol/L dithiothreitol, pH 7.4) for 20 min in ice. Later, extracts were clarified by centrifugation at 13,000 × *g* (15 min, 4 °C). Supernatants were collected and proteins were measured by Bradford method. For assays, 150 μg proteins were mixed with 200 μL of the assay buffer (20 mmol/L Hepes, 0.1% CHAPS, 5 mmol/L dithiothreitol, 2 mmol/L EDTA, pH 7.4) plus 20 μM Ac-DEVD-AMC (Acetyl-Asp-Glu-Val-Asp-7-amido-4-methylcoumarin), a caspase-3 specific substrate. Caspase-3-mediated substrate cleavage was monitored for 1 h (37 °C) in a fluorimetric reader (excitation 360 nm/emission 460 nm) [17].

### 2.7. Cellular fractionation

For nuclear extracts preparation, cells (~$5 \times 10^6$, 70–80% confluence) were washed with cold phosphate-buffered saline (PBS) and suspended in 0.4 mL hypotonic lysis buffer (10 mmol/L HEPES (pH 7.9), 1.5 mmol/L $MgCl_2$, 10 mmol/L KCl, 0.5 mmol/L phenylmethylsulfonyl fluoride, 0.5 mmol/L dithiothreitol plus protease inhibitor cocktail (Roche)) for 15 min. Cells were then lysed with 12.5 μL 10% Nonidet P-40. The homogenate was centrifuged (13,000 × *g*, 30 s), and supernatants containing the cytoplasmic extracts (fraction 1) were stored at −80 °C. The nuclear pellet was resuspended in 100 μL ice-cold hypertonic extraction buffer (10 mmol/L HEPES (pH 7.9), 0.42 M NaCl, 1.5 mmol/L $MgCl_2$, 10 mmol/L KCl, 0.5 mmol/L phenylmethylsulfonyl fluoride, 1 mmol/L dithiothreitol plus protease inhibitors). After 40 min of intermittent mixing, extracts were centrifuged (13,000 × *g*, 10 min, 4 °C), and supernatants containing nuclear proteins were secured. To detect cytochrome c release from mitochondria, mitochondria-free cytoplasmic extracts were obtained from centrifugation of the cytoplasmic extracts (fraction 1) at 14,000 × *g*, 20 min, 4 °C. The resultant supernatant (mitochondria-free cytosolic proteins) and mitochondrial pellets were stored at −80 °C. The protein content was measured by the Bradford method [17,26].

### 2.8. NFκB-p65 ELISA assay for the determination of NFκB activity

A total of 10 μg of nuclear extracts was used to determine NFκB activation (NFκB p65 ELISA kit, Stressgen/Assays designs) as per the manufacturer protocols. This ELISA-based chemiluminescent detection method rapidly detects activated NFκB complex binding (p65 detection) to a plate-adhered NFκB consensus oligonucleotide sequence. Kit-provided nuclear extracts prepared from TNF-stimulated Hela cells were used as a positive control for NFκB activation. To demonstrate assay specificity, a 50-fold excess of an NFκB consensus oligonucleotide was used as competitor to block NFκB binding. In addition, a mutated consensus NFκB oligonucleotide (which do not binds NFκB) is provided for the determination of binding reactions' specificity [15].

### 2.9. siRNA knockdown of the NFκB protein p65

The Silencer® Select Validated NFκB-p65 siRNA (siRNA ID# s11914; Ambion® Inc.) was transfected using the siPORT™ NeoFX™ Transfection Agent (Ambion®, Applied Biosystems Inc.) in agreement with manufacturer's protocol. U138MG cells were transfected with 50–100 nM of NFκB-p65 siRNA by reverse transfection and then incubated for 72 h in Opti-MEM to allow knockdown of the p65 protein, which was confirmed by Western blotting. Silencer® Select Negative Control#1 siRNA containing scrambled sequences was used as negative control.

### 2.10. Immunocytochemistry for NFκB p65 localization

For the determination of subcellular distribution of NFκB, cells were cultured up to 60–70% confluence in 12-well plates. After a brief washing with PBS, cells were fixed in 4% (v/v) formaldehyde in PBS for 20 min at room temperature. Fixed cells were rinsed three times with PBS and then permeabilized with 0.5% Triton X-100 in PBS for 15 min at room temperature. After that, cells were washed with PBS and blocked with 5% BSA for 1 h. At the end of incubation, cells were incubated with rabbit anti-p65 polyclonal antibody (1:500; overnight at 4 °C), and then incubated with a goat anti-rabbit IgG Alexa 594-conjugated antibody (1:500) for 2 h at room temperature. Cells were visualized in a fluorescence microscope (Nikon Eclipse TE 300) [27].

### 2.11. Western blotting

Proteins (20 μg) were separated by SDS-PAGE on 10% (w/v) acrylamide, 0.275% (w/v) bisacrylamide gels, and electrotransfered onto nitrocellulose membranes. Membranes were incubated in TBS-T (20 mmol/L Tris–HCl, pH 7.5, 137 mmol/L NaCl, 0.05% (v/v) Tween 20) containing 1% (w/v) non-fat milk powder for 1 h at room temperature. Subsequently, the membranes were incubated for 12 h with the appropriate primary antibody (dilution range 1:500–1:1000), rinsed with TBS-T, and exposed to horseradish peroxidase-linked anti-IgG antibodies for 2 h at room temperature. Chemiluminescent bands were detected using X-ray films, and densitometry analyses were performed using Image-J® software.

### 2.12. Mitochondria membrane potential (JC-1 assay)

For the determination of the mitochondrial membrane potential (MMP), treated cells ($5 \times 10^5$) were incubated for 30 min at 37 °C with the lipophilic cationic probe JC-1 (5,5′,6,6′-tetrachloro-1,1′,3,3′ tetraethylbenzimidazolcarbocyanine iodide, 2 μg/mL). After that, JC-1-loaded cells were centrifuged and washed once with PBS. Cells were transferred to a 96-well plate and assayed in a fluorescence plate reader with the following settings: excitation at 485 nm, emission at 540 and 590 nm, and cutoff at 530 nm (SpectraMax M2, Molecular Devices, USA). $\Delta\Psi_m$ was calculated using the ratio of 590 nm (J-aggregates)/540 nm (monomeric form) [28].

### 2.13. Clonogenic potential

Exponentially growing cells ($1 \times 10^6$) were plated in Petri plates overnight, and then incubated for 36 h with either vehicle or NFκB inhibitors. After treatments, the medium containing NFκB inhibitors was replaced by a new medium without the tested compounds, and remaining cells were maintained for additional 24 h to growth. Survival cells were gently washed and trypsinized, and viability was assessed by Trypan Blue staining. Viable cells ($10^4$ cells) were re-plated in 6-well plates and maintained for additional 6 days in complete culture medium. Cell growth was estimated by colony counting followed by MTT assay [15,29]. The percentage of colony forming efficiency was calculated in relation to values of untreated cells.

### 2.14. Soft agar colony assay

Cells ($1 \times 10^5$) were resuspended in 2 mL DMEM supplemented with 15% FBS and mixed with 1 mL of 1.6% agarose (final conditions: 0.53% agarose and 10% FBS) at 37 °C. Cell suspensions were placed on top of a base layer comprising 2 mL of DMEM with 10% FBS and 0.8% agarose in each well of a six-well plate. Cells were then covered with 2 mL of complete media and, after 3 days, a new medium containing NFκB inhibitors was added. Media containing treatments or vehicle were replaced every 72 h. At the end of 9 days, MTT (1 mg/mL) was added to the cultures and the number of colonies was scored using a microscope [15].

### 2.15. NFκB gene/protein-association network and landscape analysis of gene expression

The NFκB gene/protein interaction network was constructed by associating 46 NFκB-induced and cancer-related human genes involved in antiapoptotic defenses (14 genes), proliferation (8 genes), inflammation (10 genes) and invasion/metastasis/angiogenesis (9 genes), besides the NFκB subunits (5 genes). Genes were selected based on current literature [7,11,30,31]. Briefly, the network is generated using STRING database [32] with input

options 'databases', 'experiments', 'textmining' and 0.700 confidence level. STRING integrates different curate and public databases containing information on direct and indirect functional protein–protein associations/interactions. Each protein is identified according to both HUGO Gene Symbol [33] and Ensembl Peptide ID [34]. The selected gene list is applied in the STRING database and the links (interaction strength) between two different genes are saved in data files, which were handled in the Medusa software [35].

After being constructed, the NFκB gene network was analyzed by the ViaComplex software, which was previously developed and validated in our laboratory [36]. ViaComplex plots the gene expression activity over the Medusa network topology. To do this, ViaComplex overlaps functional information (micro-array expression data) with interaction information (the NFκB network) and distributes the microarray signal according to the coordinates of the network objects (i.e. nodes and links) thus constructing 3D landscape modules. Microarray expression data were collected from the international repository Gene Expression Omnibus (GEO-accession number: GSE12657; Platform: GPL8300, Affymetrix), and were composed of 20 human gliomas – 7 GBM; 7 oligodendroglioma (ODG); 6 pilocytic astrocytoma (PA) – which were compared to 5 healthy brain (HB) control biopsies. For each gene, means of each gene expression in each glioma type was plotted over the expression of the same gene in healthy brains (HB), and landscapes were constructed. Gene expression in GBM, ODG and PA versus HB tissues was statistically analyzed by *t*-test, and *p*-values were calculated.

### 2.16. Statistical analysis

Data are expressed as means ± SD and were analyzed by one-way ANOVA followed by Duncan's post hoc test. Differences were considered significant at $p < 0.05$.

## 3. Results

### 3.1. NFκB as potential target to cell death induction in GBMs

Initially, we treated U138MG and C6 cells with inhibitors of some signaling pathways which are described as dysregulated in GBMs and other cancers [2–4]. Inhibitors of PI3K/Akt (LY294002, wortmannin), EGFR (PD158780), MEK/ERK1/2 (UO126), JNK1/2 (SP600129), p38 MAPK (SB203580), PKC (Gö6983), proteasome/NFκB (MG132) and IKK/NFκB (BAY117082) were tested at different concentrations (1–60 μM) based on the literature range and manufacturer instructions, which describe $IC_{50}$ values < 20 μM for all the tested drugs. At the end of 36 h incubation, only the compounds with NFκB inhibitory activity (BAY11082 and MG132) promoted significant decreases in GBM viability compared to inhibitors of other tested signaling pathways (Table 1). NFκB inhibitors reduced viability as assessed by MTT assays, increased LDH release in culture medium and altered cell

**Table 1**
Effect of cell signaling pathway inhibitors on viability of GBMs.

| Treatments | Viability (MTT assay) | | LDH | Qualitative morphology |
|---|---|---|---|---|
| | C6 | U138MG | U138MG | U138MG |
| Untreated | 100 ± 4 | 100 ± 6 | 100 ± 11 | Normal |
| UO126 (30 μM) | 93 ± 15 | 96 ± 7 | 92 ± 10 | Normal |
| SP600129 (30 μM) | 103 ± 11 | 101 ± 4 | 109 ± 6 | Normal |
| SB203580 (30 μM) | 98 ± 10 | 95 ± 6 | 101 ± 5 | Normal |
| LY294002 (50 μM) | 64 ± 17* | 74 ± 4* | 108 ± 9 | Low-density |
| Wortmannin (10 μM) | 85 ± 5* | 75 ± 9* | 102 ± 4 | Low-density |
| Gö6983 (30 μM) | 96 ± 9 | 95 ± 7 | 111 ± 7 | Normal |
| PD158780 (50 μM) | 99 ± 4 | 96 ± 5 | 112 ± 6 | Normal |
| MG132 (5 μM) | 21 ± 14* | 23 ± 17* | 223 ± 38* | Dead cells |
| BAY117082 (30 μM) | 15 ± 6* | 36 ± 9* | 554 ± 39* | Dead cells |

C6 and U138MG cells were treated for 36 h with well-established pathway inhibitors and MTT, LDH and qualitative microscopy assays were performed. Experiments were repeated three times ($n = 3$) in triplicate, and data were expressed in mean ± SD.
* Different from untreated cells in each type of assay.

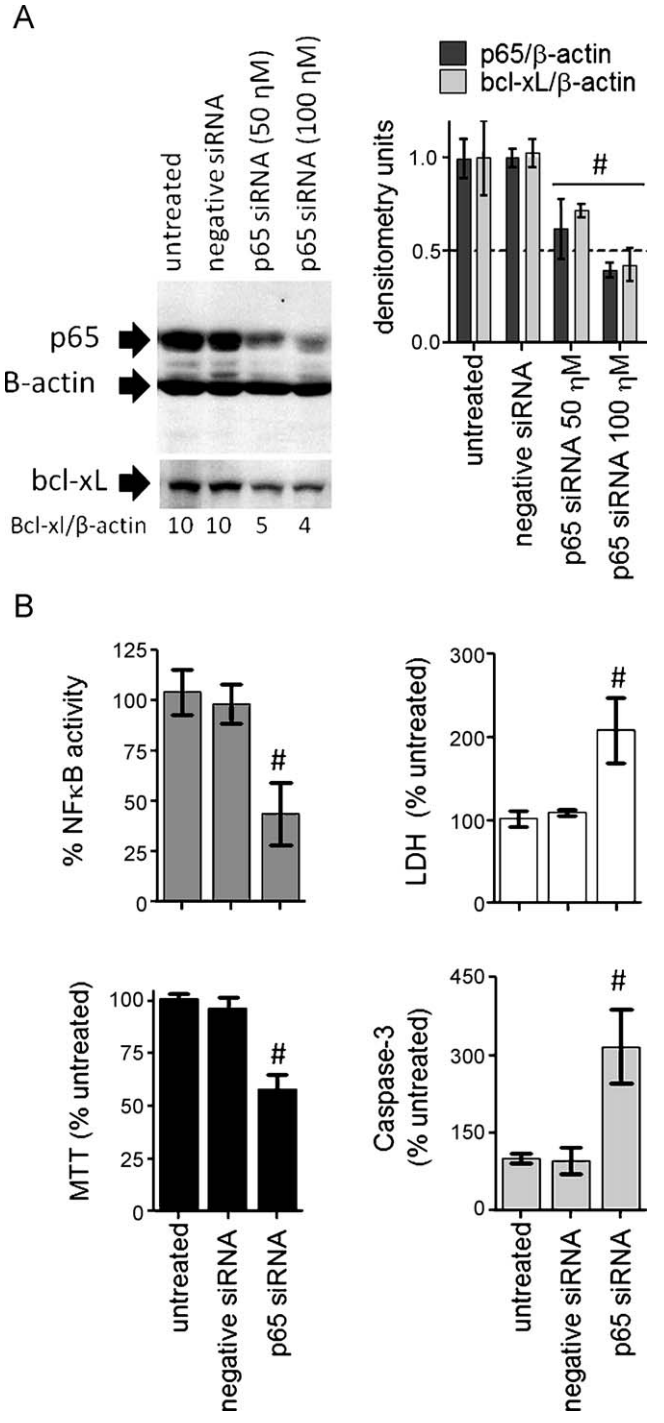


**Fig. 1.** NFκB-p65 knockdown induces apoptotic cell death in U138MG cells. (A) Representative immunoblotting and densitometry for the determination of p65 knockdown efficiency and bcl-xL levels. U138MG cells were incubated for 72 h with 50 or 100 nM p65 siRNA and cellular extracts were collected. (B) MTT, LDH, caspase-3 activity and NFκB ELISA assays in p65-downregulated U138MG cells. For these experiments, cells were incubated for 72 h with 100 nM p65 siRNA. All experiments were performed in triplicate. Graphs were expressed in mean ± SD. #Different from untreated cells from its respective assay.

morphology as indicative of cell death (Table 1 and Fig. 3A). Although the PI3K/Akt inhibitors LY294002 and wortmannin decreased MTT values, the absence of both LDH release and alterations in cell morphology, besides the observed decreases in cell density, suggests that PI3K/Akt inhibition affected GBM cell proliferation, but not induced cell death (Table 1). Thus, we decided to perform our further experiments with NFκB inhibitors. MAPKs (JNK, p38 and ERK1/2), EGFR, PKC inhibitors did not present cytotoxic effects up to 60 μM (data not shown). As control, we also performed Western blotting for the detection of the basal levels of phosphorylated forms of MAPKs (JNK, p38 and ERK1/2), Akt and PKC substrates; ELISA assay was performed to detect NFκB activity. Of the tested pathways, only PI3K/Akt and NFκB were detected at basal/non-stimulated conditions (data not shown).

### 3.2. NFκB-p65 member knockdown induces apoptosis in GBM cells

To assess the specific role of NFκB in GBM cells survival, we performed siRNA experiments to knockdown the NFκB p65 member in human U138MG cells. Immunoblotting confirmed the p65 siRNA protocol efficiency to down p65 protein after 72 h incubation with siRNAs (Fig. 1A). p65 knockdown was accompanied by the inhibition of NFκB DNA-binding activity (Fig 1B, upper left panel) and by decreases in bcl-xL protein levels (Fig. 1A), a classical antiapoptotic NFκB target gene product [7,11,13], thus confirming the effect of p65 knockdown upon NFκB signaling. As a consequence of NFκB downregulation, cell viability decreased by 45–55% as assessed by MTT. Detection of increased LDH release into culture medium and caspase-3 activation confirmed cell death induction in p65-silenced cells (Fig. 1B).

### 3.3. NFκB is up-regulated in GBMs compared to non-tumor astrocytes

NFκB overstimulation has been observed in several cancer cell lines as a consequence of cytokine overproduction, mutations, cell cycle dysregulation and apoptosis resistance [8,15,19]. In C6 and U138MG, we found a 5–10-fold increase in the basal activity of NFκB compared to primary astrocytes as assessed by NFκB p65 ELISA (Fig. 2A). LPS-treated cells (0.5 μg/mL, 3 h) were used as positive control for NFκB activation. Assay specificity was assessed by the incubation of nuclear extracts with a 50-fold excess of an unlabeled oligonucleotide containing the NFκB consensus sequence, which completely inhibited the constitutive NFκB binding (C6 + 50X lane). In addition, mutated NFκB oligonucleotides did not alter the constitutive NFκB activity confirming the specificity of binding reactions (C6 + mut lane, Fig. 2A). Determination of total and nuclear p65 immunocontent confirmed that a significant fraction of p65 is found in nuclear compartment of GBM cells whereas astrocytes expressed predominantly cytoplasmic/latent p65 (Fig. 2B). In C6 cells, nuclear accumulation of p65 was more accentuated. Detection of Lamin B and absence of Adenine Nucleotide Translocator (ANT) were assessed to confirm the purity of nuclear extracts (Fig. 2B). Immunocytochemistry to p65 confirmed the accumulation of p65 in nuclear compartment of C6 cells, corroborating with the Western blotting data shown in Fig. 2C.

### 3.4. Landscape analysis of NFκB target genes expression in human gliomas

Besides in vitro detection of NFκB in GBM cell lines (Fig. 2), we decided to test whether the cancer-related NFκB target genes are

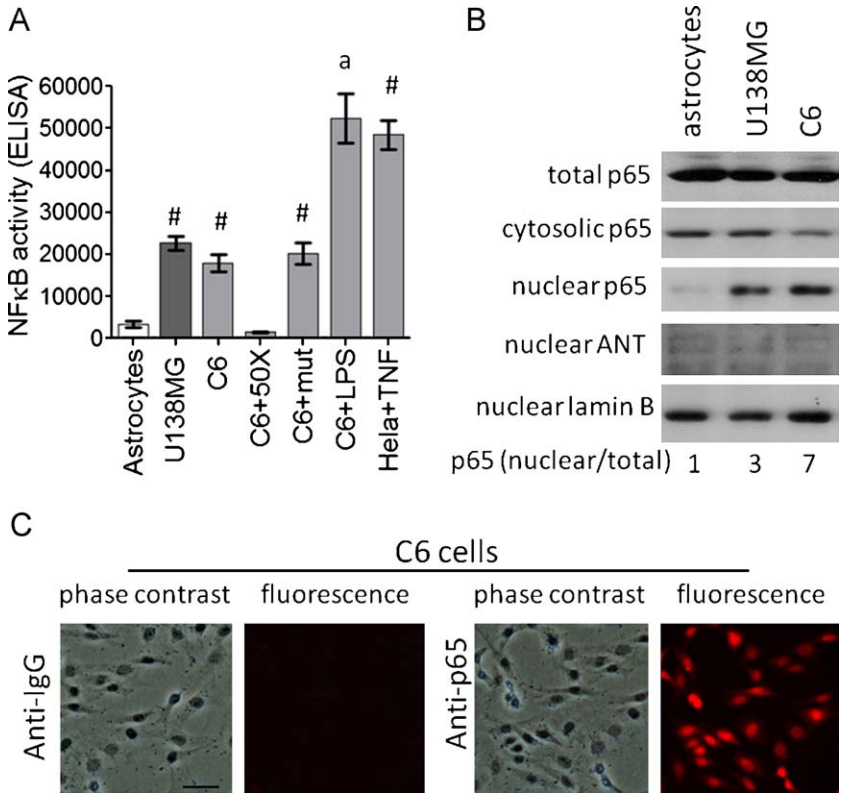


**Fig. 2.** NFκB is up-regulated in GBMs compared to primary astrocytes. (A) Basal NFκB activation in nuclear extracts isolated from C6, U138MG and astrocytes as assessed by ELISA. (B) Representative Western blotting showing p65 protein compartmentalization in C6, U138MG and astrocytes. (C) Representative immunocytochemistry for p65 in C6 cells (20× magnification). In these experiments, cells were maintained in basal conditions (complete culture medium for 48 h) and nuclear and cytoplasmic extracts were isolated to detect NFκB activity, p65 immunocontent, or fixed for immunocytochemistry. Lamin B and ANT levels in nuclear extracts were used as controls of nuclear extract purity. [#]Different from astrocytes; [a]different from its respective untreated cell line ($p < 0.05$, ANOVA, $n = 3$).

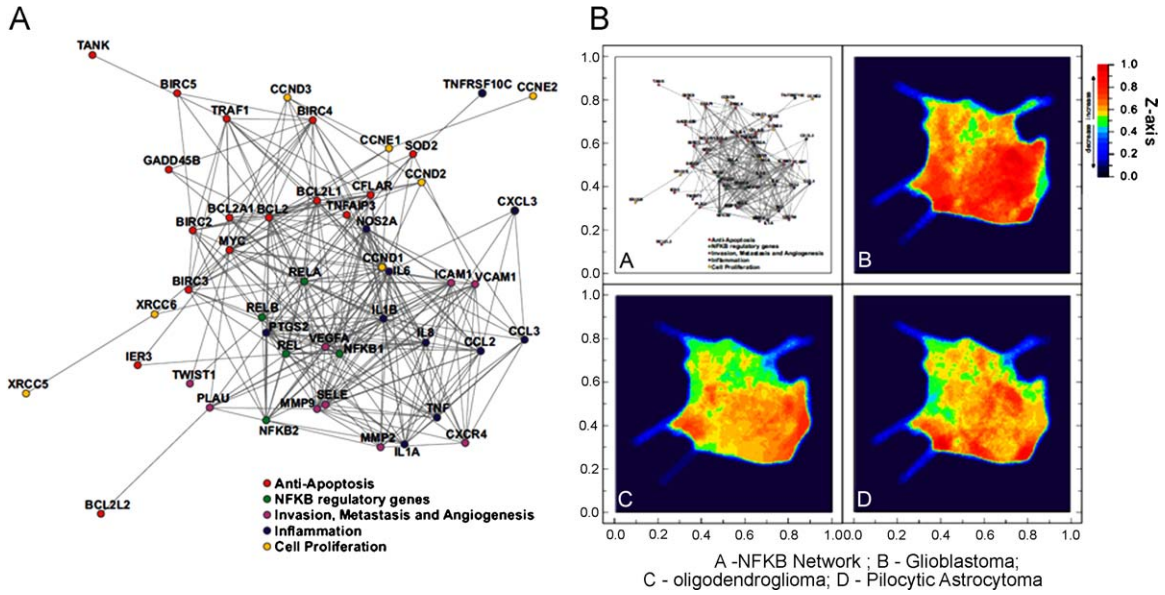


**Fig. 3.** Landscape analysis of NFκB gene/protein interaction networks in gliomas. (A) NFκB-target gene interaction network. Network was generated using STRING database. Gene symbol was collected from HUGO, and interactions were handled in Medusa software for network construction. (B) Landscape analysis of NFκB network gene expression in clinical specimens of glioblastoma (B panel), oligodendroglioma (C panel) and pilocytic astrocytoma (D panel). Gene expression in different types of glioma was plotted against gene expression in healthy brain tissues, and *Z*-axis for relative gene expression was constructed using the ViaComplex software.

modulated in human GBM biopsies. We collected microarray experiments containing the gene expression pattern for different glioma grades [pilocytic astrocytoma (PA), oligodendroglioma (ODG) and glioblastoma multiforme (GBM)], besides health brain (HB) biopsies. First, we constructed an NFκB gene/protein interactions network (Fig. 3A), which was subsequently analyzed by ViaComplex software as described in Section 2. ViaComplex landscapes were constructed by plotting gene expression values of each different glioma types over HB gene expression. ViaComplex-constructed *Z*-axis gives the relative gene expression in gliomas over gene expression in healthy brains. Fig. 3B shows that NFκB gene interaction network was up-regulated in the 3 grades of

**Table 2**
Normalized expression of NFκB-target genes in healthy brains (HB), glioblastoma (GBM), oligodendroglioma (ODG) and pilocytic astrocytoma (PA) specimens.

| Gene function | Invasion/angiogenesis/metastasis | | | | | | | | Antiapoptosis | | | | Inflammation | |
|---|---|---|---|---|---|---|---|---|---|---|---|---|---|---|
| | MMP9 | MMP2 | CXCR4 | ICAM1 | PLAU | VCAM1 | VCAM2 | VEGFA | SOD2 | MYC | A20 | IER3 | CCL2 | IL8 |
| HB1 | 102 | 130 | 304 | 106 | 102 | 148 | 136 | 92 | 70 | 118 | 177 | 112 | 320 | 97 |
| HB2 | 109 | 114 | 61 | 107 | 73 | 38 | 89 | 88 | 10 | 107 | 121 | 65 | 30 | 139 |
| HB6 | 99 | 72 | 44 | 98 | 44 | 117 | 91 | 98 | 251 | 60 | 71 | 112 | 20 | 95 |
| HB7 | 95 | 93 | 63 | 93 | 54 | 136 | 91 | 113 | 394 | 71 | 67 | 81 | 27 | 85 |
| HB11 | 94 | 91 | 28 | 96 | 226 | 61 | 93 | 108 | 102 | 143 | 67 | 131 | 100 | 85 |
| GBM1 | 256 | 149 | 1525 | 3512 | 882 | 5629 | 2755 | 2320 | 1400 | 506 | 1077 | 372 | 825 | 103 |
| GBM4 | 383 | 221 | 277 | 92 | 4776 | 305 | 144 | 1176 | 22 | 1051 | 140 | 8 | 12 | 124 |
| GBM6 | 98 | 301 | 448 | 1866 | 2702 | 9004 | 5019 | 180 | 841 | 257 | 232 | 92 | 777 | 76 |
| GBM7 | 11,212 | 214 | 2392 | 23,316 | 5237 | 6452 | 4164 | 19,305 | 2078 | 1235 | 2619 | 1334 | 2800 | 74,989 |
| GBM10 | 2951 | 129 | 2805 | 2531 | 190 | 6931 | 3034 | 6413 | 916 | 175 | 960 | 315 | 297 | 965 |
| GBM12 | 4490 | 256 | 911 | 141 | 484 | 363 | 312 | 7849 | 111 | 180 | 282 | 261 | 1219 | 434 |
| GBM13 | 36,827 | 296 | 1021 | 17,323 | 11,240 | 4757 | 2020 | 3791 | 921 | 490 | 1331 | 916 | 2858 | 59,217 |
| *p*-Value | 0.017 | 0.005 | 0.005 | 0.048 | 0.005 | 0.003 | 0.006 | 0.016 | 0.049 | 0.040 | 0.010 | 0.035 | 0.073 | 0.103 |
| ODG1 | 102 | 129 | 577 | 80 | 46 | 324 | 425 | 543 | 81 | 1081 | 177 | 452 | 174 | 120 |
| ODG3 | 107 | 225 | 647 | 110 | 73 | 1213 | 656 | 43 | 87 | 2559 | 121 | 542 | 554 | 149 |
| ODG4 | 222 | 163 | 50 | 115 | 91 | 91 | 104 | 162 | 9 | 189 | 71 | 95 | 153 | 185 |
| ODG5 | 117 | 149 | 27 | 121 | 74 | 62 | 224 | 223 | 99 | 3196 | 67 | 371 | 194 | 1761 |
| ODG6 | 109 | 247 | 226 | 118 | 101 | 425 | 298 | 150 | 9 | 1269 | 67 | 221 | 201 | 146 |
| ODG7 | 104 | 144 | 257 | 120 | 124 | 2069 | 2062 | 88 | 34 | 419 | 97 | 509 | 783 | 128 |
| ODG8 | 77 | 112 | 252 | 76 | 48 | 270 | 255 | 207 | 224 | 181 | 105 | 49 | 45 | 60 |
| *p*-Value | 0.190 | 0.020 | 0.340 | 0.270 | 0.930 | 0.073 | 0.0092 | 0.220 | 0.270 | 0.0025 | 0.930 | 0.036 | 0.073 | 0.310 |
| PA1 | 88 | 220 | 1278 | 112 | 1556 | 215 | 78 | 156 | 14 | 298 | 805 | 619 | 333 | 97 |
| PA2 | 88 | 139 | 1492 | 472 | 183 | 715 | 375 | 126 | 135 | 143 | 729 | 292 | 243 | 90 |
| PA3 | 126 | 123 | 2938 | 1011 | 4179 | 65 | 93 | 376 | 106 | 875 | 1016 | 479 | 276 | 90 |
| PA5 | 100 | 137 | 453 | 3318 | 14345 | 59 | 137 | 174 | 92 | 899 | 150 | 459 | 179 | 82 |
| PA6 | 93 | 132 | 1049 | 5745 | 4805 | 81 | 75 | 228 | 43 | 181 | 781 | 421 | 342 | 63 |
| PA12 | 86 | 342 | 1153 | 85 | 372 | 62 | 75 | 249 | 12 | 257 | 835 | 98 | 159 | 68 |
| *p*-Value | 0.25 | 0.069 | 0.007 | 0.082 | 0.0087 | 0.790 | 0.850 | 0.017 | 0.530 | 0.010 | 0.135 | 0.006 | 0.033 | 0.123 |

Mean of expression of each gene in HB was plotted as 100% (±SD) and the respective gene expression in glioma (GBM, ODG or PA) specimens was compared to these values and percentage was calculated. Percentage and *p*-values were expressed. Other details are provided in Section 2.

glioma, although GBM samples presented the higher levels of gene expression for the NFκB-regulated genes as evidenced by the red colors in *Z*-axis plots. Grouping NFκB genes by biological functions, we found that 8/9 (89%) of the selected NFκB-regulated genes described as involved in angiogenesis, invasiveness and metastasis (VEGFA, MMP2, MMP9, ICAM1, VCAM1, VCAM2, CXCR4 and PLAU) and in antiapoptotic defenses (MYC, SOD2, A20/TNFAIP3 and IER3) were markedly up-regulated in GBM patients (up to 64-fold increases, $p < 0.05$) compared to HB tissues (Table 2). Increases in the inflammatory IL8 and CCL2 mRNAs ($p < 0.1$) also were observed in GBM patients. Gene expression for NFκB subunits (RELA, REL, NFKB2 and RELB, except NFKB1) was comparable to HB, suggesting that NFκB is regulated at the activation level, not at subunit expression (data not shown). Besides increasing in GBMs, MYC, CCL2 and IER3 genes also were increased in the lower grades of glioma (ODG and PA; Table 2).

**Table 3**
$IC_{50}$ levels of NFκB inhibitors in a panel of GBMs and in primary astrocytes.

| Treatments | $IC_{50}$ (μM) | | | | |
|---|---|---|---|---|---|
| | U138MG | C6 | U87 | U373 | Astrocytes |
| BAY117082 | 17 ± 5* | 15 ± 6* | 9.5 ± 7* | 15 ± 4* | 75 ± 8 |
| Parthenolide | 22 ± 5* | 29 ± 6* | 17 ± 4* | 13 ± 5* | 186 ± 10 |
| MG132 | 2.5 ± 0.8* | 3.9 ± 0.7* | 5 ± 1* | 2.7 ± 1* | 35 ± 5 |
| Curcumin | 23 ± 5* | 25 ± 4* | 20 ± 6* | 21 ± 3* | 135 ± 12 |
| Arsenic trioxide | 4.6 ± 2* | 4.2 ± 1.5* | 3.6 ± 2* | 5 ± 1* | 18 ± 2 |

Cells (U138MG, U87, C6, U373 and astrocytes) were treated for 36 h with different concentrations of NFκB signaling inhibitors (BAY117082, curcumin, parthenolide, MG132 and arsenic trioxide; 1–200 μM) and cell viability was determined by MTT assay. Experiments were repeated three times ($n = 3$) in triplicate, and data were expressed in mean ± SD.

* Different from untreated cells, and from its respective astrocytic $IC_{50}$ value ($p < 0.05$).

### 3.5. Pharmacological inhibitors of NFκB selectively induce cell death in GBMs

Data from Table 1, and Figs. 2 and 3, indicate that NFκB could be a potential target pathway to cell death induction in GBMs. Thus, we decided to test the cytotoxic effect of some NFκB pathway inhibitors such as BAY117082, parthenolide, arsenic trioxide, MG132 and curcumin in a panel of GBM cell lines. In parallel, primary astrocyte cultures were treated in order to evaluate the drug selectivity to cancer cells. GBMs and astrocytes were incubated with different concentrations of NFκB inhibitors for 36 h, and MTT assays were performed. Results show that astrocytes were less sensitive to NFκB inhibitors than GBM cell lines, indicating selectivity of NFκB inhibitors to tumor cells (Table 3). For BAY117082, parthenolide, MG132, curcumin and arsenic trioxide, the $IC_{50}$ values in MTT assay were, respectively, at least 4.4, 6.4, 7, 4 and 3.6-fold lower in the GBM cell lines compared to astrocytes as shown in Table 3. Thus, for further experiments, we used ~$IC_{50}$ concentrations for NFκB inhibitors (17 μM BAY117082; 25 μM curcumin; 3 μM MG132; 4 μM arsenic trioxide; 25 μM parthenolide) and C6/U138MG cell lines. To determine whether the effects of pharmacological NFκB inhibitors are directly NFκB related, indirectly related to NFκB inhibition, or have nothing to do with NFκB, we evaluated different concentrations of the compounds on NFκB activity and on cell viability as shown in Table 4. Correlations between NFκB inhibition and decreases in cell viability were calculated (Table 4). Data showed that pharmacological agent-induced NFκB inhibition significantly correlated with decreases in cell viability of both C6 and U138MG cells. As control, we also determined that inhibitors of the signaling pathways which were previously tested in Table 1 did not affect NFκB activity (Table 5). Taken together, data from Tables 1, 4 and 5 suggest that the antiglioma effects of the tested compounds were directly related to their NFκB inhibitory activity.

### 3.6. NFκB inhibitors induce anchorage-independent cell death and reduce the clonogenic potential in GBMs

Results from clonogenic survival assay showed that 36 h treatment with NFκB inhibitors followed by 6-day washout significantly decreased the clonogenic proliferation in GBMs, suggesting that the antiglioma effects of NFκB inhibition were long-term thus remaining after drug withdrawal (Fig. 4B). In addition, data from soft agar experiments showed that NFκB

**Table 4**
NFκB inhibition is correlated with decreases in cell viability in GBMs.

| Treatments | Concentration (μM) | NFκB activity (%, mean ± SD) | | % cell viability (MTT assay) | | Correlation ($r^2$) Viability × NFκB | |
|---|---|---|---|---|---|---|---|
| | | C6 | U138MG | C6 | U138MG | C6 | U138MG |
| Untreated | 0 | 100 ± 11 | 100 ± 12 | 100 ± 7 | 100 ± 6 | | |
| BAY117082 | 5 | 85 ± 14 | 87 ± 15 | 86 ± 6 | 95 ± 7 | 0.931# | 0.952# |
| | 25 | 47 ± 15* | 35 ± 10* | 17 ± 9* | 37 ± 12* | | |
| | 50 | 13 ± 9* | 17 ± 5* | 5 ± 3* | 15 ± 4* | | |
| Parthenolide | 5 | 92 ± 13 | 88 ± 12 | 80 ± 12 | 91 ± 5 | 0.846# | 0.971# |
| | 25 | 24 ± 11* | 34 ± 21* | 54 ± 5* | 48 ± 7* | | |
| | 50 | 15 ± 14* | 20 ± 9* | 15 ± 6* | 19 ± 4* | | |
| MG132 | 1 | 72 ± 9* | 79 ± 6* | 66 ± 11* | 71 ± 6* | 0.974# | 0.981# |
| | 5 | 37 ± 13* | 21 ± 17* | 26 ± 5* | 23 ± 7* | | |
| | 10 | 12 ± 6* | 14 ± 8* | 15 ± 7* | 11 ± 5* | | |
| Curcumin | 5 | 93 ± 8 | 99 ± 10 | 94 ± 5 | 89 ± 4 | 0.978# | 0.962# |
| | 25 | 47 ± 12* | 49 ± 22* | 46 ± 7* | 40 ± 9* | | |
| | 50 | 24 ± 13* | 11 ± 7* | 9 ± 8* | 21 ± 11* | | |
| Arsenic | 1 | 82 ± 7* | 91 ± 12 | 95 ± 9 | 92 ± 7 | 0.954# | 0.975# |
| | 5 | 25 ± 13* | 29 ± 18* | 41 ± 7* | 45 ± 4* | | |
| | 10 | 18 ± 6* | 24 ± 9* | 17 ± 11* | 27 ± 9* | | |

C6 and U138MG cells were treated with different concentrations of BAY117082, curcumin, parthenolide, MG132 or arsenic trioxide. MTT was performed after 36 h treatment; ELISA assays for NFκB-p65 DNA-binding activity were performed in nuclear extracts isolated from 6 h-treated GBMs. Cell viability and NFκB inhibition were expressed as percentage compared to untreated cells. *R* squared ($R^2$) was calculated using GraphPad Prism software®. Experiments were repeated three times ($n = 3$) in duplicate; data were expressed as mean ± SD.

* Different from untreated cells.

\# Positive correlation.

inhibitor-induced cell death was independent of cell anchorage since NFκB inhibitors decreased cell colony formation in soft agar (Fig. 4C). At the end of 36 h treatment with NFκB inhibitors, we also observed significant alterations in cell morphology, which were accompanied by PI uptake, cell detachment and LDH release as indicative of cell death (Fig. 4A). PI uptake did not occur in all cells with morphological changes, suggesting that morphological alterations preceded the losses in cell membrane integrity. These effects suggest a programmed mechanism of cell death induction by NFκB inhibitors thus stimulating us to evaluate apoptotic markers (Fig. 4A).

### 3.7. NFκB inhibitors cell cycle arrest and apoptosis in GBMs

PI staining of chromatin showed that NFκB inhibitors induced chromatin condensation and apoptotic body formation in U138MG cells (Fig. 5A). The results were similar in C6 cells (data not shown). Determination of caspase-3 activity showed that all the tested NFκB inhibitors promoted caspase-3 activation in C6 whereas only MG132 and arsenic trioxide increased caspase-3 activity in the p53/PTEN mutant U138MG, suggesting that apoptosis can be caspase-3 dependent or independent depending on cell type and on NFκB inhibitor (Fig. 5B). Analysis of cell cycle distribution evidenced that, after 18 h treatment, NFκB inhibitors caused accumulation of cells in the G2/M phase of the cell cycle followed by the formation of sub-G1 apoptotic cells at 36 h, suggesting that arrest in G2/M phase preceded apoptosis (Fig. 5C).

### 3.8. Mitochondrial dysfunction precedes apoptosis in NFκB inhibitor-treated cells

We also evaluated the mitochondrial function in NFκB inhibitor-treated GBMs. In time-effect experiments, we determined that NFκB inhibitors promoted an early decrease in MMP (JC-1 assay) which was observed between 8 and 16 h treatment whereas cell membrane integrity (PI uptake assay) only decreased at later time points (24 h treatment) (Fig. 6A). It suggests that mitochondrial dysfunction occurred at the early steps of NFκB inhibitor-induced

**Table 5**
Effect of MAPKs, EGFR, PKC and PI3K/Akt inhibitors on NFκB activity.

| Treatments | Concentration (μM) | NFκB activity (%, mean ± SD) |
|---|---|---|
| Untreated | 0 | 100 ± 8 |
| UO126 | 10 | 110 ± 11 |
| | 30 | 112 ± 22 |
| SP600129 | 10 | 106 ± 12 |
| | 30 | 114 ± 7 |
| SB203508 | 10 | 88 ± 22 |
| | 30 | 95 ± 16 |
| PD158780 | 10 | 90 ± 8 |
| | 30 | 106 ± 14 |
| LY294002 | 10 | 88 ± 11 |
| | 30 | 86 ± 21 |
| Gö6983 | 10 | 112 ± 13 |
| | 30 | 93 ± 9 |
| Wortmannin | 1 | 89 ± 15 |
| | 10 | 93 ± 11 |
| BAY117082 | 30 | 39 ± 12* |

C6 cells were treated with different concentrations of pharmacological inhibitors of MEK/ERK (UO126), JNK1/2 (SP600129), p38 (SB203508), EGFR (PD158780), PI3K/Akt (LY294002 and wortmannin) and PKC (Gö6983). BAY117082 was used as control for NFκB inhibition. ELISA assays for NFκB-p65 DNA-binding activity were performed in nuclear extracts isolated from 6 h-treated cells. NFκB activity was expressed as percentage compared to untreated cells (mean ± SD). Experiments were performed in triplicate.
* Different from untreated cells ($p < 0.05$).

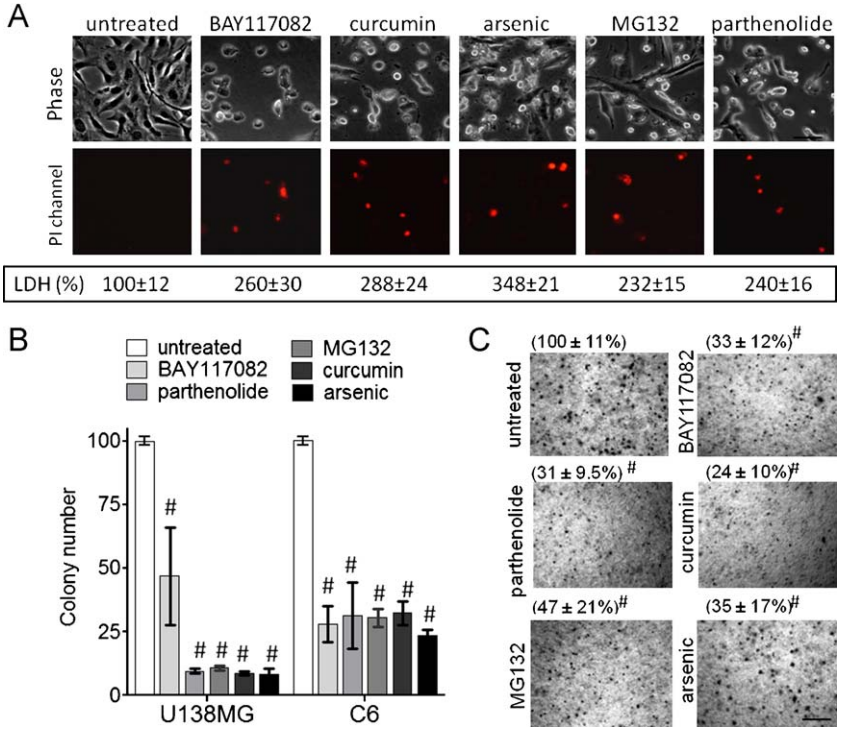


**Fig. 4.** NFκB inhibitors induce anchorage-independent cell death and reduce clonogenic potential of GBMs. (A) Representative microphotographs (20× magnification) showing cell morphology and PI uptake in U138MG cells after 36 h treatment with NFκB inhibitors. Below microphotographs are presented as means ± SD of the LDH activity detected in the culture medium of GBMs. (B) Clonogenic survival in U138MG cells after treatment with NFκB inhibitors. (C) Representative microphotographs and quantification of colonies in soft agar growing C6 cells (see details in Section 2). In these experiments were used $IC_{50}$ concentrations of NFκB inhibitors. #Different from untreated cells ($n = 3$).

cell death. Like observed in p65 knockdown experiments (Fig. 1), pharmacological inhibitors also decreased the levels of the NFκB-regulated mitochondrial cytoprotective protein bcl-xL [7,10,11] (Fig. 6B). Mitochondrial dysfunction also was accompanied by the release of the pro-apoptotic factor cytochrome c from mitochondrial to cytoplasmic fraction as assessed after 16 h treatment with NFκB inhibitors (Fig. 6B).

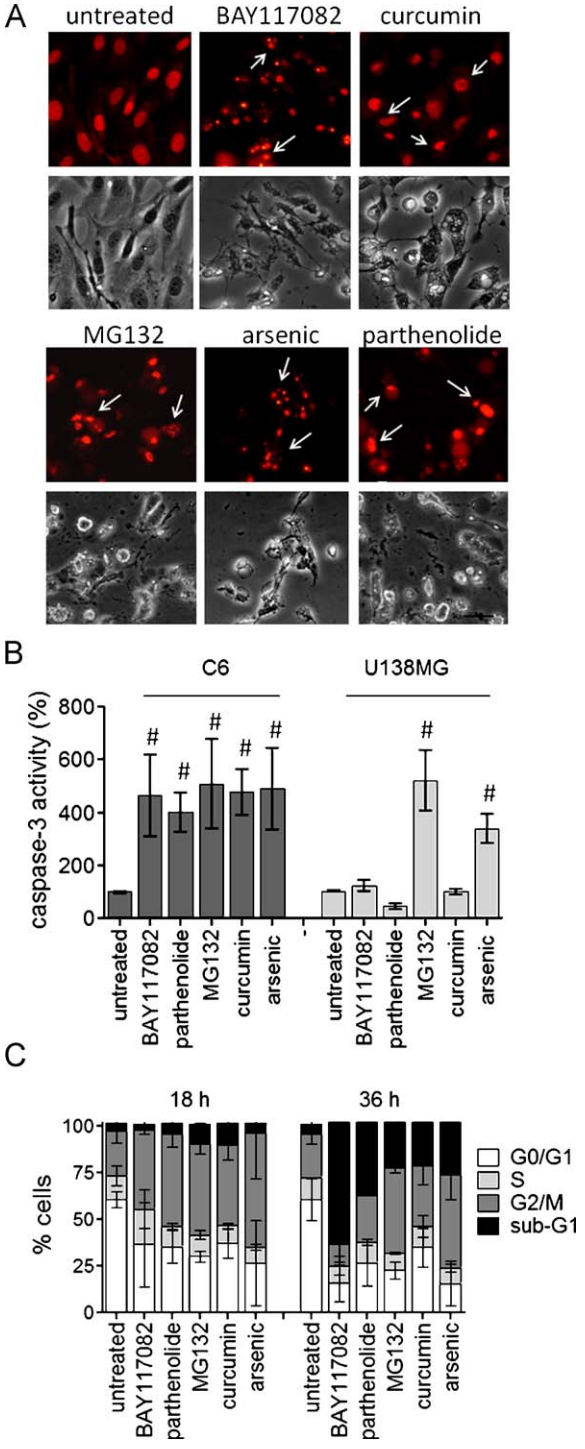


**Fig. 5.** NFκB inhibitors induce apoptosis in GBMs. (A) Representative fluorescent and phase contrast microphotographs (20×) showing chromatin condensation and apoptotic body formation after 36 h incubation with NFκB inhibitors. U138MG cells were fixed, and chromatin was stained with propidium iodide. (B) Caspase-3 protease activity after 36 h treatment with pharmacological inhibitors in C6 and U138MG cell lines. (C) Quantification of cell population distribution between sub-G1, G1/G0, S and G2/M phases of the cell cycle after 18 or 36 h treatment of U138MG cells with NFκB inhibitors. In Fig. 7 experiments, NFκB inhibitors were incubated using $IC_{50}$ concentrations. #Different from untreated cells ($n = 3$, $p < 0.05$, ANOVA).

### 3.9. NFκB inhibitors synergize with the anticancer drugs cisplatin and doxorubicin

An interesting field in the NFκB research is the possibility of combination of NFκB inhibitors with classical chemotherapy in order to decrease chemotherapy doses and adverse cytotoxicity to normal tissues [9]. In synergism/antagonism experiments, we established two protocols: (1) 6 h pre-treatment with apoptotic levels of NFκB inhibitors, washout, and 48 h mono-treatment with doxorubicin or cisplatin; (2) 6 h pre-treatment with sub-apoptotic concentrations of NFκB inhibitors followed by 48 h co-incubation with doxorubicin or cisplatin. At the end of the treatments, MTT assays were performed. Results showed that NFκB inhibitors synergized with doxorubicin and cisplatin in both apoptotic and sub-apoptotic concentrations potentiating the anticancer effects of these drugs in C6 and U138MG lines (Table 6).

### 3.10. NFκB inhibitors overcame cisplatin resistance in GBM

In other approach, we selected cisplatin-resistant cells by incubating C6 cells with 50 μM cisplatin for 48 h followed by a 20–

**Table 6**
NFκB inhibitors synergize with cisplatin and doxorubicin to induce GBM cell death.

| Treatments | Viability (mean ± SD) | |
|---|---|---|
| | C6 | U138MG |
| Untreated | 100 ± 6 | 100 ± 7 |
| Cisplatin 5 μM | 73 ± 3* | 84 ± 8* |
| Cisplatin + BAY 7.5 μM | 55 ± 12# | 64 ± 8# |
| Cisplatin + BAY 25 μM | 19 ± 5# | 34 ± 16# |
| Cisplatin + Part 10 μM | 56 ± 4# | 74 ± 6 |
| Cisplatin + Part 25 μM | 38 ± 11# | 22 ± 4# |
| Cisplatin + MG132 1 μM | 60 ± 14 | 68 ± 4# |
| Cisplatin + MG132 5 μM | 33 ± 10# | 23 ± 1# |
| Cisplatin + curcumin 10 μM | 46 ± 6# | 47 ± 13# |
| Cisplatin + curcumin 25 μM | 36 ± 5# | 28 ± 2# |
| Cisplatin + arsenic 0.5 μM | 51 ± 10# | 56 ± 1# |
| Cisplatin + arsenic 15 μM | 29 ± 9# | 25 ± 3# |
| Doxorubicin 2.5 μM | 70 ± 8* | 75 ± 7* |
| Doxorubicin + BAY 7.5 μM | 24 ± 12# | 61 ± 6.5 |
| Doxorubicin + BAY 25 μM | 21 ± 12# | 29 ± 10# |
| Doxorubicin + Part 10 μM | 46 ± 11# | 23 ± 5# |
| Doxorubicin + Part 25 μM | 23 ± 2# | 19 ± 1# |
| Doxorubicin + MG132 1 μM | 32 ± 7# | 22 ± 18# |
| Doxorubicin + MG132 5 μM | 7 ± 1# | 2 ± 3# |
| Doxorubicin + curcumin 10 μM | 67 ± 5 | 59 ± 2# |
| Doxorubicin + curcumin 25 μM | 46 ± 5# | 39 ± 3# |
| Doxorubicin + arsenic 0.5 μM | 61 ± 6 | 25 ± 2# |
| Doxorubicin + arsenic 15 μM | 30 ± 5# | 25 ± 1# |
| BAY 7.5 μM | 102 ± 13 | 103 ± 10 |
| BAY 25 μM | 37 ± 5* | 53 ± 12* |
| Part 10 μM | 92 ± 9 | 90 ± 7 |
| Part 25 μM | 58 ± 13* | 45 ± 13* |
| MG132 1 μM | 114 ± 8 | 82 ± 10* |
| MG132 5 μM | 77 ± 11* | 28 ± 4* |
| Curcumin 10 μM | 94 ± 7 | 74 ± 12* |
| Curcumin 25 μM | 75 ± 17* | 53 ± 11* |
| Arsenic 0.5 μM | 110 ± 18 | 90 ± 12 |
| Arsenic 15 μM | 58 ± 11* | 49 ± 10* |

Wild-type U138MG and C6 glioma cell lines were treated with different concentrations of NFκB inhibitors as described in Section 3, followed by exposure to 5 μM cisplatin or 2.5 μM doxorubicin (approximately $IC_{25}$ levels) for 48 h. After that, MTT assays were performed. Data were expressed as percentage compared to untreated cells (mean ± SD). Experiments were repeated three times ($n = 3$) in quadruplicate. BAY (BAY117082); Part (Parthenolide).

* Different from untreated cells.

# Different from untreated and from cisplatin or doxorubicin-treated cells ($p < 0.05$).

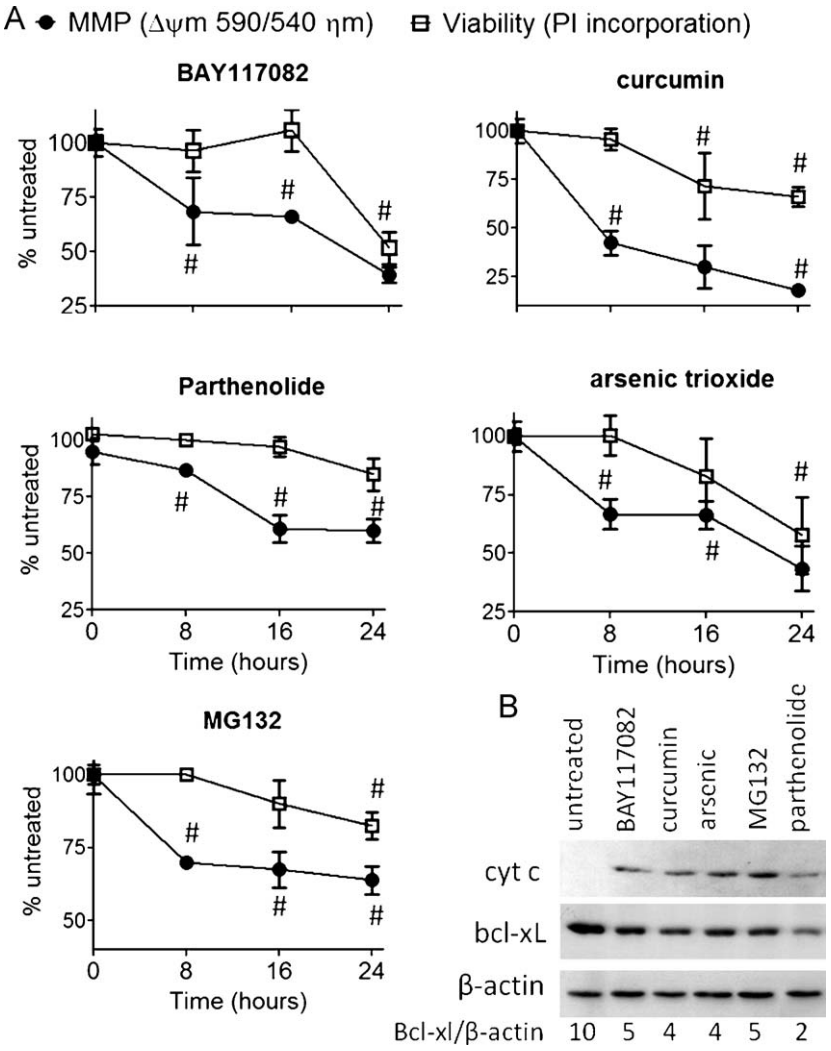


**Fig. 6.** Mitochondrial dysfunction precedes apoptosis in NFκB inhibitor-treated cells. (A) Time course effect of NFκB inhibitors on MMP was co-evaluated with PI incorporation for the determination of cell membrane integrity. U138MG was treated for different times and, at the end of treatments, cells were trypsinized and different aliquots were assayed by JC-1 or PI incorporation. (B) Western blotting detection of cytochrome c in the cytosolic fraction, and total bcl-xL protein levels in U138MG cells after 16 h treatment with NFκB inhibitors. Experiments were performed in triplicate, and graphs were expressed in mean ± SD. #Different from untreated cells.

25 day washout for the recovery of survival clones. After that, cells were tested for cisplatin resistance. $IC_{50}$ values increased by almost 8-fold (from 20 to 155 μM) confirming the resistance to the alkylating agent (Fig. 7A). Interestingly, NFκB was found over-stimulated in cisplatin-resistant cells compared to wild-type C6 (Fig. 7B). The antiglioma potential of NFκB inhibitors was independent of cisplatin resistance, since drugs were effective to induce cell death in the cisplatin-resistant C6 cell line. Interestingly, co-treatment of cisplatin ($IC_{25}$ concentration = 75 μM) plus NFκB inhibitors overcame cisplatin resistance, finally inducing high rates of cell death after 48 h treatment when compared to mono-treatments of NFκB inhibitors or cisplatin (Fig. 7C). Altogether, data showed that increased NFκB correlated with cisplatin resistance, and NFκB inhibitors efficiently induced cell death in resistant cells besides overcoming cisplatin resistance. Importantly, cell resistance to cisplatin was transitory and decreased after 3–4 passages.

## 4. Discussion

GBMs are associated with a poor prognosis due to intrinsic malignance and drug/radiation resistance, besides limited therapeutic opportunities such as neurosurgery and temozolomide/radiotherapy regimens [1,15,25]. Studies reported that NFκB activation correlates with therapeutic implications and worse prognosis in human gliomas [21–23,37–39]. Aberrant NFκB activity was found critical for focal necrosis formation, invasive phenotype establishment [22] and resistance to $O^6$ alkylating agents in GBMs [40]. In vitro, the expression of an IκB super-repressor protein decreased C6 cell viability [21]. Also, the literature indicates that most of the factors that mediate proliferation, invasion, angiogenesis and apoptotic resistance in cancer, including GBMs, such as EGF/EGFR, VEGF, PDGF, MCP-1, MMPs, VCAM, bcl-xL and FLICE are activators of or products of NFκB-regulated genes, conferring to NFκB a potential role on GBM growth and thus a potential target pathway [7,8,11,41,42]. In this way, some experimental drugs possessing antiglioma activities showed mechanisms involving NFκB inhibition [43–46].

In this work, knockdown of the NFκB member p65 and pharmacological inhibition of NFκB caused significant decreases in GBM cell viability whereas inhibitors of other signaling pathways such as MEK/ERK, JNK, p38, EGFR and PKC had no significant effects, except for a cytostatic activity following PI3K/Akt inhibition. Corroborating, Carapancea et al. showed that inhibitors of PDGF, EGFR, PI3K and MEK1/2 (AG1433, AG1024, LY294002 and PD98059, respectively) failed to induce cell death in MO59J and

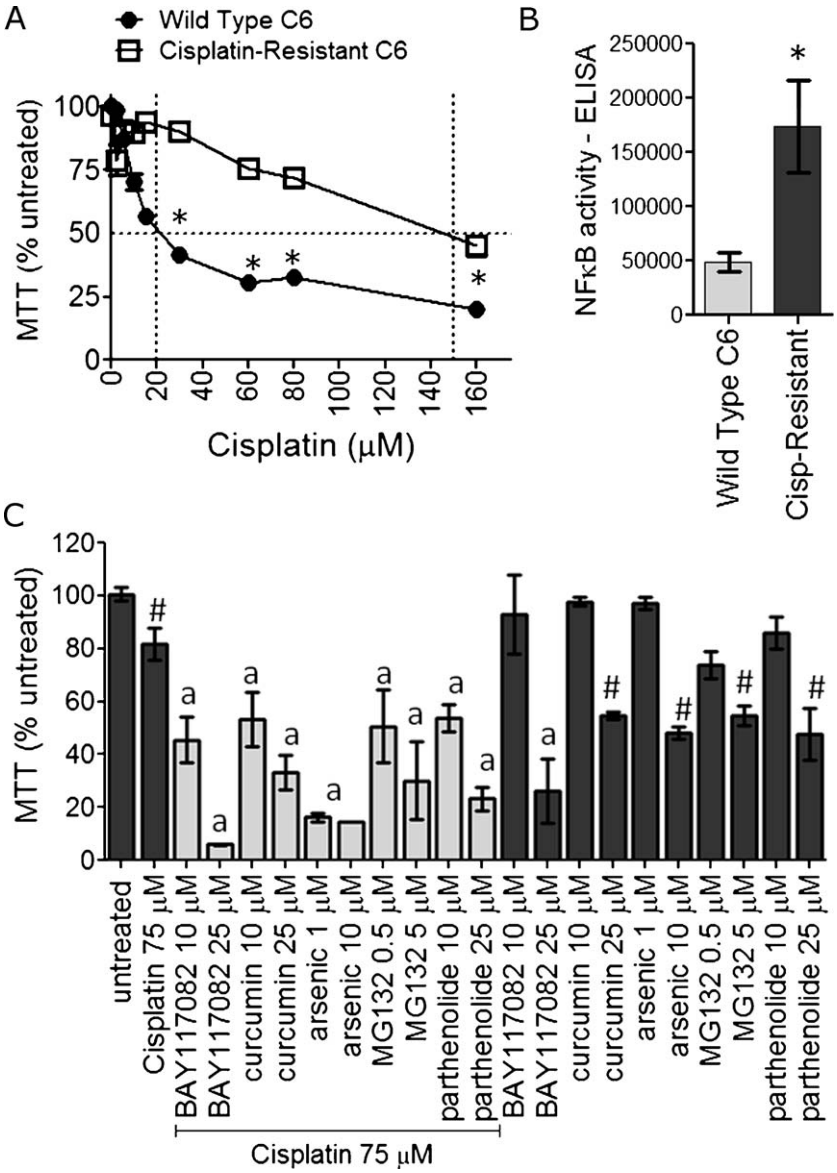


**Fig. 7.** NFκB inhibitors overcame cisplatin resistance GBM cells. (A) Representative MTT assay showing the validation of cisplatin resistance in C6 cells. (B) NFκB ELISA assay showing that NFκB DNA-binding activity is increased in cisplatin-resistant compared to that of wild-type C6 cells. (C) NFκB inhibition abolishes cisplatin resistance in cisplatin-resistant cells. Cells were treated with $IC_{25}$ concentrations of cisplatin in the presence or absence of NFκB inhibitors ($IC_{50}$ levels) for 48 h, and viability was determined by MTT. Resistance induction was performed twice, and experiments were performed in triplicate. *Different from C6-wild type cells; #different from untreated cells; [a]different from cisplatin and from its respective NFκB inhibitor alone treatment.

MO59K cell lines, and in primary cultures derived from GBM patients [47]. NFκB inhibitors induced cell death in liquid and soft agar growing cells regardless of the p53 or PTEN mutational status since cytotoxicity was similar for C6 (p53 and PTEN normal), U87 (PTEN mutant), U373 (p53 and PTEN mutant) and U138MG (p53 and PTEN mutant) cell lines. NFκB was found overstimulated in GBMs, and its inhibitors were selective to cell death induction in tumor cells as compared to astrocytes. The antiglioma potential of the pharmacological agents correlated with NFκB inhibition as demonstrated in Tables 4 and 5. Tumor-specific targeting represents an improvement over classical chemotherapeutics, which adversely affect both diseased and normal brain in a non-specific manner [6,9,13]. Nuclear p65 was found in GBMs whereas latent/cytosolic p65 was detected in astrocytes. Total p65 protein was similar between GBM and astrocytes suggesting that NFκB was modulated at the level of activation. Nonetheless, landscapes analysis for NFκB gene interaction network revealed that NFκB target genes were up-regulated in the three tumor grades (GBM, oligodendroglioma and astrocytoma) compared to healthy brain tissues. Landscapes evidenced a high expression of NFκB target genes in the most aggressive form of glioma, GBM; marked increases were observed in VEGFA, MMP2, MMP9, PLAU, VCAM1, ICAM1, IER3, SOD2, MYC, CCL2 and IL8 gene expression. In agreement with these results, Xie et al. showed that constitutive NFκB regulates the expression of VEGF and IL-8 and tumor angiogenesis in human GBM [12]. This exacerbated activation of NFκB has been pivotal to explain the selective toxicity of NFκB inhibitors to cancer cells [10,13,17,19].

Previous works showed that downregulation of NFκB leads to mitochondrial dysfunction due to decreases in the expression of mitochondrial cytoprotective genes such as bcl-xL and SOD2, which result in cytotoxicity [11,15,17,26]. Jiang et al. reported that selective bcl-xL knockdown rendered U87 and NS008 GBM cells to apoptosis [48]. In our model, NFκB inhibitors caused bcl-xL protein downregulation, mitochondrial depolarization and release of the apoptotic factor cytochrome c, which preceded the losses in cell

membrane integrity and apoptosis, thus implying that mitochondrial dysfunction is an early step of NFκB inhibitor-induced cell death [7,11,15,48]. In previous studies, arsenic trioxide induced G2/M arrest in the U87 and T98G [49], and mitochondrial aggregation and cytochrome c release in A172 GBMs [50]. Here, all NFκB inhibitors elicited cell arrest in the G2/M phase of the cell cycle before sub-G1 induction, apoptotic body formation and caspase-3 activation. The herein reported impairment on mitochondrial function and induction of G2/M arrest were previously demonstrated by our group and others during curcumin [51], parthenolide [52], BAY117082 and MG132 [17] treatment in other types of cancer cells, but not in gliomas.

In GBMs, defects in caspase-mediated apoptotic signaling due to p53 mutations limit the effectiveness of chemotherapy thus promoting chemoresistance and poor clinical outcome [53–56]. Induction of caspase-independent mechanisms of cell death could be useful for circumventing GBM resistance. In our model, all tested NFκB inhibitors activated caspase-3 in C6 whereas only MG132, arsenic trioxide and p65 siRNA stimulated caspase-3 in the p53-mutant U138MG; curcumin, BAY117082 and parthenolide exerted caspase-independent cell death in U138MG. Besides the distinct genetic aberrations between C6 and U138MG cell lines, differences in the action mechanisms of the tested NFκB inhibitors and possible off-target effects could explain their differential effects upon caspase-3. BAY117082 is a specific IKK-beta inhibitor ($IC_{50} \sim 10\ \mu M$) [57]; parthenolide inhibits NF-κB both indirectly by blocking IKK-beta at cys179 and directly by inhibiting p65 at the cysteine residue in its activation loop ($IC_{50} \sim 10\ \mu M$) [58,59]; MG132 inhibits proteasome ($IC_{50} \sim 0.1\ \mu M$) and proteasome-dependent IκB-alpha degradation ($IC_{50} \sim 3\ \mu M$) thus blocking the nuclear activity of NFκB; arsenic trioxide inhibits degradation and up-regulates expression of IκB-alpha [60]; curcumin inhibits IKKs ($IC_{50} \sim 13\ \mu M$), although unspecific effects upon activator protein-1 and glyoxalase I activity, for example, were described [15,61,62]. In U138MG, the IKK inhibitors did not increase caspase-3 in contrast to inhibitors of IκB degradation such as MG132 and arsenic. In T98G and U87 GBMs, curcumin induces caspase- and calpain-independent cell death irrespective of the p53 status of the cells [15]. Thus, elucidation of these mechanistic differences requires further investigation.

Besides their apoptotic activity per se, NFκB inhibitors presented adjuvant activity by potentiating the anticancer effect of cisplatin and doxorubicin in both C6 and U138MG cells, besides overcoming cisplatin resistance in cisplatin-resistant C6. Several lines of evidence suggest NFκB as a key mediator of cancer cells resistance to chemotherapy and anticancer therapy failure in vivo [9,18,40]. Bredel et al. reported that NFκB mediates GBM resistance to the alkylating agents, temozolomide and BCNU, in primary GBM cultures [40]. In addition, Weaver et al. demonstrated that chemotherapy-induced DNA damage may activate NFκB, and inhibition of NFκB by mutant IκB-alpha enhances BCNU, carboplatin and TNF-induced cell death in U87 and U251 cells [63]. In our model, NFκB activity was up-regulated in cisplatin-resistant C6 cells compared to that in wild-type C6. Cisplatin-resistant cells remained sensitive to NFκB inhibitors, and combination of cisplatin plus NFκB inhibitors overcame cisplatin resistance, suggesting that alkylation resistance involved NFκB pathway. In agreement, previous studies reported that the proteasome inhibitors LLnL and MG132, which are known by acting through NFκB inhibition, sensitized GBMs to TRAIL-induced apoptosis [18]. Clinically, the adjuvant potential of NFκB inhibitors could be used for therapeutic advantage in order to potentiate the efficacy of classical anticancer drugs in chemotherapy-resistant patients thus decreasing the anticancer agents' doses and the frequently observed collateral effects to healthy tissues [9,15].

As above cited, some previous studies exploited the antiglioma effects of some of the herein used compounds as arsenic trioxide [49,50,64], curcumin [15,65–67], parthenolide [68] and proteasome/NFκB inhibitors [3,18,63,69,70] in GBMs. Here, we suggest that a mechanism by which they induce GBM cells death is mediated by their NFκB inhibitory activity. We add information by evaluating inhibitors of different signaling pathways, NFκB pathway activation in cell lines and in clinical specimens, and effect of different NFκB inhibitors in a panel of GBM cell lines; p65 knockdown also was evaluated. Importantly, selectivity to cancer cells, mitochondrial dysfunction, adjuvant potential and ability of NFκB inhibitors to abolish chemoresistance were examined. The results were positive and support a rationale for further testing inhibition of NFκB pathway in animal models of GBMs, and possibly other cancers.

## Disclosure statement

The authors report no conflicts of interest. The authors alone are responsible for the content and writing of the paper.

## Acknowledgements

We acknowledge the Brazilian funds CAPES, FINEP/IBNNet (01060842-00) and CNPq for financial support, and Dr Rafael Roesler (Hospital de Clinicas de Porto Alegre, HCPA) for kindly providing U87 and U373 cell lines.

## References

[1] Stewart LA. Chemotherapy in adult high-grade glioma: a systematic review and meta-analysis of individual patient data from 12 randomised trials. Lancet 2002;359:1011–8.
[2] Soni D, King JA, Kaye AH, Hovens CM. Genetics of glioblastoma multiforme: mitogenic signaling and cell cycle pathways converge. J Clin Neurosci 2005;12:1–5.
[3] Yu C, Friday BB, Yang L, Atadja P, Wigle D, Sarkaria J, et al. Mitochondrial Bax translocation partially mediates synergistic cytotoxicity between histone deacetylase inhibitors and proteasome inhibitors in glioma cells. Neuro Oncol 2008;10(3):309–19.
[4] Brennan C, Momota H, Hambardzumyan D, Ozawa T, Tandon A, Pedraza A, et al. Glioblastoma subclasses can be defined by activity among signal transduction pathways and associated genomic alterations. PLoS ONE 2009; 4(11):e7752.
[5] Gerstner ER, Sorensen AG, Jain RK, Batchelor TT. Anti-vascular endothelial growth factor therapy for malignant glioma. Curr Neurol Neurosci Rep 2009;9(3):254–62.
[6] Mercer RW, Tyler MA, Ulasov IV, Lesniak MS. Targeted therapies for malignant glioma: progress and potential. BioDrugs 2009;23(1):25–35.
[7] Barkett M, Gilmore TD. Control of apoptosis by Rel/NFkB transcription factors. Oncogene 1999;18:6910–24.
[8] Rayet B, Gélinas C. Aberrant rel/NFκB genes and activity in human cancer. Oncogene 1999;18(49):6938–47.
[9] Nakanishi C, Toi M. Nuclear factor-kappaB inhibitors as sensitizers to anticancer drugs. Nat Rev Cancer 2005;5(4):297–309.
[10] Baud V, Karin M. Is NF-kB a good target for cancer therapy? Hopes and pitfalls. Nat Rev Drug Discov 2009;8:33–40.
[11] Aggarwal BB. Nuclear factor-kappaB: the enemy within. Cancer Cell 2004;6(3):203–8.
[12] Xie TX, Xia Z, Zhang N, Gong W, Huang S. Constitutive NF-kappaB activity regulates the expression of VEGF and IL-8 and tumor angiogenesis of human glioblastoma. Oncol Rep 2010;23(3):725–32.
[13] Orlowski RZ, Baldwin Jr AS. NF-kappa B as a therapeutic target in cancer. Trends Mol Med 2002;8:385–9.
[14] Li B, Li YY, Tsao SW, Cheung AL. Targeting NF-kappaB signaling pathway suppresses tumor growth, angiogenesis, and metastasis of human esophageal cancer. Mol Cancer Ther 2009;8(9):2635–44.
[15] Dhandapani KM, Mahesh VB, Brann DWJ. Curcumin suppresses growth and chemoresistance of human glioblastoma cells via AP-1 and NFkappaB transcription factors. J Neurochem 2007;102(2):522–38.
[16] Xie TX, Aldape KD, Gong W, Kanzawa T, Suki D, Kondo S, et al. NF-kappaB activity is critical in focal necrosis formation of human glioblastoma by regulation of the expression of tissue factor. Int J Oncol 2008;33(1):5–15.
[17] Zanotto-Filho A, Delgado-Cañedo A, Schröder R, Becker M, Klamt F, Moreira JC. The pharmacological NFkappaB inhibitors BAY117082 and MG132 induce cell arrest and apoptosis in leukemia cells through ROS–mitochondria pathway activation. Cancer Lett 2010;288(2):192–3.

[18] Kasuga C, Ebata T, Kayagaki N, Yagita H, Hishii M, Arai H, et al. Sensitization of human glioblastomas to tumor necrosis factor-related apoptosis-inducing ligand (TRAIL) by NF-kappaB inhibitors. Cancer Sci 2004;95(10):840–4.
[19] Pickering BM, de Mel S, Lee M, Howell M, Habens F, Dallman CL, et al. Pharmacological inhibitors of NF-kB accelerate apoptosis in chronic lymphocytic leukemia cells. Oncogene 2007;26:1166–77.
[20] Domingo-Domènech J, Pippa R, Tápia M, Gascón P, Bachs O, Bosch M. Inactivation of NF-kappaB by proteasome inhibition contributes to increased apoptosis induced by histone deacetylase inhibitors in human breast cancer cells. Breast Cancer Res Treat 2008;112(1):53–62.
[21] Robe PA, Bentires-Alj M, Bonif M, Rogister B, Deprez M, Haddada H, et al. In vitro and in vivo activity of the nuclear factor-kappaB inhibitor sulfasalazine in human glioblastomas. Clin Cancer Res 2004;10(16):5595–603.
[22] Raychaudhuri B, Han Y, Lu T, Vogelbaum MA. Aberrant constitutive activation of nuclear factor kappaB in glioblastoma multiforme drives invasive phenotype. J Neurooncol 2007;85(1):39–47.
[23] Brown RE, Law A. Morphoproteomic demonstration of constitutive nuclear factor-kappaB activation in glioblastoma multiforme with genomic correlates and therapeutic implications. Ann Clin Lab Sci 2006;36(4):421–6.
[24] da Frota Jr ML, Braganhol E, Canedo AD, Klamt F, Apel MA, Mothes B, et al. Brazilian marine sponge Polymastia janeirensis induces apoptotic cell death in human U138MG glioma cell line, but not in a normal cell culture. Invest New Drugs 2009;27(1):13–20.
[25] Braganhol E, Zamin LL, Cañedo AD, Horn F, Tamajusuku AS, Wink MR, et al. Antiproliferative effect of quercetin in the human U138MG glioma cell line. Anticancer Drugs 2006;17(6):663–71.
[26] Zanotto-Filho A, Gelain DP, Schröder R, Souza LF, Pasquali MA, Klamt F, et al. The NFkappaB-mediated control of RS and JNK signaling in vitamin A-treated cells: duration of JNK–AP-1 pathway activation may determine cell death or proliferation. Biochem Pharmacol 2009;77:1291–301.
[27] Bharti AC, Donato N, Singh S, Aggarwal BB. Curcumin (diferuloylmethane) down-regulates the constitutive activation of nuclear factor-kappa B and IkappaBalpha kinase in human multiple myeloma cells, leading to suppression of proliferation and induction of apoptosis. Blood 2003;101(3):1053–62.
[28] Klamt F, Shacter E. Taurine chloramine, an oxidant derived from neutrophils, induces apoptosis in human B lymphoma cells through mitochondrial damage. J Biol Chem 2005;280:21346–52.
[29] Hirose Y, Berger MS, Pieper RO. p53 affects both the duration of G2/M arrest and the fate of temozolomide-treated human glioblastoma cells. Cancer Res 2001;61:1957–63.
[30] Kucharczak J, Simmons MJ, Fan Y, Gélinas C. To be, or not to be: NF-kappaB is the answer: role of Rel/NF-kappaB in the regulation of apoptosis. Oncogene 2003;22(56):8961–82.
[31] Kim HJ, Hawke N, Baldwin AS. NF-kappaB and IKK as therapeutic targets in cancer. Cell Death Differ 2006;13(5):738–47.
[32] von Mering C, Jensen LJ, Snel B, Hooper SD, Krupp M, Foglierini M, et al. STRING: known and predicted protein–protein associations, integrated and transferred across organisms. Nucleic Acids Res 2005;33:433–7.
[33] Wain HM, Lush MJ, Ducluzeau F, Khodiyar VK, Povey S. Genew: the Human Gene Nomenclature Database, 2004 updates. Nucleic Acids Res 2004;32:255–7.
[34] Birney E, Andrews D, Caccamo M, Chen Y, Clarke L, Coates G, et al. Ensembl 2006. Nucleic Acids Res 2006;34:556–61.
[35] Hooper SD, Bork P. Medusa: a simple tool for interaction graph analysis. Bioinformatics 2005;21:4432–3.
[36] Castro MAA, Rybarczyk Filho JL, Dalmolin RJS, Sinigaglia M, Moreira JCF, Mombach JCM, et al. ViaComplex: software for landscape analysis of gene expression networks in genomic context. Bioinformatics 2009;25(11):1468–9.
[37] Park S, Hatanpaa KJ, Xie Y, Mickey BE, Madden CJ, Raisanen JM, et al. The receptor interacting protein 1 inhibits p53 induction through NF-kappaB activation and confers a worse prognosis in glioblastoma. Cancer Res 2009;69(7):2809–16.
[38] Park S, Zhao D, Hatanpaa KJ, Mickey BE, Saha D, Boothman DA, et al. RIP1 activates PI3K–Akt via a dual mechanism involving NF-kappaB-mediated inhibition of the mTOR–S6K–IRS1 negative feedback loop and down-regulation of PTEN. Cancer Res 2009;69(10):4107–11.
[39] Wang H, Wang H, Zhang W, Huang HJ, Liao WS, Fuller GN. Analysis of the activation status of Akt, NFkappaB, and Stat3 in human diffuse gliomas. Lab Invest 2004;84(8):941–51.
[40] Bredel M, Bredel C, Juric D, Duran GE, Yu RX, Harsh GR, et al. Tumor necrosis factor-alpha-induced protein 3 as a putative regulator of nuclear factor-kappaB-mediated resistance to $O^6$-alkylating agents in human glioblastomas. J Clin Oncol 2006;24(2):274–87.
[41] Kapoor GS, Zhan Y, Johnson GR, O'Rourke DM. Distinct domains in the SHP-2 phosphatase differentially regulate epidermal growth factor receptor/NF-kappaB activation through Gab1 in glioblastoma cells. Mol Cell Biol 2004;24(2):823–36.
[42] Sethi G, Ahn KS, Chaturvedi MM, Aggarwal BB. Epidermal growth factor (EGF) activates nuclear factor-kappaB through IkappaBalpha kinase-independent but EGF receptor-kinase dependent tyrosine 42 phosphorylation of Ikappa-Balpha. Oncogene 2007;26(52):7324–32.
[43] Gao X, Deeb D, Jiang H, Liu Y, Dulchavsky SA, Gautam SC. Synthetic triterpenoids inhibit growth and induce apoptosis in human glioblastoma and neuroblastoma cells through inhibition of prosurvival Akt, NF-kappaB and Notch1 signaling. J Neurooncol 2007;84(2):147–57.
[44] Kotliarova S, Pastorino S, Kovell LC, Kotliarov Y, Song H, Zhang W, et al. Glycogen synthase kinase-3 inhibition induces glioma cell death through c-MYC, nuclear factor-kappaB, and glucose regulation. Cancer Res 2008;68(16):6643–51.
[45] Sharma V, Tewari R, Sk UH, Joseph C, Sen E. Ebselen sensitizes glioblastoma cells to Tumor Necrosis Factor (TNFalpha)-induced apoptosis through two distinct pathways involving NF-kappaB downregulation and Fas-mediated formation of death inducing signaling complex. Int J Cancer 2008;123(9):2204–12.
[46] Kuwayama K, Matsuzaki K, Mizobuchi Y, Mure H, Kitazato KT, Kageji T, et al. Promyelocytic leukemia protein induces apoptosis due to caspase-8 activation via the repression of NFkappaB activation in glioblastoma. Neuro Oncol 2009;11(2):132–41.
[47] Carapancea M, Alexandru O, Fetea AS, Dragutescu L, Castro J, Georgescu A, et al. Growth factor receptors signaling in glioblastoma cells: therapeutic implications. Neurooncology 2009;92(2):137–47.
[48] Jiang Z, Zheng X, Rich KM. Down-regulation of Bcl-2 and Bcl-xL expression with bispecific antisense treatment in glioblastoma cell lines induce cell death. J Neurochem 2003;84:273–81.
[49] Zhao S, Tsuchida T, Kawakami K, Shi C, Kawamoto K. Effect of $As_2O_3$ on cell cycle progression and cyclins D1 and B1 expression in two glioblastoma cell lines differing in p53 status. Int J Oncol 2002;21(1):49–55.
[50] Haga N, Fujita N, Tsuruo T. Involvement of mitochondrial aggregation in arsenic trioxide ($As_2O_3$)-induced apoptosis in human glioblastoma cells. Cancer Sci 2005;96(11):825–33.
[51] Chiu TL, Su CC. Curcumin inhibits proliferation and migration by increasing the Bax to Bcl-2 ratio and decreasing NF-kappaB p65 expression in breast cancer MDA-MB-231 cells. Int J Mol Med 2009;23(4):469–75.
[52] Hayashi S, Sakurai H, Hayashi A, Tanaka Y, Hatashita M, Shioura H. Inhibition of NF-kappaB by combination therapy with parthenolide and hyperthermia and kinetics of apoptosis induction and cell cycle arrest in human lung adenocarcinoma cells. Int J Mol Med 2010;25(1):81–7.
[53] Sidransky D, Mikkelsen T, Schwechheimer K, Rosenblum ML, Cavanee W, Vogelstein B. Clonal expansion of p53 mutant cells is associated with brain tumour progression. Nature 1992;355:846–7.
[54] Lowe SW, Bodis S, McClatchey A, Remington L, Ruley HE, Fisher DE, et al. p53 status and the efficacy of cancer therapy in vivo. Science 1994;266:807–10.
[55] Lowe SW, Ruley HE, Jacks T, Housman DE. p53-dependent apoptosis modulates the cytotoxicity of anticancer agents. Cell 1993;74:957–67.
[56] Igney FH, Krammer PH. Death and anti-death: tumour resistance to apoptosis. Nat Rev Cancer 2002;2:277–88.
[57] Pierce JW, Schoenleber R, Jesmok G, Best J, Moore SA, Collins T, et al. Novel inhibitors of cytokine-induced IκBα phosphorylation and endothelial cell adhesion molecule expression show anti-inflammatory effects in vivo. J Biol Chem 1997;272:21096–103.
[58] Kwok BH, Koh B, Ndubuisi MI, Elofsson M, Crews CM. The anti-inflammatory natural product parthenolide from the medicinal herb Feverfew directly binds to and inhibits IκB kinase. Chem Biol 2001;8:759–66.
[59] Hehner SP, Hofmann TG, Droge W, Schmitz ML. The antiinflammatory sesquiterpene lactone parthenolide inhibits NF-κB by targeting the IκB kinase complex. J Immunol 1999;163:5617–23.
[60] Han SS, Kim K, Hahm ER, Park CH, Kimler BF, Lee SJ, et al. Arsenic trioxide represses constitutive activation of NF-kappaB and COX-2 expression in human acute myeloid leukemia, HL-60. J Cell Biochem 2005;94:695–7.
[61] Kasinski AL, Du Y, Thomas SL, Zhao J, Sun SY, Khuri FR, et al. Inhibition of IkappaB kinase–nuclear factor-kappaB signaling pathway by 3,5-bis(2-flurobenzylidene)piperidin-4-one (EF24), a novel monoketone analog of curcumin. Mol Pharmacol 2008;74:654–61.
[62] Santel T, Pflug G, Hemdan NY, Schäfer A, Hollenbach M, Buchold M, et al. Curcumin inhibits glyoxalase 1: a possible link to its anti-inflammatory and anti-tumor activity. PLoS ONE 2008;3(10):e3508.
[63] Weaver KD, Yeyeodu S, Cusack Jr JC, Baldwin Jr AS, Ewend MG. Potentiation of chemotherapeutic agents following antagonism of nuclear factor kappa B in human gliomas. J Neurooncol 2003;61:187–96.
[64] Pucer A, Castino R, Mirković B, Falnoga I, Slejkovec Z, Isidoro C, et al. Differential role of cathepsins B and L in autophagy-associated cell death induced by arsenic trioxide in U87 human glioblastoma cells. Biol Chem 2010;391(5):519–31.
[65] Perry MC, Demeule M, Régina A, Moumdjian R, Béliveau R. Curcumin inhibits tumor growth and angiogenesis in glioblastoma xenografts. Mol Nutr Food Res 2010;54(8):1192–201.
[66] Karmakar S, Banik NL, Ray SK. Curcumin suppressed anti-apoptotic signals and activated cysteine proteases for apoptosis in human malignant glioblastoma U87MG cells. Neurochem Res 2007;32(12):2103–13.
[67] Liu E, Wu J, Cao W, Zhang J, Liu W, Jiang X, et al. Curcumin induces G2/M cell cycle arrest in a p53-dependent manner and upregulates ING4 expression in human glioma. J Neurooncol 2007;85(3):263–70.
[68] Anderson KN, Bejcek BE. Parthenolide induces apoptosis in glioblastomas without affecting NF-kappaB. J Pharmacol Sci 2008;106(2):318–20.
[69] Wagenknecht B, Hermisson M, Groscurth P, Liston P, Krammer PH, Weller M. Proteasome inhibitor-induced apoptosis of glioma cells involves the processing of multiple caspases and cytochrome c release. J Neurochem 2000;75(6):2288–97.
[70] Wagenknecht B, Hermisson M, Eitel K, Weller M. Proteasome inhibitors induce p53/p21-independent apoptosis in human glioma cells. Cell Physiol Biochem 1999;9(3):117–25.

III.1 – Artigo 4

# The curry spice curcumin selectively inhibits cancer cells growth in vitro and in preclinical model of glioblastoma.

Journal of Nutritional Biochemistry, 2012; 23(6): 591-601.

doi:10.1016/j.jnutbio.2011.02.015

Available online at www.sciencedirect.com

SciVerse ScienceDirect

Journal of Nutritional Biochemistry 23 (2012) 591–601

Journal of Nutritional Biochemistry

# The curry spice curcumin selectively inhibits cancer cells growth *in vitro* and in preclinical model of glioblastoma☆

Alfeu Zanotto-Filho[a,*], Elizandra Braganhol[b], Maria Isabel Edelweiss[c], Guilherme A. Behr[a], Rafael Zanin[b], Rafael Schröder[a], André Simões-Pires[a], Ana Maria Oliveira Battastini[b], José Cláudio Fonseca Moreira[a]

[a]*Centro de Estudos em Estresse Oxidativo, Departamento de Bioquímica, Universidade Federal do Rio Grande do Sul (UFRGS), Porto Alegre, Rio Grande do Sul, Brasil*
[b]*Laboratório de Enzimologia, Departamento de Bioquímica, Universidade Federal do Rio Grande do Sul (UFRGS), Porto Alegre, Rio Grande do Sul, Brasil*
[c]*Laboratório de Patologia, Hospital de Clínicas de Porto Alegre (HCPA), Porto Alegre, Rio Grande do Sul, Brasil*

Received 14 December 2010; received in revised form 30 January 2011; accepted 24 February 2011

**Abstract**

Previous studies suggested that curcumin is a potential agent against glioblastomas (GBMs). However, the *in vivo* efficacy of curcumin in gliomas remains not established. In this work, we examined the mechanisms underlying apoptosis, selectivity, efficacy and safety of curcumin from *in vitro* (U138MG, U87, U373 and C6 cell lines) and *in vivo* (C6 implants) models of GBM. *In vitro*, curcumin markedly inhibited proliferation and migration and induced cell death in liquid and soft agar models of GBM growth. Curcumin effects occurred irrespective of the p53 and PTEN mutational status of the cells. Interestingly, curcumin did not affect viability of primary astrocytes, suggesting that curcumin selectivity targeted transformed cells. In U138MG and C6 cells, curcumin decreased the constitutive activation of PI3K/Akt and NFkappaB survival pathways, down-regulated the antiapoptotic NFkappaB-regulated protein bcl-xl and induced mitochondrial dysfunction as a prelude to apoptosis. Cells developed an early G2/M cell cycle arrest followed by sub-G1 apoptosis and apoptotic bodies formation. Caspase-3 activation occurred in the p53-normal cell type C6, but not in the p53-mutant U138MG. Besides its apoptotic effect, curcumin also synergized with the chemotherapeutics cisplatin and doxorubicin to enhance GBM cells death. In C6-implanted rats, intraperitoneal curcumin (50 mg $kg^{-1}$ $d^{-1}$) decreased brain tumors in 9/11 (81.8%) animals against 0/11 (0%) in the vehicle-treated group. Importantly, no evidence of tissue (transaminases, creatinine and alkaline phosphatase), metabolic (cholesterol and glucose), oxidative or hematological toxicity was observed. In summary, data presented here suggest curcumin as a potential agent for therapy of GBMs.


*Keywords:* Curcumin; Glioblastoma; Apoptosis; *In vitro*; Preclinical

## 1. Introduction

Glioblastoma (GBM) is an aggressive, invasive and difficult to treat primary brain tumor. Standard therapy includes surgical resection, external beam radiation and chemotherapy, with no known curative therapy [1,2]. A number of deregulated signaling cascades have been described in GBMs, including the nuclear factor kappa-B (NFkappaB), the phosphoinositide-3-kinase (PI3K/Akt) pathway and the Ras/MEK/ERK mitogen-activated protein kinase pathway. Deregulation of these pathways is driven by mutation, amplification or overexpression of multiple genes such as PTEN, EGFr, PDGFR-a, p53 and mTOR [3–5]. Understanding these deregulated pathways has provided the basis for designing molecular targeted therapies as well as new combination therapies and drug delivery systems [6–8]. Despite the aforementioned findings, median survival in GBM has remained approximately 1 year for decades [1,2]. Therefore, validation of new antiglioma drugs may offer new therapeutic opportunities to patients.

Curcumin (diferuloylmethane), a naturally occurring polyphenol derived from the root of the rhizome *Curcuma longa*, possesses anti-inflammatory, antioxidant and anticancer properties by inhibition of signaling pathways such as NFkappaB, PI3K/Akt and activator protein-1 (AP-1) [9]. Recently, curcumin entered into phase I clinical trials for the treatment of some high-risk cancers [10]. In GBMs, an emerging *in-vitro*-based literature [11–16] suggests that curcumin exerts antiglioma effects through enhancement of TRAIL-induced apoptosis [11], inhibition of metalloproteinase-9 expression [12,14] and induction of apoptosis in T98G and U87MG cell lines [13,15,16]. However, the apoptotic mechanisms, selectivity to transformed cells and principally the *in vivo* efficacy of curcumin in GBMs remain to be better studied. In this work, we examined the mechanisms underlying curcumin anti-GBM effects based on *in vitro* (C6, U138MG, U87 and U373 cell lines) and *in vivo* (C6 implants in rat brain) models of the disease. *In vitro*, we evaluated curcumin effects on proliferation, apoptosis and migration as well as antagonism with classical GBM survival pathways (PI3K/Akt and NFkappaB), selectivity to cancer

☆ Conflict of interest statement: The authors report that there are no conflicts of interest.

* Corresponding author. Depto. Bioquímica (ICBS-UFRGS), Rua Ramiro Barcelos, 2600/Anexo, CEP 90035-003, Porto Alegre, Rio Grande do Sul, Brazil. Tel.: +55 51 3308 5578; fax: +55 51 3308 5535.

*E-mail address:* alfeuzanotto@hotmail.com (A. Zanotto-Filho).

0955-2863/$ - see front matter © 2012 Elsevier Inc. All rights reserved.
doi:10.1016/j.jnutbio.2011.02.015

cells and adjuvant potential. *In vivo*, we tested the hypothesis that curcumin may decrease glioma growth without inducing toxicity to healthy tissues.

## 2. Materials and methods

### 2.1. Reagents

Curcumin, propidium iodide (PI), Hepes, CHAPS, dithiothreitol, EDTA, trypsin, 3-(4,5-dimethyl)-2,5-diphenyl tetrazolium bromide (MTT), Nonidet-P40, spermin tetrahydrochloride, RNAse A and culture analytical-grade reagents were purchased from Sigma Chemical Co. (St. Louis, MO, USA). Anti-lamin B (C-20) and anti-p65 NFkappaB antibodies were from Santa Cruz Biotechnologies; anti-β-actin, anti-phospho-Akt(ser$^{473}$) , anti-Akt and anti-bcl-xl were from Cell Signaling Technology. Parthenolide (PTL) and LY294002 were from Biomol International (Plymouth Meeting, PA, USA). Electrophoresis and immunoblotting reagents were from Bio-Rad Laboratories (Hercules, CA, USA). Kits for biochemical analysis were acquired from Labtest Diagnostica (MG, Brazil).

### 2.2. Cell cultures

The rat (C6) and human (U138MG, U87 and U373) malignant GBM cell lines were obtained from American Type Culture Collection (Rockville, MD, USA). The cells were grown and maintained in low-glucose Dulbecco's modified Eagle's medium (DMEM; Gibco BRL, Carlsbad, CA, USA) containing 0.1% Fungizone and 100 U/L gentamicin and supplemented with 10% fetal bovine serum (FBS). Cells were kept at 37°C in a humidified atmosphere with 5% $CO_2$. Primary astrocyte cultures were prepared as previously described [17]. Briefly, cortex of newborn Wistar rats (1–2 days old) were removed and dissociated mechanically in a $Ca^{+2}$ and $Mg^{+2}$ free balanced salt solution, pH 7.4, (137 mmol/L NaCl, 5.36 mmol/L KCl, 0.27 mmol/L $Na_2HPO4$, 1.1 mmol/L $KH_2PO4$, 6.1 mmol/L glucose). After centrifugation at 1000 rpm for 5 min, the pellet was resuspended in DMEM supplemented with 10% FBS. The cells ($2\times10^5$) were plated in poly-L-lysine-coated 48-well plates. After 4-h plating, plates were gently shaken and phosphate-buffered saline (PBS)-washed, and medium was changed to remove neuron and microglia contaminants. Cultures were allowed to grow to confluence by 20–25 days. Medium was replaced every 4 days.

### 2.3. MTT and lactate dehydrogenase assays

Dehydrogenases-dependent MTT reduction (MTT assay) and lactate dehydrogenase release into culture medium [lactate dehydrogenase (LDH) assay] were used as an estimative of cell viability [18]. Cells were plated in 96-well plates ($10^4$/well) and treated at 60%–70% confluence. At the end of incubations, MTT and LDH assays were performed. Lactate dehydrogenase activity in the culture medium was determined in agreement with manufacturer instructions (CytoTox 96-NonRadioactive Cytotoxicity Assay, Promega). Cell morphology was evaluated by light microscopy (Nikon Eclipse TE 300).

### 2.4. PI incorporation and staining of chromatin

For determination of PI uptake in cells with losses in membrane integrity, treated cells were incubated with 2 μg/ml PI in complete medium for 1 h. Propidium iodide fluorescence was excited at 515–560 nm using an inverted microscope (Nikon Eclipse TE 300) fitted with a standard rhodamine filter. Representative microphotographs (at least five per well) were collected [19]. For detection of the morphological alterations in chromatin (condensation and fragmentation) and apoptotic bodies formation, cells were fixed in methanol/acetone (1:1) for 5 min and washed with PBS (three times). Afterward, chromatin was stained with PI (0.5 μg/ml, 10 min) followed by fluorescent microscopy (Nikon Eclipse TE 300).

### 2.5. Cell cycle analysis

For cell cycle analysis, cells were trypsinized, centrifuged and resuspended in a lysis buffer containing 3.5 mmol/L trisodium citrate, 0.1% vol/vol Nonidet P-40, 0.5 mmol/L Tris-HCl, 1.2 mg/ml spermine tetrahydrochloride, 5 μg/ml RNAse, 5 mmol/L EDTA and 1 μg/ml PI, pH 7.6. Afterward, cells were incubated for at least 10 min on ice for cell lysis. DNA content was determined by flow cytometry. Ten thousand events were counted per sample. FACS analyses were performed in the CellQuest Pro Software (BD Biosciences, CA, USA) [18].

### 2.6. Caspase-3 activity

Caspase-3 activity was assessed in agreement with CASP3F Fluorometric kit (Sigma, Saint Louis, MI, USA). Treated cells were harvested and incubated in a lysis buffer (50 mmol/L Hepes, 5 mmol/L CHAPS and 5 mmol/L dithiothreitol, pH 7.4) for 20 min in ice. Afterward, extracts were clarified by centrifugation at 13,000*g* (15 min, 4°C). Supernatants were collected, and proteins were measured by Bradford method. For assays, 150 μg proteins were mixed with 200 μl of the assay buffer (20 mmol/L Hepes, 0.1% CHAPS, 5 mmol/L dithiothreitol, 2 mmol/L EDTA, pH 7.4) plus 20 μM Ac-DEVD-AMC (Acetyl-Asp-Glu-Val-Asp-7-amido-4-methylcoumarin), a caspase-3-specific substrate. Caspase-3-mediated substrate cleavage was monitored during 1 h (37°C) in a fluorometric reader (excitation 360 nm/emission 460 nm) [18].

### 2.7. Cellular fractionation

For nuclear extracts preparation, cells (~$5\times10^6$, 70%–80% confluence) were washed with cold PBS and suspended in 0.4-ml hypotonic lysis buffer [10 mmol/L HEPES (pH 7.9), 1.5 mmol/L $MgCl_2$, 10 mmol/L KCl, 0.5 mmol/L phenylmethylsulfonyl fluoride, 0.5 mmol/L dithiothreitol plus protease inhibitor cocktail (Roche)] for 15 min. Cells were then lysed with 12.5 μl 10% Nonidet P-40. The homogenate was centrifuged (13,000*g*, 30 s), and supernatants containing the cytoplasmic extracts were stored at −80°C. The nuclear pellet was resuspended in 100-μl ice-cold hypertonic extraction buffer [10 mmol/L HEPES (pH 7.9), 0.42 M NaCl, 1.5 mmol/L $MgCl_2$, 10 mmol/L KCl, 0.5 mmol/L phenylmethylsulfonyl fluoride, 1 mmol/L dithiothreitol plus protease inhibitors]. After 40 min of intermittent mixing, extracts were centrifuged (13,000*g*, 10 min, 4°C), and supernatants containing nuclear proteins were secured. The protein content was measured by the Bradford method [18–20].

### 2.8. NFκB-p65 enzyme-linked immunosorbent assay for determination of NFκB activity

A total of 10 μg of nuclear extracts was used to determine the NFκB DNA-binding activity [NFκB p65 enzyme-linked immunosorbent assay (ELISA) kit, Stressgen/Assays designs] per manufacturer's protocols. This ELISA-based chemiluminescent detection method rapidly detects activated NFκB complex binding (p65 detection) to a plate-adhered NFκB consensus oligonucleotide sequence. Kit-provided nuclear extracts prepared from TNF-stimulated Hela cells were used as a positive control for NFκB activation. To demonstrate assay specificity, a 50-fold excess of an NFκB consensus oligonucleotide was used as competitor to block NFκB binding. In addition, a mutated consensus NFκB oligonucleotide (which does not bind NFκB) is provided for determination of binding reactions' specificity [21].

### 2.9. Western blotting

Proteins (20 μg) were separated by sodium dodecyl sulfate polyacrylamide gel electrophoresis on 10% (wt/vol) acrylamide and 0.275% (wt/vol) bisacrylamide gels and electrotransferred onto nitrocellulose membranes. Membranes were incubated in TBS-T [20 mmol/L Tris–HCl, pH 7.5, 137 mmol/L NaCl, 0.05% (vol/vol) Tween 20] containing 1% (wt/vol) nonfat milk powder for 1 h at room temperature. Subsequently, the membranes were incubated for 12 h with the appropriate primary antibody (dilution range 1:500–1:1000), rinsed with TBS-T and exposed to horseradish-peroxidase-linked anti-IgG antibodies for 2 h at room temperature. Chemiluminescent bands were detected using X-ray films, and densitometry analyses were performed using Image-J software.

### 2.10. Mitochondria membrane potential (JC-1 assay)

For determination of the mitochondrial membrane potential (MMP), treated cells ($5\times10^5$) were incubated for 30 min at 37°C with the lipophilic cationic probe JC-1 (5,5′,6,6′-tetrachloro-1,1′,3,3′ tetraethylbenzimidazolcarbocyanine iodide, 2 μg/ml). Afterward, JC-1-loaded cells were centrifuged and washed once with PBS. Cells were transferred to a 96-well plate and assayed in a fluorescence plate reader with the following settings: excitation at 485 nm, emission at 540 and 590 nm and cutoff at 530 nm (SpectraMax M2, Molecular Devices, USA). $\Delta\Psi m$ was calculated using the ratio of 590 nm (J-aggregates)/540 nm (monomeric form) [22].

### 2.11. Clonogenic potential

Exponentially growing cells ($1\times10^6$) were plated in petri plates overnight and then incubated for 36 h with either vehicle or curcumin. After treatments, the medium containing curcumin was replaced by a curcumin-free medium, and remaining cells were maintained for additional 24 h to growth. Survival cells were gently washed and

Table 1
$IC_{50}$ levels of curcumin in a panel of GBMs and astrocytes

| Cell lines | Curcumin $IC_{50}$ (μM) |
|---|---|
| U138MG | 29±5[a] |
| C6 | 25±4[a] |
| U87 | 19±7[a] |
| U373 | 21±3[a] |
| Astrocytes | 135±12 |

Legend: Cells (U138MG, U87, C6, U373 and astrocytes) were treated for 36 h with different concentrations of curcumin (1–150 μM), and cell viability was determined by MTT assay. Experiments were repeated three times ($n$=3) in triplicate, and data were expressed in mean±S.D.

[a] Different from astrocytic $IC_{50}$ value ($P$<.05, $t$ test).

Table 2
LDH release and cellular viability in curcumin-treated C6 and astrocytes

| Curcumin (μM) | C6 cells | | Astrocytes | |
|---|---|---|---|---|
| | Viability (MTT, %) | LDH (%) | Viability (MTT, %) | LDH (%) |
| 0 | 100±3 | 100±14 | 100±9 | 100±11 |
| 7.5 | 90±2[a] | 113±21 | 101±3 | 102±13 |
| 15 | 78±5[b] | 120±36 | 103±4 | 98±19 |
| 25 | 67±2[b] | 276±92[a] | 102±17 | 89±9 |
| 50 | 28±3[b] | 907±105[b] | 108±13 | 121±13 |
| 100 | 10±5[b] | 1251±57[b] | 110±15 | 115±33 |
| 120 | 3±1[b] | 1290±154[a] | 81±9[a] | 169±14[a] |

Legend: Cells were treated with curcumin for 36 h; medium was collected for LDH activity determination, and cells were used for viability estimation by MTT assay. Experiments were repeated three times ($n$=3) in triplicate, and data were expressed in mean±S.D.
[a] Different from untreated cells.
[b] Different from untreated cells and from the immediately lower curcumin concentration ($P$<.05, ANOVA).

trypsinized, and viability was assessed by trypan blue staining. Viable cells ($10^4$ cells) were replated in six-well plates and maintained for additional 6 days in complete culture medium. Cell growth was estimated by colony counting followed by MTT assay [21]. The percentage of colony forming efficiency was calculated in relation to values of untreated cells.

### 2.12. Soft agar colony assay

Cells ($1\times10^5$) were resuspended in 2 ml DMEM supplemented with 15% FBS and mixed with 1 ml of 1.6% agarose (final conditions: 0.53% agarose and 10% FBS) at 37°C. Cell suspensions were placed on top of a base layer comprised of 2 ml of DMEM with 10% FBS and 0.8% agarose in each well of a six-well plate. Cells were then covered with 2 ml of complete media, and after 3 days, a new medium containing curcumin was added. Medium containing treatments or vehicle was replaced every 72 h. At the end of 9 days, MTT (1 mg/ml) was added to the cultures, and the number of colonies was scored using a microscope [21].

### 2.13. Migration assay

The monolayer of confluent C6 and U138MG cells was pretreated for 12 h with curcumin and subsequently scratched with a 200 μl pipette tip to create a wound. Cells were washed twice with PBS to remove floating cells and then incubated in DMEM with 2% FBS plus treatments. Cells were incubated for additional 16–18 h, and the rate of wound closure was investigated through photographs (100×) taken at final time points. Migration of treated cells was compared to untreated cells and expressed as percentage [23].

### 2.14. Proliferation assay

For proliferation assay, 24-well-plated cells were treated at 50%–60% confluence during 72 h (chronic exposure) with curcumin inhibitors. After treatments, cells were fixed in ethanol:acetone (1:1) for 5 min followed by PBS washing (three times). Fixed cells were stained with trypan blue 0.4% (Sigma, CA, USA) for 30 min and washed three times with PBS. Trypan-stained cells were lysed with 1 N NaOH for 5 min. Afterward, equal volume of distillated water was added, and trypan blue color was estimated in spectrophotometer at 595 nm [24]. Sample absorbance was compared to controls and expressed as percentage of untreated cells.

### 2.15. Preclinical study: glioma in vivo experiments

#### 2.15.1. Implantation

*In vivo* model of rat C6 glioma was carried out as previously described by Takano et al. [25] and validated in our laboratory [26,27]. Exponentially growing C6 cells were trypsinized, washed once in DMEM, spun down and resuspended at $10^6$ cells/3 μl DMEM. Cells were injected using a 5-μl Hamilton microsyringe coupled in the infusion pump (1 μl/min) at a depth of 6.0 mm into the right striatum (coordinates with regard to bregma: 0.5 mm posterior and 3.0 mm lateral) of adult male Wistar rats (8 weeks old, 220–260 g) previously anesthetized by intraperitoneal (ip) administration of

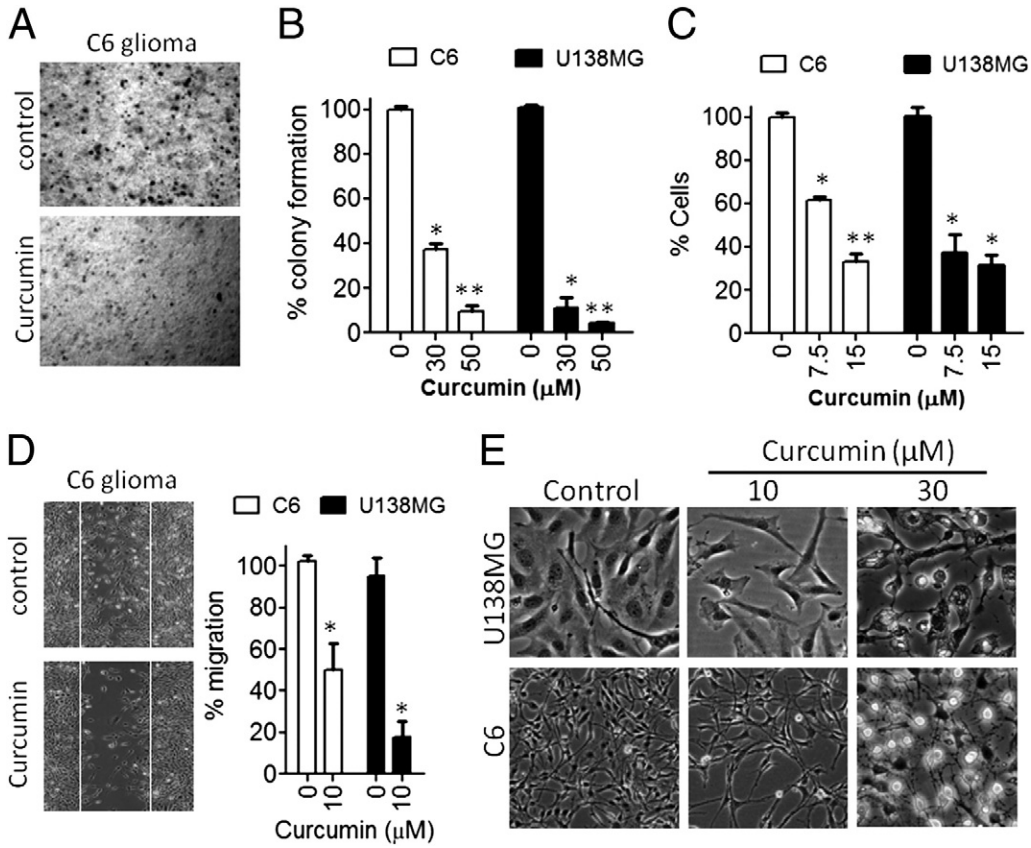


Fig. 1. Curcumin inhibits GBM cells growth. (A) Curcumin 30 μM inhibits the growth of C6 cells in soft agar. (B) Short-term incubation with curcumin reduces clonogenic potential of C6 and U138MG cells. (C) Effect of subtoxic concentrations of curcumin on proliferation of C6 and U138MG cell lines. Cells were treated for 72 h with 7.5 or 15 μM curcumin, fixed and stained with trypan blue for estimation of cell density. Cell morphology was monitored by light microscopy. *Different from untreated cells; **different from the immediately lower curcumin concentration, $P$<.05, ANOVA. (D) Subtoxic concentrations of curcumin (10 μM) decrease U138MG and C6 cells migration. *Different from untreated cells, $P$<.05, $t$ test. (E) Representative microphotographs (20×) showing the effect of cytotoxic (30 μM) and subapoptotic (10 μM) concentrations of curcumin on morphology of U138MG and C6 cells. All experiments were repeated at least four times ($n$=4).

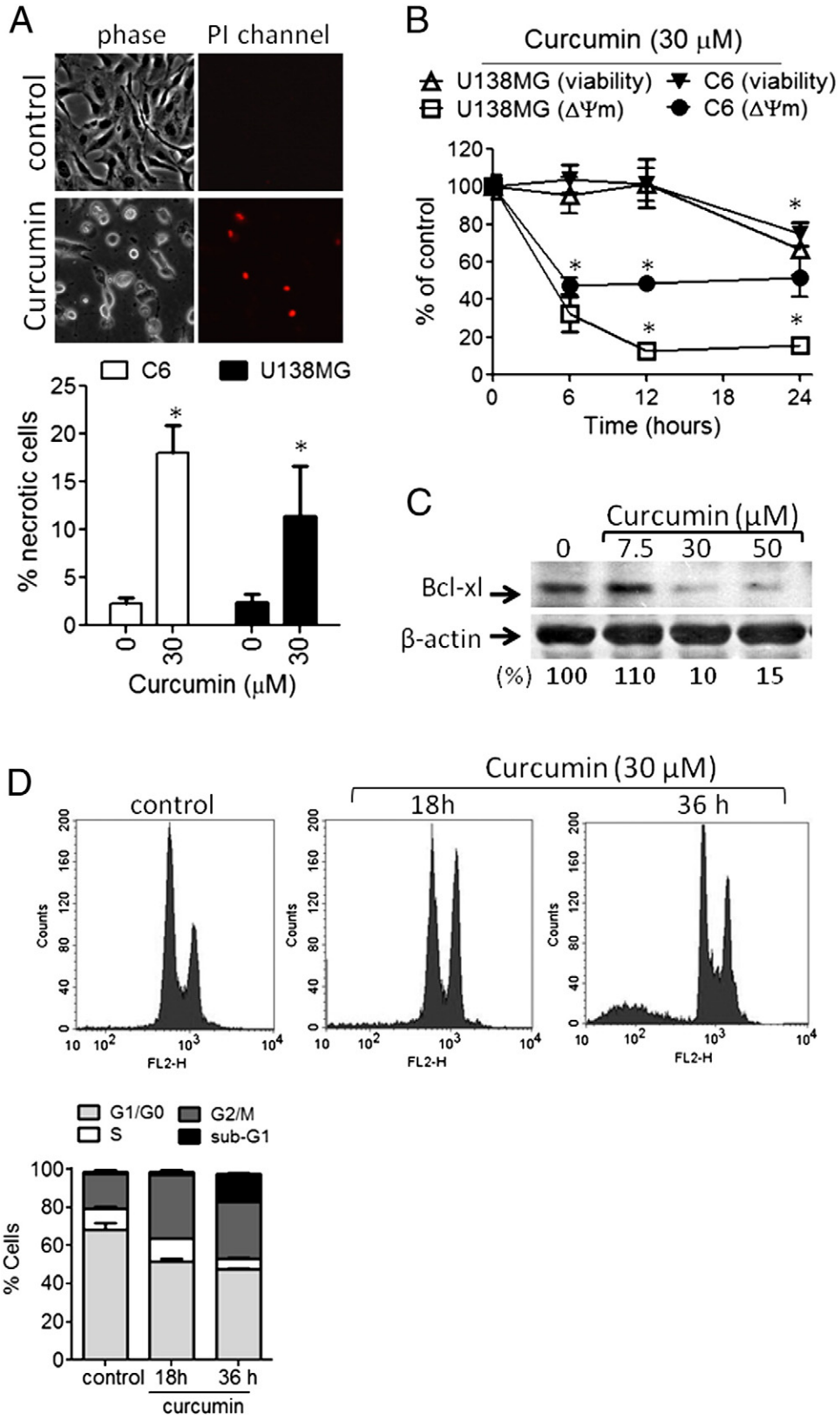


Fig. 2. Curcumin induces mitochondrial dysfunction and programmed cell death in GBMs. (A) Propidium iodide incorporation in U138MG cells. After 36-h treatment with 30 μM curcumin, cells were incubated with PI diluted in culture medium. Fluorescence and phase contrast microphotographs were taken (20×). The percentage of PI-stained cells was quantified. *Different from untreated cells, $P<.05$, $t$ test. (B) Time course effect of curcumin on MMP was co-evaluated with PI incorporation for determination of cell membrane integrity. U138MG cells were treated for different times and trypsinized, and different aliquots were collected for JC-1 or PI incorporation assays. *Different from untreated cells, $P<.05$, $t$ test. (C) Curcumin decreases bcl-xL protein immunocontent as assessed by Western blotting in total cell extracts of 12-h-treated U138MG cells. (D) Flow cytometry for determination of cell cycle distribution (sub-G1, G1/G0, S and G2/M) in untreated and 30 μM curcumin-treated (18–36 h) U138MG cells. All experiments were repeated at least three times ($n=3$).

ketamine/xylazine. The number of animals for 95% confidence was statistically calculated in agreement with our previously determined standard deviations ($S$) and means ($\mu$) of tumor size for the *in vivo* model of glioma [26]. Data/legends: A=DMSO-treated rats (control); B=alkylation-agent-treated rats (control for antiglioma activity); statistical parameters: $\mu_A$=73 mm$^3$; $\mu_B$=27 mm$^3$; $S_A$=13 mm$^3$; $S_B$=37 mm$^3$; $\alpha$=0.05, power=1−$\beta$=0.9; $\beta$=0.1; $t_\alpha$=2.101; $u_\beta$=1,734; $n_0$=10. Formula: $n=((S_A)^2+(S_b)^2)/(\mu_A-\mu_b)^2\times(t_\alpha+u_\beta)^2$; $n$=11 rats/group. All procedures used in the present study followed the "Principles of Laboratory Animal Care" of the National Institutes of Health and were approved by the Ethical Committee of the Hospital de Clinicas de Porto Alegre.

#### 2.15.2. Treatments

Ten days after glioma implantation, animals were divided into two groups ($n$=11 per group) as follows: (a) DMSO/vehicle-treated group and (b) curcumin-treated group (50 mg/kg/day curcumin solubilized in sterile DMSO). The formulations were administered ip for 10 consecutive days.

#### 2.15.3. Analysis

After 20 days (10 days for glioma implantation+10 days for treatments), rats were anesthetized and decapitated. The brain was removed, sectioned and fixed with 10% paraformaldehyde. Cerebellum, liver and kidney were also removed and frozen at −80°C for biochemical analysis. Blood samples were collected for determination of glucose, total cholesterol, creatinine, alkaline phosphatase, alanine aminotransferase (ALT) and aspartate aminotransferase (AST) activity in serum, which were used as markers of metabolic and tissue toxicity. These experiments were performed in a LabMax 240 analyzer (Labtest Diagnostica, Brazil). Hematological parameters were evaluated in a Sysmex KX-21-N hematologic analyzer (Sysmex, Lille, France). The oxidative stress parameters TBARS (lipoperoxidation), protein sulfhydryl and carbonyl groups, catalase, superoxide dismutase and glutathione *S*-transferase (GST) activity were evaluated in cerebellum, liver and kidney in agreement with our previously described protocols [28].

For tumor volume quantification, three hematoxylin and eosin (H&E) coronal sections (2–3 μm thick, paraffin embedded) from each animal were analyzed. Images were captured using a digital camera connected to a microscope (Nikon Eclipse TE300), and the tumor area (mm$^2$) was determined using Image Tool Software. The total volume (mm$^3$) of the tumor was computed by the multiplication of the slice sections and by summing the segmented areas [26,27]. In animals with detectable tumor mass, histopathological parameters were evaluated by two expert pathologists.

### 2.16. Statistical analysis

The statistical significance among three or more groups was assessed by one-way analysis of variance (ANOVA) followed by Tukey's test. The statistical significance between DMSO-treated and curcumin-treated groups and other two-group analyses were carried out by means of unpaired Student's $t$ test (Prism GraphPad Software, San Diego, CA, USA). For qualitative data (Table 4 experiments), $Z$-test for two proportions and Fisher's Exact Test were chosen. Significant differences among groups were calculated at $P$<.05.

## 3. Results

### 3.1. Curcumin inhibits proliferation and induces cell death in GBMs but not in astrocytes

First, we examined the effect of curcumin on viability of GBMs by treating a panel of GBM cell lines (C6, U138MG, U87, U373) with different concentrations of curcumin for 36 h. At the end of incubation, MTT assays were carried out. In parallel, primary astrocytes cultures were used as a nontransformed model of glial cells in order to test the selectivity of curcumin. Curcumin markedly decreased the viability of the four GBM cells lines ($IC_{50}$ range=19–28 μM), whereas astrocytes were much less sensitive to curcumin treatment ($IC_{50}$=135 μM) as assessed by MTT (Table 1). Curcumin also caused a dose-dependent release of LDH into culture medium of GBMs, indicating losses in cell membrane integrity. Curcumin-induced LDH release was associated with decreases in cell viability as assessed by MTT (Table 2). In astrocytes, toxicity only was observed at high curcumin concentrations (120 μM). Taken together, these data suggest that the cytotoxic effects of curcumin selectively targeted GBMs (Table 2). For further experiments, we used ~$IC_{50}$ concentrations of curcumin, and the C6 and U138MG cell lines since (a) they have different patterns of p53 mutations, (b) curcumin mechanisms were not determined in these cell lines and (c) C6 cells were used in *in vivo* experiments.

Curcumin-induced growth inhibition was independent on cell anchorage to extracellular matrix as evaluated by soft agar growth experiments (Fig. 1A). In addition, results from clonogenic survival assays showed that curcumin treatment (24 h) followed by 6-day washout significantly decreased the clonogenic proliferation in GBMs, suggesting that curcumin effects were prolonged and persisted after drug withdrawal (Fig. 1B). Significant morphological alterations and cell detachment were observed in 30 μM curcumin-treated cells (Fig. 1E). At low concentrations (≤15 μM), curcumin caused decreases in cell viability and cell density (Table 2 and Fig.

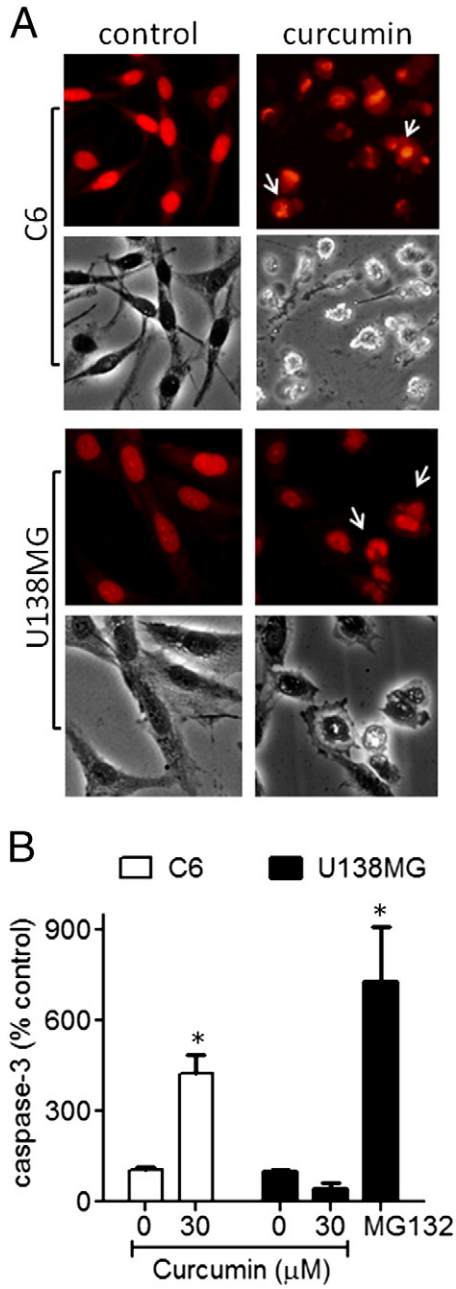


Fig. 3. Curcumin promotes chromatin condensation and modulates caspase-3 in GBMs. (A) Representative fluorescence and phase contrast microphotographs (40×) showing the effect of 30 μM curcumin (36-h treatment) on condensation of chromatin and formation of apoptotic bodies in C6 and U138MG cells. (B) Caspase-3 activity after 36-h treatment with 30 μM curcumin in C6 and U138MG. *Different from untreated cells, $P$<.05, $t$ test, $n$=4.

1E), but induced neither LDH release nor alterations in cell morphology (Fig. 1E), indicating a cytostatic/antiproliferative effect of curcumin at noncytotoxic concentrations. Therefore, we decided to test whether a long-term exposure to subtoxic curcumin could decrease cell proliferation. Curcumin (7.5 and 15 μM) decreased cell proliferation by up to 73%±12% after 72-h exposure when compared

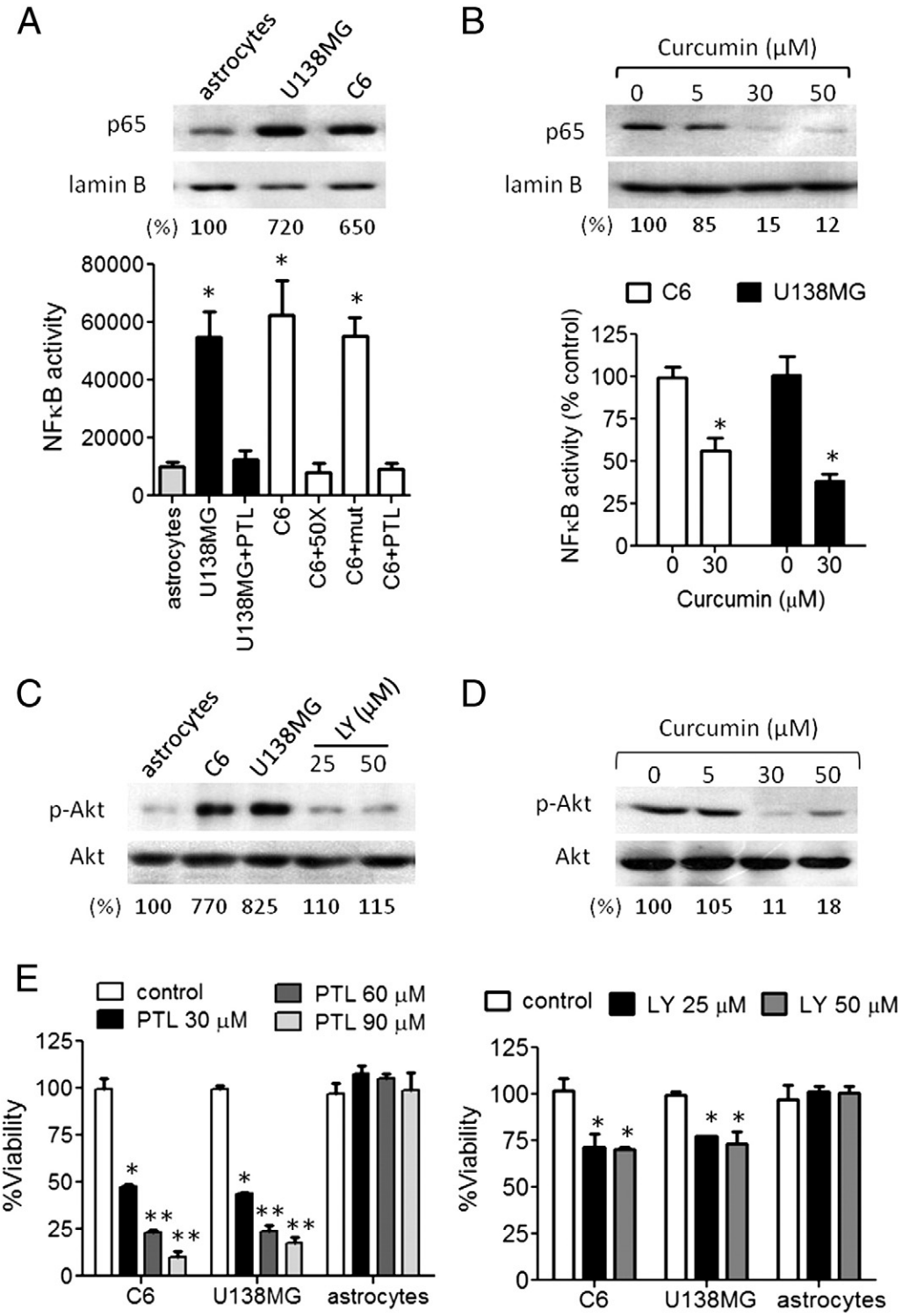


Fig. 4. Curcumin suppresses activation of NFkappaB and PI3K/Akt in GBMs. (A) Constitutive NFkappaB activation and nuclear levels of p65 in C6, U138MG and astrocytes. Cells were maintained in equal basal conditions (complete culture medium for 48 h), and nuclear extracts were isolated for detection of NFkappaB activity (ELISA kit) and p65 immunocontent (Western blotting). Lamin B was used as loading control for nuclear extracts. *Different from astrocytes, $P<.05$, ANOVA. (B) Curcumin inhibits NFkappaB DNA-binding activity and p65 translocation in GBM. The ELISA assays and Western blots were carried out in nuclear extracts isolated from 6-h-treated U138MG cells. [a]Different from untreated cells, $P<.05$, $t$ test. (C) Constitutive PI3K/Akt pathway activation in C6, U138MG and astrocytes. Cells were maintained in basal conditions (above cited), and Western blotting for p-Akt and total-Akt forms was performed in total extracts. Beta-actin was used as loading control (not shown). (D) Curcumin inhibits Akt phosphorylation. U138MG cells were treated for 6 h with 5 to 60 μM curcumin followed by Western blotting for p-Akt protein detection. (E) The MTT assays showing the effect of different concentrations of PTL or LY294002 (LY) on viability of GBM cell lines and astrocytes. *Different from untreated cells; **different from untreated and from the immediately lower concentration of PTL or LY, $P<.05$, ANOVA, $n=3$.

Table 3
Curcumin synergizes with classical chemotherapy

| Treatments | Viability (MTT, %) | |
|---|---|---|
| | U138MG | C6 |
| Untreated | 100±5.7 | 100±2.1 |
| Cisplatin | 63±6.0[a] | 42±3.3[a] |
| Cisplatin+curcumin 10 μM | 46±5.9[b] | 29±2.4[b] |
| Cisplatin+curcumin 25 μM | 30±3.2[b] | 10±4.2[b] |
| Doxorubicin | 66±2.0[a] | 73±4.2[a] |
| Doxorubicin+curcumin 10 μM | 48±3.3[b] | 61±3.0[b] |
| Doxorubicin+curcumin 25 μM | 36±4.6[b] | 46±5.4[b] |
| Curcumin 10 μM | 76±1.2[a] | 88±5.1[a] |
| Curcumin 25 μM | 55±5.0[a] | 75±7.3[a] |

Legend: U138MG and C6 cells lines were treated with different concentrations of curcumin, followed by exposure to cisplatin or doxorubicin for 48 h. Data were collected from three independent experiments ($n$=3) performed in triplicate.
[a] Different from untreated cells.
[b] Different from its respective cisplatin or doxorubicin monotreatment, $P$<.05, ANOVA.

to untreated cells (Fig. 1B). In addition, subtoxic curcumin (10 μM) also inhibited the migration of both C6 and U138MG cells as assessed by scratching assay (Fig. 1C).

### 3.2. Curcumin induces mitochondrial dysfunction, cell cycle arrest and apoptosis in GBMs

At the end of 36-h incubation, we observed significant morphological alterations in curcumin-treated cells, which were accompanied by PI uptake (Fig. 2A). However, PI uptake did not occur in all cells with changes in morphology, suggesting that morphological alterations preceded the losses in cell membrane permeability (Fig. 2A). These events suggest a programmed mechanism of cell death. Curcumin caused an early collapse in the MMP ($\Delta\Psi$m, Fig. 2B) and decreased the immunocontent of the cytoprotective mitochondrial protein bcl-xL (Fig. 2C). These events preceded curcumin-induced losses in plasmatic membrane integrity (PI incorporation assays, Fig. 2B). Curcumin-induced decreases in MMP and bcl-xl protein were clearly observed at 12-h treatment, whereas PI uptake only increased at later time points (24 h). By flow cytometry, we determined that curcumin caused cell arrest in the G2/M phase of the cell cycle at 18-h treatment, which cumulated in formation of a significant population of hypodiploid (sub-G1) cells at 36 h, indicating that G2/M arrest preceded apoptosis in curcumin-treated cells (Fig. 2D). Staining of chromatin with PI showed that curcumin induced chromatin condensation and formation of apoptotic bodies in GBMs after 36-h incubation (Fig. 3A). Activation of the executor caspase-3 was detectable in C6 cells but not in the p53-mutant U138MG (Fig. 3B). The proteasome inhibitor MG132 was used as a positive control for caspase-3 activation in order to confirm the noneffect of curcumin on caspase-3 in U138MG.

### 3.3. Curcumin inhibits PI3K/Akt and NFkappaB survival pathways in GBMs

NFkappaB and PI3K/Akt are considered as two important GBMs survival pathways [29,30]. NFkappaB was found up-regulated in the GBM cell lines (six- to sevenfold) compared to astrocytes as detected by ELISA assays for NFkappaB activity and Western blotting for nuclear p65 protein (Fig. 4A). Treatment with curcumin for 6 h decreased both NFkappaB activity and nuclear accumulation of p65 (Fig. 4B). Taking into account that curcumin also decreased the NFkappaB-regulated protein bcl-xl (Fig. 3B), these results indicate that curcumin inhibits NFkappaB signaling in GBMs. The ELISA assay specificity was confirmed by incubation of nuclear extracts with kit-provided 50× unlabeled oligonucleotides, which inhibited completely NFkappaB basal binding (C6+50× lane). In addition, mutant oligonucleotides did not alter NFkappaB activity, confirming the specificity of the binding reactions (C6+mut lane). The pharmacological NFkappaB inhibitor PTL was used as a control for NFkappaB inhibition (Fig. 4A); LPS was used as a control for NFkappaB activation (not shown).

PI3K/Akt pathway also was found up-regulated (seven- to eightfold increase) in C6 and U138MG cell lines compared to astrocytes (Fig. 4C). Curcumin inhibited about 80% the constitutive activation of the PI3K/Akt pathway as detected from levels of the phosphorylated forms of Akt, a surrogate to evaluate PI3K/Akt pathway activation in GBMs. Total forms of Akt were not altered, indicating that the protein was modulated in the posttranslational level (Fig. 4D). Controls for specific PI3K/Akt inhibition were performed by incubating cells with LY294002 (see Fig. 4C, LY lanes).

To evaluate/confirm whether NFkappaB and PI3K/Akt pathways, which were blocked by curcumin, play a role in survival of GBMs, we treated C6, U138MG and astrocytes with inhibitors of NFkappaB (PTL) and PI3K/Akt (LY294002) for 36 h; MTT assays were performed. NFkappaB and PI3K inhibitors decreased the cellular viability in GBM cell lines but exerted no effects on astrocytic viability (Fig. 4E).

### 3.4. Curcumin synergizes with clinically utilized anticancer drugs

Adjuvant therapy has the therapeutic advantage of potentiating the effect of classical anticancer drugs, thereby decreasing the frequently observed systemic side effects and damage to healthy tissues [31]. To explore the potential of curcumin as a chemotherapeutic adjuvant, we pretreated U138MG and C6 cells with subapoptotic (12-h pretreatment followed by 48-h coincubation) or apoptotic (12-h curcumin pretreatment, washout and subsequent 48-h incubation with anticancer drugs alone) concentrations of curcumin either alone or in combination with the alkylation agent cisplatin (5 μM) or the topoisomerase inhibitor doxorubicin (2.5 μM). The MTT assays showed that curcumin synergized with the anticancer drugs in both apoptotic and subapoptotic concentrations, potentiating the effects of the cisplatin and doxorubicin in the two tested cell lines (Table 3).

### 3.5. Curcumin inhibits GBM growth in vivo

In order to determine whether curcumin antiglioma potential *in vitro* could be achieved *in vivo*, we treated C6-implanted Wistar rats with 50 mg/kg/day curcumin, ip, from the 10th to the 20th day after glioma implantation. This *in vivo* model is one of the most useful tools to evaluate the pharmacologic potential of a drug in the growth of gliomas since tumor cells are induced to grow in the brain of immune-competent animals, thus simulating much of the *in vivo* conditions of GBMs [25–27]. Of the curcumin-treated rats, only 7/11 (63%) developed detectable tumors vs. 11/11 (100%) in the DMSO-treated

Table 4
Histological analysis of H&E-stained brain sections of glioma-implanted rats

| Histology | DMSO | Curcumin | $Z$-value/confidence |
|---|---|---|---|
| Rats with tumor development | 11/11 (100%) | 7/11 (64%) | 1.66[a]/96%[a] |
| Coagulative necrosis | 10/11 (91%) | 5/7 (71%) | 0.43/67% |
| Intratumoral hemorrhage | 9/11 (82%) | 3/7 (43%) | 1.2/88% |
| Lymphocytic infiltration | 9/11 (82%) | 4/7 (57%) | 0.6/72% |
| Peritumoral edema | 9/11 (82%) | 5/7 (71%) | −0.065/47% |
| Peripheral pseudopalisading | 6/11 (54%) | 5/7 (71%) | −0.065/47% |

Legend: The proportion of animals that developed a defined tumor mass as evaluated by H&E analysis. The histological variables (coagulative necrosis, intratumoral hemorrhage, lymphocytic infiltration, peritumoral edema, peripheric pseudopalisading) were regarded as present or absent.
[a] Different from DMSO-treated rats at $\alpha$>95 % confidence level (DMSO vs. curcumin , $Z$-test).

group (Table 4) as evaluated by histochemistry. Quantification of tumor volume was carried out exclusively in animals presenting a body mass that could be quantified. In the curcumin-treated rats with detectable tumors (seven rats), we observed decreases in tumor volume in five of seven (71%) animals, whereas all DMSO-treated rats (11/11) presented marked tumor masses (Fig. 5A). Results showed

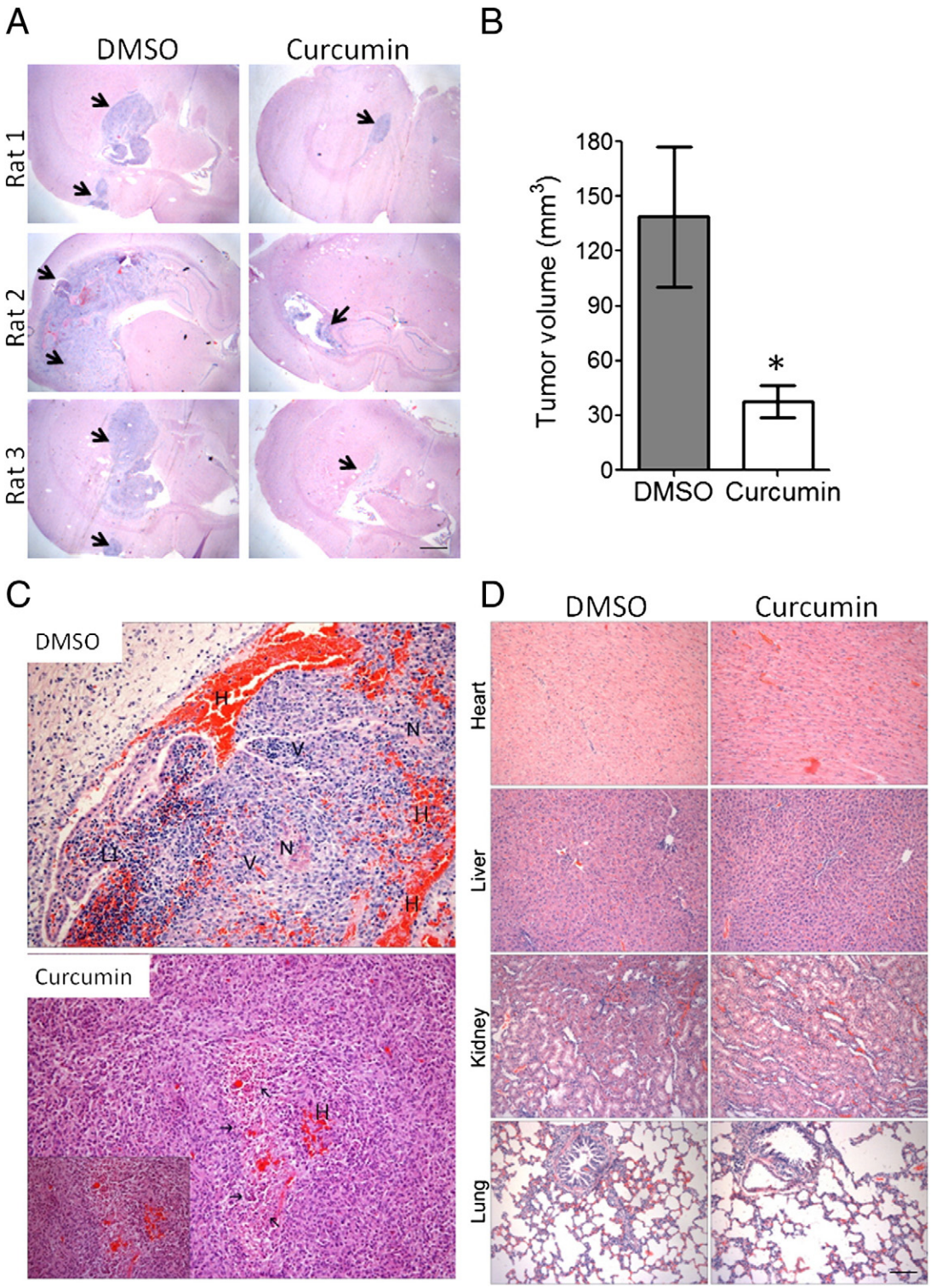


Fig. 5. Curcumin inhibits GBM growth *in vivo*. Animals were treated, and samples were analyzed as described in Materials and Methods. (A) Representative H&E-stained brain coronal sections of C6 tumors (arrows) of three representative animals of the control group (DMSO treated) and of the curcumin-treated group. Scale bars=1 mm. (B) Tumor volume ($mm^3$) quantification of implanted gliomas. *Different from DMSO-treated controls, $P<.05$, DMSO vs. curcumin , *t* test, mean±S.D. (C) Histopathology of C6 tumors. Legends: DMSO-treated group: (N) necrosis, (H) hemorrhages, (V) vascular proliferation, (LI) lymphocytic infiltration; curcumin-treated group: pathological characteristics of tumor in involution; arrows: apoptotic cells; (H) hemorrhages. Magnification 20×; insert 40×. (D) Representative microphotographs showing H&E-stained sections of liver, lung, kidney and heart of DMSO-treated and curcumin-treated glioma-implanted rats; magnification 10×.

Table 5
Hematological parameters and tissue damage serum markers in curcumin- and DMSO-treated C6 implanted rats

| | DMSO | Curcumin |
|---|---|---|
| White blood cells ($\times 10^3$/mm$^3$) | 4.8±1.2 | 4.92±1.6 |
| Red blood cells ($\times 10^6$/mm$^3$) | 7.38±0.7 | 7.37±0.6 |
| Hematocrit (%) | 40±4 | 41±3 |
| Platelets ($\times$103/mm$^3$) | 872±67 | 850±140 |
| RDW (%) | 14±0.4 | 15.1±0.5 |
| Lymphocytes (%) | 74.3±2.5 | 75.2±5.5 |
| Granulocytes (%) | 15.3±3.2 | 15.7±3.6 |
| Monocytes (%) | 10.3±2.4 | 9.1±2.1 |
| AST (U/L) | 186±30 | 194±35 |
| ALT (U/L) | 82±9 | 71±5 |
| Alkaline phosphatase (U/L) | 240±61 | 166±78 |
| Creatinine (mg/dl) | 0.5±0.05 | 0.49±0.1 |
| Glucose (mg/dl) | 161±33 | 143±35 |
| Total cholesterol (mg/dl) | 41±3 | 44±8 |

that the animals treated with curcumin displayed a significant reduction in tumor size (mean±S.D.: 37±9 mm$^3$, $n$=7) compared to the DMSO-treated (mean±S.D.=138±37 mm$^3$, $n$=11) group (Fig. 5B). Representative H&E-stained tumor sections are shown in Fig. 5A (arrows indicate tumor areas). It is important to cite that, of the 11 tumor-implanted animals in the DMSO group, two animals presented losses in body weight and motor impairment and died between the 18th and 19th day of experiment due to glioma complications.

Besides reducing tumors size, curcumin increased the number of apoptotic cells in tumors as detected by microscopic analysis of H&E-stained brain sections (Fig. 5C, arrows show apoptotic areas). On the other hand, although the percentage/proportion of animals with intratumoral hemorrhage (curcumin: 3/7 vs. DMSO: 9/11) and lymphocytic infiltration (curcumin: 4/7 vs. DMSO: 9/11) appeared to be lower in curcumin-treated rats, the proportions, which were based on qualitative analysis of "presence or absence" of the alterations, were not statistically different from DMSO-treated rats (Table 4). However, the hemorrhagic areas in curcumin-treated rats were clearly reduced when compared to DMSO-treated rats (Fig. 5C, red regions indicate intratumoral hemorrhage, H).

Importantly, curcumin neither altered hematological parameters (leukogram and hemogram) nor exerted tissue or metabolic toxicity as evaluated from determination of ALT, AST (liver damage marker), creatinine (kidney damage marker), alkaline phosphatase (pancreas, liver and bone unspecific damage markers), glucose and total cholesterol (Table 5). Means in curcumin-treated group did not differ from means in DMSO-treated rats ($t$ test; $P$>.05). In addition, curcumin did not alter oxidative stress parameters in cerebellum, liver and kidney as evaluated from quantification of TBARS, protein carbonyl, sulfhydryl and antioxidant enzymes activity (Table 6). Microscopic investigation of liver, kidney, lungs and hearts by H&E analysis also demonstrated absence of tissue toxicity in curcumin-treated rats. Representative histologies of liver, kidney, lungs and heart tissues in curcumin- and DMSO-treated rats are shown in Fig. 5D.

## 4. Discussion

The present study showed a potent and selective cytotoxic effect of the dietary compound curcumin in a panel of GBM cell lines and in glioma implants. Curcumin effect occurred in both adhered and agar-growing GBMs, evidencing an anchorage-independent mechanism. In addition, the antiglioma activity of curcumin was prolonged and persisted for several days after drug withdrawal as assessed by clonogenic assays. Besides cell death induction at cytotoxic levels, low concentrations of curcumin decreased proliferation and migration and synergized with classical anticancer drugs, suggesting that subtoxic concentrations of curcumin also could be taken for therapeutic advantage.

Curcumin appeared to act irrespective of the p53 or PTEN mutational status of the cells, since U138MG, U373 (PTEN mutated/p53 mutated), U87 (PTEN mutates/p53 wild-type) and C6 (PTEN wild-type/p53 wild-type), which possess different mutations, were sensitive to curcumin. Defects in apoptotic signaling pathways as p53 mutations and caspases down-regulation promote chemoresistance and limit the effectiveness of chemotherapeutics [32–37]. Curcumin stimulated effector caspase-3 in C6 but not in the p53-mutant U138MG, indicating that curcumin can activate either caspase-dependent or caspase-independent cell death pathways depending on the cell line. In agreement, prior studies reported that curcumin exerts caspases, calpains and p53-independent cell death via inhibition of NFkappaB in the p53-mutated T98G cell line [21]. Thus, curcumin's ability to induce caspase/p53-independent cell death circumvents two frequent aberrations that contribute to GBM resistance.

Curcumin suppressed NFkappaB and PI3K/Akt, which are two pivotal survival pathways in GBMs [38–44]. Mutations in the tensin homolog PTEN, a negative regulator of PI3K, leads to losses in PTEN activity and to constitutive activation of the PI3K/Akt pathway in most of gliomas [40,45]. On the other hand, NFkappaB up-regulation has been attributed to cytokine overproduction, deregulation of PI3K/Akt [40], RIP-1 [41] and EGFR pathways [42]. Aberrant activation of NFkappaB has been reported in GBM biopsies, and focal necrosis formation, invasive phenotypes [43] and resistance to $O^6$ alkylating agents [39] paralleled the activity of this pathway in these tumors. In high-grade astrocytoma and GBM, a positive correlation between phospho-Akt, NFκB activation and glioma progression was observed [43]. Therefore, PI3K/Akt and NFkappaB pathways become important therapeutic targets for these tumors. We found a constitutive activation of PI3K/Akt and NFkappaB in GBM cell lines but not in astrocytes. Inhibition of NFkappaB and PI3K/Akt with the pharmacological inhibitors LY294002 and PTL selectively decreased cellular viability in GBMs, confirming the role of these pathways in GBM cells survival. Taking into account the aforementioned, the mechanisms whereby curcumin is protective in normal cells, yet death inducing in tumor cells, could be explained by its ability to block survival pathways that are constitutively active in cancer but not in healthy cells, such as PI3K/Akt and NFkappaB [31,43,44]. Although markedly

Table 6
Oxidative stress markers in liver, kidney and cerebellum of C6 implanted rats after 10 days of DMSO or curcumin treatment

| | DMSO | Curcumin |
|---|---|---|
| Liver | | |
| TBARS (nmol/mg protein) | 0.092±0.031 | 0.078±0.026 |
| Sulfhydryl (μmol/mg protein) | 76.1±3.9 | 78.6±1.0 |
| Carbonyl (nmol/mg protein) | 1.1±0.3 | 0.77±0.35 |
| Catalase (U/mg protein) | 113±14.5 | 107±9.1 |
| SOD (U/mg protein) | 48.4±2.2 | 48.9±1.9 |
| GST (U/mg protein) | 2.70±0.12 | 2.68±0.11 |
| Kidney | | |
| TBARS (nmol/mg protein) | 0.64±0.05 | 0.59±0.04 |
| Sulfhydryl (μmol/mg protein) | 73.8±1.2 | 71.5±2.0 |
| Carbonyl (nmol/mg protein) | 1.47±0.6 | 1.15±0.25 |
| Catalase (U/mg protein) | 29.9±1.7 | 27.6±0.8 |
| SOD (U/mg protein) | 62.8±1.8 | 63.1±1.4 |
| GST (U/mg protein) | 1.1±0.02 | 1.2±0.08 |
| Cerebellum | | |
| TBARS (nmol/mg protein) | 0.50±0.04 | 0.47±0.03 |
| Sulfhydryl (μmol/mg protein) | 79.6±3.4 | 78±1.8 |
| Carbonyl (nmol/mg protein) | 1.2±0.31 | 0.95±0.4 |
| Catalase (U/mg protein) | 2.25±0.11 | 2.32±0.12 |
| SOD (U/mg protein) | 35.5±0.84 | 33.7±0.63 |
| GST (U/mg protein) | 2.08±0.13 | 2.23±0.12 |

cytotoxic to GBMs, curcumin spared nontransformed cells, except for a minor reduction in astrocytic viability after 100 μM, which may be restricted to proliferating astrocytes in culture; a property not shared *in vivo* [21]. The arrest in the G2/M phase as an early step of the apoptotic mechanism also could contribute to curcumin selectivity, since cancer cells are in constant cell cycle progression through S to G2/M phase, in contrast to nonproliferative cells. Previous studies showed that curcumin seems unlikely to affect normal brain function and, in fact, is neuroprotective in animal models of ischemic stroke and Alzheimer's disease [46–49].

Despite aggressive neurosurgery and chemotherapy, GBMs frequently exhibit chemoresistance [39,48–51]. Identifying novel strategies to overcome drug resistance may aid in the development of improved therapeutics. In C6 and U138MG, curcumin decreased the nuclear activity of NFkappaB, causing reduction of the bcl-xl protein immunocontent, which is a classical NFkappaB-regulated mitochondrial antiapoptotic protein. Moreover, curcumin synergized with the chemotherapeutics doxorubicin and cisplatin to cause toxicity in GBMs. This implies that curcumin may be a potential adjuvant by decreasing the antiapoptotic threshold, leading to sensitization to anticancer drugs' apoptotic stimuli. Previous studies have shown that curcumin decreases the expression of NFkappaB-regulated genes as bcl-xL, XIAP, cIAPs and survivin in T98G cells, which contribute to chemoresistance [21,52,53]. We previously reported that down-regulation of NFkappaB by BAY117082 and MG132 leads to mitochondrial dysfunction due to decreases in bcl-xL and SOD2 in leukemic cell lines [18]. Selective bcl-xL knockdown rendered U87 and NS008 GBM cells apoptosis [53], suggesting that bcl-xL down-regulation may induce mitochondrial dysfunction that ultimately results in cytotoxicity. Here, curcumin decreased bcl-xL and caused mitochondrial depolarization, which preceded the losses in cell membrane integrity, suggesting the mitochondrial dysfunction as an early step of curcumin-induced cell death. These findings corroborate with the reported caspase-9 activation in curcumin-treated T98G cells [16].

Despite the promising results in cell culture models of cancer at concentrations as low as 10 μM, curcumin blood levels are unlikely to reach these concentrations via dietary consumption in humans due to limited mucosal absorption [54]. Oral administration of 8 g/day produced peak blood levels around 2 μM of curcumin in patients [54]. These findings show a gap between the basic and clinical applications of curcumin. On the other hand, studies have found anticancer activities associated with oral, ip and intravenous administration of curcumin in xenografts [55–58]. In our model, we used ip curcumin in order to circumvent the problems associated with its oral absorption. Moreover, ip curcumin may cross the brain blood barrier [57,58]; 50 mg/kg/day was chosen based on the reported literature range (10–120 mg/kg/day) [55–58]. In our model, curcumin significantly reduced the size of brain tumors in C6-implanted rats. Interestingly, curcumin treatment did not induce toxicity to health tissues as evaluated from quantification of serum biomarkers of tissue damage, oxidative stress, hematological parameters and tissue histochemistry. Corroborating with *in vitro* data, these findings suggest a selective toxicity of curcumin against cancer cells *in vivo*. Recently, Perry et al. reported that ip curcumin (60 and 120 mg/kg/day) decreased the subcutaneous growth of U87 tumors in xenografts [58]. In that study, 120 mg/kg/day of curcumin also increased the survival rate in nude mice bearing brain-implanted U87 tumors, although the size of the tumors was not quantified [58]. In brain-implanted B16F10 melanoma cells, tail vein and intracerebral injection of curcumin blocked tumor formation in C57BL6 mice [57]. Therefore, application of injectable formulations of curcumin or direct delivery into the surgical resection cavity could be useful to circumvent the poor oral absorption into a safe therapeutic strategy for treating brain tumors.

This work is the second report of an *in vivo* antiglioma effect of curcumin, but the first using immune-competent rats. The C6 model maintains the immunological and inflammatory surveillances founded *in vivo*, which are critical for gliomas growth and resistance to apoptosis [59]. Perry et al. used immune-compromised mice to implant U87 human cells, and the results also were positive [58]. Given the documented safety of curcumin in humans [54], data presented here and data from Perry et al. provide a provocative foundation for further studies testing and improving the ability of curcumin to limit human brain tumors.

## Acknowledgments

We acknowledge the Brazilian funds CAPES, CNPq and FINEP/IBNNet (01060842-00) for financial support.

## References

[1] Singh SK, Hawkins C, Clarke ID, Squire JA, Bayani J, Hide T, et al. Identification of human brain tumour initiating cells. Nature 2004;432:396–401.
[2] Legler JM, Ries LA, Smith MA, Warren JL, Heineman EF, Kaplan RS, et al. Cancer surveillance series [corrected]: brain and other central nervous system cancers: recent trends in incidence and mortality. J Natl Cancer Inst 1999; 91:1382–90.
[3] Soni D, King JA, Kaye AH, Hovens CM. Genetics of glioblastoma multiforme: mitogenic signaling and cell cycle pathways converge. J Clin Neurosci 2005;12: 1–5.
[4] Yu C, Friday BB, Yang L, Atadja P, Wigle D, Sarkaria J, et al. Mitochondrial Bax translocation partially mediates synergistic cytotoxicity between histone deacetylase inhibitors and proteasome inhibitors in glioma cells. Neuro Oncol 2008;10(3):309–19.
[5] Brennan C, Momota H, Hambardzumyan D, Ozawa T, Tandon A, Pedraza A, et al. Glioblastoma subclasses can be defined by activity among signal transduction pathways and associated genomic alterations. PLoS One 2009;4(11):e7752.
[6] Roesler R, Brunetto AT, Abujamra AL, de Farias CB, Brunetto AL, Schwartsmann G. Current and emerging molecular targets in glioma. Expert Rev Anticancer Ther 2010;10(11):1735–51.
[7] Gerstner ER, Sorensen AG, Jain RK, Batchelor TT. Anti-vascular endothelial growth factor therapy for malignant glioma. Curr Neurol Neurosci Rep 2009; 9(3):254–62.
[8] Mercer RW, Tyler MA, Ulasov IV, Lesniak MS. Targeted therapies for malignant glioma: progress and potential. BioDrugs 23(1), 25–35.
[9] Singh S, Khar A. Biological effects of curcumin and its role in cancer chemoprevention and therapy. Anticancer Agents Med Chem 2006;6(3):259–70 [Review].
[10] Cheng AL, Hsu CH, Lin JK, Hsu MM, Ho YF, Shen TS, et al. Clinical trial of curcumin, a chemopreventive agent, in patients with high-risk or pre-malignant lesions. Anticancer Res 2001;21:2895–900.
[11] Gao X, Deeb D, Jiang H, Liu YB, Dulchavsky AS, Gautam SC. Curcumin differentially sensitizes malignant glioma cells to TRAIL/Apo2L-mediated apoptosis through activation of procaspases and release of cytochrome c from mitochondria. J Exp Ther Oncol 2005;5:39–48.
[12] Kim SY, Jung SH, Kim HS. Curcumin is a potent broad spectrum inhibitor of matrix metalloproteinase gene expression in human astroglioma cells. Biochem Biophys Res Commun 2005;337:510–6.
[13] Nagai S, Kurimoto M, Washiyama K, Hirashima Y, Kumanishi Y, Endo S. Inhibition of cellular proliferation and induction of apoptosis by curcumin in human malignant astrocytoma cell lines. J Neurooncol 2005;74:105–11.
[14] Woo MS, Jung SH, Kim SY, Hyun JW, Ko KH, Kim WK, et al. Curcumin suppresses phorbol ester-induced matrix metalloproteinase-9 expression by inhibiting the PKC to MAPK signaling pathways in human astroglioma cells. Biochem Biophys Res Commun 2005;335:1017–25.
[15] Belkaid A, Copland IB, Massillon D, Annabi B. Silencing of the human microsomal glucose-6-phosphate translocase induces glioma cell death: potential new anticancer target for curcumin. FEBS Lett 2006;580:3746–52.
[16] Karmakar S, Banik NL, Patel SJ, Ray SK. Curcumin activated both receptor-mediated and mitochondria-mediated proteolytic pathways for apoptosis in human glioblastoma T98G cells. Neurosci Lett 2006;407:53–8.
[17] da Frota Jr ML, Braganhol E, Canedo AD, Klamt F, Apel MA, Mothes B, et al. Brazilian marine sponge *Polymastia janeirensis* induces apoptotic cell death in human U138MG glioma cell line, but not in a normal cell culture. Invest New Drugs 2009;27(1):13–20.
[18] Zanotto-Filho A, Delgado-Cañedo A, Schröder R, Becker M, Klamt F, Moreira JC. The pharmacological NFkappaB inhibitors BAY117082 and MG132 induce cell arrest and apoptosis in leukemia cells through ROS-mitochondria pathway activation. Cancer Lett 2010;288(2):192–203.
[19] Braganhol E, Zamin LL, Cañedo AD, Horn F, Tamajusuku AS, Wink MR, et al. Antiproliferative effect of quercetin in the human U138MG glioma cell line. Anticancer Drugs 2006;17(6):663–71.

[20] Zanotto-Filho A, Gelain DP, Schröder R, Souza LF, Pasquali MA, Klamt F, et al. The NFkappaB-mediated control of RS and JNK signaling in vitamin A-treated cells: duration of JNK-AP-1 pathway activation may determine cell death or proliferation. Biochem Pharmacol 2009;77:1291–301.
[21] Dhandapani KM, Mahesh VB, Brann DWJ. Curcumin suppresses growth and chemoresistance of human glioblastoma cells via AP-1 and NFkappaB transcription factors. J Neurochem 2007;102(2):522–38.
[22] Klamt F, Shacter E. Taurine chloramine, an oxidant derived from neutrophils, induces apoptosis in human B lymphoma cells through mitochondrial damage. J Biol Chem 2005;280:21346–52.
[23] Lin HJ, Su CC, Lu HF, Yang JS, Hsu SC, Ip SW, et al. Curcumin blocks migration and invasion of mouse-rat hybrid retina ganglion cells (N18) through the inhibition of MMP-2, -9, FAK, Rho A and Rock-1 gene expression. Oncol Rep 2010;23(3): 665–70.
[24] Uliasz TF, Hewett SJ. A microtiter trypan blue absorbance assay for the quantitative determination of excitotoxic neuronal injury in cell culture. J Neurosci Methods 2000;100(1–2):157–63.
[25] Takano T, Lin JHC, Arcuino G, Gao Q, Yang J, Nedergaard M. Glutamate release promotes growth of malignant gliomas. Nature Med 2001;7:1010–5.
[26] Morrone FB, Oliveira DL, Gamermann P, Stella J, Wofchuk S, Wink MR, et al. In vivo glioblastoma growth is reduced by apyrase activity in a rat glioma model. BMC Cancer 2006;6:226–36.
[27] Braganhol E, Morrone FB, Bernardi A, Huppes D, Meurer L, Edelweiss MI, et al. Selective NTPDase2 expression modulates in vivo rat glioma growth. Cancer Sci 2009;100(8):1434–42.
[28] De Oliveira MR, Moreira JC. Impaired redox state and respiratory chain enzyme activities in the cerebellum of vitamin A-treated rats. Toxicology 2008;253(1–3): 125–30.
[29] Brown RE, Law A. Morphoproteomic demonstration of constitutive nuclear factor-kappaB activation in glioblastoma multiforme with genomic correlates and therapeutic implications. Ann Clin Lab Sci 2006;36(4):421–6.
[30] Gao X, Deeb D, Jiang H, Liu Y, Dulchavsky SA, Gautam SC. Synthetic triterpenoids inhibit growth and induce apoptosis in human glioblastoma and neuroblastoma cells through inhibition of prosurvival Akt, NF-kappaB and Notch1 signaling. J Neurooncol 2007;84(2):147–57.
[31] Nakanishi C, Toi M. Nuclear factor-kappaB inhibitors as sensitizers to anticancer drugs. Nat Rev Cancer 2005;5(4):297–309.
[32] Yahanda AM, Bruner JM, Donehower LA, Morrison RS. Astrocytes derived from p53-deficient mice provide a multistep in vitro model for development of malignant gliomas. Mol. Cell Biol 1995;15:4249–59.
[33] Lowe SW, Bodis S, McClatchey A, Remington L, Ruley HE, Fisher DE, et al. p53 Status and the efficacy of cancer therapy in vivo. Science 1994;266:807–10.
[34] Lowe SW, Ruley HE, Jacks T, Housman DE. p53-Dependent apoptosis modulates the cytotoxicity of anticancer agents. Cell 1993;74:957–67.
[35] Devarajan E, Sahin AA, Chen JS, Krishnamurthy RR, Aggarwal N, Brun AM, et al. Down-regulation of caspase 3 in breast cancer: a possible mechanism for chemoresistance. Oncogene 2002;21:8843–51.
[36] Igney FH, Krammer PH. Death and anti-death: tumour resistance to apoptosis. Nat. Rev Cancer 2002;2:277–88.
[37] Jaattela M. Multiple cell death pathways as regulators of tumour initiation and progression. Oncogene 2004;23:2746–56.
[38] Ansari SA, Safak M, Del Valle L, Enam S, Amini S, Khalili K. Cell cycle regulation of NF-kappa b-binding activity in cells from human glioblastomas. Exp. Cell Res 2001;265:221–33.
[39] Bredel M, Bredel C, Juric D, Duran GE, Yu RX, Harsh GR, et al. Tumor necrosis factor-alpha-induced protein 3 as a putative regulator of nuclear factor-kappaB-mediated resistance to O6-alkylating agents in human glioblastomas. J Clin Oncol 2006;24(2):274–87.
[40] Wang H, Wang H, Zhang W, Huang HJ, Liao WS, Fuller GN. Analysis of the activation status of Akt, NFkappaB, and Stat3 in human diffuse gliomas. Lab Invest 2004;84(8):941–51.
[41] Park S, Hatanpaa KJ, Xie Y, Mickey BE, Madden CJ, Raisanen JM, et al. The receptor interacting protein 1 inhibits p53 induction through NF-kappaB activation and confers a worse prognosis in glioblastoma. Cancer Res 2009;69(7):2809–16.
[42] Sethi G, Ahn KS, Chaturvedi MM, Aggarwal BB. Epidermal growth factor (EGF) activates nuclear factor-kappaB through IkappaBalpha kinase-independent but EGF receptor-kinase dependent tyrosine 42 phosphorylation of IkappaBalpha. Oncogene 2007;26(52):7324–32.
[43] Raychaudhuri B, Han Y, Lu T, Vogelbaum MA. Aberrant constitutive activation of nuclear factor kappaB in glioblastoma multiforme drives invasive phenotype. J Neurooncol 2007;85(1):39–47.
[44] Robe PA, Bentires-Alj M, Bonif M, Rogister B, Deprez M, Haddada H, et al. In vitro and in vivo activity of the nuclear factor-kappaB inhibitor sulfasalazine in human glioblastomas. Clin Cancer Res 2004;10(16):5595–603.
[45] Sansal I, Sellers WR. The biology and clinical relevance of the PTEN tumor suppressor pathway. J Clin Oncol 2004;22(14):2954–63.
[46] Lim GP, Chu T, Yang F, Beech W, Frautschy SA, Cole GM. The curry spice curcumin reduces oxidative damage and amyloid pathology in an Alzheimer transgenic mouse. J Neurosci 2001;21:8370–7.
[47] Thiyagarajan M, Sharma SS. Neuroprotective effect of curcumin in middle cerebral artery occlusion induced focal cerebral ischemia in rats. Life Sci 2004;74:969–85.
[48] Opel D, Westhoff MA, Bender A, Braun V, Debatin KM, Fulda S. Phosphatidylinositol 3-kinase inhibition broadly sensitizes glioblastoma cells to death receptor- and drug-induced apoptosis. Cancer Res 2008;68(15):6271–80.
[49] Weaver KD, Yeyeodu S, Cusack Jr JC, Baldwin AS, Ewend MG. Potentiation of chemotherapeutic agents following antagonism of nuclear factor kappa B in human gliomas. J Neurooncol 2003;61:187–96.
[50] Stewart LA. Chemotherapy in adult high-grade glioma: a systematic review and meta-analysis of individual patient data from 12 randomised trials. Lancet 2002;359:1011–8.
[51] Nagane M, Levitzki A, Gazit A, Cavenee WK, Huang HJ. Drug resistance of human glioblastoma cells conferred by a tumor-specific mutant epidermal growth factor receptor through modulation of Bcl-XL and caspase-3-like proteases. Proc Natl Acad Sci USA 1998;95:5724–9.
[52] Cheng Q, Lee HH, Li Y, Parks TP, Cheng G. Upregulation of Bcl-x and Bfl-1 as a potential mechanism of chemoresistance, which can be overcome by NF-kappaB inhibition. Oncogene 2000;19:4936–40.
[53] Jiang Z, Zheng X, Rich KM. Down-regulation of Bcl-2 and Bcl-xL expression with bispecific antisense treatment in glioblastoma cell lines induce cell death. J Neurochem 2003;84:273–81.
[54] Anand P, Kunnumakkara AB, Newman RA, Aggarwal BB. Bioavailability of curcumin: problems and promises. Mol Pharm 2007;4(6):807–18 [Review].
[55] Shankar S, Ganapathy S, Chen Q, Srivastava RK. Curcumin sensitizes TRAIL resistant xenografts: molecular mechanisms of apoptosis, metastasis and angiogenesis. Mol Cancer 2008;7:16–29.
[56] Dujic J, Kippenberger S, Ramirez-Bosca A, Diaz-Alperi J, Bereiter-Hahn J, Kaufmann R, et al. Curcumin in combination with visible light inhibits tumor growth in a xenograft tumor model. Int J Cancer 2009;124(6):1422–8.
[57] Purkayastha S, Berliner A, Fernando SS, Ranasinghe B, Ray I, Tariq H, et al. Curcumin blocks brain tumor formation. Brain Res 2009;1266:130–8.
[58] Perry MC, Demeule M, Régina A, Moumdjian R, Béliveau R. Curcumin inhibits tumor growth and angiogenesis in glioblastoma xenografts. Mol Nutr Food Res 2010;54:1–10.
[59] Albesiano E, Han JE, Lim M. Mechanisms of local immunoresistance in glioma. Neurosurg Clin N Am 2010;21(1):17–29.

# IV – DISCUSSÃO

## IV. DISCUSSÃO

A hipótese testada neste estudo é que o fator de transcrição NFκB poderia ser um componente central na proliferação, controle dos mecanismos de morte celular e resistência, especialmente em tumores, caracterizando-se como um novo alvo para o desenvolvimento de novos fármacos. Neste projeto, investigamos o papel do NFκB em modelos celulares de tumores sólidos e hematopoiéticos, gliomas e leucemias, visando à avaliação funcional, no que se refere à sua atividade e essencialidade em células tumorais. Além disso, avaliamos o papel do NFκB no controle do estresse oxidativo celular em modelo de indução por vitamina A. Para a investigação dos mecanismos, foram utilizados métodos bastante variados como western blotting, shif assays (EMSA), citometria de fluxo, siRNA, inibidores farmacológicos, oligonucleotídeos decoy, marcadores fluorescentes, análises por biologia de sistemas, e ensaios simples de viabilidade celular (MTT e LDH). Os modelos de leucemia e gliomas foram escolhidos como modelos de processos neoplásicos não-sólidos e sólidos, respectivamente.

Os nossos estudos e dados de outros grupos vêm corroborando no que se refere ao papel de NFκB como um potencial alvo para indução de morte celular em tumores (Dancey et al., 2002; Demuth e Berens, 2004). Como já descrito, NFκB é um fator de transcrição intimamente ligado à indução de genes anti-apoptóticos recentemente descrito como um importante fator de desenvolvimento, metástase e resistência tumoral (Coussens e Werb, 2002; Espinosa et al., 2003). O desfecho destes estudos, inclusive os nossos trabalhos, tem demonstrado que NFκB é superativado em diversos tipos de neoplasias como leucemias (Pikarsky et al., 2004; artigo 2), linfomas (Sishodia

e Aggarwal, 2002; Piva et al., 2005; Saglio et al., 2006), tumores de mama (Haffner et al., 2006), carcinoma prostático (Yemelyanov et al., 2006), gliomas (artigo 3) entre outros (Orlowsky et al., 2002; Shen e Tergaonkar, 2009). Um ponto importante a ser considerado no potencial apoptótico da inibição de NFκB é a aumentada expressão e ativação de NFκB que tem sido relatada em células tumorais quando comparado às células sadias (García et al., 2005; Piva et al., 2005; Cilloni et al., 2006; 2007). Embora os dados apontem uma aumentada expressão/ativação de NFκB, poucos têm avaliado o efeito dos inibidores deste fator de transcrição no crescimento de células tumorais in vitro, e no desenvolvimento de tumores in vivo, o que gera um distanciamento entre o potencial terapêutico da modulação desta via de sinalização, e o potencial terapêutico real (Kasuga et al., 2004; García et al., 2005).

Em gliomas humanos, estudos demonstraram que a ativação e expressão aberrantes de NFκB estão correlacionadas a fenótipos invasivos (Brown e Law, 2006; Raychaudhuri et al., 2007; Xie et al., 2008). Ilustrando o acima exposto, dois estudos correlacionaram ativação exacerbada de NFκB em biópsias de glioma com mau prognóstico (Brown e Law, 2006; Raychaudhuri et al., 2007). A ativação exacerbada de NFκB foi encontrada no tecido tumoral ao passo que a região peritumoral apresentava baixa estimulação do fator de transcrição. Por Western bloting, os autores observaram a ativação de NFκB em mais de 70 % das biópsias (Brown e Law, 2006). Nos experimentos apresentados nesta tese, observamos que tanto em células de glioblastoma com diferentes perfis mutacionais (mutações em PTEN e P53) quanto em células leucêmicas de diferentes origens hematopoiéticas (Jurkat T, K562 e U937) a atividade de NFκB foi aumentada, em nível de translocação nuclear de NFκB, quando

comparado a células leucocitárias ou astrocíticas saudáveis. A inibição de NFκB com os inibidores farmacológicos (BAY117082, MG132, partenolide, trioxido de arsênio) causou uma massiva indução de morte celular nas células malignas ao passo que as células sadias não foram afetadas, o que reforça o potencial de indução de morte celular e, principalmente, a seletividade dos inibidores desta via de sinalização. Interessantemente, e de grande potencial para investigação em estudos clínicos, inibidores de outras vias de sinalização classicamente envolvidas na regulação da proliferação celular como Map cinases (JNK1/2, p38 e ERK1/2), PI3K/Akt, EGFR e PKC e PKA não causaram qualquer alteração na viabilidade celular nos dois tipos de neoplasia, sugerindo que, entre diferentes rotas clássicas de proliferação celular, NFκB parece ter uma importância diferenciada. Através de experimentos de silenciamento transitório da subunidade RelA/p65 com siRNA, foi possível diminuir a atividade ligante do fator de transcrição, diminuir a viabilidade celular e ativar os mecanismos de morte celular apoptótica, como acessado pelo ensaio de ativação da caspase-3 efetora.

Em acordo com os estudos de Brown e Law (2006) e Raychaudhuri e colaboradores (2007), as análises de rede de NFκB pelo software ViaComplex mostraram a expressão exacerbada de diversos genes regulados por NFκB e envolvidos nos processos tumorais. Tal aumento correlacionou-se com o grau de malignidade dos gliomas, sendo o glioblastoma o tipo de glioma com a maior expressão de genes regulados por NFκB. Dentre os genes aumentados, muitos são classicamente descritos em processos de angiogênese (VEGFA), invasividade (MMP2, MMP9, PLAU), adesão celular (ICAM1, VCAM1/2), genes inflamatórios (CXCR4, IL8, CCL2), antioxidantes (SOD2) e antiapoptóticos

(MYC, TNFAIP3 e IER3), alguns apresentando variações de até 64 vezes mais que os tecidos sadios. Pelas análises de microarranjo, alterações na expressão de genes das subunidades de NFκB (RELA, REL, NFKB2 e RELB, exceto NFKB1) não foram observadas, sugerindo uma regulação em nível de ativação. Entretanto, imuno-histoquímicas dos implantes de células C6 em cérebro de rato demonstraram um aumentado imunoconteúdo de p65 (total e fosforilado/ativo), IKK e IkB fosforiladas (ativas) co-localizadas com o marcador de indiferenciação celular, Nestina, confirmando o aumento da ativação da via de NFκB no tecido tumoral (Anexo 1).

Não apenas sob condições basais celulares, a ativação exacerbada da via de NFκB contribui, também, para a proliferação descontrolada e resistência aos agentes antitumorais em pacientes refratários aos protocolos de quimioterapia (García et al., 2005; Furman et al., 2000; Pickering et al., 2007; Philip e Ruland, 2007). Tal hiperativação em resposta à quimioterapia tem sido correlacionada com a falha terapêutica associada tanto a drogas clássicas como o taxol, etoposídeo (Morotti et al., 2006), vincristina, vimblastina (García et al., 2005) quanto a fármacos de nova geração como o imatinib (Cilloni et al., 2006). Neste contexto, os estudos vêm especulando que o uso combinado de inibidores de NFκB com antitumorais clássicos pode potencializar a morte celular ou, até mesmo, quebrar a resistência celular a esses compostos. Por exemplo, o tratamento de linhagens celulares de leucemia mielóide crônica (LMC) com PS1145, um inibidor de IKK, quebrou a resistência celular e induziu apoptose em linhagens celulares resistentes ao fármaco de escolha para LMC, o imatinib (Cilloni et al., 2006 e 2007). Em acordo com estes estudos, demonstramos que o tratamento combinado de doxorubicina e BAY117082 ou MG132 foi capaz de

abolir a resistência de uma linhagem de células K562 resistente à doxorubicina *in vitro* (artigo 2). Em gliomas, selecionamos células C6 resistentes para o agente alquilante cisplatina. Nas células resistentes, observamos uma aumentada ativação de NFκB basal quando comparado com células C6 selvagens, e tratamentos com BAY117082, partenolideo, curcumina e MG132 aboliu a resistência celular (artigo 3). Os dados obtidos com os experimentos em células leucêmicas e gliomas resistentes sugerem um papel para NFκB na indução de resistência e o potencial dos inibidores na reversão de tal fenótipo. Em células de gliomas extraídas de espécimens tumorais e selecionadas para resistência in vitro, Bredel e colaboradores demonstraram uma superativação de NFκB relacionada com a resistência. Naquela ocasião, os autores detectaram uma redução nos níveis do inibidor de NFκB TNFAIP3/A20 em células de gliomas resistentes comparado aos gliomas sensíveis ao tratamento alquilante (Bredel et al., 2006). Logo, a terapia adjuvante de inibidores de NFκB com antitumorais clássicos pode proporcionar a utilização de ambos compostos em doses menores que aquelas utilizadas quando em monoterapia, o que seria útil na diminuição da toxicidade frequentemente observada nos pacientes recebendo altas doses de antitumorais como a cisplatina, doxorubicina, etoposídeo entre outros (Friedman et al., 2000; Morotti et al., 2006).

Na última década, a procura por fitocompostos com atividade anticâncer aumentou exponencialmente. Dentre as moléculas potencialmente ativas descobertas, a curcumina - pigmento alaranjado extraído de um rizoma tipicamente indiano, a *Curcuma longa* - destacou-se por apresentar potencial antiproliferativo e protetor em diversos modelos in vitro e alguns modelos pré-clínicos de doenças como o câncer, Alzheimer, Mal de Parkinson e doenças

cardiovasculares, além de uma baixa toxicidade em seres humanos (Dhandapani et al., 2007; Khan et al., 2008; Aggarwal et al., 2009). Entretanto, o translado entre os achados in vitro e a aplicação clínica desta substância ainda não ocorreu efetivamente tanto que, por exemplo, na área específica de oncologia, foco deste trabalho, a eficácia clínica da curcumina ainda não foi validada em protocolos antitumorais. Além disso, a baixa disponibilidade via oral e a pouca solubilidade nos líquidos corporais também têm se caracterizado como fatores importantes que afetam o potencial da curcumina. Nesse contexto, estratégias tecnológicas para contornar tais problemas têm sido buscadas. Assim, o potencial da curcumina na terapia anticâncer permanece subestimado. Por exemplo, nossos estudos - e dados de outros grupos - demonstraram que a curcumina é um potente inibidor de NFκB (Ichikawa et al., 2007; Kunnumakkara et al., 2008; Khan et al., 2008). Por exemplo, uma seleção de diversos estudos mostra que a cucumina inibe a expressão de diversos genes regulados por NFκB como VCAM-1, Bcl-2, Bcl-xL, ICAM-1, Survivin, Cyclin D1, XIAP, VEGF, COX-2, iNOS, MMP-9, TNF*α*, IL-6 e IL-8 os quais estão diretamente relacionados com processos de proliferação, resistência quimioterápica, metástase e angiogênese em câncer (Aggarwal et al., 2009; Ichikawa et al., 2007; Khan et al., 2008).

No estudo publicado no periódico Journal of Nutritional Biochemistry, demonstramos que o tratamento com curcumina reduziu significativamente o crescimento de tumores de células de glioma C6 implantados no cérebro de ratos Wistar sem causar alterações nos níveis de marcadores bioquímicos séricos (transaminases, creatinina, fosfatase alcalina e outros) e teciduais de toxicidade. Adicionalmente, em 2 linhagens de glioma (C6, U138), a curcumina

induziu apoptose, inibição de rotas de sobrevida celular (NFκB e PI3K/Akt) além de potencializar os efeitos tóxicos da cisplatina e doxorubicina in vitro. Quando da data de publicação, tais dados foram inéditos na área, demonstrando pela primeira vez o efeito biológico da curcumina em monoterapia contra gliomas in vivo, o que abriu uma nova perspectiva na utilização desta fitomolécula no tratamento desta doença. Nossos achados com curcumina foram recentemente comprovados por estudos em outros modelos animais da doença (Weissenberger et al., 2010).

Em uma evolução bastante rápida, nos últimos 3 anos, diferentes grupos de pesquisa vêm desenvolvendo e aprimorando a tecnologia de nanocápsulas contendo curcumina na tentativa de aumentar seu efeito em nível de sistema nervoso central e distribuição tecidual periférica (Sun et al., 2010; Tsai et al., 2011). Em um trabalho realizado em parceria com o Laboratório de Nanotecnologia da Faculdade de Farmácia da UFRGS, em colaboração com o Dr. Ruy Beck e a aluna Karine Coradini, observamos que nanocápsulas carreadoras de curcumina apresentaram efeito bastante significativo no crescimento de gliomas C6 em ratos e na sobrevida dos animais quando comparado à curcumina solúvel (manuscrito em fase de preparação). Entretanto, esses dados não foram adicionados como capítulo da tese, em função de uma colaboração igual e divisão de dados entre os alunos de doutorado dos diferentes laboratórios envolvidos. Assim como a curcumina, o inibidor de IKK, BAY117082, também aumentou significantemente a sobrevida de ratos submetidos ao implante cerebral de gliomas, como demonstrado no Anexo 2. Coletivamente, esses dados mostram que a inibição de NFκB além de promissora in vitro, também apresenta potencial terapêutico in vivo.

Um achado bastante interessante observado nos diferentes modelos de estudo se refere aos mecanismos observados na indução de morte celular pelos inibidores de NFκB. Todos diferentes inibidores de NFκB utilizados, independente do tipo de linhagem, induziram parada na fase G2/M do ciclo celular em tempos mais iniciais de tratamento, ao passo que aumento nos níveis de células hipodiplóides (sub-G1) ocorreu em tempos maiores de incubação, sugerindo um mecanismo programado/coordenado, diferente da necrose. De fato, uma vez parada na fase G2/M, a impossibilidade de completar o processo de mitose, e a presença de uma quantidade elevada de DNA promovem instabilidade cromossômica e indução de processos de morte celular (Alberts et al., 2006). Embora avaliados por diferentes procedimentos experimentais, todos os inibidores de NFκB testados induziram modificações na estrutura da cromatina sugestivas de processos apoptóticos em gliomas. O mesmo aconteceu com os inibidores (BAY117082 e MG132) testados em células leucêmicas (ensaios PI/YOPRO-1 e AnnexinaV/PI). Por outro lado, algumas diferenças nos perfis de ativação de caspases foram observadas dependendo do mecanismo específico de inibição de NFκB. Por exemplo, o inibidor da degradação proteassômica de IκB, MG132, induziu ativação de caspases em todas as linhagens tumorais estudadas. Por outro lado, os inibidores de IKK, BAY117082, partenolide e curcumina, causaram ativação de caspases apenas na linhagem C6 de gliomas, ao passo que a linhagem p53/PTEN mutante U138MG não ativou caspase-3. Essas diferenças podem ser atribuídas aos diferentes perfis mutacionais e sensibilidade à ativação de caspases que as diferentes linhagens podem apresentar (Dhandapani et al., 2007). Outra marca presente em todos os tipos tumorais foi a diminuição do

potencial de membrana mitocondrial após o tratamento com inibidores de NFκB. Em gliomas, a inibição de NFκB por siRNA para p65, ou curcumina, causou uma significante diminuição do conteúdo proteico da proteína antiapoptótica mitocondrial bcl-xl. Resultados similares foram observados em células K562 tratadas com BAY117082 e MG132. Bcl-xl é uma importante proteína antiapoptótica cujo gene é positivamente regulado por NFκB. Jiang e colaboradores descreveram que o silenciamento de bcl-xL por siRNA nas linhagens U87 e NS008 de glioma induz morte celular espontânea, sugerindo a importância dos níveis basais de bcl-xL à viabilidade de gliomas (Jiang et al., 2003).

Em células K562, a diminuição de bcl-xl e do potencial de membrana mitocondrial ocorreu concomitantemente com a liberação de citocromo c. Em concordância, o pré-tratamento das células com o inibidor do poro de permeabilidade transitória mitocondrial, ácido boncréico, inibiu a diminuição do potencial de membrana mitocondrial e a apoptose induzida por BAY117082 e MG132, sugerindo a função mitocondrial como um dos processos afetados pela inibição de NFκB. Em células leucêmicas, o tratamento antioxidante com Trolox® ou TCEP bloqueou a disfunção mitocondrial e a morte celular induzida pela inibição de NFκB, sugerindo que o fator de transcrição em estudo controla o estado redox celular e sua inibição está associada a aumento na produção de ERO. A partir dos experimentos com células de Sertoli, observamos que o NFκB pode controlar a ativação de rotas de morte de celular como JNK/AP-1 através da modulação do estresse oxidativo mitocondrial. A partir destes achados, pode-se pensar que uma vez afetado, a ausência de atividade NFκB parece comprometer as células tumorais mesmo em condições basais (não-

tratadas com quimioterápicos), e até mesmo células sadias sob estresse oxidativo.

A partir dos estudos com células de Sertoli, observamos que a inibição concomitante de NFκB por BAY117082 sob a ação estressora mitocondrial da vitamina A, causou um grande aumento no estresse oxidativo celular, induzindo elevada citotoxicidade. Por outro lado, em presença de NFκB ativo, o estresse oxidativo foi apenas transitório e atuou como um fator que estimulou a proliferação destas células. Embora o bcl-xL não tenha sido dosado naquela oportunidade, foi observado, através de experimentos com oligonucleotídeos decoy, que NFκB controlou a expressão da enzima antioxidante mitocondrial SOD2, a qual é bem descrita por atuar na eliminação do radical superóxido mitocondrial, o qual foi gerado no estresse causado pelo tratamento com retinol. Um achado muito interessante foi o mecanismo pelo qual NFκB controla a proliferação/resistência celular no tratamento com altas doses de retinol. Na presença de NFκB ativo, a via de JNK/AP-1 sofreu uma ativação transitória e sua inibição bloqueou os efeitos de proliferação induzidos pelos baixos níveis de radicais gerados pelo retinol. Com inibição de NFκB por BAY117082 ou oligonucleotídeos decoy específicos, o estresse oxidativo causado por retinol permaneceu alto por um período de tempo maior e a indução da enzima SOD2 não ocorreu, gerando uma ativação duradoura de JNK1/2, a qual interessantemente mediou um aumento significante na morte celular em células de Sertoli. Previamente, demonstramos que a modulação de SOD2 é correlacionada com a radiorresistência em células MO59J, U87 e U138MG de glioma humano (Dal-Pizzol et al., 2003). Nas análises de microarranjos das biópsias de pacientes com glioma (artigo 3), a SOD2 foi um dos genes

superestimulados em amostras tumorais. De fato, é bem estabelecido que os tumores possuem níveis de produção de ERO maiores que os tecidos normais em função dos altos índices de proliferação, microambientes de hipóxia/reoxigenação, elevada sinalização por citocinas (TNF-α e IL-s) e presença de infiltrado inflamatório, os quais são bem conhecidos como sistemas geradores de ERO (Aggarwal et al., 2002).

De fato, ainda não é possível precisar quais são os mecanismos responsáveis pela ativação de NFκB observada em tumores. Alguns estudos já demonstraram mutações em alguns genes da via de NFκB, mas tal fenômeno é observado apenas em subgrupos de pacientes, ao passo que a ativação da via, independente da presença ou ausência de mutação em algum de seus genes componentes, pareça ocorrer eu uma porcentagem maior de amostras. Por exemplo, em glioblastomas, as mutações frequentes observadas na rota de PTEN levam à superativação de Akt, a qual é bem conhecida por induzir fosforilação de IKK e ativação da via (Dan et al., 2008). Recentemente foi demonstrado que o miRNA, miRNA30*, liga o mRNA de IκB-α e inibe a tradução de IκB, portanto inibindo o loop de feedback negativo de NFκB. Adicionalmente, níveis elevados de miRNA30e* foram encontrados em amostras de pacientes com glioma, as quais correlacionaram positivamente com a grau de malignidade dos tumores (Jiang et al., 2012). Logo, é bastante plausível que a ativação aumentada de NFκB observada nos modelos tumorais in vitro e em espécimes tumorais humanos possa ser consequência não apenas de uma ativação consequente de mutações em vias de NFκB, mas também por outros mecanismos regulatórios. Embora nossos experimentos tenham demonstrado uma ativação basal de NFκB nas células de glioma e

leucemia em um ambiente in vitro (cultivo celular), a ativação e presença constante de células imunológicas infiltradas nos tumores, e a decorrente produção de citocinas neste microambiente, também podem colaborar para ativação de NFκB in vivo, uma vez que grande parte dos mediadores inflamatórios sinaliza através da via clássica de NFκB (Coussens e Werb, 2002; Baud e Karin, 2009).

Embora diferentes papéis de NFκB na regulação dos níveis de estresse celular - quimioterapia, condições basais e exposição a oxidantes – tenham sido investigados nesse estudo, e o grande potencial dos inibidores de NFκB como agentes antitumorais parece ser digno de investimentos em futuros estudos, não podemos excluir alguns possíveis efeitos adversos a serem previstos na terapia com inibidores de transdução de sinal de NFκB. Considerando que NFκB é extremamente importante nos processos de resposta inflamatória e imunológica, são necessários estudos adicionais in vivo para validar tanto a eficácia farmacológica dos mais diversos inibidores desta via, assim como o seu potencial efeito imunossupressor em longo prazo, de modo a tirar o melhor resultado dessa promissora estratégia terapêutica.

# V - CONCLUSÃO

## V – CONCLUSÕES

A partir dos resultados obtidos nesta Tese, podemos sugerir que:

- NFκB é um fator ativado durante situações de estresse oxidativo. Tal ativação atua como central no controle dos níveis de estresse oxidativo e dano celular induzido por retinol, através da modulação dos níveis da enzima antioxidante SOD2 e consequentemente a redução do efeito citotóxico das espécies reativas de oxigênio (ERO) produzidas na mitocôndria. Nesse processo, NFκB participa como fator antiapoptótico por controlar os níveis de ERO e o perfil de ativação da via JNK/AP-1, modulando a "decisão celular" entre a proliferação e a indução de morte sob tal insulto pró-oxidante.

- NFκB mostrou-se superestimulado em células tumorais de leucemia, linhagens de glioblastoma, espécimes tumorais de gliomas humanos e glioma animal quando comparado a células polimorfonucleares normais, astrócitos e tecidos cerebrais sadios.

- Inibição de NFκB com inibidores farmacológicos de IKKs e da degradação proteassômica de IκB, assim como siRNA para p65, são capazes de reduzir a viabilidade de células tumorais (C6, U87, U373, U138 de glioblastoma e K562, U937 e Jurkat T de leucemia), com uma seletividade alta em comparação com células não-transformadas de mesma origem histológica (astrócitos e leucócitos periféricos)

- In vitro, NFκB esteve superestimulado em células resistentes aos quimioterápicos cisplatina e doxorubicina, e o tratamento com inibidores de NFκB parece reverter o fenótipo resistente, além de potencializar o efeitos destes antitumorais em linhagens selvagens, evidenciando tanto um papel de NFκB na quimioresistência como o potencial adjuvante dos seus inibidores.

- Como mecanismo, a mitocôndria parece ser uma das estruturas celulares afetadas durante a inibição de NFκB tanto m células de Sertoli sob estresse oxidativo como em células tumorais. A despolarização mitocondrial foi um efeito observado nos tratamentos com inibidores de NFκB em células tumorais, assim como a modificação do conteúdo de proteínas antiapoptóticas mitocondriais como bcl-xl e SOD2. Outro efeito observado foi a parada em fase G2/M do ciclo celular em células tumorais tratadas com inibidores de NFκB como passo inicial no fenômeno de morte celular programada observado.

- O inibidor de NFκB curcumina foi capaz de reduzir o crescimento dos implantes tumorais de glioma C6 em ratos sem indução de toxicidade sistêmica no modelo de estudo, assim como o BAY117082 foi capaz de prolongar a sobrevida animal.

Portanto, a validação da eficácia e segurança de inibidores de NFκB como antitumorais in vivo e, além disso, a identificação dos tipos de tumores que requerem a ativação de NFκB para a manutenção da viabilidade celular, proliferação e metástase pode justificar a potencial utilidade clínica do o uso de inibidores desta via de transdução como agentes em monoterapia, assim como em combinação com drogas classicamente empregadas no tratamento do câncer.

# Vi - PERSPECTIVAS

# VI - PERSPECTIVAS

As principais perspectivas de seguimento deste trabalho.

1) Desenvolvimento de linhagem tumoral expressando plasmídeo codificante para proteína dominante negativo de IkB com sequencia para ativação in vivo.
2) Avaliação dos efeitos antitumorais dos inibidores específicos de NFκB, BAY117082, partenolideo e QNZ, em modelos tumorais in vivo, enfatizando tanto a eficácia e a toxicidade aguda e crônica.
3) Avaliação do potencial adjuvante dos inibidores de NFκB em combinação com agentes anticâncer in vivo.
4) Análise, por ferramentas de bioinformática, das redes de interação gênicas de NFκB com outras vias de sinalização em câncer na busca de outros potenciais genes de interesse.

REFERÊNCIAS BIBLIOGRÁFICAS


[1] Adams J, Palombella VJ, Sausville EA, Johnson J, Destree A, Lazarus DD, Maas J, Pien CS, Prakash S, Elliott PJ. Proteasome inhibitors: a novel class of potent and effective anti-tumor agents. Cancer Res 59, 1999: 2615–2622.

[2] Aggarwal BB, Van Kuiken ME, Iyer LH, Harikumar KB, Sung B. Molecular targets of nutraceuticals derived from dietary spices: potential role in suppression of inflammation and tumorigenesis. Exp Biol Med (Maywood) 2009, 234: 825–849.

[3] Alberts B, Bray D, Hopkin K, Johnson A. Fundamentos da Biologia Celular, 2ª. ed. Porto Alegre: Artmed, 2006.

[4] Anand P, Nair HB, Sung B, Kunnumakkara AB, Yadav VR, Tekmal RR, Aggarwal BB. Design of curcumin-loaded PLGA nanoparticles formulation with enhanced cellular uptake, and increased bioactivity in vitro and superior bioavailability in vivo, Biochem Pharmacol 79, 2010: 330-338.

[5] Baker SJ, Reddy EP. Targeted inhibition of kinases in cancer therapy. Mt Sinai J Med 77, 2010: 573–586.

[6] Bargou RC, Leng C, Krappmann D, Emmerich F, Mapara MY, Bommert K, Royer HD, Scheidereit C, Dorken B. High-level nuclear NF-kB and Oct-2 is a common feature of cultured Hodgkin/Reed-Sternberg cells. Blood 87, 1996:4340- 4347.

[7] Baud V, Karin M. Is NF-kappaB a good target for cancer therapy? Hopes and pitfalls. Nat Rev Drug Discov 8, 2009:33-40.

[8] Birbach A, Gold P, Binder BR, Hofer E, de Martin R, Schmid JA. Signaling molecules of the NF-kB pathway shuttle constitutively between cytoplasm and nucleus. J Biol Chem 277, 2002:10842- 10851.

[9] Bredel M, Bredel C, Juric D, Duran GE, Yu RX, Harsh GR, Vogel H, Recht LD, Scheck AC, Sikic BI. Tumor necrosis factor-alpha-induced protein 3 as a putative regulator of nuclear factor-kappaB-mediated resistance to O6-alkylating agents in human glioblastomas. J Clin Oncol 24, 2006:274-287.

[10] Brown RE, Law A. Morphoproteomic demonstration of constitutive nuclear factor-kappaB activation in glioblastoma multiforme with genomic correlates and therapeutic implications. Ann Clin Lab Sci 36, 2006: 421-426.

[11] Cabannes E, Khan G, Aillet F, Jarrett RF, Hay RT. Mutations in the IkBa gene in Hodgkin's disease suggest a tumour suppressor role for IkBa. Oncogene 18, 1999: 3063- 3070.

[12] Chauhan D, Uchiyama H, Akbarali Y, Urashima M, Yamamoto K, Libermann TA, Anderson KC. Multiple myeloma cell adhesioninduced interleukin-6 expression in bone marrow stromal cells involves activation of NF-kB. Blood 87, 1996: 1104- 1112.

[13] Cilloni D, Martinelli G, Messa F, Baccarani M, Saglio G. NF-kappa B as a target for new drug development in myeloid malignancies. Haematologica 92, 2007: 1224-1229.

[14] Cilloni D, Messa F, Arruga F, Defilippi I, Morotti A, Messa E, Carturan S, Giugliano E, Pautasso M, Bracco E, Rosso V, Sen A, Martinelli G, Baccarani M, Saglio G. The NF-kappaB pathway blockade by the IKK

inhibitor PS1145 can overcome imatinib resistance. Leukemia 20, 2006: 61-67.

[15] Coussens LM, Werb Z. Inflammation and cancer. Nature 2002, 420:860-867.

[16] Cramer P, Hallek M. Hematological cancer in 2011: New therapeutic targets and treatment strategies. Nat Rev Clin Oncol 9, 2012:72-74.

[17] Cuni S, Perez-Aciego P, Perez-Chacon G, Vargas JA, Sanchez A, Martin-Saavedra FM. A sustained activation of PI3K/NF-kappaB pathway is critical for the survival of chronic lymphocytic leukemia B cells. Leukemia 18, 2004: 1391–1400.

[18] Dal-Pizzol F, Ritter C, Klamt F, Andrades M, da Frota ML Jr, Diel C, de Lima C, Braga Filho A, Schwartsmann G, Moreira JC. Modulation of oxidative stress in response to gamma-radiation in human glioma cell lines. J Neurooncol 61, 2003:89-94. Erratum in: J Neurooncol 62, 2003:361.

[19] Dan HC, Cooper MJ, Cogswell PC, Duncan JA, Ting JPY, Baldwin AS. Akt-dependent regulation of NF-kB is controlled by mTOR and Raptor in association with IKK. Genes Dev 22, 2008:1490–1500.

[20] de l, I, Konopka G, Lim KL, Nutt CL, Bromberg JF, Frank DA, Mischel PS, Louis DN, Bonni A. Deregulation of a STAT3-interleukin 8 signaling pathway promotes human glioblastoma cell proliferation and invasiveness. J Neurosci 2008, 28:5870-5878.

[21] Delhase M, Hayakawa M, Chen Y, Karin M. Positive and negative regulation of IkB kinase activity through IKKb subunit phosphorylation. Science 284, 1999: 309- 313.

[22] Demuth T, Berens ME. Molecular mechanisms of glioma cell migration and invasion. J Neurooncol 2004, 70:217-228.

[23] Desbaillets I, Diserens AC, Tribolet N, Hamou MF, Van Meir EG. Upregulation of interleukin 8 by oxygen-deprived cells in glioblastoma suggests a role in leukocyte activation, chemotaxis, and angiogenesis. J Exp Med 1997, 186:1201-1212.

[24] Dhandapani KM, Mahesh VB, Brann DWJ. Curcumin suppresses growth and chemoresistance of human glioblastoma cells via AP-1 and NFkappaB transcription factors. J Neurochem 102, 2007:522–538.

[25] Emmerich F, Theurich S, Hummel M, Haeffker A, Vry MS, Dohner K, Bommert K, Stein H, Dorken B. Inactivating I kappa B epsilon mutations in Hodgkin/Reed-Sternberg cells. J Pathol 201, 2003: 413- 420.

[26] Espinosa E, Zamora P, Feliu J, Baron MG. Classification of anticancer drugs-a new system based on therapeutic targets. Cancer Treat Reviews 29, 2003: 515–523.

[27] Fiumara P, Snell V, Li Y, Mukhopadhyay A, Younes M, Gillenwater AM, Cabanillas F, Aggarwal BB, Younes A. Functional expression of receptor activator of nuclear factor kB in Hodgkin disease cell lines. Blood 98, 2001:2784- 2790.

[28] Friedman HS, Kerby T, Calvert H. Temozolomide and treatment of malignant glioma. Clin Cancer Res 6, 2000:2585-2597.

[29] Furman RR, Asgary Z, Mascarenhas JO, Liou HC, Schattner EJ. Modulation of NF-kappa B activity and apoptosis in chronic lymphocytic leukemia B cells. J Immunol 164, 2000: 2200–2206.

[30] Gandhirajan RK, Poll-Wolbeck SJ, Gehrke I, Kreuzer KA. Wnt/β-catenin/LEF-1 signaling in chronic lymphocytic leukemia (CLL): a target for current and potential therapeutic options. Curr Cancer Drug Targets 10, 2010: 716-727.

[31] García MG, Alaniz L, Lopes EC, Blanco G, Hajos SE, Alvarez E. Inhibition of NF-κB activity by BAY 11-7082 increases apoptosis in multidrug resistant leukemic T-cell lines. Leukemia Res 29, 2005: 1425–1434.

[32] Gill JS, Zhu X, Moore MJ, Lu L, Yaszemski MJ, Windebank AJ: Effects of NFkappaB decoy oligonucleotides released from biodegradable polymer microparticles on a glioblastoma cell line. Biomaterials 2002, 23:2773-2781.

[33] Goff LK, Neat MJ, Crawley CR, Jones L, Jones E, Lister TA, Gupta RK. The use of real-time quantitative polymerase chain reaction and comparative genomic hybridization to identify amplification of the REL gene in follicular lymphoma. Br J Haematol 111, 2000: 618- 625.

[34] Guo D, Teng Q, Ji C. NOTCH and phosphatidylinositide 3-kinase/phosphatase and tensin homolog deleted on chromosome ten/AKT/mammalian target of rapamycin (mTOR) signaling in T-cell development and T-cell acute lymphoblastic leukemia. Leuk Lymphoma 52, 2011:1200-1210.

[35] Haffner MC, Berlato C, Doppler W. Exploiting our knowledge of NF-kappaB signaling for the treatment of mammary cancer. J Mammary Gland Biol Neoplasia 11, 2006:63-73.

[36] Han SS, Kim K, Hahm ER, Park CH, Kimler BF, Lee SJ, Lee SH, Kim WS, Jung CW, Park K, Kim J, Yoon SS, Lee JH, Park S. Arsenic trioxide represses constitutive activation of NF-kappaB and COX-2 expression in human acute myeloid leukemia, HL-60. J Cell Biochem 94, 2005:695–697.

[37] Hayden MS, Ghosh S. Signaling to NF-kB. Genes Dev 18, 2004: 2195-2224.

[38] Hehner SP, Hofmann TG, Droge W, Schmitz ML. The antiinflammatory sesquiterpene lactone parthenolide inhibits NF-kB by targeting the IkB kinase complex. J Immunol 163, 1999:5617–5623.

[39] Houldsworth J, Mathew S, Rao PH, Dyomina K, Louie DC, Parsa N, Offit K, Chaganti RS. REL proto-oncogene is frequently amplified in extranodal diffuse large cell lymphoma. Blood 87, 1996: 25- 29.

[40] Huang TT, Miyamoto S. Postrepression activation of NF-kB requires the amino-terminal nuclear export signal specific to IkBa. Mol Cell Biol 21, 2001: 4737-4747.

[41] Hurley LH. DNA and its associated processes as targets for cancer therapy. Nat Rev Cancer 2, 2002:188–200.

[42] Ichikawa H, Nakamura Y, Kashiwada Y, and Aggarwal BB. Anticancer drugs designed by mother nature: ancient drugs but modern targets. Curr Pharm Des 13, 2007: 3400–3416.

[43] Jiang L, Lin C, Song L, Wu J, Chen B, Ying Z, Fang L, Yan X, He M, Li J, Li M. MicroRNA-30e* promotes human glioma cell invasiveness in an orthotopic xenotransplantation model by disrupting the NFκB/IkBalpha negative feedback loop. J Clin Invest 122, 2012:33–47.

[44] Jiang Z, Zheng X, Rich KM. Down-regulation of Bcl-2 and Bcl-xL expression with bispecific antisense treatment in glioblastoma cell lines induce cell death. J Neurochem 84, 2003:273–281.

[45] Jost PJ, Ruland J. Aberrant NF-kappaB signaling in lymphoma: mechanisms, consequences, and therapeutic implications. Blood 109, 2007:2700-2707.

[46] Kandel ES. NFkappaB inhibition and more: a side-by-side comparison of the inhibitors of IKK and proteasome. Cell Cycle 8, 2009:1819-1820.

[47] Karin M, Ben-Neriah Y. Phosphorylation meets ubiquitination: the control of NF-kB activity. Annu Rev Immunol 18, 2000: 621- 663.

[48] Kasuga C, Ebata T, Kayagaki N, Yagita H, Hishii M, Arai H, Sato K, Okumura K. Sensitization of human glioblastomas to tumor necrosis factor-related apoptosis-inducing ligand (TRAIL) by NF-kappaB inhibitors. Cancer Sci 95, 2004:840-844.

[49] Khan N, Afaq F, Mukhtar H: Cancer chemoprevention through dietary antioxidants: progress and promise. Antioxid Redox Signal 2008, 10: 475–510

[50] Koukourakis GV, Kouloulias V, Zacharias G, Papadimitriou C, Pantelakos P, Maravelis G, Fotineas A, Beli I, Chaldeopoulos D, Kouvaris J. Temozolomide with radiation therapy in high grade brain gliomas: pharmaceuticals considerations and efficacy; a review article. Molecules 14, 2009:1561-1577.

[51] Krappmann D, Emmerich F, Kordes U, Scharschmidt E, Dorken B, Scheidereit C : Molecular mechanisms of constitutive NFκB/ Rel

activation in Hodgkin/Reed-Sternberg cells. Oncogene 18, 1999: 943-953.

[52] Kunnumakkara AB, Diagaradjane P, Guha S, Deorukhkar A, Shentu S, et al.: Curcumin sensitizes human colorectal cancer xenografts in nude mice to gamma-radiation by targeting nuclear factor-kappaB-regulated gene products. Clin Cancer Res 2008, 14: 2128–2136.

[53] Kwok BH, Koh B, Ndubuisi MI, Elofsson M, Crews CM. The anti-inflammatory natural product parthenolide from the medicinal herb Feverfew directly binds to and inhibits IkB kinase. Chem Biol 8, 2001:759–766.

[54] Li Q, Verma IM. NF-κB regulation in the immune system. Nat Rev Immunol 2, 2002:725- 734.

[55] Li ZW, Chu W, Hu Y, Delhase M, Deerinck T, Ellisman M, Johnson R, Karin M. The IKKb subunit of IkB kinase (IKK) is essential for nuclear factor kB activation and prevention of apoptosis. J Exp Med 189, 1999: 1839-1845.

[56] Mao H, Lebrun DG, Yang J, Zhu VF, Li M. Deregulated signaling pathways in glioblastoma multiforme: molecular mechanisms and therapeutic targets. Cancer Invest. 2012, 30(1):48-Review.

[57] Martin-Subero JI, Gesk S, Harder L, Sonoki T, Tucker PW, Schlegelberger B, Grote W, Novo FJ, Calasanz MJ, Hansmann ML, Dyer MJ, Siebert R. Recurrent involvement of the REL and BCL11A loci in classical Hodgkin lymphoma. Blood 99, 2002:1474- 1477.

[58] May MJ, Ghosh S. Rel/NF-kB and IkB proteins: an overview. Semin Cancer Biol 8, 1997:63-73.

[59] McKeithan TW, Takimoto GS, Ohno H, Bjorling VS, Morgan R, Hecht BK, Dube I, Sandberg AA, Rowley JD : BCL3 rearrangements and t ( 14 ; 19) in chronic lymphocytic leukemia and other B-cell malignancies : a molecular and cytogenetic study. Genes Chromosomes Cancer 20, 1997: 64- 72.

[60] Mellinghoff IK, Lassman AB, Wen PY. Signal transduction inhibitors and antiangiogenic therapies for malignant glioma. Glia 59, 2011:1205-1212.

[61] Mercer RW, Tyler MA, Ulasov IV, Lesniak MS. Targeted therapies for malignant glioma: progress and potential. BioDrugs 2009; 23: 25-35.

[62] Mitsiades CS, Mitsiades NS, McMullan CJ, Poulaki V, Shringarpure R, Akiyama M, Hideshima T, Chauhan D, Joseph M, Libermann TA, Garcia-Echeverria C, Pearson MA, Hofmann F, Anderson KC, Kung AL. Inhibition of the insulin-like growth factor receptor-1 tyrosine kinase activity as a therapeutic strategy for multiple myeloma, other hematologic malignancies, and solid tumors. Cancer Cell 5, 2004: 221- 230.

[63] Momoko Nishikori. Classical and Alternative NF-kB Activation Pathways and Their Roles in Lymphoid Malignancies. J Clin Exp Hematopathol 45, 2005: 14-24.

[64] Morotti A, Cilloni D, Pautasso M, Messa F, Arruga F, Defilippi I, Carturan S, Catalano R, Rosso V, Chiarenza A, Taulli R, Bracco E, Rege-Cambrin G, Gottardi E, Saglio G. NF-κB inhibition as a strategy to enhance etoposide-induced apoptosis in K562 cell line. Am J Hematol 81, 2006: 938-945.

[65] Munzert G, Kirchner D, Stobbe H, Bergmann L, Schmid RM, Dohner H. Tumour necrosis factor receptor associated factor 1 gene overexpression in B-cell chronic lymphocytic leukemia: analysis of NF-kappa B/Rel regulated inhibitors of apoptosis. Blood 100, 2002: 3749–3756.

[66] Nefedova Y, Cheng P, Alsina M, Dalton WS, Gabrilovich DI. Involvement of Notch-1 signaling in bone marrow stromamediated de novo drug resistance of myeloma and other malignant lymphoid cell lines. Blood 103, 2004: 3503- 3510.

[67] Nishikori M, Maesako Y, Ueda C, Kurata M, Uchiyama T, Ohno H : High-level expression of BCL3 differentiates t (2 ; 5) (p23 ; q35)-positive anaplastic large cell lymphoma from Hodgkin disease. Blood 101, 2003: 2789- 2796.

[68] Ohno H, Doi S, Yabumoto K, Fukuhara S, McKeithan TW. Molecular characterization of the t (14; 19) (q32; q13) translocation in chronic lymphocytic leukemia. Leukemia 7, 1993: 2057- 2063.

[69] Ohno H, Takimoto G, McKeithan TW. The candidate protooncogene bcl-3 is related to genes implicated in cell lineage determination and cell cycle control. Cell 60, 1990: 991- 997.

[70] Orlowski RZ, Stinchcombe TE, Mitchell BS, Shea TC, Baldwin AS, Stahl S, Adams J, Esseltine DL, Elliott PJ, Pien CS, Guerciolini R, Anderson JK, Depcik-Smith ND, Bhagat R, Lehman MJ, Novick SC, O'Connor OA, Soignet SL. Phase I trial of the proteasome inhibitor PS-341 in patients with refractory hematologic malignancies. J Clin Oncol 20, 2002: 4420–4427.

[71] Orlowski RZ, Baldwin AS, Jr. NF-kappaB as a therapeutic target in cancer. Trends Mol Med 8, 2002:385-389.

[72] Philipp J, Ruland J. Aberrant NF-κB signaling in lymphoma: mechanisms, consequences, and therapeutic implications. Blood 109, 2007:2700-2707.

[73] Pickering BM, de Mel S, Lee M, Howell M, Habens F, Dallman CL, Neville LA, Potter KN, Mann J, Mann DA, Johnson PW, Stevenson FK, Packham G. Pharmacological inhibitors of NF-kappaB accelerate apoptosis in chronic lymphocytic leukaemia cells. Oncogene 26, 2007:1166-1177.

[74] Pierce JW, Schoenleber R, Jesmok G, Best J, Moore SA, Collins T, Gerritsen ME. Novel inhibitors of cytokine-induced IkBa phosphorylation and endothelial cell adhesion molecule expression show anti-inflammatory effects in vivo. J Biol Chem 272, 1997:21096–21103.

[75] Pikarsky E, Porat RM, Stein I, Abramovitch R, Amit S, Kasem S, Gutkovich-Pyest E, Urieli-Shoval S, Galun E, Ben Neriah Y. NF-kappaB functions as a tumour promoter in inflammation-associated cancer. Nature 431, 2004:461-466.

[76] Piva R, Gianferretti P, Ciucci A, Taulli R, Belardo G, Gabriella Santoro M. 15-Deoxy-delta12, 14-prostaglandin J2 induces apoptosis in human malignant B cells: an effect associated with inhibition of NF-κB activity and down-regulation of anti-apoptotic proteins. Blood 105, 2005: 1750-1758.

[77] Raychaudhuri B, Han Y, Lu T, Vogelbaum MA. Aberrant constitutive activation of nuclear factor kappaB in glioblastoma multiforme drives invasive phenotype. J Neurooncol 85, 2007:39-47

[78] Rayet B, Gelinas C. Aberrant rel/NFκB genes and activity in human cancer. Oncogene 18, 1999: 6938- 6947.

[79] Richardson PG, Barlogie B, Berenson J, Singhal S, Jagannath S, Irwin D, Rajkumar SV, Srkalovic G, Alsina M, Alexanian R, Siegel D, Orlowski RZ, Kuter D, Limentani SA, Lee S, Hideshima T, Esseltine DL, Kauffman M, Adams J, Schenkein DP, Anderson KC : A phase 2 study of bortezomib in relapsed, refractory myeloma. N Engl J Med 348, 2003: 2609- 2617.

[80] Sathornsumetee S, Reardon DA. Targeting multiple kinases in glioblastoma multiforme. Expert Opin Investig Drugs 18, 2009:277-92.

[81] Sen R, Baltimore D. Inducibility of kappa immunoglobulin enhancer-binding protein NF-kappa B by a posttranslational mechanism. Cell 47, 1986: 921- 928.

[82] Senftleben U, Cao Y, Xiao G, Greten FR, Krahn G, Bonizzi G, Chen Y, Hu Y, Fong A, Sun SC, Karin M. Activation by IKKa of a second, evolutionary conserved, NF-kB signaling pathway. Science 293, 2001: 1495- 1499.

[83] Shen HM, Tergaonkar V. NFkappaB signaling in carcinogenesis and as a potential molecular target for cancer therapy. Apoptosis 14, 2009:348-363.

[84] Shishodia S, Aggarwal BB. Nuclear factor-kappaB activation: a question of life or death. J Biochem Mol Biol 35, 2002:28-40.

[85] Silverman N, Maniatis T. NF-kB signaling pathways in mammalian and insect innate immunity. Genes Dev 15, 2001: 2321- 2342.

[86] Sison EA, Brown P The bone marrow microenvironment and **leukemia**: biology and therapeutic targeting. Expert Rev Hematol 4, 2011:271-283.

[87] Skorski T. Genetic mechanisms of chronic myeloid leukemia blastic transformation. Curr Hematol Malig Rep 7, 2012:87-93.

[88] Sun M, Gao Y, Guo C, Cao F, Song Z, Xi Y, Yu A, Li A, Zhai G. Enhancement of transport of curcumin to brain in mice by poly(n-butylcyanoacrylate) nanoparticle. J Nanop Res 12, 2010: 3111-3122.

[89] Tentori L, Graziani G. Recent approaches to improve the antitumor efficacy of temozolomide. Curr Med Chem 16(2), 2009:245-257.

[90] Tsai YM, Chien CF, Lin LC, Tsai TH. Curcumin and its nano-formulation: The kinetics of tissue distribution and blood-brain barrier penetration. Int J Pharm 416, 2011: 331-338.

[91] Xie TX, Aldape KD, Gong W, Kanzawa T, Suki D, Kondo S, Lang F, Ali-Osman F, Sawaya R, Huang S. Aberrant NF-kappaB activity is critical in focal necrosis formation of human glioblastoma by regulation of the expression of tissue factor. Int J Oncol 33, 2008:5-15.

[92] Xiong-Zhi Wu. A new classification system of anticancer drugs – Based on cell biological mechanisms. Medical Hypotheses 66, 2006:883–887.

[93] Yemelyanov A, Gasparian A, Lindholm P, Dang L, Pierce JW, Kisseljov F, Karseladze A, Budunova I. Effects of IKK inhibitor PS1145 on NF-kappaB function, proliferation, apoptosis and invasion activity in prostate carcinoma cells. Oncogene 25, 2006: 387-398.

[94] Zhang S, Zhong-Ning L, Yang C, Shi X, Ong C-N, Shen H. Suppressed

NF-kB and sustained JNK activation contribute to the sensitization effect of parthenolide to TNF-a-induced apoptosis in human cancer cells. Carcinogenesis 25, 2004: 2191-2199.

ANEXOS

**Anexo 1**: Expressão de p65, fosfo-p65, fosfo-IKK e Nestina em cérebro de ratos Wistar submetidos a implantes intracerebrais de linhagem C6 de gliomas.

**Anexo 2**: Curva de Sobrevida de ratos Wistar submetidos a implantes intracerebrais de linhagem C6 de gliomas com ou sem tratamento com os inibidores BAY117082 ou curcumina.

**Anexo 3:** Artigo publicado: Proteasome inhibitor MG132 induces selective apoptosis in glioblastoma cells through inhibition of PI3K/Akt and NFκB pathways, mitochondrial dysfunction, and activation of p38-JNK1/2 signaling. Investigational New Drugs, 2012 (In Press). DOI: 10.1007/s10637-012-9804-z

Anexo 1:

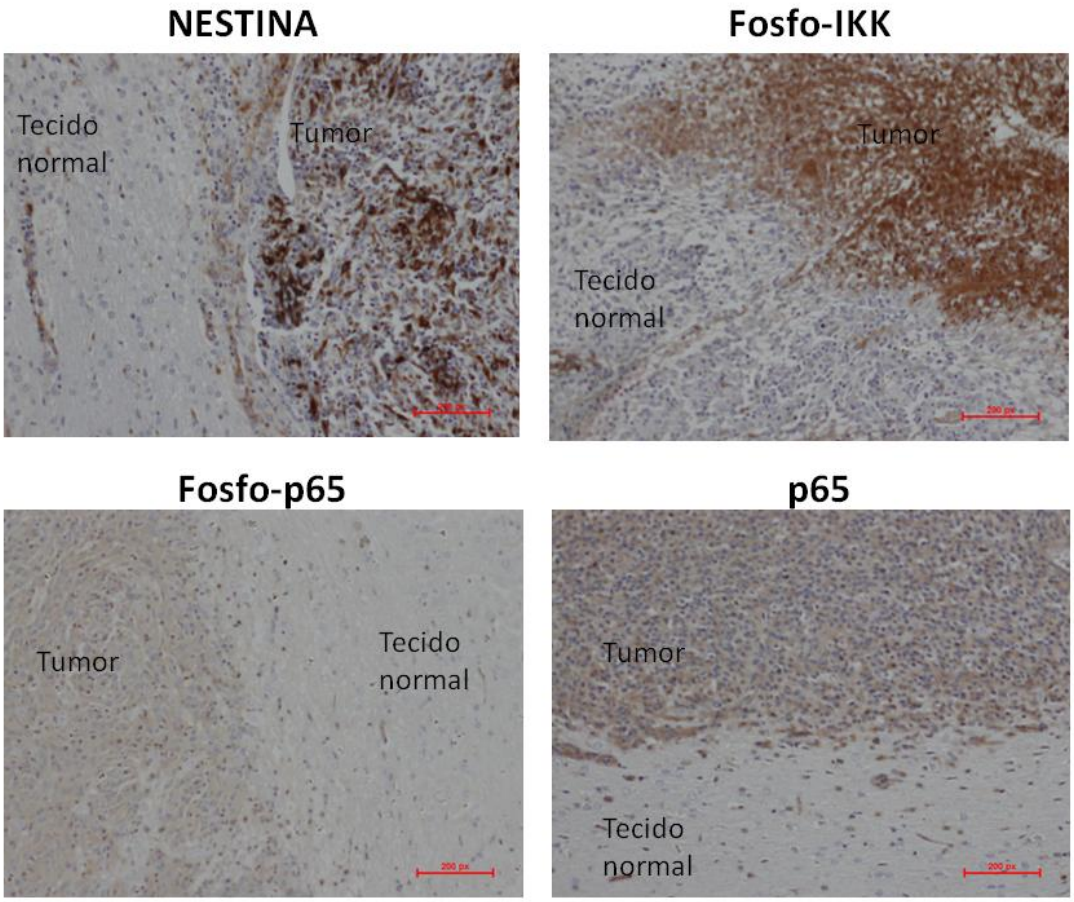
NESTINA
Tecido normal
Tumor
Fosfo-IKK
Tumor
Tecido normal
Fosfo-p65
Tumor
Tecido normal
p65
Tumor
Tecido normal

Anexo 2:

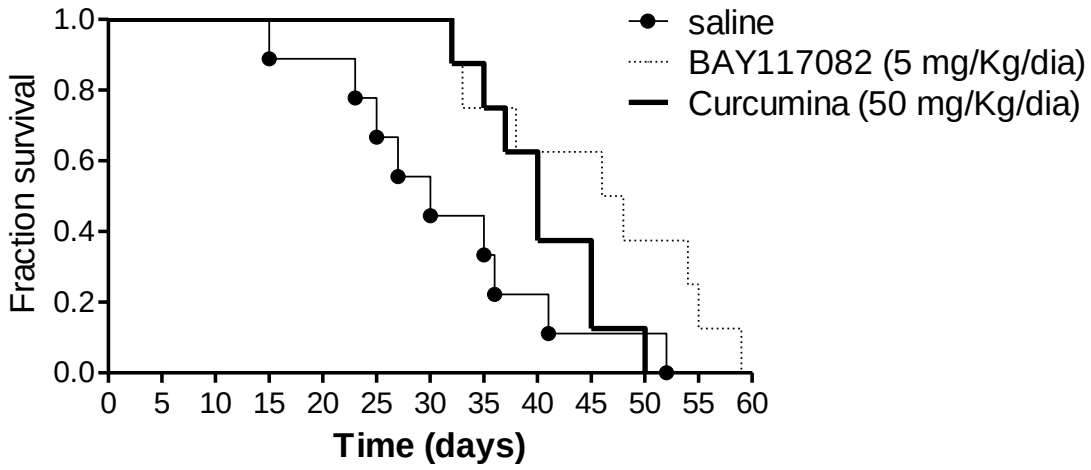


**Legenda: Curva de sobrevivência animal.**

**Metodologia**: Ratos Wistar (n=10 por grupo) foram implantados com glioma C6 (vide método no artigo 4) e, após 10 dias para crescimento dos tumores, os animais foram tratados com injeções intraperitoneais de inibidores de NFκB, BAY117082 (5 mg/Kg/dia) ou curcumina (50 mg/Kg/dia), por 10 dias adicionais. Os animais foram monitorados para sintomas neurológicos (alterações locomotoras, perda de consciência) e o tempo de sobrevida foi monitorado dia a dia até 60 dias. Dados foram analisados pelo teste Chi-quadrado considerando $p<0,05$. **Resultado:** Grupos tratados com BAY117082 e Curcumina tiveram sobrevida média estatisticamente maior que os animais tratados com salina. **Sobrevida média:** Salina: 30 dias; BAY117082: 47 dias; Curcumina: 40 dias

Invest New Drugs
DOI 10.1007/s10637-012-9804-z

PRECLINICAL STUDIES

# Proteasome inhibitor MG132 induces selective apoptosis in glioblastoma cells through inhibition of PI3K/Akt and NFkappaB pathways, mitochondrial dysfunction, and activation of p38-JNK1/2 signaling

**Alfeu Zanotto-Filho · Elizandra Braganhol · Ana Maria Oliveira Battastini · José Cláudio Fonseca Moreira**

Received: 2 January 2012 / Accepted: 15 February 2012


**Summary** Proteasome inhibitors are emerging as a new class of anticancer agents. In this work, we examined the mechanisms underlying cytotoxicity, selectivity and adjuvant potential of the proteasome inhibitor MG132 in a panel of glioblastoma (GBM) cells (U138MG, C6, U87 and U373) and in normal astrocytes. MG132 markedly inhibited GBM cells growth irrespective of the p53 or PTEN mutational status of the cells whereas astrocytic viability was not affected, suggesting a selective toxicity of MG132 to cancerous glial cells. Mechanistically, MG132 arrested cells in G2/M phase of the cell cycle and increased $p21^{WAF1}$ protein immunocontent. Following cell arrest, cells become apoptotic as shown by annexin-V binding, caspase-3 activation, chromatin condensation and formation of sub-G1 apoptotic cells. MG132 promoted mitochondrial depolarization and decreased the mitochondrial antiapoptotic protein bcl-xL; it also induced activation of JNK and p38, and inhibition of NFkappaB and PI3K/Akt survival pathways. Pre-treatment of GBMs with the mitochondrial permeability transition pore inhibitor, bongkrekic acid, or pharmacological inhibitors of JNK1/2 and p38, SP600125 and SB203580, attenuated MG132-induced cell death. Besides its apoptotic effect alone, MG132 also enhanced the antiglioma effect of the chemotherapeutics cisplatin, taxol and doxorubicin in C6 and U138MG cells, indicating an adjuvant/chemosensitizer potential. In summary, MG132 exerted profound and selective toxicity in GBMs, being a potential agent for further testing in animal models of the disease.

**Keywords** MG132 · Glioblastoma · Apoptosis · Chemotherapy

A. Zanotto-Filho · J. C. F. Moreira
Centro de Estudos em Estresse Oxidativo,
Departamento de Bioquímica,
Universidade Federal do Rio Grande do Sul (UFRGS),
Porto Alegre, Rio Grande do Sul, Brasil

E. Braganhol · A. M. O. Battastini
Laboratório de Enzimologia, Departamento de Bioquímica,
Universidade Federal do Rio Grande do Sul (UFRGS),
Porto Alegre, Rio Grande do Sul, Brasil

E. Braganhol
Centro de Ciências Químicas, Farmacêuticas e de Alimentos,
Universidade Federal de Pelotas (UFPel),
Pelotas, Rio Grande do Sul, Brasil

A. Zanotto-Filho (✉)
Departamento de Bioquímica (ICBS-UFRGS),
Rua Ramiro Barcelos, 2600/Anexo,
CEP 90035-003 Porto Alegre, Rio Grande do Sul, Brasil
e-mail: alfeuzanotto@hotmail.com

## Introduction

Glioblastoma multiforme (GBM) is a highgrade brain malignancy arising from astrocytes, and despite aggressive surgical approaches, and optimized radiation and chemotherapy regimens, the median survival of GBM patients from time of diagnosis is approximately 14 months, which has not changed in decades [35, 36]. A number of deregulated signaling cascades have been described in GBMs, including the PI3K/Akt, NFkappaB, MEK/ERK and PLC/PKC pathways [5, 32, 35]. Deregulation of these pathways is driven by mutation, amplification or

Published online: 28 February 2012

overexpression of multiple genes such as *PTEN*, *EGFR*, *PDGFR*-a, *p53*, and *mTOR* [5, 23, 32, 35]. Understanding of these GBM deregulated pathways should provide the basis for drug discovery and development of new therapy protocols.

The ubiquitin–proteasome pathway is involved in proteolysis of most nuclear and cytosolic proteins, and in particular, many of the short-lived regulatory proteins that govern cell cycle progression, transcription factor activation, and signaling [1, 44]. The proteasome, therefore, represents a novel target for cancer therapy. Novel proteasome inhibitors as lactacystin, MG132, PS341, Epoxomicin, SC68896 have been described, although much of their anticancer potential and selectivity in different types of neoplasia remains to be determined [1, 8]. Clinically, bortezomib (PS341), an FDA-approved drug for the treatment of multiple myeloma, remains the first proteasome inhibitor to demonstrate in vitro activity against 60 types of tumor cell lines besides preclinical activity in solid tumor models, including carcinomas of the breast, lung, colon, bladder, ovary, pancreas and prostate [1, 8, 12, 17, 34, 44]. Single agent activity of bortezomib in murine and human prostate xenograft models is associated with enhanced apoptosis, specifically against transformed cells [8, 12]. Inactivation of the transcription factor NFkappaB is one of its major modes of action as well as accumulation of the cyclin-dependent kinase inhibitors p21WAF1 and p27, which trigger growth arrest and apoptosis [17, 34, 44]. Recently, siRNA screening showed that 22% (12/55) of the genes important for GBM cells survival are constituents of the 20S and 26S proteasome subunits, suggesting the proteasome as a potential molecular target in GBM [37]. In contrast to bortezomib [18, 28, 44], sensitivity of GBM to other proteasome inhibitors as G5 [11], LLnL (leucinyl-leucinyl-norleucinal) [14, 24], SC68896 [33] and MG132 [19] has not been extensively studied thus requiring investigation. Taken the aforementioned, this work was undertaken in order to evaluate the antiglioma effect and mechanisms of the well-established proteasome inhibitor MG132 (Z-Leu-Leu-Leu-CHO) (Fig. 1). MG132 was tested in a panel of GBM cell lines with different mutations: U138MG and U373 (p53-mutant/PTEN-mutant), U87 (PTEN-mutant/p53-normal), and C6 (chemotherapy-induced glioma, PTEN-normal/p53-normal). Apoptosis, selectivity to cancer cells, adjuvant and chemo-sensitizer potential as well as the role for mitochondria, NFkappaB, PI3K/Akt, p38 and JNK1/2 signaling pathways were investigated.

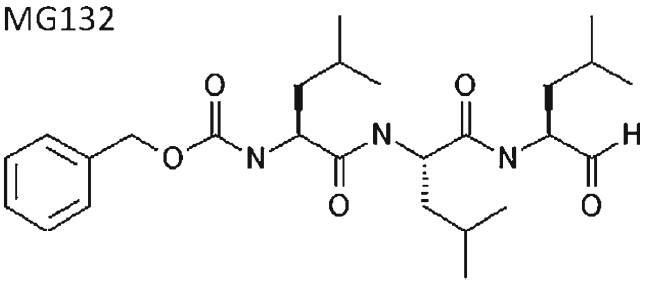


Formal name: N-[(phenylmethoxy)carbonyl]-L-leucyl-N-[(1S)-1-formyl-3-methylbutyl]-L-leucinamide
Synonyms: Z-Leu-Leu-Leu-CHO; Z-Leu-Leu-Leu-al
Molecular formula: $C_{26}H_{41}N_3O_5$
CAS Number: 133407-82-6

**Fig. 1** Structure, formal name, molecular formula, synonym and CAS number of MG132

## Materials and methods

### Reagents

MG132 (Z-Leu-Leu-Leu-CHO),propidium iodide, Hepes, CHAPS, dithiothreitol, EDTA, trypsin, MTT (3-(4,5-dimethyl)-2,5-diphenyl tetrazolium bromide), taxol, cisplatin, doxorubicin, Nonidet-P40, spermin tetrahydrochloride, RNAse A and culture analytical grade reagents were purchased from Sigma Chemical Co (St. Louis, MO, USA). Anti-phospho-JNK1/2 (G7), anti-JNK (FL), anti-phospho-p38 and anti-p38 were from Santa Cruz Biotechnologies; anti-β-actin, anti-bcl-xL, anti-phospho-Akt ($ser^{473}$), anti-Akt were from Cell Signaling Technology; SP600129 and SB203580 were from Promega Corporation (Madison, USA). BAY117082 and LY294002 were from Biomol International (Plymouth Meeting, PA). Electrophoresis/immunoblotting reagents were from Bio-Rad Laboratories (Hercules, CA, USA).

### Cell cultures

The rat (C6), and human (U138MG, U87 and U373) malignant GBM cell lines were obtained from American Type Culture Collection (Rockville, Maryland, USA). The cells were grown and maintained in low glucose Dulbecco's modified Eagle's medium (DMEM; Gibco BRL, Carlsbad, USA) containing 0.1% Fungizone, 100 U/l gentamicin and supplemented with 10% fetal bovine serum. Cells were kept at 37°C in a humidified atmosphere with 5% $CO_2$. Primary astrocytes cultures were prepared as previously described [9]. Briefly, cortex of newborn Wistar rats (1–2 days old) were removed, and dissociated mechanically in a $Ca^{+2}$ and $Mg^{+2}$ free balanced salt solution pH 7.4, (137 mmol/L NaCl, 5.36 mmol/L KCl, 0.27 mmol/L $Na_2HPO4$, 1.1 mmol/L $KH_2PO4$, 6.1 mmol/L glucose). After centrifugation at 1,000 rpm for 5 min, the pellet was resuspended in DMEM supplemented with 10% FBS. The cells ($2\times10^5$) were plated in poly-L-lysine-coated 48-well plates. After 4 h platting, plates were gently shaken, PBS-washed, and medium was changed to remove neuron and microglia contaminants. Cultures were allowed to grow to confluence by 20–25 days. Medium was replaced every 4 days.

### MTT and LDH viability assays

Dehydrogenases-dependent MTT reduction (MTT assay) and lactate dehydrogenase release into culture medium (LDH assay) were used as an estimative of cell viability [9, 46]. Cells were plated in 96-well plates ($10^4$/well) and treated at 60–70% confluence. At the end of incubations, MTT and LDH assays were performed. Lactate dehydrogenase (LDH) activity in the culture medium was determined in agreement with manufacturer instructions (CytoTox 96-NonRadioactive Cytotoxicity Assay, Promega). Cell morphology was evaluated by light microscopy (Nikon Eclipse TE 300).

### Annexin-V binding assay

At the end of treatments, cells were trypsinized, and externalized phosphatidylserine was labeled (15 min, ice-cold) with 3 μl FITC-conjugated annexin V in 100 μl binding buffer (10 mM HEPES pH 7.4, 145 mM NaCl, 5 mM KCl, 1.0 mM $MgCl_2.6H_2O$, 1.8 mM $CaCl_2$. $2H_2O$). Propidium iodide (PI, 1 μg/mL) was added 10 min prior to analysis. Cells were analyzed in a FACScalibur flow cytometer (BD PharMingen). Viable (annexin-/PI-), apoptotic (annexin+/PI-) and late apoptotic/necrotic (annexin+/PI+) cells were characterized as previously described [45].

### Propidium iodide uptake and staining of chromatin

For determination of propidium iodide (PI) uptake in cells with losses in membrane integrity, treated cells were incubated with 2 μg/mL PI in complete medium for 1 h. PI fluorescence was excited at 515–560 nm using an inverted microscope (Nikon Eclipse TE 300) fitted with a standard rhodamine filter. Representative microphotographs (at least 5/well) were collected [3]. For detection of the morphological alterations in chromatin (condensation and fragmentation) and apoptotic bodies formation, cells were fixed in methanol/acetone (1:1) for 5 min and subsequently washed with PBS (3 times). After, chromatin was stained with PI (0.5 μg/mL, 10 min) and analyzed by fluorescence microscopy (Nikon Eclipse TE 300).

### Cell cycle analysis

Cells were trypsinized, centrifuged and resuspended in a lysis buffer containing 3.5 mmol/L trisodium citrate, 0.1% v/v Nonidet P-40, 0.5 mmol/L Tris–HCl, 1.2 mg/mL spermine tetrahydrochloride, 5 μg/ml RNAse, 5 mmol/L EDTA, 1 μg/mL propidium iodide, pH 7.6. After, cells were incubated for at least 10 min on ice for cell lysis. The DNA content was determined by flow cytometry. Ten thousand events were counted per sample. FACS analyses were performed in the CellQuest Pro Software (BD Biosciences, CA) [45].

### Caspase-3 activity

Caspase-3 activity was assessed in agreement with CASP3F Fluorimetric kit (Sigma, Saint Louis/MI). Treated cells were harvested and incubated in a lysis buffer (50 mmol/L Hepes, 5 mmol/L CHAPS and 5 mmol/L dithiothreitol, pH 7.4) for 20 min on ice. After, extracts were clarified by centrifugation at 13,000 × g (15 min, 4°C). Supernatants were collected and proteins were measured by Bradford method. For assays, 150 μg proteins were mixed with 200 μL of the assay buffer (20 mmol/L Hepes, 0.1% CHAPS, 5 mmol/L dithiothreitol, 2 mmol/L EDTA, pH 7.4) plus 20 μM Ac-DEVD-AMC (Acetyl-Asp-Glu-Val-Asp-7-amido-4-methylcoumarin), a caspase-3 specific substrate. Caspase-3-mediated substrate cleavage was monitored during 1 h at 37°C in a fluorimetric reader (excitation 360 nm/emission 460 nm) [45].

### Cellular fractionation

For nuclear extracts preparation, cells (~$5\times10^6$, 70–80% confluence) were washed with cold phosphate-buffered saline (PBS) and suspended in 0.4 mL hypotonic lysis buffer (10 mmol/L HEPES (pH 7.9), 1.5 mmol/L $MgCl_2$, 10 mmol/L KCl, 0.5 mmol/L phenylmethylsulfonyl fluoride, 0.5 mmol/L dithiothreitol plus protease inhibitor cocktail (Roche)) for 15 min. Cells were then lysed with 12.5 μL 10% Nonidet P-40. The homogenate was centrifuged (13,000 × g, 30 seg), and supernatants containing the cytoplasmic extracts were stored at −80°C. The nuclear pellet was resuspended in 100 μL ice-cold hypertonic extraction buffer (10 mmol/L HEPES (pH 7.9), 0.42 M NaCl, 1.5 mmol/L $MgCl_2$, 10 mmol/L KCl, 0.5 mmol/L phenylmethylsulfonyl fluoride, 1 mmol/L dithiothreitol plus protease inhibitors). After 40 min of intermittent mixing, extracts were centrifuged (13,000 × g, 10 min, 4°C), and supernatants containing nuclear proteins were secured. The protein content was measured by the Bradford method [45, 46].

### NFkappaB-p65 ELISA assay for determination of NFkappaB activity

A total of 10 μg of nuclear extracts was used to determine NFkappaB DNA-binding activity (NFkappaB p65 Elisa kit, Stressgen/Assays designs) per manufacturer's protocols. This ELISA-based chemiluminescent detection method rapidly detects activated NFkappaB complex binding (p65 detection) to a plate-adhered NFkappaB consensus oligonucleotide sequence. Kit-provided nuclear extracts prepared from TNF-alpha-stimulated Hela cells were used as a positive control for NFkappaB activation. To demonstrate assay specificity, a 50-fold excess of an NFkappaB consensus oligonucleotide was used as competitor to block NFkappaB binding. In addition, a mutated consensus NFkappaB oligonucleotide (which do not

binds NFkappaB) is provided for determination of binding reactions' specificity [10].

### Western blotting

Proteins (20 μg) were separated by SDS-PAGE on 10% (w/v) acrylamide, 0.275% (w/v) bisacrylamide gels and electrotransfered onto nitrocellulose membranes. Membranes were incubated in TBS-T (20 mmol/L Tris–HCl, pH 7.5, 137 mmol/L NaCl, 0.05% (v/v) Tween 20) containing 1% (w/v) non-fat milk powder for 1 h at room temperature. Subsequently, the membranes were incubated for 12 h with the appropriate primary antibody (dilution range 1:500–1:1000), rinsed with TBS-T, and exposed to horseradish peroxidase-linked anti-IgG antibodies for 2 h at room temperature. Chemiluminescent bands were detected using X-ray films, and densitometry analyses were performed using Image-J® software.

### Mitochondrial membrane potential (JC-1 assay)

For determination of the Mitochondrial Membrane Potential (MMP), treated cells ($5\times10^5$) were incubated for 30 min at 37°C with the lipophilic cationic probe JC-1 (5,5′,6,6′-tetrachloro-1,1′,3,3′ tetraethylbenzimidazolcarbocyanine iodide, 2 μg/ml). After, JC-1-loaded cells were centrifuged and washed once with PBS. Cells were transferred to a 96-well plate and assayed in a fluorescence plate reader with the following settings: excitation at 485 nm, emission at 540 and 590 nm, and cutoff at 530 nm (SpectraMax M2, Molecular Devices, USA). $\Delta\Psi m$ was calculated using the ratio of 590 nm (J-aggregates)/ 540 nm (monomeric form) [16, 45].

### Statistical analysis

Data are expressed as means±S.D and were analyzed by one-way ANOVA followed by Duncan's post hoc test. Differences were considered significant at $p<0.05$.

## Results

### MG132 selectively induces cell death in GBM cell lines but not in astrocytes

We examined the effect of MG132 on viability of gliomas by treating a panel of GBM cell lines with different concentrations of MG132 for 48 h. At the end of incubation, MTT and LDH assays were performed. In parallel, primary astrocytes cultures were used as a non-transformed model of glial cells in order to evaluate the selectivity of MG132. MG132 caused a dose dependent decrease in the viability of the four GBM cell lines ($IC_{50}$ range: 2–5 μM) whereas astrocytic viability was not significantly altered up to 10 μM MG132 (Fig. 2a). These results suggest that MG132 preferentially targeted cancer cells. U138MG and C6 cell lines were used for further experiments. Simultaneously with the decreases in cellular viability, MG132 >1 μM promoted a significant leakage of LDH into culture medium (Fig. 2b), indicating losses in cell membrane integrity. In addition, marked increases in PI incorporation besides significant morphological alterations and cell detachment were observed in MG132-treated cells (Fig. 2c).

### MG132 promotes cell cycle arrest and mitochondria-mediated apoptosis in GBMs

Staining of chromatin with propidium iodide (PI) showed that MG132 promoted chromatin condensation and formation of apoptotic bodies in GBM (Fig. 3a). By flow cytometry, we found that 5 μM MG132 elicited externalization (flip-flop) of phophatydylserine in approximately 30% cells (Annexin V+/ PI-cells), suggesting apoptosis (Fig. 3b).

To understand the mechanism of action of MG132, we initially studied its effects on mitochondrial function. MG132 caused and early collapse in the mitochondrial membrane potential (MMP) which was clearly detected from 12 h incubation of C6 and U138MG cells with the proteasome inhibitor (Fig. 3c and d). MG132 also caused an early (12 h) decrease in the immunocontent of bcl-xL, which is an important antiapoptotic mitochondrial protein (Fig. 3e). To determine the role of the aforementioned mitochondrial impairments in MG132-induced apoptosis, cells were pre-incubated with 100 μM bongkrekic acid (BK), a specific mitochondrial permeability transition pore (mPTP) opening inhibitor, for 1 h prior MG132 treatment. BK inhibited MG132-induced cell death, suggesting that mitochondrial collapse and mPTP opening are involved in the apoptotic effect of the proteasome inhibitor (Fig. 3f). Concomitantly to decreases in MMP and bcl-xL, MG132 promoted a 14 to 25-fold increase in caspase-3 activation, a classical apoptotic effector protease (Fig. 4b).

By flow cytometry, we observed that MG132 treatment caused arrest in the G2/M phase of the cell cycle at 24 h incubation, which cumulated in formation of a massive population sub-G1 cells (>50% events) after 48 h treatment, suggesting that G2/M arrest preceded DNA fragmentation during MG132-induced apoptosis (Fig. 4a). MG132 also promoted accumulation of the cyclin-dependent kinase inhibitior (CDKi) $p21^{WAF1}$, a marker of cell cycle arrest (Fig. 4c).

### MG132 inhibits PI3K/Akt and NFkappaB survival pathways and induces JNK/p38-dependent cell death

One of the major effects of proteasome inhibitors in many cell types is the reduction of NFkappaB activity. NFkappaB is a GBM-overstimulated transcription factor which increases the

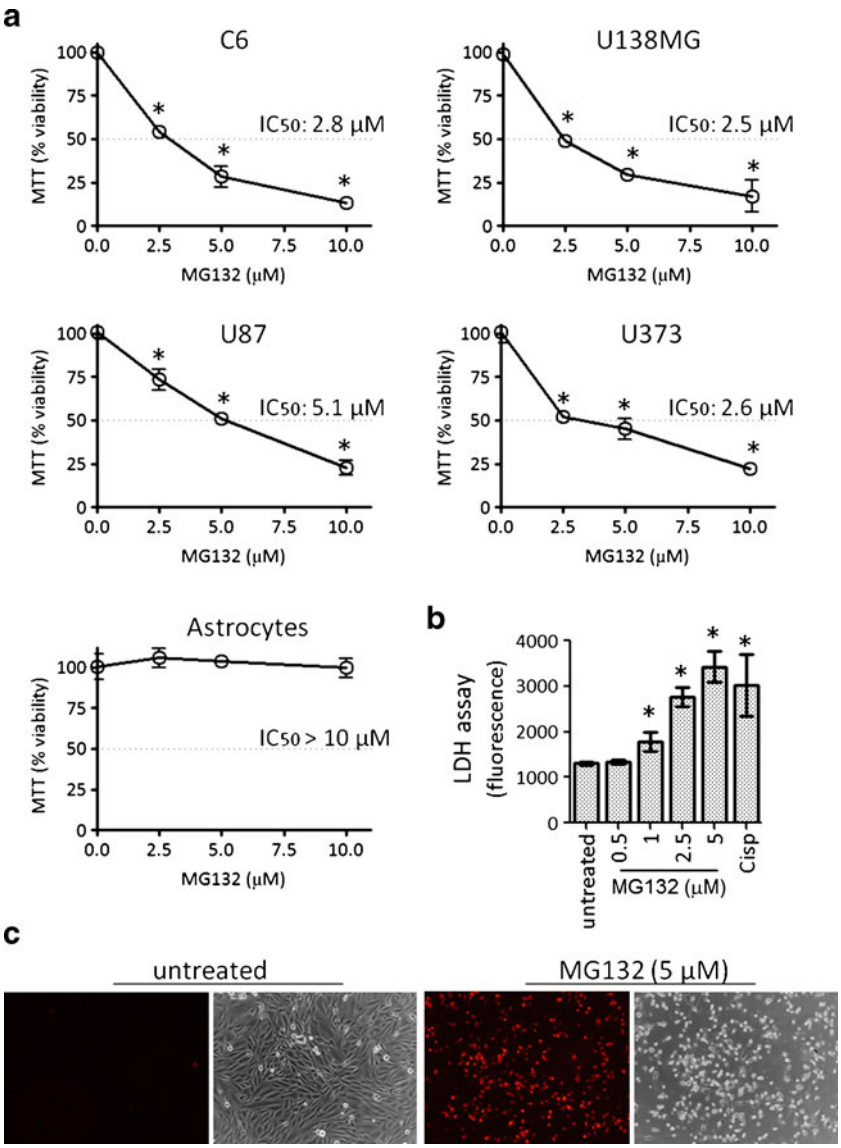


**Fig. 2** Effect of MG132 on viability of GBMs and astrocytes. **a** A panel of GBM cell lines (C6, U87, U373 and U138MG) and normal astrocytes were treated for 48 h with different concentrations of MG132 (μM), and MTT assays were carried out. **b** LDH activity in the culture medium of 48 h-treated U138MG cells. **c** Propidium iodide incorporation in U138MG cells after 48 h treatment with 5 μM MG132. Cell morphology and fluorescence were analyzed by fluorescence and phase contrast microscopy (10 × magnification). Legends: Cisp (cisplatin 10 μM). * different from untreated cells (ANOVA, $p<0.05$)

expression of diverse antiapoptotic genes as bcl-xl, c-IAP1/2 and XIAP, and modulates the activation state of other signaling pathways as JNK1/2 [17, 44, 46]. Besides NFkappaB, PTEN/homotensin homologue mutations leading to overstimulation of PI3K/Akt pathway also play a critical role in GBM cells survival [10, 27, 43]. Thus, we explored the effect of MG132 on NFkappaB, PI3K/Akt, JNK1/2 and p38 signaling, and the role of these pathways in GBM survival and in MG132 effects. By Western blotting, we determined that 12 h treatment with MG132 markedly increased the levels of phospho-JNK1/2 and phospho-p38 (active forms). Phospho-JNK1/2 and phospho-p38 were not detected upon basal conditions as determined by western blotting (Fig. 5a). In contrast, we detected a constitutive activation of the PI3K/Akt pathway, which was evaluated from levels of phospho-Akt, a surrogate for determination of PI3K/Akt pathway activation in GBM [27, 43]. MG132 (5 μM, 12 h) decreased Akt phosphorylation, suggesting inhibition of the PI3K/Akt pathway (Fig. 5a). MG132 also inhibited about 51% the constitutive activation of the transcription factor NFkappaB, as assessed by ELISA assay (Fig. 5b). ELISA specificity for NFkappaB was confirmed by incubation of nuclear extracts with kit-provided 50X unlabeled oligonucleotides, which inhibited completely NFkappaB basal binding (untreated +50X lane). In addition, mutant oligonucleotides did not alter NFκB activity confirming the specificity of the binding reactions (see untreated+mut lane, Fig. 5b).

To determine the role of NFkappaB, PI3K/Akt, JNK1/2 and p38 in MG132-induced cell death, the cells were cultured with MG132 (5 μM) either alone or in combination with inhibitors of NFkappaB (BAY117082), PI3K/Akt (LY294002), JNK1/2 (SP600129) and p38 (SB203580) for 48 h, and MTT assays were carried out. NFkappaB and PI3K inhibitors potentiated whereas JNK1/2 and p38 inhibitors

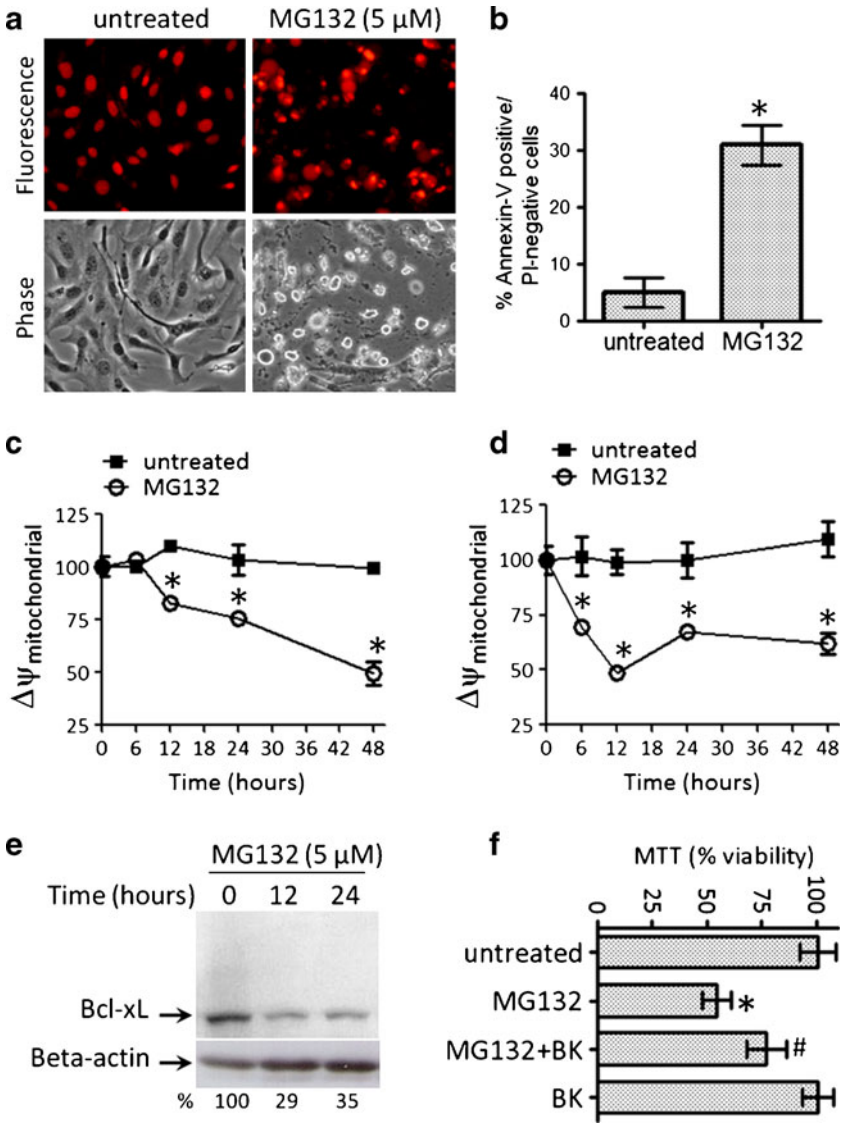


**Fig. 3** MG132 induces chromatin condensation, phosphatydilserine flip-flop and mitochondrial dysfunction in GBMs. **a** U138MG cells were treated, fixed, and chromatin was stained with propidium iodide. Cells were visualized by fluorescence microscopy (20 × magnifications). **b** Flow cytometry experiments for quantification of apoptotic cells (annexin-V+/PI-) in MG132-treated U138MG cells. Cell were treated for 48 h. **c**, **d** JC-1 assay for determination of mitochondrial membrane potential (MMP, $\Delta\Psi m$) in C6 and U138MG cell lines (C and D, respectively). Data were expressed as percentage of untreated cells. **e** Effect of MG132 on immunocontent of bcl-xl protein in U138MG cells. Cells were treated for different times, and total extracts were analyzed by western blotting. Beta-actin was used as loading control. **f** MTT assay showing the effect bongkrekic acid pre-treatment (BK 100 μM, 1 h) on MG132-induced cell death. U138MG cells were incubated for 48 h with 5 μM MG132. * different from untreated cells; # different from untreated and from MG132-treated cells (ANOVA, $p<0.05$)

blunted the MG132 ability to decrease GBM cells viability (Fig. 5c). MG132 reduced cellular viability by about 40%; on the other hand under similar conditions, only about 20% reduction in cell viability was observed when the cells were cultured with the combination MG132 and the JNK or p38 inhibitors ($p<0.05$). In addition, the NFkappaB and PI3K inhibitors, but not JNK and p38 inhibitors, mono-treatments also decreased the cellular viability of GBMs, confirming the described role of these pathways in survival of this type of cancer (Fig. 5c).

### MG132 sensitizes GBM cell lines to classical anticancer drugs

To explore the potential of MG132 as adjuvant, we pre-treated U138MG and C6 cells with different concentrations of MG132 (1 and 5 μM) for 6 h followed by 48 h incubation either alone or in combination with the alkylation agent cisplatin (5 μM), or the topoisomerase inhibitor doxorubicin (5 μM) or the antimitotic taxane Taxol (0.2 μM). MTT assays showed that the ability of the cisplatin, doxorubicin and taxol to induce GBM cells death was enhanced by MG132 in both tested GBM cell lines, suggesting that MG132 pre-treatment sensitized GBMs to chemotherapeutics (Fig. 6a and b).

## Discussion

Recently, siRNA screening studies showed that proteasome constituents are essential for survival of LNZ-308, LNZ-428, A172 and T98G GBM cell lines [37], suggesting that pharmacological inhibition of proteasome could be a strategy for cell death induction in this type of cancer. However, little has

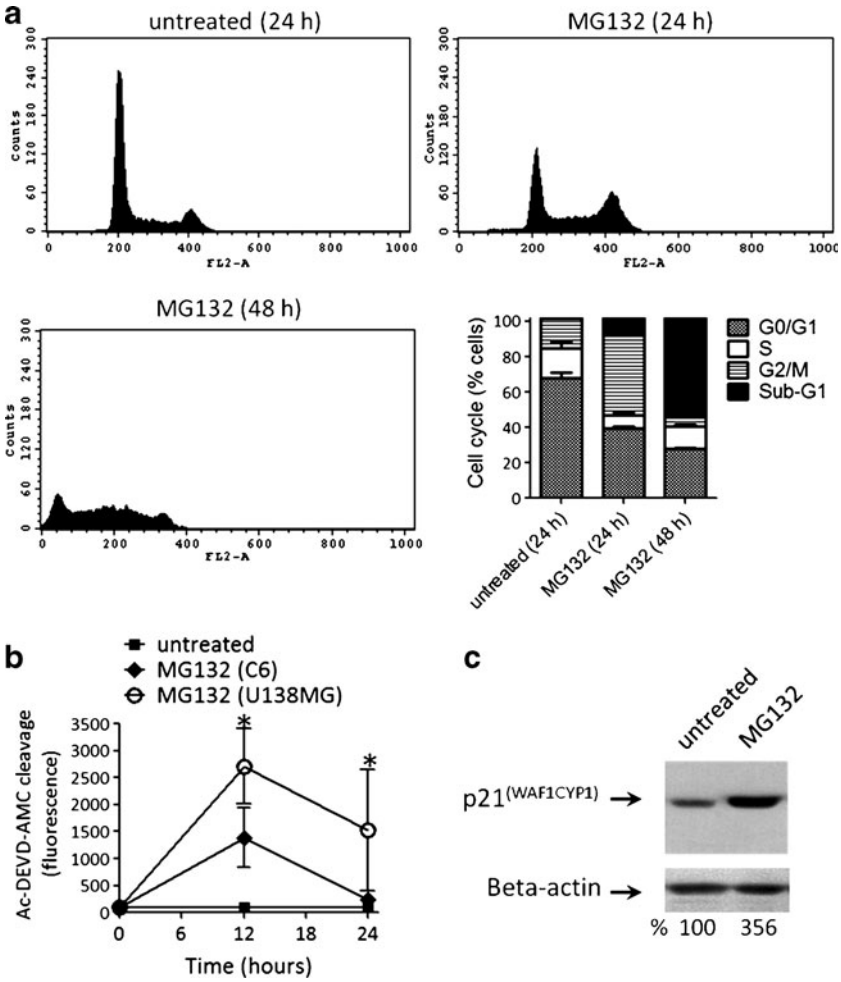


**Fig. 4** MG132 induces cell cycle arrest and caspase-3 activation in GBMs. **a** Flow cytometry for cell cycle analysis, and quantification of cell cycle distribution in 24 and 48 h MG132-treated cells. **b** MG132 promotes caspase-3 activation in C6 and U138MG cell lines. **c** Representative western blotting for determination of the CDK inhibitor p21WAF1immunocontent in 24 h-treated U138MG cells. Beta-actin was used as loading control. In Fig. 4 experiments, cells were incubated with 5 μM MG132 * different from untreated cells (ANOVA, $p<0.05$)

been reported of the effect and mechanisms of the well-known proteasome inhibitor MG132 on GBM cells [39, 40]. Previous works showed that MG132 can induce caspase-3 activation and cytochrome c release in LN-18 and LN-308 cell lines [39, 40]. In this work, we expanded the knowledge of MG132 effects and mechanisms in GBMs. MG132 induced cell death in a panel of GBM cell lines with different mutations: U138MG and U373 (PTEN mutant/p53 mutant), U87 (PTEN mutant/p53 wild-type) and C6 (nitrosurea-induced glioma, p53 wild-type/PTEN wild-type). Of great relevance, MG132 was selectively cytotoxic to GBM cell lines and spared normal glial cells, since astrocytic viability was not affected by the proteasome inhibitor. Tumor-selectivity has the advantage of minimizing toxicity to normal tissues, thereby decreasing systemic side effects and damage to healthy tissues. Previous studies showed that the proteasome inhibitor PS-341 blocked cells of different types of solid tumors in the G2/M phase of the cell cycle [2, 22, 39]. This effect was associated with increases in the CDK inhibitors $p21^{WAF1}$ and/or $p27^{KIP1}$, since proteasome inhibition can block their degradation/turnover in proliferative cells [2, 22, 44]. The increased turnover of cell cycle regulating proteins in cancer cells compared to normal cells has explained, at least in part, the cancer cells selectivity of PS-341 [1, 8, 34, 44] and MG132. For example, our findings showed that MG132-treated GBMs accumulated in the G2/M phase of the cell cycle associated with increased levels of $p21^{WAF1}$ at the early steps of apoptosis; similar results were previously observed in LN-18 cells [39].

The p53 protein plays a pivotal role in cell cycle regulation, apoptosis and chemoresistance (Kuerbitz et al., 1992; Wu and Levine, 1994). Previous studies suggested that PS-341 [21, 44], calpain inhibitor-I, lactacystin and LLnL [15, 39] inhibit growth of tumor cells in a p53-independent manner; others suggest that proteasome inhibitors effects occur in a p53-dependent way [38]. In agreement with the reported for PS-341 [21, 44], we found that both p53-wild type (C6 and U87) and p53–mutant (U138MG and U373) cell lines were equally sensitive to growth inhibition mediated by MG132. About 35% of GBMs have mutant p53 [29, 44], emphasizing the importance of selecting a therapy that can function independent of p53 mutational status of the tumors. Besides p53 mutations, PI3K/Akt and NFkappaB

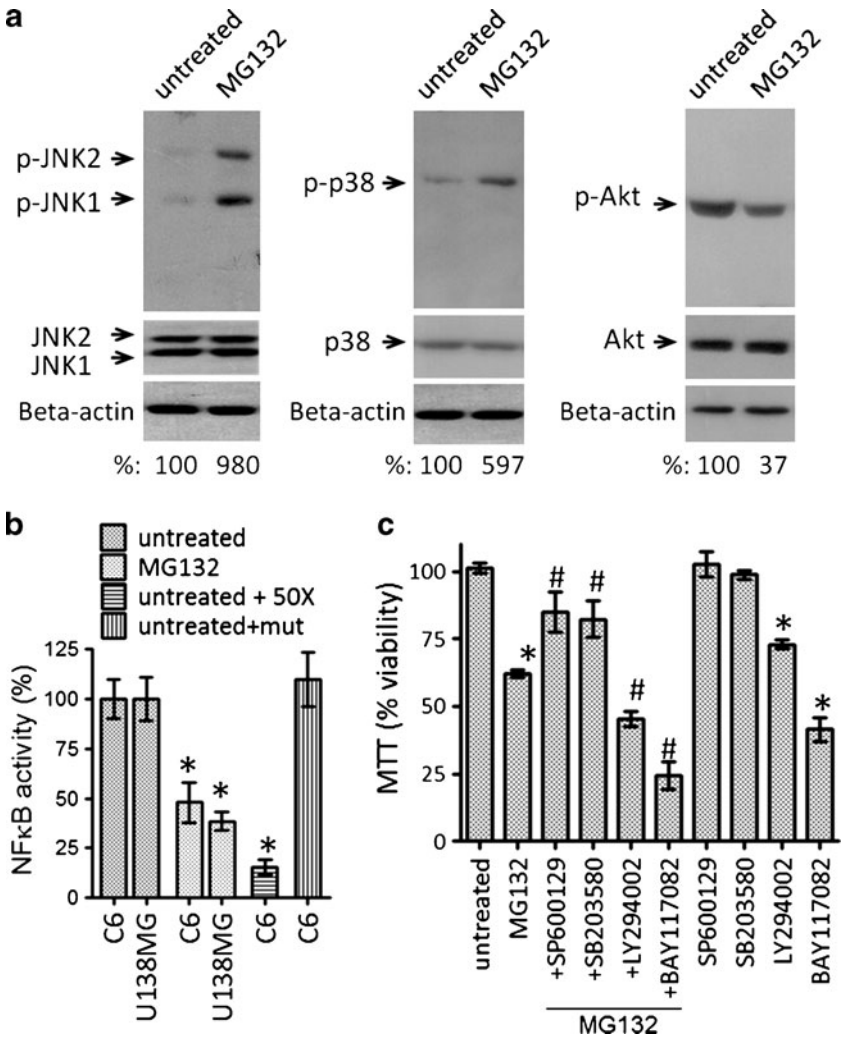


**Fig. 5** MG132 modulates apoptotic and survival pathways in GBMs. **a** Effect of MG132 on the phosphorylation state of p38, JNK1/2 and Akt in U138MG cells. Cells were treated with 5 μM MG132 for 12 h, and total extracts were analyzed by western blotting. Total forms of the proteins were determined; beta-actin was used as loading control. **b** ELISA assay for determination of NFkappaB activity in nuclear extracts of 5 μM MG132-treated GBMs. **c** MTT assay showing the effect of NFkappaB (BAY117082, 15 μM), PI3K/Akt (LY294002, 25 μM), JNK1/2 (SP600129, 15 μM) and p38 (SB203580, 15 μM) inhibitors on MG132-induced cell death. U138MG cells were pre-treated for 1 h with inhibitors. After, MG132 was added to culture medium at a final concentration of 5 μM; cells were incubated for additional 48 h. * different from untreated cells; # different from MG132-treated cells and from its respective inhibitor mono-treatment group (ANOVA, $p<0.05$)

pathways play pivotal roles in GBM cells survival and tumor progression in vivo [27, 30, 31, 43]. Mutations in PTEN and homotensin homologue, which are negative regulators of PI3K, lead to constitutive activation of the PI3K/Akt pathway in most of GBMs [27, 43]. Aberrant activation of NFkappaB also has been reported in GBM biopsies, driving focal necrosis formation, invasive phenotypes [6, 30] and resistance to $O^6$ alkylating agents [4]. In high-grade astrocytoma and GBM patients a positive correlation between phospho-Akt, NFκB activation and glioma progression was observed [41]. Thus, PI3K/Akt and NFkappaB pathways become important therapeutic targets for these tumors. We found a constitutive activation of PI3K/Akt and NFkappaB in GBM cell lines, and inhibition of these pathways with the specific pharmacological inhibitors LY294002 and BAY117082 decreased cell viability, confirming the role of these pathways in GBM cells survival. MG132 decreased the nuclear activity of NFkappaB, causing reduction of the bcl-xl protein immunocontent, which is a classical NFkappaB-regulated mitochondrial cytoprotective protein. PI3K-mediated Akt phosphorylation also was significantly inhibited. Moreover, MG132 synergized with NFkappaB and PI3K inhibitors to cause toxicity in GBMs. NFkappaB activation depends on phosphorylation and ubiquitination of the inhibitory protein IkappaB-alpha. Proteasome inhibitors can stabilize IkappaB-alpha by inhibiting the chymotryptic activity of the proteasome ultimately inhibiting NFkappaB [1, 8, 44]. In agreement, previous studies showed that PS-341 could significantly decrease the NFkappaB activity in T98G cells [44]. Taken together, MG132 effects on PI3K/Akt and NFkappaB pathways, which are up-regulated in GBMs but not in healthy cells/astrocytes, contribute to MG132 apoptotic potential and possibly to its selectivity.

Previous works from our group and others have shown that NFkappaB inhibition induces impairment on mitochondrial function leading to apoptotic JNK activation in different cell types [7, 20, 46]. NFkappaB inhibition sensitizes the cells to apoptosis by decreasing the levels of antiapoptotic proteins as bcl-xl, SOD2 and ferritin heavy chain, leading to a stress-dependent activation of JNK-mediated apoptosis. We found that MG132 decreased the levels of bcl-xl, inducing

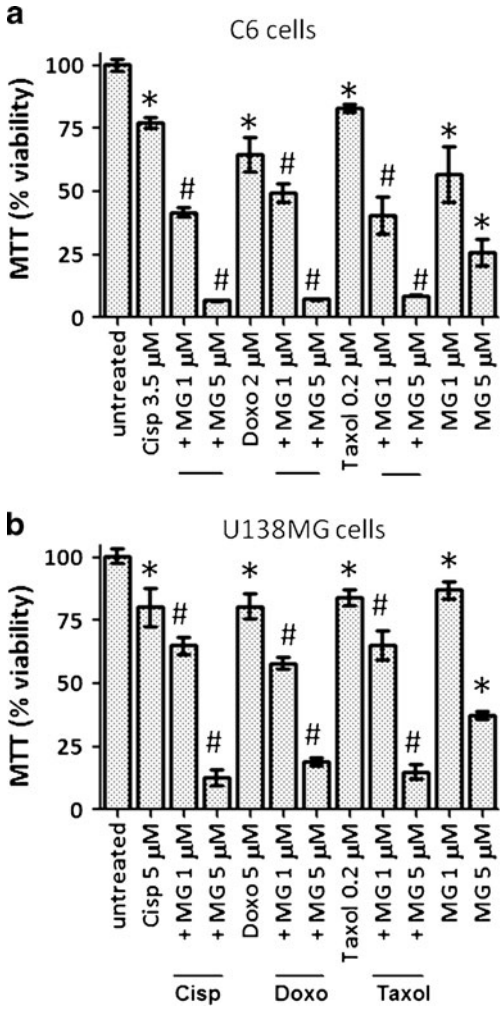


**Fig. 6** MG132 synergizes with chemotherapeutic agents. **a**, **b** C6 and U138MG (A and B graphs, respectively) were treated with different concentrations of MG132, followed by exposure to 5 μM cisplatin, 0.2 μM taxol or 5 μM doxorubicin for 48 h. Data were collected from three independent experiments ($n=3$). Legends: Cisp (cisplatin), Doxo (doxorubicin), MG (MG132). * Different from untreated cells; # different from its respective cisplatin, taxol or doxorubicin monotreatment ($p<0.05$, ANOVA)

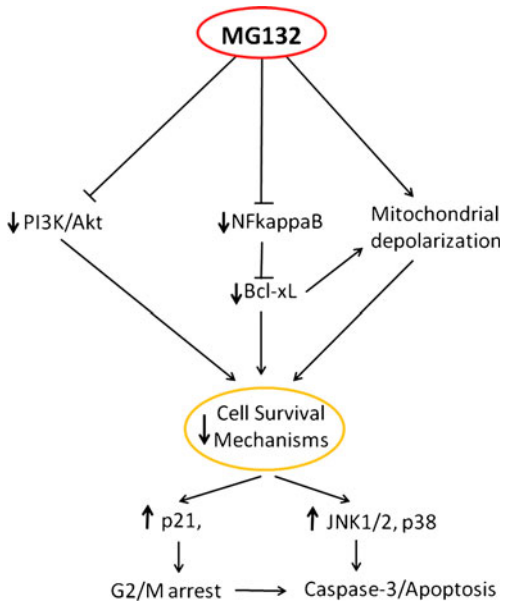


**Fig. 7** Schematic representation of MG132 effects on glioblastoma cell lines

mitochondrial depolarization, mPTP opening and phosphorylation of JNK1/2 and p38; inhibition of mPTP with bongkrekic acid and JNK and p38 inhibitors partially reversed MG132-induced cell death, suggesting that impairments on mitochondrial function and activation of stress-related pathways as JNK and p38 are involved in MG132 toxicity. In agreement, previous studies showed that PS-341-induced apoptosis was associated with JNK activation in HepG2 [20], U87 and T98G cell lines [44]. Also, Jiang et al. reported that selective bcl-xL knockdown rendered U87 and NS008 cells to apoptosis, evidencing a key role for the NFkappaB-regulated mitochondrial protein bcl-xl in GBMs survival [13]. In addition, bcl-xl mediates drug resistance in EGFR-mutated GBMs [25]. Taken together, data suggest that MG132 can blunt pivotal components of the GBM antiapoptotic threshold as NFkappaB/bcl-xl and PI3K/Akt, cumulating in mitochondrial dysfunction and pro-apoptotic stimulation of p38, JNK1/2 and caspase-3 cascades.

Besides the apoptotic activity per se, MG132 markedly synergized with the chemotherapeutics cisplatin, doxorubicin and taxol, suggesting that MG132 may be a clinically useful adjunct to classical anticancer drugs. Nonetheless, chemotherapeutics frequently exert cytotoxicity to healthy tissues leading to therapy failure and poor prognosis [4, 35, 36, 42]. Therefore, the adjuvant potential of MG132 also could be used for therapeutic advantage in order to reduce the doses of classical anticancer agents thus minimizing the frequently observed side effects to healthy tissues [4, 26, 36, 42].

In summary, we have demonstrated that proteasome inhibitor MG132 has important effects on GBM cells by inhibiting their growth and by inducing apoptotic cell death (Fig. 7). This was mediated by inhibition NFkappaB and PI3K/Akt, which are two major survival pathways in GBM cells, and accompanied by decreases in the NFkappaB-regulated anti-apoptotic mitochondrial protein bcl-xL, mitochondrial depolarization and mPTP opening. In conjunction with these changes, cells were arrested in G2/M at the early stages of treatment with concomitant increases in the CDK inhibitor $p21^{WAF1}$. These events cumulated in activation of caspase-3 and JNK1/2 and p38-dependent cell death (Fig. 6). Finally, MG132 probed potential as adjuvant for combined therapy with clinically utilized agents. These findings suggest that MG132 may be a candidate for further testing in pre-clinical studies of the disease.

**Acknowledgements** We acknowledge the Brazilian funds CAPES, CNPq, and FINEP/IBNNet (01060842–00) for financial support. We

thank Dr. Rafael Roesler (HCPA, Porto Alegre, Brazil) for gently provided U87 and U373 cell lines.

**Conflict of interest statement** The authors declare that there are no conflicts of interest.

## References


1. Adams J, Palombella VJ, Sausville EA, Johnson J, Destree A, Lazarus DD, Maas J, Pien CS, Prakash S, Elliott PJ (1999) Proteasome inhibitors: a novel class of potent and effective antitumor agents. Cancer Res 59:2615–2622
2. Baiz D, Pozzato G, Dapas B, Farra R, Scaggiante B, Grassi M, Uxa L, Giansante C, Zennaro C, Guarnieri G, Grassi G (2009) Bortezomib arrests the proliferation of hepatocellular carcinoma cells HepG2 and JHH6 by differentially affecting E2F1, p21 and p27 levels. Biochimie 91:373–382. doi:10.1016/j.biochi.2008.10.015
3. Braganhol E, Zamin LL, Cañedo AD, Horn F, Tamajusuku AS, Wink MR, Salbego C, Battastini AM (2006) Antiproliferative effect of quercetin in the human U138MG glioma cell line. Anticancer Drugs 17:663–671. doi:10.1097/01.cad.0000215063.23932.02
4. Bredel M, Bredel C, Juric D, Duran GE, Yu RX, Harsh GR, Vogel H, Recht LD, Scheck AC, Sikic BI (2006) Tumor necrosis factor-alpha-induced protein 3 as a putative regulator of nuclear factor-kappaB-mediated resistance to O6-alkylating agents in human glioblastomas. J Clin Oncol 24:274–287. doi:10.1200/JCO.2005.02.9405
5. Brennan C, Momota H, Hambardzumyan D, Ozawa T, Tandon A, Pedraza A, Holland E (2009) Glioblastoma subclasses can be defined by activity among signal transduction pathways and associated genomic alterations. PLoS One 4:e7752. doi:10.1371/journal.pone.0007752
6. Brown RE, Law A (2006) Morphoproteomic demonstration of constitutive nuclear factor-kappaB activation in glioblastoma multiforme with genomic correlates and therapeutic implications. Ann Clin Lab Sci 36:421–426
7. Bubici C, Papa S, Pham CG, Zazzeroni F, Franzoso G (2006) The NF-kappaB-mediated control of ROS and JNK signaling. Histol Histopathol 21:69–80
8. Chari A, Mazumder A, Jagannath S (2010) Proteasome inhibition and its therapeutic potential in multiple myeloma. Biologics 4:273–287. doi:10.2147/BTT.S3419
9. da Frota ML, Braganhol E, Canedo AD, Klamt F, Apel MA, Mothes B, Lerner C, Battastini AM, Henriques AT, Moreira JC (2009) Brazilian marine sponge Polymastia janeirensis induces apoptotic cell death in human U138MG glioma cell line, but not in a normal cell culture. Invest New Drugs 27:13–20. doi:10.1007/s10637-008-9134-3
10. Dhandapani KM, Mahesh VB, Brann DWJ (2007) Curcumin suppresses growth and chemoresistance of human glioblastoma cells via AP-1 and NFkappaB transcription factors. J Neurochem 102:522–538. doi:10.1111/j.1471-4159.2007.04633.x
11. Foti C, Florean C, Pezzutto A, Roncaglia P, Tomasella A, Gustincich S, Brancolini C (2009) Characterization of caspase-dependent and caspase-independent deaths in glioblastoma cells treated with inhibitors of the ubiquitin-proteasome system. Mol Cancer Ther 8:3140–3150. doi:10.1158/1535-7163.MCT-09-0431
12. Frankel A, Man S, Elliott P, Adams J, Kerbel RS (2000) Lack of multicellular drug resistance observed in human ovarian and prostate carcinoma treated with the proteasome inhibitor PS-341. Clin Cancer Res 6:3719–3728
13. Jiang Z, Zheng X, Rich KM (2003) Down-regulation of Bcl-2 and Bcl-xL expression with bispecific antisense treatment in glioblastoma cell lines induce cell death. J Neurochem 84:273–281. doi:10.1046/j.1471-4159.2003.01522.x
14. Kasuga C, Ebata T, Kayagaki N, Yagita H, Hishii M, Arai H, Sato K, Okumura K (2004) Sensitization of human glioblastomas to tumor necrosis factor-related apoptosis-inducing ligand (TRAIL) by NF-kappaB inhibitors. Cancer Sci 95:840–844. doi:10.1111/j.1349-7006.2004.tb02191.x
15. Kitagawa H, Tani E, Ikemoto H, Ozaki I, Nakano A, Omura S (1999) Proteasome inhibitors induce mitochondria-independent apoptosis in human glioma cells. FEBS Lett 443:181–186. doi:10.1016/S0014-5793(98)01709-8
16. Klamt F, Shacter E (2005) Taurine chloramine, an oxidant derived from neutrophils, induces apoptosis in human B lymphoma cells through mitochondrial damage. J Biol Chem 280:21346–21352. doi:10.1074/jbc.M501170200
17. Ko BS, Chang TC, Chen CH, Liu CC, Kuo CC, Hsu C, Shen YC, Shen TL, Golubovskaya VM, Chang CC, Shyue SK, Liou JY (2010) Bortezomib suppresses focal adhesion kinase expression via interrupting nuclear factor-kappa B. Life Sci 86:199–206. doi:10.1016/j.lfs.2009.12.003
18. Koschny R, Holland H, Sykora J, Haas TL, Sprick MR, Ganten TM, Krupp W, Bauer M, Ahnert P, Meixensberger J, Walczak H (2007) Bortezomib sensitizes primary human astrocytoma cells of WHO grades I to IV for tumor necrosis factor-related apoptosis-inducing ligand-induced apoptosis. Clin Cancer Res 13:3403–3412. doi:10.1158/1078-0432.CCR-07-0251
19. La Ferla-Brühl K, Westhoff MA, Karl S, Kasperczyk H, Zwacka RM, Debatin KM, Fulda S (2007) NF-kappaB-independent sensitization of glioblastoma cells for TRAIL-induced apoptosis by proteasome inhibition. Oncogene 26:571–582. doi:10.1038/sj.onc.1209841
20. Lauricella M, Emanuele S, D'Anneo A, Calvaruso G, Vassallo B, Carlisi D, Portanova P, Vento R, Tesoriere G (2006) JNK and AP-1 mediate apoptosis induced by bortezomib in HepG2 cells via FasL/caspase-8 and mitochondria-dependent pathways. Apoptosis 11:607–625. doi:10.1007/s10495-006-4689-y
21. Ling YH, Liebes L, Jiang JD, Holland JF, Elliott PJ, Adams J, Muggia FM, Perez-Soler R (2003) Mechanisms of proteasome inhibitor PS-341-induced G(2)-M-phase arrest and apoptosis in human non-small cell lung cancer cell lines. Clin Cancer Res 9:1145–1154
22. Lu G, Punj V, Chaudhary PM (2008) Proteasome inhibitor Bortezomib induces cell cycle arrest and apoptosis in cell lines derived from Ewing's sarcoma family of tumors and synergizes with TRAIL. Cancer Biol Ther 7: 603–608. doi: http://dx.doi.org/10.4161/cbt.7.4.5564
23. Mercer RW, Tyler MA, Ulasov IV, Lesniak MS (2009) Targeted therapies for malignant glioma: progress and potential. BioDrugs 23:25–35. doi:10.2165/00063030-200923010-00003
24. Monticone M, Biollo E, Fabiano A, Fabbi M, Daga A, Romeo F, Maffei M, Melotti A, Giaretti W, Corte G, Castagnola P (2009) z-Leucinyl-leucinyl-norleucinal induces apoptosis of human glioblastoma tumor-initiating cells by proteasome inhibition and mitotic arrest response. Mol Cancer Res 7:1822–1834. doi:10.1158/1541-7786.MCR-09-0225
25. Nagane M, Levitzki A, Gazit A, Cavenee WK, Huang HJ (1998) Drug resistance of human glioblastoma cells conferred by a tumor-specific mutant epidermal growth factor receptor through modulation of Bcl-XL and caspase-3-like proteases. Proc Natl Acad Sci USA 95:5724–5729
26. Nakanishi C, Toi M (2005) Nuclear factor-kappaB inhibitors as sensitizers to anticancer drugs. Nat Rev Cancer 5:297–309. doi:10.1038/nrc1588
27. Opel D, Westhoff MA, Bender A, Braun V, Debatin KM, Fulda S (2008) Phosphatidylinositol 3-kinase inhibition broadly sensitizes glioblastoma cells to death receptor- and drug-induced apoptosis. Cancer Res 68:6271–6280. doi:10.1158/0008-5472.CAN-07-6769
28. Phuphanich S, Supko JG, Carson KA, Grossman SA, Burt Nabors L, Mikkelsen T, Lesser G, Rosenfeld S, Desideri S, Olson JJ

(2010) Phase 1 clinical trial of bortezomib in adults with recurrent malignant glioma. J Neurooncol 100:95–103. doi:10.1007/s11060-010-0143-7

29. Rao SK, Edwards J, Joshi AD, Siu IM, Riggins GJ (2010) A survey of glioblastoma genomic amplifications and deletions. J Neurooncol 96:169–179. doi:10.1007/s11060-009-9959-4
30. Raychaudhuri B, Han Y, Lu T, Vogelbaum MA (2007) Aberrant constitutive activation of nuclear factor kappaB in glioblastoma multiforme drives invasive phenotype. J Neurooncol 85:39–47. doi:10.1007/s11060-007-9390-7
31. Robe PA, Bentires-Alj M, Bonif M, Rogister B, Deprez M, Haddada H, Khac MT, Jolois O, Erkmen K, Merville MP, Black PM, Bours V (2004) In vitro and in vivo activity of the nuclear factor-kappaB inhibitor sulfasalazine in human glioblastomas. Clin Cancer Res 10:5595–5603. doi:10.1158/1078-0432.CCR-03-0392
32. Roesler R, Brunetto AT, Abujamra AL, de Farias CB, Brunetto AL, Schwartsmann G (2010) Current and emerging molecular targets in glioma. Expert Rev Anticancer Ther 10:1735–1751. doi:10.1586/era.10.167
33. Roth P, Kissel M, Herrmann C, Eisele G, Leban J, Weller M, Schmidt F (2009) SC68896, a novel small molecule proteasome inhibitor, exerts antiglioma activity in vitro and in vivo. Clin Cancer Res 15:6609–6618. doi:10.1158/1078-0432.CCR-09-0548
34. Russo A, Bronte G, Fulfaro F, Cicero G, Adamo V, Gebbia N, Rizzo S (2010) Bortezomib: a new pro-apoptotic agent in cancer treatment. Curr Cancer Drug Targets 10:55–67
35. Soni D, King JA, Kaye AH, Hovens CM (2005) Genetics of glioblastoma multiforme: mitogenic signaling and cell cycle pathways converge. J Clin Neurosci 12:1–5. doi:10.1016/j.jocn.2004.04.001
36. Stewart LA (2002) Chemotherapy in adult high-grade glioma: a systematic review and meta-analysis of individual patient data from 12 randomised trials. Lancet 359:1011–1018. doi:10.1016/S0140-6736(02)08091-1
37. Thaker NG, Zhang F, McDonald PR, Shun TY, Lewen MD, Pollack IF, Lazo JS (2009) Identification of survival genes in human glioblastoma cells by small interfering RNA screening. Mol Pharmacol 76:1246–1255. doi:10.1124/mol.109.058024
38. Vaziri SA, Hill J, Chikamori K, Grabowski DR, Takigawa N, Chawla-Sarkar M, Rybicki LR, Gudkov AV, Mekhail T, Bukowski RM, Ganapathi MK, Ganapathi R (2005) Sensitization of DNA damage-induced apoptosis by the proteasome inhibitor PS-341 is p53 dependent and involves target proteins 14-3-3-sigma and survivin. Mol Cancer Ther 4:1880–1890. doi:10.1158/1535-7163.MCT-05-0222
39. Wagenknecht B, Hermisson M, Eitel K, Weller M (1999) Proteasome inhibitors induce p53/p21-independent apoptosis in human glioma cells. Cell Physiol Biochem 9:117–125. doi:10.1159/000016308
40. Wagenknecht B, Hermisson M, Groscurth P, Liston P, Krammer PH, Weller M (2000) Proteasome inhibitor-induced apoptosis of glioma cells involves the processing of multiple caspases and cytochrome c release. J Neurochem 75:2288–2297. doi:10.1046/j.1471-4159.2000.0752288.x
41. Wang H, Wang H, Zhang W, Huang HJ, Liao WS, Fuller GN (2004) Analysis of the activation status of Akt, NFkappaB, and Stat3 in human diffuse gliomas. Lab Invest 84:941–951. doi:10.1038/labinvest.3700123
42. Weaver KD, Yeyeodu S, Cusack JC, Baldwin AS, Ewend MG (2003) Potentiation of chemotherapeutic agents following antagonism of nuclear factor kappa B in human gliomas. J Neurooncol 61:187–196. doi:10.1023/A:1022554824129
43. Yang Y, Shao N, Luo G, Li L, Zheng L, Nilsson-Ehle P, Xu N (2010) Mutations of PTEN gene in gliomas correlate to tumor differentiation and short-term survival rate. Anticancer Res 30:981–985
44. Yin D, Zhou H, Kumagai T, Liu G, Ong JM, Black KL, Koeffler HP (2005) Proteasome inhibitor PS-341 causes cell growth arrest and apoptosis in human glioblastoma multiforme (GBM). Oncogene 24:344–354. doi:10.1038/sj.onc.1208225
45. Zanotto-Filho A, Delgado-Cañedo A, Schröder R, Becker M, Klamt F, Moreira JC (2010) The pharmacological NFkappaB inhibitors BAY117082 and MG132 induce cell arrest and apoptosis in leukemia cells through ROS-mitochondria pathway activation. Cancer Lett 288:192–203. doi:10.1016/j.canlet.2009.06.038
46. Zanotto-Filho A, Gelain DP, Schröder R, Souza LF, Pasquali MA, Klamt F, Moreira JCF (2009) The NFkappaB-mediated control of RS and JNK signaling in vitamin A-treated cells: duration of JNK-AP-1 pathway activation may determine cell death or proliferation. Biochem Pharmacol 77:1291–1301. doi:10.1016/j.bcp.2008.12.010